Molecular mechanisms underlying the surface organization of the NMDA receptors during development

Nathan Benac

université de BORDEAUX

THÈSE PRÉSENTÉE

POUR OBTENIR LE GRADE DE

DOCTEUR DE

L'UNIVERSITÉ DE BORDEAUX

ÉCOLE DOCTORALE SCIENCES DE LA VIE ET DE LA SANTÉ

SPÉCIALITÉ NEUROSCIENCES

Par Nathan BENAC

Etude des mécanismes moléculaires responsables de l'organisation à la surface des récepteurs NMDA au cours du développement

Molecular mechanisms underlying the surface organization of NMDA receptors during development

Sous la direction de Laurent GROC

Soutenue le 3 octobre 2024

Membres du jury :

M. HERRY, Cyril	Directeur de Recherche, Université de Bordeaux	Président
Mme. LEVI, Sabine	Directeur de Recherche, ESPCI Paris	Rapporteur
Mme. CHARRIER, Cécile	Directeur de Recherche, ENS Paris	Rapporteur
M. DITYATEV, Alexander	Professeur, Université de Magdeburg	Examinateur
M. GROC, Laurent	Directeur de Recherche, Université de Bordeaux	Directeur de thèse

Title Molecular mechanisms underlying the surface organization of NMDA receptors during development

Abstract Understanding how neurons develop to form the organized pattern of synaptic connections remains a central question in neuroscience. The vast majority of excitatory synapses are formed early in development during a synaptogenesis window. N-methyl-D-aspartate receptors (NMDAR) have long been a strong candidate to drive synaptogenesis as both *in vivo* and *in vitro* data show a key role for NMDAR during that phase. Furthermore, the facts that NMDAR are found in the developmentally immature "silent" synapses and among the first receptors to accumulate at the site of nascent synapses together lead to the assumption that NMDAR's clustering is a nucleation point. Yet, the mechanisms underpinning the early clustering of NMDAR into synaptogenic assemblies remain enigmatic. Evidences that NMDAR can directly interact with other surface proteins, including receptors, has promoted the possibility that surface protein-protein interaction (PPI) represents a potent way to cluster receptors. Using a combination of live imaging and super-resolution microscopy, we observed that the interaction between D1R-GluN1-NMDAR were promoted in immature neurons, during the synaptogenesis phase. We showed that the D1R-GluN1-NMDAR interaction directly shapes the organization of NMDAR, allowing their functional clustering and synaptogenesis. Indeed, preventing the interaction in immature neurons, and not in mature neurons, altered the formation of excitatory post-synapses. We then focused on the intracellular and extracellular regulatory mechanisms of the interaction. We demonstrated a role of metabotropic glutamate receptors (mGluR) and casein kinase 1 (CK1) in promoting the interaction between D1R and GluN1-NMDAR. On the other hand, the facts that the hyaluronic acid (HA), one of the main components of the extracellular matrix (ECM), is enriched early in the immature brain and it regulates the surface diffusion of macromolecules opens the hypothesis that the ECM regulates the ability of NMDAR to interact with other surface macromolecules, including D1R. Yet, classical approaches have mainly focused on degrading the ECM. Herein, we aimed at increasing the ECM content in HA by over-expressing both the wild-type form of the rat hyaluronan synthase 2 (HAS2) or one bearing the two point-mutations present in the naked mole rat (NMR; N178S and N301S) which produces very high molecular weight HA (vHMW-HA). We observed that increasing the matrix impaired the development of the neuron and modified both

the surface organization and trafficking of NMDAR. These findings validate our strategy, and open new paths for investigating the role of the ECM on neuronal development.

Keywords NMDA receptor, protein-protein interaction, dopamine type I receptor, synaptogenesis, super-resolution microscopy, brain extracellular matrix, hyaluronic acid, naked mole rat

---

Unité de recherche

Institut Interdisciplinaire de Neurosciences, Université de Bordeaux, UMR5297, Centre Broca Nouvelle Aquitaine, 146 rue Léo Saignat 33076 Bordeaux Cedex (France)

Titre Etude des mécanismes moléculaires responsables de l'organisation à la surface des récepteurs NMDA au cours du développement

Résumé Comprendre comment les neurones se développent pour former le schéma organisé des connexions synaptiques reste une question centrale en neurosciences. La grande majorité des synapses excitatrices se forment tôt au cours du développement pendant une fenêtre de synaptogenèse. Les récepteurs N-méthyl-D-aspartate (NMDAR) sont depuis longtemps considérés comme un candidat important pour stimuler la synaptogenèse, car les données in vivo et in vitro montrent un rôle clé des NMDAR pendant cette phase. De plus, le fait que les NMDAR se trouvent dans les synapses « silencieuses », immatures sur le plan développemental, et parmi les premiers récepteurs à s'accumuler et s'agréger au site des synapses naissantes conduit à l'hypothèse que l'agrégation des NMDAR est un point de départ dans la formation des synapses. Cependant, les mécanismes moléculaires précoces sous-tendant l'agrégation des NMDAR en assemblages pro-synaptogéniques restent peu connus. De précédents travaux montrant que les NMDAR peuvent interagir directement avec d'autres protéines de surface, y compris des récepteurs, ont favorisé la possibilité que les interactions protéine-protéine (PPI) à la surface des neurones représentent un moyen puissant pour agréger les récepteurs. En utilisant une combinaison d'imagerie en direct et de microscopie super-résolution, nous avons observé que l'interaction entre les D1R-GluN1-NMDAR était favorisée dans les neurones immatures, pendant la phase de synaptogenèse. Nous avons montré que l'interaction D1R-GluN1-NMDAR façonne directement l'organisation des NMDAR, permettant leur agrégation fonctionnelle et la synaptogenèse. En effet, empêcher l'interaction dans les neurones immatures, et non dans les neurones matures, a altéré la formation des synapses excitatrices. Nous nous sommes ensuite concentrés sur les mécanismes de régulation intracellulaire et extracellulaire de l'interaction. Nous avons démontré un rôle des récepteurs métabotropes du glutamate (mGluR) et de la caséine kinase 1 (CK1) dans la promotion de l'interaction entre les D1R et les GluN1-NMDAR. D'autre part, le fait que l'acide hyaluronique (HA), l'un des principaux composants de la matrice extracellulaire (ECM), soit enrichi tôt dans le cerveau immature et régule la diffusion de surface des macromolécules ouvre l'hypothèse que l'ECM régule la capacité des NMDAR à interagir avec d'autres macromolécules de surface, y compris le D1R. Pourtant, les approches classiques se sont principalement concentrées sur la

dégradation de l'ECM. Ici, nous avons visé à augmenter le contenu de l'ECM en HA en surexprimant à la fois la forme sauvage de la hyaluronane synthase de type synthase 2 de rat (HAS2) ou une forme portant les deux mutations ponctuelles présentes chez le rat-taupe nu (NMR; N178S et N301S) qui est connu pour produire de l'HA de très haut poids moléculaire (vHMW-HA). Nous avons observé que l'augmentation de la matrice entravait le développement des neurones et modifiait à la fois l'organisation et le trafic de surface des NMDAR. Ces résultats valident notre stratégie et ouvrent de nouvelles voies pour enquêter sur le rôle de l'ECM dans le développement neuronal.

Mots clés Récepteur NMDA, interactions protéines – protéines, récepteur à la dopamine de type I, synaptogenèse, microscopie super-résolution, matrice extracellulaire, rat-taupe nu

Acknowledgments

I would like to express my gratitude to the members of the committee: Cécile Charrier, Sabine Levi, Alexander Dityatev, and Cyril Herry. Thank you for your time and your willingness to evaluate my PhD work.

Un grand merci à toi Laurent. Merci de m'avoir accueilli au sein de ton équipe, mais surtout merci pour ta confiance, ton soutien, et la liberté presque totale que tu m'as accordé. Je ne pense pas avoir déjà eu un "non" de ta part, pas même quand mes idées étaient farfelues, et je t'en remercie.

Merci à tous les membres de l'équipe, anciens et actuels. Ce fût un plaisir de travailler avec vous tout au long de ces années. A vous tous, Delphine, Julien, Olivier, Frédéric, François, Hélène, Joana, Emily, Ezequiel, Elise, Constance, Elodie, Morgane, Magalie, Flávia, Ivo, Juan, Zoë, Floriane, Dominique, Daniel, Mar, Léa, Adèle, Romain, Thomas L, Thomas G, Camille, Laurine, Carlos – et tous ceux que j'ai peut-être oublié. Votre investissement, votre exigence et votre enthousiasme ont été, et resteront, un exemple.

My PhD work relied on collaborations with many talented scientists from IINS to whom I am extremely grateful: Rémi Galland, Jean-Baptiste Sibarita, Corey Butler, Anushka Nair (I will never forget the night we saw this ridiculously dim band on the agarose gel…), Jonathan Elegheert. Je voudrais également remercier Christelle Breillat. Merci pour ton aide précieuse mais surtout pour ta bienveillance.

A special thanks to my past and current, quite extraordinary, office-mates and friends: Floriane, Zoë, Flávia, Dominique, Morgane, Ivo, and Juan. Thank you for the countless coffee breaks and discussions, but most of all, for your kindness and support.

Finalement, merci à ma famille et à toi, Sylvain. Merci pour votre soutien sans faille.

Table of content

Introduction

Overall context. The purpose of the introduction section is to outline our current understanding of the glutamatergic synapse, its components, focusing mainly on the glutamatergic NMDA receptor, and how these elements assemble during the formation of synapses. Many fundamental questions on these topics remain obviously without answers, my PhD project aiming to shed new light on a specific question: how the glutamatergic NMDA receptor cluster at the surface of immature neurons?

Generally, the brain is composed of billions of neuronal cells, also known as neurons, that are tightly inter-connected to one another and serves as the fundamental basis for all cognitive processes. Each neuron makes thousands of connections with cognate neurons from the same or distant regions, creating sophisticated neural networks. Within those networks, neurons communicate through a process known as synaptic transmission. Nerve impulses are conveyed as electrical signals, along the neuronal axons, in the form of action potential before being passed to a second neuron through a synapse (figure 1). Chemical synapses are the main type of synapses in the central nervous system (CNS). In opposition to electrical synapses, chemical synapses are composed of two highly specialized compartments, known as the pre- and post-synapse, that are separated by the synaptic cleft.

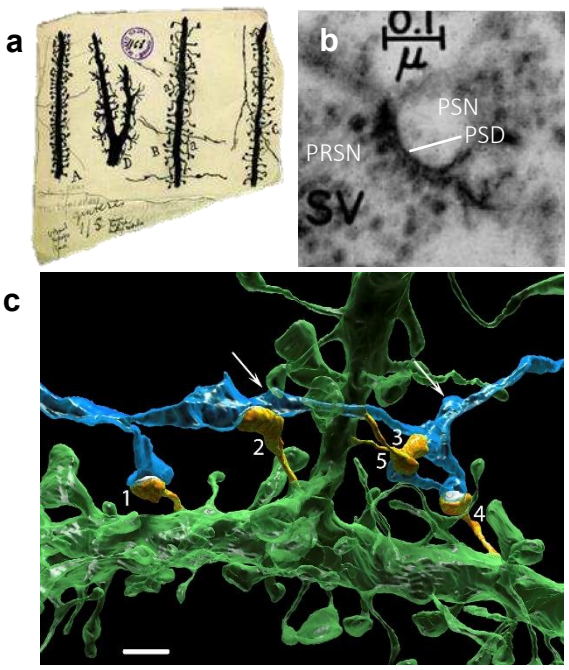

Figure 1. The chemical synapse. *Initially considered as an artifact from the Golgi staining, spines were first described by Ramon y Cajal. In opposition to the reticular theory, this observation changed the field of neuroscience: neuronal cells are independent units. In comparison to intestinal villi, Ramon y Cajal proposed that such extensions of the membrane allow to increase its surface, therefore increasing the capacity to connect.* ***a****, Ramon y Cajal drawing of dendritic spines. Adapted from (Yuste, 2015)* ***b****, First electron microscopy image of a synapse. PSN post-synaptic neuron, PSD post-synaptic density, PRSN pre-synaptic neuron, SV synaptic vesicles. Adapted from (De Robertis and Bennett, 1955)* ***c****, 3D-reconstruction of synaptic contacts from the mouse neocortex. In this example, a single axon connects with several dendritic*

spines from the same neuron (noted from 1 to 5); the arrows show synaptic contacts with spines from other neurons. Adapted from (Kasthuri et al., 2015).

The propagation of an action potential in the pre-synapse leads to the release of neurotransmitters in the synaptic cleft that bind to their receptors located onto the post-synapse membrane within the post-synaptic density (PSD). The activation of neurotransmitter receptors then generates a specific response within the receiving neuron. The efficacy of the synaptic transmission can be modified, either enhanced (e.g. long-term potentiation, LTP) or reduced (e.g. long-term depression, LTD). These mechanisms, collectively known as synaptic plasticity, are considered as the molecular basis for learning and memory. The efficacy of synaptic transmission *R* is determined by presynaptic transmitter release properties (number of active zones *n* and probability of release *p*) and post-synaptic receptor numbers and properties (e.g. through post-translational modifications) *q,* which gives the equation: $R = npq$

The glutamatergic synapse is the main excitatory synapse in the vertebrate brain. Glutamate receptors can be divided into two groups, the ionotropic (iGluR) and metabotropic (mGluR) receptors. iGluR are composed by N-Methyl-D-Aspartate Receptors (NMDAR, GluN1-3), α-Amino-3-hydroxy-5-Methyl-4-isoxazolePropionic Acid Receptors (AMPAR, GluA1-4), Kainate Receptors (KAR, GluK1-5) and delta glutamate receptors (GluD1 and 2). iGluR generate a fast response by fluxing cations into the cell whereas G protein-coupled receptor (GPCR), e.g. metabotropic glutamate receptors or mGluR (type I mGluR 1/5, type II mGluR 2/3, type III mGluR 4/6-8), are responsible for slower changes by generating protein G-mediated signal transduction cascades. Similarly, inhibitory transmission is mediated through γ-aminobutyric acid (GABA)-ergic synapses. Inhibitory signals are transduced by two classes of receptors, the metabotropic $GABA_B$ receptors and the ionotropic $GABA_A$ receptors which are permeable to the anion chloride. The balance between excitation and inhibition is central to the normal functioning of the brain and its disruption is associated to neurodevelopmental disorders. Noteworthy, I will only focus the introduction on the excitatory glutamatergic synapse, hence referred to as synapse.

Chapter 1. NMDAR

1. Composition, structure, and expression of NMDAR

1.1 NMDAR composition

NMDAR are heterotetrametric assemblies consisting of two obligatory $_{D}$-serine or glycine-binding GluN1 subunit and two glutamate-binding GluN2 (A, B, C, or D) subunits, two glycine-binding GluN3 (GluN3A and GluN3B) subunits or a mixture of GluN2- and GluN3-subunits (reviewed in (Hansen et al., 2018; Paoletti et al., 2013; Pérez-Otaño et al., 2016). The GluN1 subunit is encoded by a single gene (*GRIN1*) with 8 splice variants (figure 2A) (Durand et al., 1992; Hollmann et al., 1993; Nakanishi et al., 1992; Sugihara et al., 1992). This alternative splicing is due to the alternative inclusion of the exon 5 in the N-terminal domain (NTD), and of the exons 21 (which encodes the cassette C1) and 22 (which encodes the cassette C2 or C2' as a result of alternative splicing) in the carboxyl terminal domain (CTD). The GluN2 subunits (A-D) also encoded by a single gene (*GRIN2A*, *GRIN2B*, *GRIN2C*, *GRIN2D*). The human GluN2A subunit has 2 splice variants (GluN2A-Full and GluN2A-short) of different CTD length. The GluN3 subunit is encoded by two genes (*GRIN3A* and *GRIN3B*). In rodents, both GluN3A and GluN3B subunits are undergoing alternatively splicing with 2 splice variants for GluN3A subunit (long and short) and five splice variants for GluN3B subunit. As a result, there may be as many as 300 unique NMDAR expressed across the CNS. The subunit composition of NMDAR varies depending on the central nervous system (CNS) region, developmental stage, neuronal subtype or disease state (Akazawa et al., 1994).). In the hippocampus and cortex, which are the brain structures that have been most studies over the past decades, synapses primarily exhibit GluN2A and GluN2B subunits (Paoletti et al., 2013)) in a dihetero- or triheteromeric form (Chazot and Stephenson, 1997; Hansen et al., 2018; Luo et al., 1997).

1.2 Structure of NMDAR

Each NMDAR subunit can be divided into 4 domains (figure 2B). The extracellular portion of the NMDAR is composed by an N-terminal domain (NTD, also known as amino-terminal domain, ATD) and a ligand-binding domain (LBD, also known as agonist-binding domain, ABD) attached by a linker. The NTD is composed of two glomerular segments and contributes (1) to the assembly of NMDAR within the endoplasmic reticulum, (2) to extracellular protein-protein interactions and (3) to allosteric modulations of the receptor (Atlason et al., 2007; Gielen et al., 2009; Yuan et al., 2009). The LBD (or ABD) is composed of two discontinuous segments S1 and S2 where agonists (NMDA or glutamate) or co-agonists (glycine and D-serine) bind to the GluN2 and to the obligatory GluN1- or the GluN3 subunits, respectively. The transmembrane domain (TMD) is made of three helices (M1, M3 and M4) as well as one re-entering loop (M2) that forms the cation-permeable pore of the receptor (with a magnesium block at resting membrane potential) (Karakas and Furukawa, 2014; Lee et al., 2014; Wollmuth, 2018). The intracellular C-terminal domain (CTD) differs substantially in size depending on the subunit with GluN1 subunit exhibiting a much shorter CTD than those of the GluN2-subunits. The CTDs are important for receptor assembly and trafficking to the plasma membrane, for its stabilization at synapses, and for modulations of the receptors through post-translational modifications, interactions with other proteins, and/or degradation (Aman et al., 2014; Lussier et al., 2015; Traynelis et al., 2010).

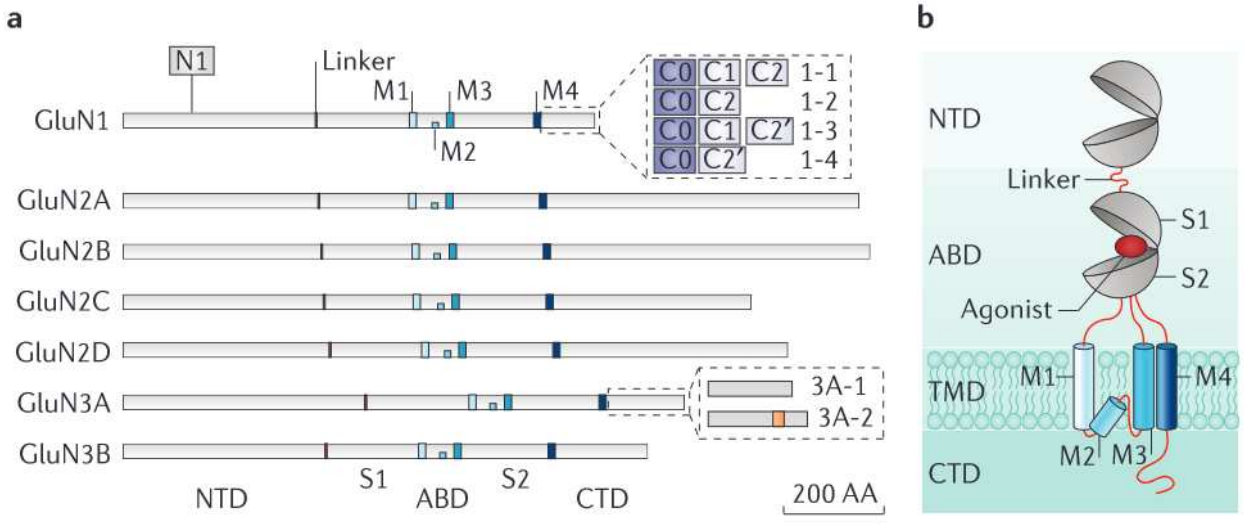

Figure 2. NMDAR topology. *A, The obligatory GluN1 subunit is encoded by a single gene (GRIN1) with 8 splice variants. This alternative splicing is due to the alternative inclusion of the exon 5 in the N-terminal domain (NTD), and of the exons 21 (which encodes the cassette C1) and 22 (which encodes the cassette C2 or C2'*

as a result of alternative splicing) in the carboxyl terminal domain (CTD). B, Organization of the different domain of the NMDAR. it is composed by a N-terminal domain (also known as amino-terminal domain, ATD) that is linked to a ligand-binding domain (also known as agonist-binding domain) where glutamate bind to the obligatory GluN1 subunit or the non-obligatory GluN3-subunit, and the co-agonist D-serine or glycine to the GluN2-subunits, four transmembrane domain and a C-terminal tail or C-terminal domain (CTDs). Adapted from (Paoletti et al., 2013).

1.3 NMDAR expression

The obligatory GluN1 subunit is expressed across development, brain regions and cell types (Laurie and Seeburg, 1994; Monyer et al., 1994; Paupard et al., 1997). On the other hand, the expression patterns of GluN2 and GluN3 subunits vary depending on the brain region, the developmental state, the neuronal subtype as well as the disease state (figure 3). GluN2A and GluN2B subunits are the prevalent non-obligatory subunits in higher brain structures (e.g. cortical and hippocampal regions) (Monyer et al., 1994; Paoletti et al., 2013; Watanabe et al., 1992). The GluN2B subunit is highly expressed early during brain development and its predominance progressively decreases with the incorporation of GluN2A-containing NMDARs during the second and third post-natal weeks in rodents (known as the GluN2B-to-GluN2A shift). In adulthood, the forebrain is the structure that retains the highest levels of GluN2B subunit. GluN2A subunit expression is widespread in the adult brain. The GluN2C subunit appears after the first week of development in rodent, and is mainly contained in the cerebellum and olfactory bulb whereas GluN2D subunit expression is high during the first postnatal week, with low level of expression in adult, in the diencephalon, brainstem, cerebellum and spinal cord. The GluN3A subunit is expressed early during brain development, with a maximum expression around the second and third postnatal week, and is rather expressed across all brain regions (Pérez-Otaño et al., 2016).

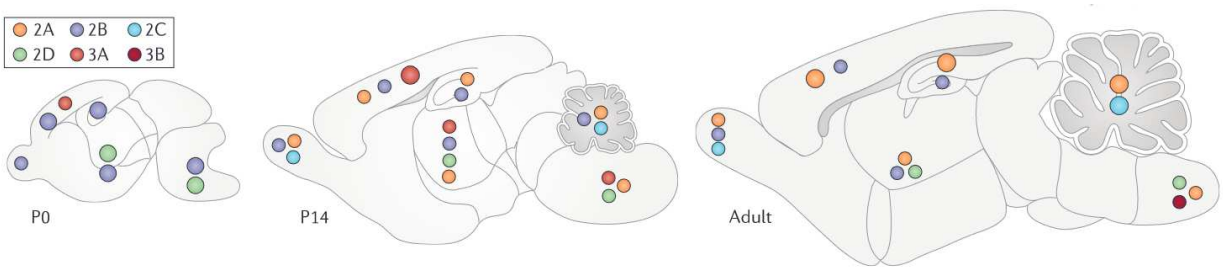

Figure 3. Developmental profile of NMDAR expression. *The expression of NMDARs changes across brain regions and developmental state. In the hippocampus, our main region of interest, GluN2B- and GluN2A-containing NMDARs are prominent. Early in development, NMDARs are mainly composed by the non-obligatory subunit GluN2B whereas they are mainly composed by GluN2A-containing NMDAR in the mature hippocampus. Adapted from (Paoletti et al., 2013).*

2. Functional properties of NMDAR

2.1 NMDAR activation

At hyperpolarized resting membrane potential, NMDARs are closed due to the trapping of magnesium ions inside their cation-permeable channel pore. Their activation required coincident presynaptic and postsynaptic activity, with the concomitant binding of both the co-agonist glycine or D-serine and glutamate to GluN1 and GluN2 subunits, respectively, together with the removal of their voltage-dependent magnesium blockade through postsynaptic depolarization. Synaptic NMDARs have thus been considered as Hebbian-like detector to sense putative changes in the presynaptic and postsynaptic compertments. Upon activation, they flux calcium into the cell which leads to the activation of intracellular signaling cascades that mediate synaptic transmission.

2.2 NMDAR composition determines NMDAR functional properties

NMDARs have distinct functional properties (e.g. gating kinetics and desensitization) depending on their composition. Briefly, GluN2A-containing NMDARs have a much faster decay time (~ 40 ms) in comparison with GluN2B-containing NMDARs (~200 ms) (Monyer et al., 1992; Traynelis et al., 2010; Vicini et al., 1998; Wyllie et al., 1998; Yuan et al., 2009). The opening probability of the

receptor will also vary significantly depending on the GluN2 subunit (0.5 for GluN2A and 0.1 for GluN2B), with thus higher opening probability for GluN2A- than GluN2B-containing NMDARs (Wyllie et al., 1998), as well as the conductance and the sensitivity to magnesium blockade. Inversely, GluN2A-containing NMDAR have a lower sensitivity to glutamate than GluN2B-containing NMDARs (Chen et al., 2008; Erreger et al., 2007; Hansen et al., 2018). GluN2C- as well as GluN2D-NMDAR have lower conductances, a lower sensitivity to magnesium and a lower permeability to calcium than GluN2A- and GluN2B-containing NMDAR (Burnashev et al., 1995; Kuner and Schoepfer, 1996; Monyer et al., 1992; Qian et al., 2005). Importantly, GluN3-NMDARs are not activated by glutamate (or NMDA) but, like the obligatory GluN1 subunits, by glycine (Pérez-Otaño et al., 2016; Stroebel et al., 2021). GluN3-containing NMDARs have a very low calcium permeability and virtually no magnesium block. Furthermore, GluN3-NMDAR are insensitive to competitive antagonist such as APV since they do not possess a binding site for glutamate as well as for open-channel blockers such as MK-801.

Different NMDARs can have distinct pharmacological modulators. For example, ifenprodil is known as specific antagonist for GluN2B-containing NMDAR whereas zinc is highly specific to GluN2A-containing NMDARs at low concentration (Chen et al., 1997). In fact, zinc and ifenprodil can be used somehow to differentiate between GluN2A- and GluN2B-contaning NMDARs (Paoletti et al., 2013), although to a very specific range of low concentrations.. Protons preferentially inhibit GluN2B- as well as GluN2D-containing NMDARs (Low et al., 2003) while extracellular polyamines preferentially enhance GluN2B-containing NMDARs. All these features have been reviewed in reviewed in (Dupuis et al., 2023; Hansen et al., 2018; Paoletti et al., 2013; Traynelis et al., 2010; Vieira et al., 2020).

2.3 Role of NMDAR on plasticity

2.3.1 Role on AMPAR-mediated synaptic plasticity

Synaptic plasticity (e.g. LTP and LTD) refers to long-term changes in the strength or efficiency of synaptic transmission. NMDARs and their transmission have traditionally been considered less “plastic” than AMPARs at synapses, where changes in AMPAR-mediated transmission are known to underlie various forms of LTP and LTD, such as the NMDAR-dependent long-term plasticity. It is

well established that NMDAR activity is essential for initiating AMPAR-mediated both NMDAR-dependent LTP and LTD. This has been extensively reviewed by (Huganir and Nicoll, 2013; Lüscher and Malenka, 2012; Malenka and Bear, 2004; Nicoll and Schulman, 2023) (figure 4).

After the release of glutamate from the presynaptic terminal, glutamate activates postsynaptic ionotropic receptors and triggers an influx of Na+ and efflux of K+, resulting in the depolarization of the postsynaptic membrane. The depolarization removes the magnesium ion block from the NMDAR channel pore, allowing calcium to enter the cell and trigger intracellular signaling cascades that modulate synaptic strength and eventually induce synaptic plasticity. It is widely accepted that correlated activity drives NMDAR-dependent LTP whereas non-correlated activity, such as low-frequency activation of the presynaptic terminal without postsynaptic depolarization and decorrelate pre- and postsynaptic activation, can drive long-term depression (LTD)(Bi and Poo, 1998; Dan and Poo, 2006; Dudek and Bear, 1992; Froemke and Dan, 2002; Mizuno et al., 2001). It has been suggested that the form of plasticity induced, i.e. LTP or LTD, depends on the amplitude of the calcium influx followed by NMDAR activation (Artola et al., 1990; Lisman, 1989). Modest or low NMDAR activation triggers LTD through the activation of calcineurin and protein phosphatase 1, resulting in a reduction in synaptic AMPAR and spine shrinkage (Dudek and Bear, 1992; Lisman, 1989; Oliet et al., 1997; Zhou et al., 2004). In contrast, strong NMDAR activation induces LTP via the activation of CaMKII, leading to an increase in AMPAR conductance, an increase in the number of synaptic AMPARs, and spine enlargement (Benke et al., 1998; Derkach et al., 1999; Ehlers, 2000; Holtmaat and Svoboda, 2009; Nicoll and Schulman, 2023).

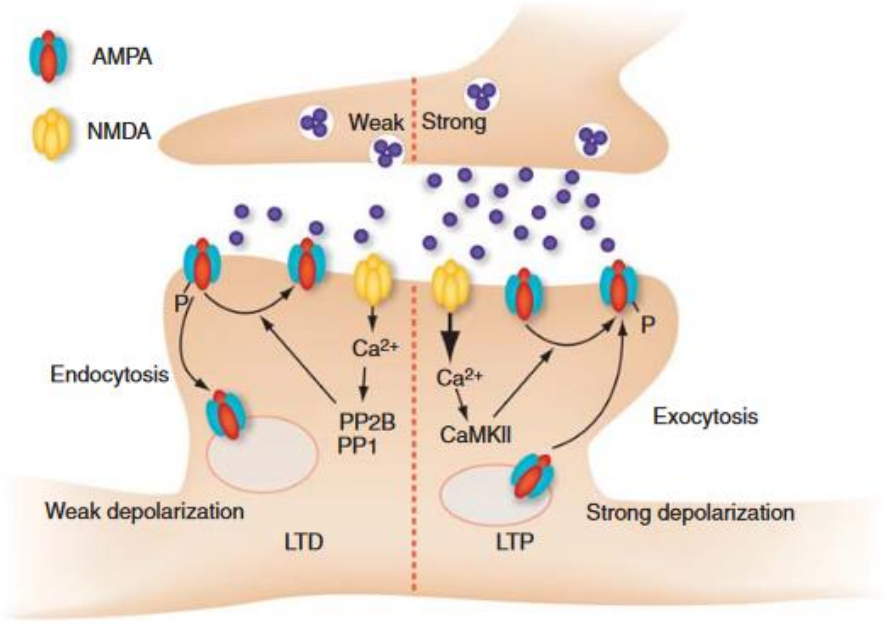

Figure 4. NMDAR-dependent AMPAR-mediated synaptic plasticity. *LTD is triggered by a modest activation of NMDARs, which leads to a low-amplitude calcium increase and the activation of PP1, which promotes AMPAR removal and endocytosis. In contrast, strong NMDAR activation causes a large calcium influx, activating CaMKII and leading to LTP (e.g. increase in the number of synaptic AMPAR). Adapted from (Lüscher and Malenka, 2012).*

2.3.2 Activity-dependent changes in NMDAR number

Both NMDAR-LTP and -LTD require the activation of NMDARs as well as a rise in intracellular calcium. It has been suggested that these induced-form of plasticity, either LTP or LTD, depends on the amplitude of the calcium increase (Bhouri et al., 2014; Harney et al., 2006; Hunt et al., 2013; Kotecha et al., 2003). In NMDAR-LTP, the rise in intracellular calcium is a consequence of the activation of either type I mGluRs or adenosine 2A receptors, that triggers depending on the cell type either PKC/SRC or PKA mediated signaling, and finally lead to an increase in the number of NMDARs at the cell surface and at the synapse (Grosshans et al., 2002; Harney et al., 2006; Rebola et al., 2008).

2.3.3 Activity-dependent changes in NMDAR properties and composition

The amplitude of NMDAR-mediated calcium influx can be modulated by PKA-mediated phosphorylation following the activation of type I mGluRs, D2R, A2AR, or GABA-B receptors (Chalifoux and Carter, 2010; Higley and Sabatini, 2010; Matta et al., 2011; Skeberdis et al., 2006). NMDAR plasiticity can also be due to changes in NMDAR-subunit composition, which is triggered by the activation of NMDAR, type I mGluR and subsequent activation of phospholipase C and PKC as well as by the subunit-dependent redistribution of NMDARs.

2.3.4 Non-ionotropic functions of the NMDARs

Over the past decades, it emerges that, in parallel to the function of the ionotropic NMDAR-mediated transmission, NMDAR can be engaged into non-ionotropic (also referred as non-canonical, metabotropic) functions; reviewed in (Dupuis et al., 2023). These emerging features and functions are still under debate and the molecular mechanisms underpinning the NMDAR non-ionotropic functions remain, to date, poorly understood.

2.3.4.1 Long-term depression

Ion-flux indendepent LTD were first reported almost 30 years ago with the observation that heterosynaptic LTD was not blocked neither by the open-channel blocker MK-801 nor by calcium chelation (Mayford et al., 1995; Nabavi et al., 2013; Scanziani et al., 1996). On the other hand, LTD was blocked by the competitive antagonist APV (which competes with agonist binding). The binding of the agonist to the NMDAR is capable of inducing a change in the conformation of receptor that is proposed to be responsible for the non-ionotropic action of NMDAR (Dore et al., 2016, 2015). Indeed, blocking the conformational change of the NMDAR, by using antibodies, is sufficient to prevent the NMDAR-mediated induction of LTD. Additionnally, NMDAR can trigger either spine growth or shrinkage independently of ion-flow through p38 MAPK-dependent signaling pathways (Birnbaum et al., 2015; Stein et al., 2021, 2020, 2015).

2.3.4.2 Long-term potentiation

While LTD can be induced in a non-ionotropic dependent manner, the expression of NMDAR-mediated LTP requires ionotropic activity (Scanziani et al., 1996). However, both ionotropic and non-ionotropic NMDAR functions may together participate in the induction of LTP with (1) classical calcium influx from synaptic GluN2A-containing NMDARs and (2) the secondary redistribution of GluN2B-containing NMDAR towards the synaptic compartment which may help redistributing key intracellular actors such as CaMKII (Dupuis et al., 2014a). In fact, preventing the redistribution of GluN2B-containing NMDARs or expressing a mutant form of GluN2B-containing NMDAR that cannot bind to CaMKII is sufficient to abolish the induction of LTP (Dupuis et al., 2014a). This feeds a model in which NMDAR-dependent LTP requires a calcium and subsequent NMDAR membrane redistribution, which favor intracellular protein kinase clustering and signaling cascades (Groc and Choquet, 2020).

3. NMDAR surface expression

3.1 NMDAR assembly and export to the plasma membrane

NMDAR subunits are first assembled as monomers in the endoplasmic reticulum (ER) and exported, as heterotetramers, to the Golgi, trans-Golgi network and finally, to the plasma membrane (figure 5) (Gardoni and Di Luca, 2021; Horak et al., 2014; Vieira et al., 2020). NMDARs can also be synthetized locally, within Golgi outposts. Indeed, local synthesis is important for certain activity-dependent modulations in synaptic NMDAR content (Dupuis et al., 2023) (figure 4).) (figure 5). Only properly assembled complexes will be exported to the plasma membrane as the obligatory GluN1 subunit bears ER-retention signal (RRR and KKK motifs) that are unmasked upon tetramerization with GluN2 subunits. The NMDAR processing is limited by the number of available GluN2 or GluN3 subunits early within the ER (Horak and Wenthold, 2009; Standley et al., 2000). Of note, ER retention signals are located on GluN1 CTD either within the cassette C1 i.e. present in GluN1-1 and GluN1-3 isoforms) as well as within the cassette C2 (GluN1-3 and GluN1-4 isoforms (Horak and Wenthold, 2009; Standley et al., 2000). Similarly, ER retention signals can be found within the ATD of the GluN2A subunit and in the CTD of GluN2B subunit (Horak et al.,

2014; Kaniakova et al., 2012; Qiu et al., 2009). As a consequence, NMDAR are considered as obligate heterotetramers.

3.2 Endo- and exocytosis of NMDAR

3.2.1 NMDAR endocytosis

The processes of endocytosis and exocytosis participate in regulating the number of surface NMDAR both at synaptic and extrasynaptic locations. Endocytois is the active process through which membrane and/or extracellular proteins, herein membrane NMDAR, are internalized (figure 5). NMDAR endocytosis is mediated by clathrin-coated pits that are located outside of PSD (Blanpied et al., 2002; Petralia et al., 2003). It is thus accepted that NMDAR first exit synapses through lateral surface diffusion before being trapped and internalized at extrasynaptic sites. The γ2 subunit of the AP-2 protein complex, which is part of the endocytic machinery, interacts with NMDAR either through an internalization motif (YELK) at the GluN2B CTDs or through tyrosine phosphorylation in the case of the GluN1 and GluN2A subunits (Lavezzari et al., 2004; Nakatsu and Ohno, 2003; Prybylowski et al., 2005; Roche et al., 2001; Scott et al., 2001; Vissel et al., 2001). NMDAR internalization is highly regulated by the association with other proteins, the binding of agonist as well as post-translational modifications of the CTDs. Indeed, NMDAR-PSD-95 association decreases AP-2-dependent internalization and increases NMDAR surface content (Roche et al., 2001). On the other hand, agonist binding and NMDAR activation both promote the internalization of NMDAR (Nong et al., 2003). Lastly, GluN2B CTDs can be phosphorylated by several kinases, including CaMKII, PKC, DABK1) in an activity-dependent manner. Phosphorylation of GluN2B subunit at the serine 1303 residue has been shown to disrupt the interaction between GluN2B CTD and CaMKII, thus reducing its internalization (Strack et al., 2000).

3.2.2 NMDAR exocytosis

Exocytosis is the active process through which proteins are integrated in the plasma membrane or released into the extracellular space (ECS) for secreted proteins. NMDAR exocytosis can occur via the N-ethylmaleimine-sensitive factor attachment protein receptor (SNARE) complex, in this case through SNAP25-VAMP1-syntaxin complex at extrasynaptic sites (Gu and Huganir, 2016;

Südhof and Rothman, 2009) (figure 5). This suggests that NMDAR need to laterally diffuse from their site of membrane insertion to the synapses. The cleavage and inactivation of SNAP-25 by botinulum toxin prevent NMDAR exocytosis (Lau et al., 2010). SNAP-23 have also been shown to be specifically involved in mediating NMDAR, but no AMPAR, exocytosis (Suh et al., 2010; Washbourne et al., 2004). Importantly, NMDAR exocytosis is regulated by neuronal activity, herein by protein kinase C (PKC) (Lan et al., 2001; Tanaka and Nishizuka, 1994). Additionally, the activation of other receptors such as dopamine receptors (DAR) and type I mGluRs have been shown to promote the insertion of NMDAR to the neuronal surface (Dunah and Standaert, 2001; Lan et al., 2001; Lee et al., 2002; Petit-Pedrol and Groc, 2021).

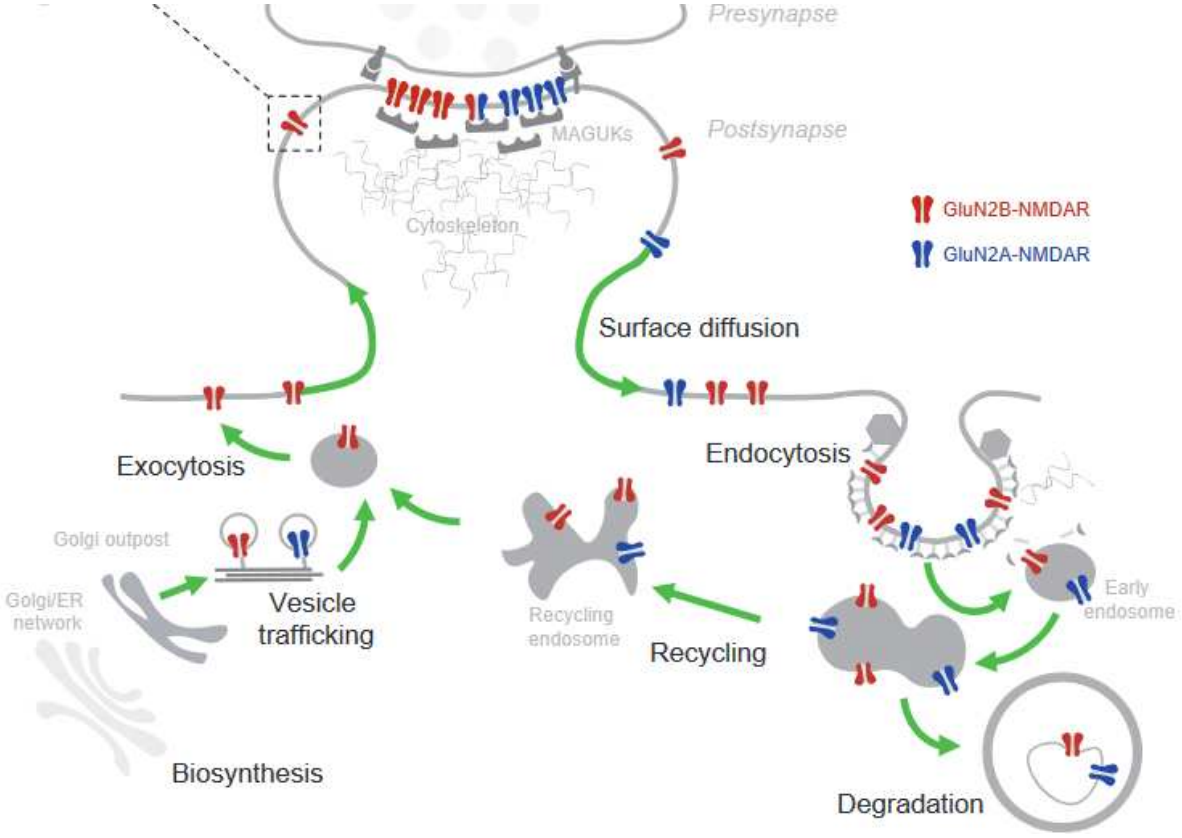

Figure 5. NMDAR assembly and export. *Following their synthesis, NMDAR are exported from the ER and the Golgi network to the membrane where they can enter synapses through lateral diffusion. NMDAR are internalized by clathrin-mediated endocytosis. Then, they can be either degraded or recycled. Adapted from (Dupuis et al., 2023).*

4. NMDAR membrane organization

4.1 Presynaptic NMDAR

The presence of presynaptic NMDARs has only been demonstrated in specific brain regions, including the cortex and the hippocampus (Banerjee et al., 2016; Bouvier et al., 2018). The composition of presynaptic NMDAR varies depending on the brain region and the identity of the postsynaptic terminal with GluN2C- and GluN2D-NMDAR predominating in the hippocampus. Functionnally, it has been shown that presynaptic NMDARs can regulate spontaneous neurotransmitter release (Abrahamsson et al., 2017) as well as participate in calcium-mediated presynaptic plasticity through the activation of nitric acid oxidase (NOS) and/or calcineurin (Andrade-Talavera et al., 2016; Bouvier et al., 2018, 2015; Larsen et al., 2014).

4.2 Synaptic NMDAR and extrasynaptic NMDAR

NMDAR can be found both in synaptic and extrasynaptic compartments (Clark et al., 1997; Harney et al., 2006; Harris and Pettit, 2007; Petralia et al., 2010; Rao and Craig, 1997; Rosenmund et al., 1995). Approximately, 20 to 50 % of surface NMDARs are localized extrasynaptically in mature hippocampal neurons. The subcellular composition of NMDAR is not homogeneous and seem to depend on the GluN2 subunit composition. While GluN2B-containing NMDARs are present at both synaptic and extra-synaptic sites, GluN2A-containing NMDARs are more abundant in synapses (Bard and Groc, 2011). The activation of extrasynaptic NMDAR is triggered by the presence of glutamate outside of the synaptic cleft, typically following glutamate spill-over (Asztely et al., 1997; Clark and Cull-Candy, 2002; Harris and Pettit, 2007; Nahir and Jahr, 2013). It has been proposed that synaptic NMDARs are preferentially gated by the co-agonist D-serine whereas extrasynaptic NMDARs are preferentially gated by glycine which results to different changes in membrane diffusion(Ferreira et al., 2017; Papouin et al., 2012). Indeed, synaptic GluN2B-containingNMDAR lateral diffusion is reduced by D-serine, but not glycine, whereas synaptic GluN2A-containing NMDAR lateral diffusion is not affected by neither D-serine nor glycine. Importantly, the activation of extrasynaptic NMDARs is involved in several brain diseases, as it is well accepted to trigger pro-

death signaling pathways (Hardingham and Bading, 2010; Martel et al., 2012; McQueen et al., 2017; Parsons and Raymond, 2014; Tu et al., 2010; Yu et al., 2023; Zong et al., 2022).

4.2.1 Nanoscale organization

At the surface of cortical and hippocampal neurons, NMDARs are aggregated into clusters of ~400 nm diameter that can be observed with conventional microscopy techniques. Thanks to the development of superresolution imaging techniques, it has been shown that synapses contain dozens of NMDAR (30-50 copies) that are organized in 1-4 nanodomains (superresolved regions of receptor aggregation that are contain within a cluster) of ~60 nm diameter (Kellermayer et al., 2018; MacGillavry et al., 2013; Willems et al., 2020) (figure 6). Similar nanoclustering have been observed for other glutamate receptors (e.g. AMPARs, mGluRs) within excitatory synapses as well as within inhibitory synapses (Ferreira et al., 2020; Kellermayer et al., 2018; MacGillavry et al., 2013; Nair et al., 2013; Pennacchietti et al., 2017; Scheefhals et al., 2023; Specht et al., 2013). The synaptic nano-organization is likely a common feature of the ionotropic neurotransmitter receptors, strengthening the view that the post-synapse is a highly complex and compartmentalized entity. It also emerged the possibility that the correct positioning of synaptic receptors in regards to presynaptic release sites, forming the so-called trans-synaptic “nanocolumns, is an additional level of regulation of the synaptic transmission (Tang et al., 2016). This is particularly important for low-affinity receptors, like AMPARs, as their probability of activation drops with the distance from the release sites (Haas et al., 2018). Whether this mechanism applies to NMDARs, which affinity to glutamate is higher, remains however unanswered. A presumed role for the NMDAR synaptic nanoclustering is on their activity-dependent inactivation, as receptors in close proximity would more efficiently inhibit one-another (Iacobucci and Popescu, 2019).

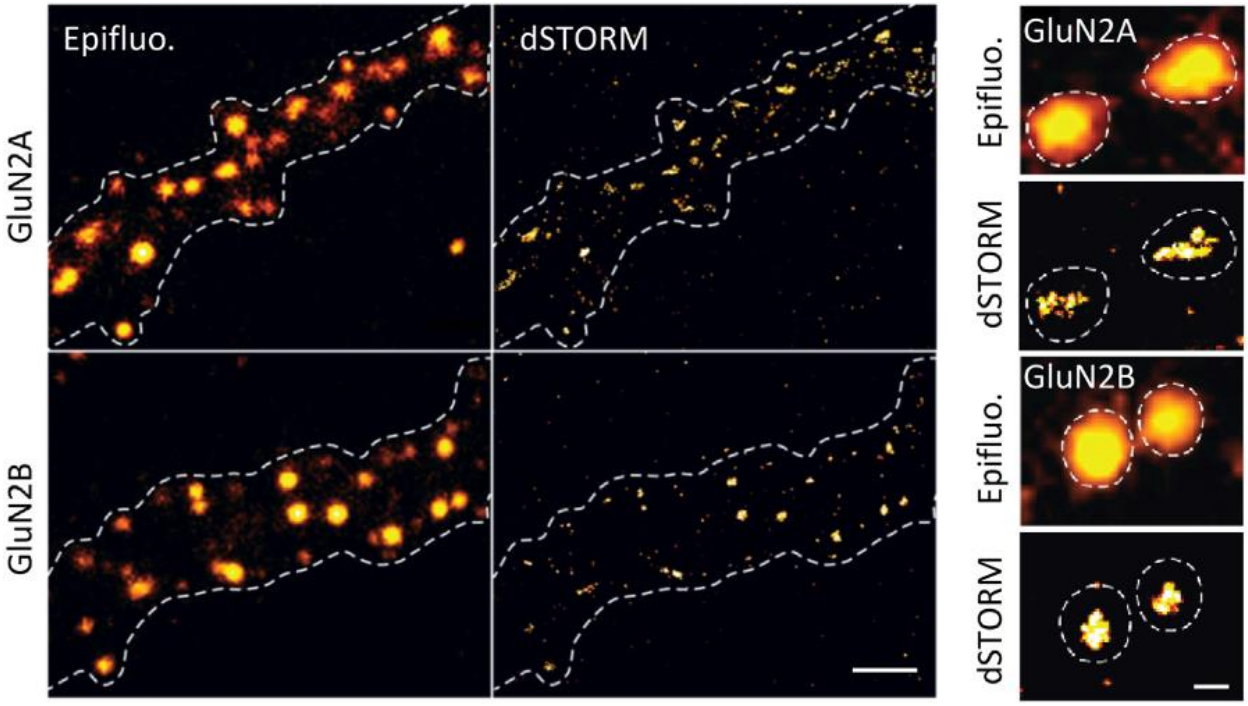

Figure 6. NMDAR are nano-organized. *Thanks to the development of superresolution microscopy techniques such as direct stochastic optical reconstruction microscopy (dSTORM), it has been shown that NMDARs are nano-organized at the cell surface. They form nanodomains of ~ 60 nm diameter. Adapted from (Kellermayer et al., 2018).*

It is well accepted that receptors are concentrated in the PSD through anchorage to intracellular scaffolds. Indeed, the membrane-associated guanylate kinase (MAGUK) proteins, such as PSD95 that directly binds to NMDAR, play an important role in their synaptic trapping (Bard et al., 2010; Barria and Malinow, 2002; Kornau et al., 1995; Prybylowski et al., 2005; Yi et al., 2007). Direct cis-interaction between NMDAR and trans-synaptic proteins have also been shown to control the synaptic localization of NMDAR. Particularly, the direct interaction between the obligatory GluN1 subunit of the NMDAR and the ephrin B2 receptor (EphB2R) (Dalva et al., 2000; Washburn et al., 2020) as well as the adhesion molecule neuroligin-1 (Nlg1) (Budreck et al., 2013) that bind to the presynaptic proteins ephrin ligand and neurexin, respectively. The interaction between NMDARs and both Nlg-1 and EphB2 have been shown to participate in both the synaptic anchoring and retention of NMDAR within the postsynaptic sites (Budreck et al., 2013; Chih et al., 2005; Dalva et al., 2000). It is important to note, however, that the interaction between NMDAR and Nlg1 have been shown by co-immunoprecipitation assays (Budreck et al., 2013) but biophysical studies have failed to detect it (Elegheert et al., 2017).

Both GluN2A- and GluN2B-containing NMDAR are differentially organized at post-synapses with only a minor fraction (30%) that is overlapping (Kellermayer et al., 2018). Such differential organization of synaptic GluN2A- and GluN2B-containing NMDAR indicate subunit-dependent regulatory processes, although the involved mechanisms have not been clearly identified. One potential target is the CaMKIIα subunit. Indeed, it has been shown that CaMKIIα binds to the CTD of GluN2B subunit and regulates its nano-organization in hippocampal neuronal cultures (Ferreira et al., 2020). Furthermore, activated CaMKIIα undergoes liquid-liquid phase separation with GluN2B CTD, which leads to the formation of synaptic protein condensates that reproduce the synaptic organization of NMDAR (Hosokawa et al., 2021). Collectively, these data suggest CaMKII acts as a postsynaptic organizer of NMDARs at the nanoscale.

5. NMDAR surface dynamics

Despite the original fluid mosaic model of the plasma membrane (Singer and Nicolson, 1972) prevailed, in neuroscience, a static view of the post-synaptic membrane: movements of post-synaptic receptors would occur during development and stop after maturation, once receptors are in place. Following this view, receptors recycling through endo- and exocytosis was the only route in and out of synapses, respectively. The developments of fluorescence imaging and single molecule localization microscopy challenged this view, highlighting the surface diffusion of neurotransmitter receptors following thermally-driven Brownian movements (Borgdorff and Choquet, 2002; Dahan et al., 2003; Groc et al., 2004, 2006b; Meier et al., 2001). It is now well accepted that, driven by a Brownian motion regime, receptors are highly mobile within the membrane plane. The number and the distribution of synaptic receptors are continuously regulated through a combination of local synthesis, endo- and exocytosis at peri- and extrasynpatic sites as well as lateral diffusion.

5.1 Methods for studying membrane receptors movements in neurons

5.1.1 Open channel block

Patch-clamp recordings a well as diffraction-limited fluorescence imaging (see the paragraph on fluorescence recovery after photobleaching) are one of the oldest techniques that have been used to monitor the membrane diffusion of receptors in neurons. It consists in monitoring the recovery of synaptic currents following their irreversible blockade (using MK-801 in the case of NMDAR, for example), and use it as a proxy to estimate the mobility of the receptors (Tovar and Westbrook, 2002). This technique has been recently used to monitor the rapid exchange between synaptic and extrasynaptic NMDAR in rat hippocampal slices (McQuate and Barria, 2020). However, this technique is only applicable to ionotropic receptors and cannot be used to monitor the surface behaviors of other types of receptors such as GPCRs, including metabotropic glutamate receptors.

5.1.2 Fluorescence Recovery After Photobleaching (FRAP)

Fluorescence Recovery After Photobleaching (FRAP) is one of the most widely used technique to measure receptor diffusion in neuronal cultures, brain slices as well as in live animals *in vivo* (Erami et al., 2016; Rasse et al., 2005). This strategy has been successfully used to monitor the average membrane diffusion of membrane protein, including both ionotropic (e.g. acetylcholine, AMPAR, and GABA-A) as well as metabotropic receptors (serotonin, dopamine, mu opioid) types (Ashby et al., 2006; D Axelrod et al., 1976; D. Axelrod et al., 1976; Pucadyil et al., 2004; Rasse et al., 2005; Saulière-Nzeh et al., 2010; Schlessinger et al., 1976; Scott et al., 2006; Thomas et al., 2005). During FRAP, fluorescently-labeled receptors are locally photobleached using a brief and focused high-intensity laser illumination and the recovery of fluorescence, due to the movement of surrounding non-photobleached receptors, is measured over time (figure 7). The plateau of recovery, normalized to the intensity in the region of interest before photobleaching, gives a proxy of the receptor mobile fraction (figure 7). For FRAP, receptors are usually tagged with a pH-sensitive version of green fluorescent protein (GFP), namely superecliptic pHluorine (SEP), that emits fluorescence at neutral pH and thus allows to specifically monitor the mobility of populations of receptors at the plasma membrane (Ashby et al., 2004). However, FRAP has heavily relied on overexpressing recombinant receptors, which could interfere with and bias mobility

measurements, for example, by saturating anchoring sites for synaptic receptors. Alternatives to the overexpression of recombinant receptors are the use of (1) chemical labeling of endogenous receptors (Nonaka et al., 2024; Wakayama et al., 2017), or (2) the use of CRISPR-Cas9 editing strategies (Fang et al., 2021; Willems et al., 2020).

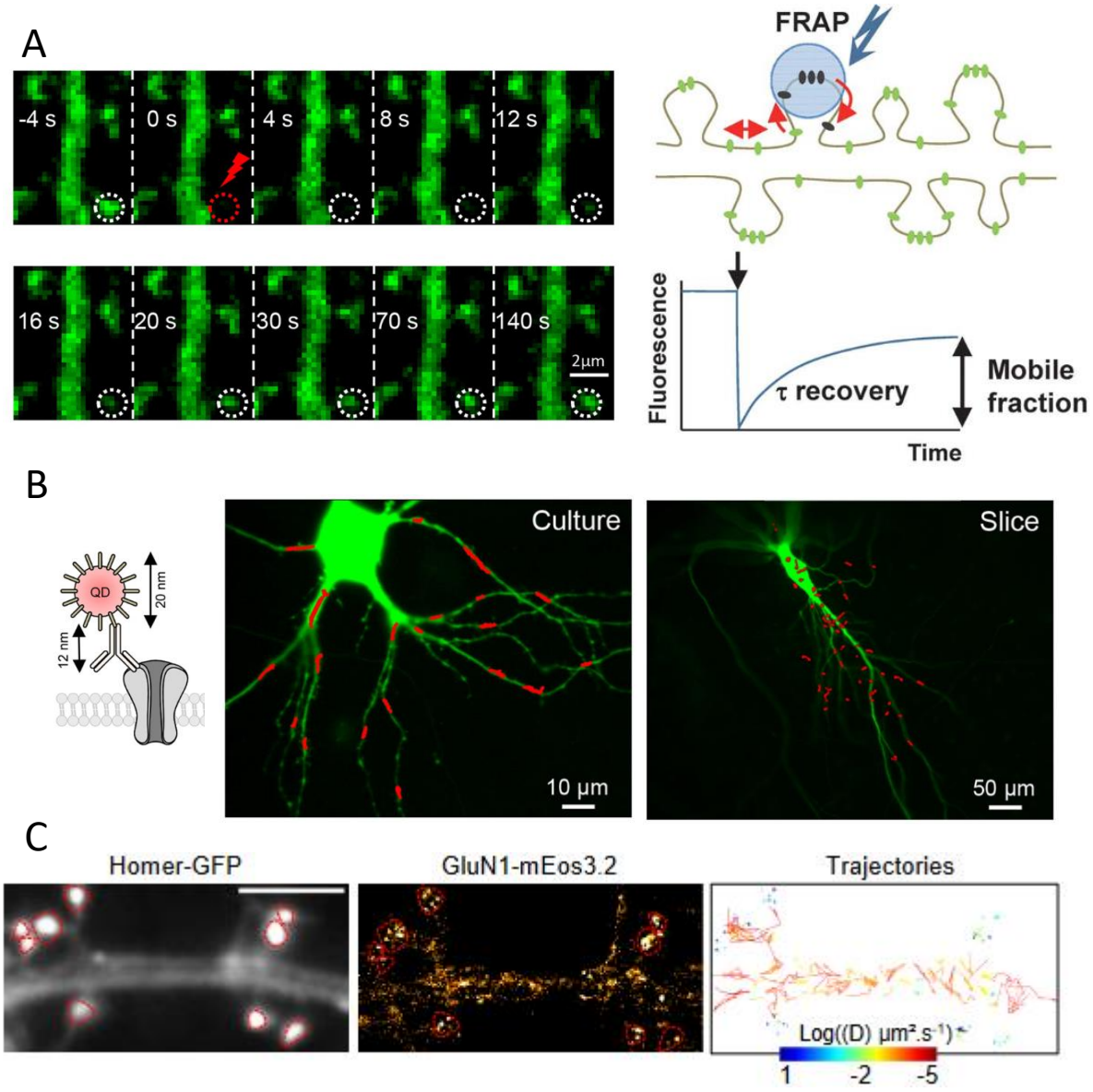

Figure 7. Imaging approaches for studying membrane receptors movements in neuron. *A. In fluorescence recovery after photobleaching (FRAP), fluorescently labeled receptors are locally photobleached and the fluorescence recovery is measured over time in the recovery area in order to measure both the diffusion rate and the fraction of mobile receptors. B. In QD-SPT, membrane receptors are labeled with a complex of primary antibody-QD. QD-SPT allows to track the surface diffusion of membrane receptors for extended period of time in both primary neuronal cultures as well as slices. C. Homer-GFP is labeling excitatory*

postsynapes. SPT-PALM allows to track the surface diffusion of a large number of receptors both in synaptic and extrasynaptic compartment. Adapted from (Dupuis and Groc, 2020; Groc and Choquet, 2020; Jamet et al., 2024)

5.1.3 Single molecule imaging

In contrast to the two techniques mentioned above, which rely on ensemble-averaging of receptor populations, the development of single molecule imaging methods has revolutionized the field by enabling the tracking of individual surface receptors. Single molecule imaging relies on decorrelating the fluorescence emission of the labelled receptors as a function of time and space, in order to achieve nanometric resolution. This is achieved by either a sparse labeling of the protein of interest that are labeled with either photobleachable florescent probes (e.g. universal point accumulation for imaging in nanoscale topography, uPAINT) (Sharonov and Hochstrasser, 2006) or photostable nanoparticles (e.g. quantum dots, QDs) for single particle tracking (SPT), or by the stochastic activation and bleaching of photoconvertible fluorescent protein that are coupled to the protein of interest (e.g. photoactivation localization microscopy, PALM).

SPT have been widely used to investigate the surface diffusion of neurotransmitter receptors both in primary cultures as well as in brain slices, both organotypic and acute (Dupuis and Groc, 2020; Heine et al., 2008; Varela et al., 2016) (figure 7). QDs are semiconductor nanocrystals that are particularly suited for single molecule imaging considering their narrow emission spectra, high brightness as well as photostability (they are virtually unbleachable); reviewed in (Walling et al., 2009). QDs allow to track the surface diffusion of receptors for extended periods of time, thus enabling the detailed exploration of the diffusion and diffusive properties of single receptors in various cell compartments. The use of QD-SPT has revealed that individual receptors can transition between freely diffusive and highly confined states at the surface of hippocampal neurons. It is important to consider that, although QD-SPT offers several advantages, including the ability to track the diffusion of endogenous receptors, their large size (a QD emitting at 655 nm is around 20 nm, and a primary antibody–QD complex is approximately 32 nm) could limit or hinder their diffusion in narrow compartments, such as the synaptic cleft (figure 7). The development and use of another single molecule imaging approach, PALM requires the expression of recombinant receptors that are fused with a photoswitchable fluorescent molecules (the green-to-red photoswitchable fluorescent protein mEOS, for example) (Betzig et al., 2006; Hess et al., 2006).

The recent development of CRISPR-Cas9 editing strategy provide a way to label endogeneously expressed receptors. PALM allows the acquisition of a large number of both synaptic and extrasynaptic receptor trajectories (figure 7). Noteworthy, PALM is not suitable to track proteins for long period of time, due to the low photostability of the fluorescent protein.

5.2 NMDAR trafficking in immature neurons

Both NMDAR membrane diffusion and endo- / exocytosis rates are developmentally regulated. NMDAR endocytosis occurs in a subunit-dependent manner at clathrin-coated vesicles (CCV) or pits, which are located laterally to the PSD (Lavezzari et al., 2004). The number and the distance of the CCV to synapses vary depending on the maturation stage. In comparison with mature neurons, CCVs are in higher number and are located closer to synapses in immature neurons (Blanpied et al., 2002; Petralia et al., 2003). Overall, it suggests that NMDAR endocytic rate is more pronounced at early stage, and reduces with neuronal development (Roche et al., 2001). Similarly, NMDAR surface diffusion changes across neuronal development. Initially high, the surface dynamics of NMDAR is decreased by around 30% in mature neurons (Groc et al., 2006b). Of note, this is not specific to NMDAR as AMPAR also show both a high recycling rate and surface diffusion in immature compare to mature neurons (Borgdorff and Choquet, 2002; Groc et al., 2006a). Altogether, these data highlight the high instability of the immature neuronal membrane.

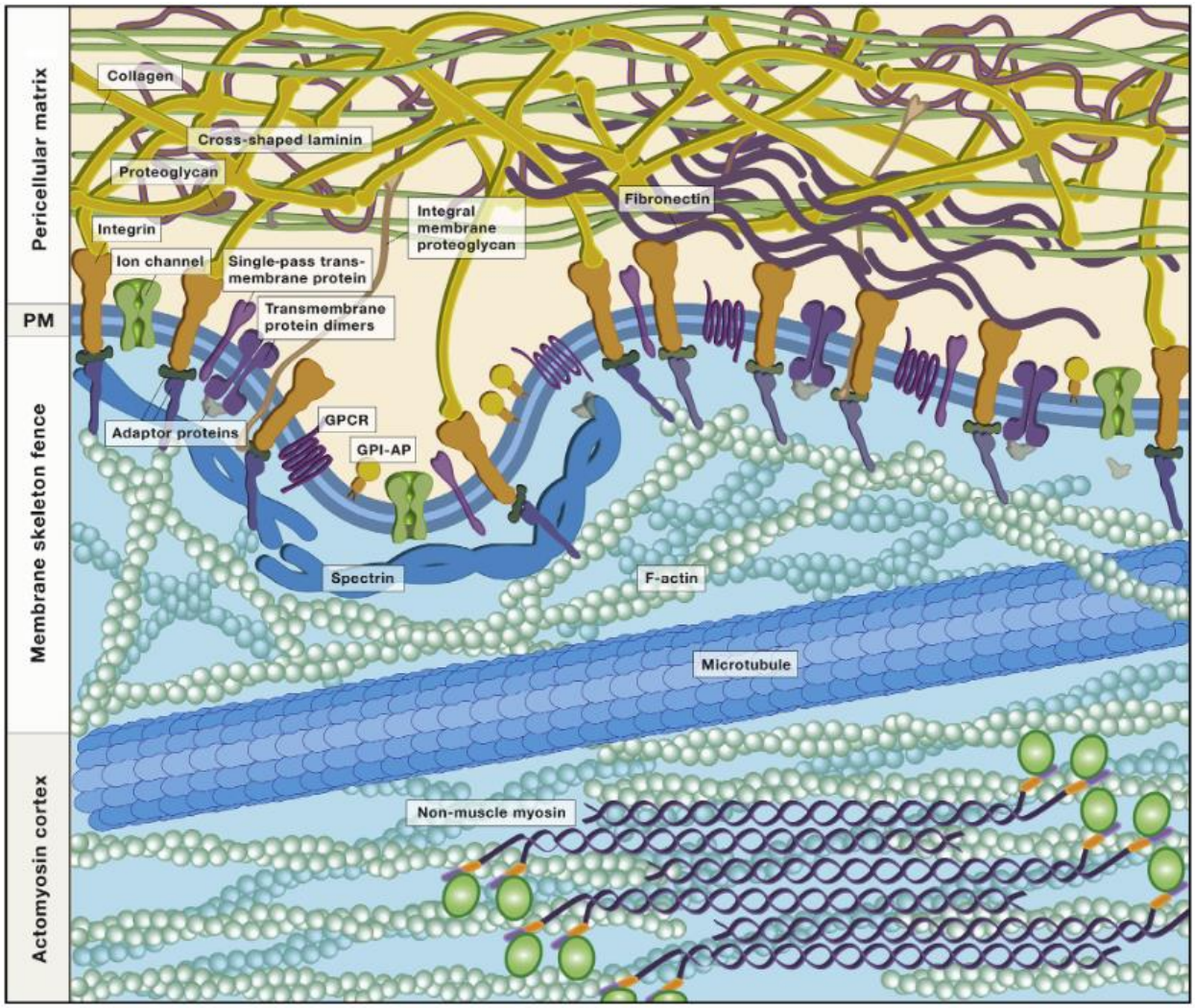

Figure 8. The plasma membrane. *Biological membrane are highly crowded structures. The density of proteins is extremely high and, according to the picket fence model which has been the main model to explain the regulation of surface diffusion, there is a continuum of connectivity between the extracellular matrix and the cytoskeleton. Adapted from (Jacobson et al., 2019).*

5.3 Regulatory mechanisms of NMDAR surface trafficking

Surface NMDARs do not exhibit unrestricted Brownian motion at the cell surface. Although biological membranes are classically pictured with low protein content, it is important to consider that the plasma membrane is filled with thousand of proteins with little remaining free lipid spaces (Engelman, 2005; Ryan et al., 1988) (figure 8). Several studies have estimated the protein density in biological membranes to be around 30,000 proteins per µm (Jacobson et al., 2019). This notion is further strengthened by recent profiling of neuronal surfaceome (i.e. total surface protein), with

an average of 1,000 protein families present at the surface of cortical neurons (Herber et al., 2018; Van Oostrum et al., 2020). The measured surface diffusion of both membrane proteins and lipids in biological membranes is lower than in reconstituted membranes, thus further indicating the presence of constraints, such as passive obstacles or active binding partners, that limit the free diffusion of membrane macromolecules(Choquet and Triller, 2013; Jacobson et al., 2019). The anchored picket fence has been a model to explain the regulation of lateral diffusion in biological membranes (Kusumi et al., 2012). Schematically, it is likely that there are multiple regulatory processes between the extracellular matrix and the intracellular cytoskeleton (fences), connected with transmembrane proteins (pickets), that segregates the membrane into subdomains (2-300 nm) where the local composition, organization and dynamic will differ from the average membrane properties. In neurons, neurotransmitter receptors are concentrated in the postsynaptic density (PSD), a protein-rich subdomain located at the inner surface of the postsynaptic neuronal membrane in front of the presynaptic site. They are also present extrasynaptically in the form of extrasynaptic clusters. Once inserted at the neuronal membrane, receptors will randomly laterally diffuse within the membrane plane, and eventually enter synapses. They alternate between different surface dynamics behaviors depending on the membrane subdomains: strongly confined diffusion within PSD when anchored to scaffold proteins, highly diffusive with low confinement in the extrasynaptic membrane, and confined diffusion within small extrasynaptic protein domains.

Driven by thermal agitation and reversible binding to intracellular, transmembrane, or extracellular components, receptors constantly alternate between mobile and immobile states (Choquet, 2018; Groc and Choquet, 2020) (figure 9). As an example, only 20 to 50% of surface NMDAR are mobile, with GluN3A-containing NMDAR being more mobile than GluN2B-containing NMDAR, which are in turn more mobile than GluN2A-containing NMDAR (González-González et al., 2023; Groc et al., 2006b; Kortus et al., 2023).

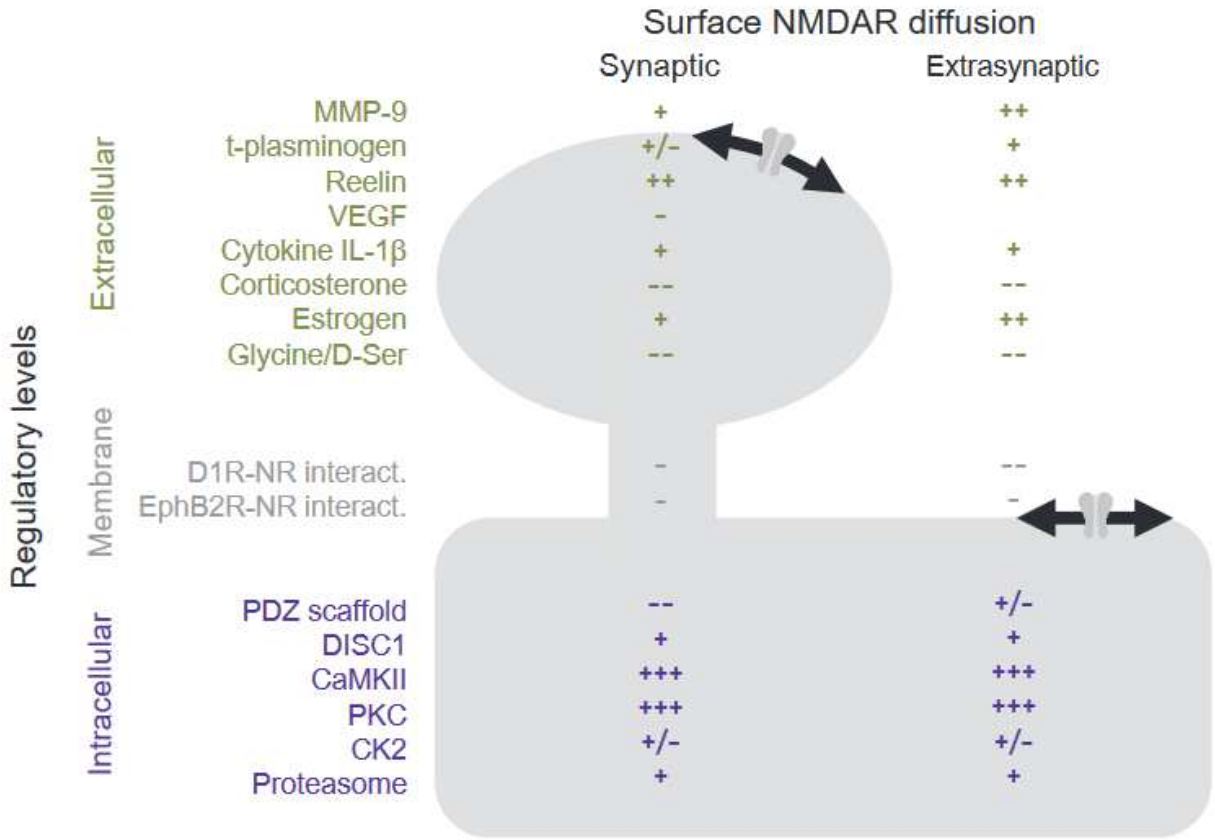

Figure 9. NMDAR membrane organization and lateral diffusion A. Example of the main known intracellular, transmembrane, and extracellular modulator of NMDAR surface diffusion. Adapted from (Dupuis et al., 2023).

5.3.1 Intracellular modulators

NMDAR interact with a large variety of molecules through their CTDs (Dupuis et al., 2023). Typically, their interaction with MAGUKs proteins, which are highly enriched at the PSD, are accepted to be responsible for the synaptic anchoring of NMDARs (Bard et al., 2010). Furthermore, several kinases, such as protein kinase C (PKC) and CaMKII, have been shown to modulate the membrane diffusion of NMDARs either through their activity (e.g. post-translational modifications) and/or through direct binding (Dupuis et al., 2014b; Ferreira et al., 2020; Groc et al., 2004). The proteasome as well as disrupted in schizophrenia (DISC1) also modulate the surface diffusion of NMDARs (Espana et al., 2021; Ferreira et al., 2021).

5.3.1 Extracellular modulators

The extracellular environment is well-known to potently modulate NMDAR surface trafficking (Dupuis et al., 2023). NMDAR surface dynamics is regulated by components of the extra-cellular matrix (ECM), a network of proteins and carbohydrates that surrounds every cell, such as reelin, the matrix metalloproteinase 9 (MMP-9) or the tissular-plasminogen (tPA), but also hormones (corticosterone and estrogen) (Groc et al., 2008; Mikasova et al., 2017; Potier et al., 2016), amino acids such as the co-agonists glycine and D-serine (Ferreira et al., 2017; Papouin et al., 2012), as well as pathological molecules such as auto-antibodies directed against the NMDAR (Hunter et al., 2024; Jamet et al., 2024; Jézéquel et al., 2017; Mikasova et al., 2012). In particular, it has been shown that reelin, a secreted glycoprotein that plays a critical role on brain development (Tissir and Goffinet, 2003) and which synaptic content increases during development, destabilizes GluN2B-containingNMDAR from synapses (Groc et al., 2007a), thus favoring the development-associated decline in GluN2B-containing NMDAR-mediated synaptic currents. Similarly, digestion of the ECM through the endopeptidase MMP-9 or tPA increase NMDAR surface trafficking (Lesept et al., 2016; Michaluk et al., 2009).

5.3.2 Transmembrane modulators

NMDAR display a large cis-interactome, composed of a variety of neurotransmitter and neuromodulator receptors, ion channels as well as adhesion molecules; reviewed in (Petit-Pedrol and Groc, 2021) (figure 10). For instance, the direct interaction between NMDARs and the adhesion molecules Neuroligin-1 and EphB2 are well known for their role on the synaptic trapping of NMDARs (Budreck et al., 2013; Dalva et al., 2000; Washburn et al., 2020). It is well accepted that the interaction between NMDAR and EphB2R, a postsynaptic cell adhesion molecule and tyrosine kinase receptor, regulate the synaptic localization and clustering of NMDARs (Dalva et al., 2000; Nolt et al., 2011; Takasu et al., 2002; Washburn et al., 2020). It has also been suggested that NMDARs interact with neurotransmitter and neuromodulator receptors at peri- and extrasynaptic sites, and that those interactions regulate the surface diffusion of the receptors, possibly leading to the local aggregation/clustering of receptors into extrasynaptic “hubs” (Petit-Pedrol and Groc, 2021).

NMDARs have been shown to interact with dopamine receptors, both D1R and D2R (Wang et al., 2012), type I mGluRs (Perroy et al., 2008), mu opioid receptors (with the GluN1 subunit but no GluN2A- or GluN2B-subunits) (Rodríguez-Muñoz et al., 2012), the sCAM EphB2 (Dalva et al., 2000) and Nlg-1 (Budreck et al., 2013), nicotinic receptors (with the GluN1- and GluN2A subunits) (Li et al., 2012; Zhang et al., 2016), the ER protein sigma 1 receptors (Sig1R) (with the GluN1 subunit in a GluN1-2A configuration) (Balasuriya et al., 2013), histamine 3 receptors (H3R) (with both GluN1 and GluN2A subunits) (Rodríguez-Ruiz et al., 2017), apolipoprotein E receptor 2 (ApoER2) (Hoe et al., 2006), interleukin-1 (IL-1) receptors (Gardoni et al., 2011; Johansson et al., 2020), purinergic (P2X) receptors (Rodriguez et al., 2020), voltage-activated potassium (BK) channels (with the GluN1 subunit) (Zhang et al., 2018), and extrasynaptically with transient receptor potential cation channel subfamily M member 4 (TRPM4) (Yan et al., 2020).

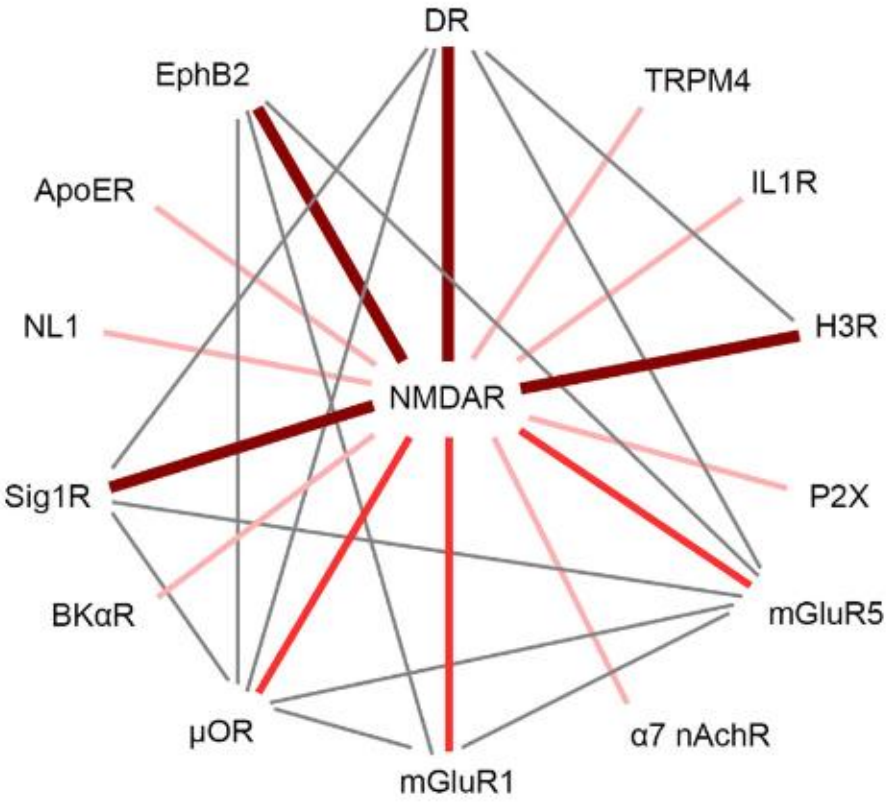

Figure 10. Known NMDAR cis-interactome. NMDAR cis-interactome comprises several neuromodulator and neurotransmitter receptors including Dopamine type I receptors and type I mGluRs (mGluR1/5), as well as sCAM such as Nlg-1 (NL1) and EphB2. Importantly, each of these surface proteins are also directly

interacting with other membrane proteins of NMDAR interactome, possibly creating assemblies or hubs of receptors at the neuronal membrane. Adapted from (Petit-Pedrol and Groc, 2021).

I will particularly emphasize on interactions dopamine type I receptors (D1Rs) and glutamate type I mGluRs (mGluR1/5) and introduce these receptors which were reported to regulate the organization of NMDARs.

5.3.2.1 D1R-GluN1-NMDAR

Dopamine (DA), one of the major brain neuromodulators, is greatly involved in motivation, reward as well as learning and memory. Dopaminergic neurons are mainly localized within the ventral midbrain, e.g. ventral tegmental area (VTA) and the substantia nigra (SN, divided into SN *pars compacta* SNc and SN *pars reticulata* SNr). Briefly, the nigrostriatal pathway, involved in motor control, originates from the SNc and projects to the striatum whereas the mesolimbinc pathways, involved in reward and motivation as well as learning and memory, originates from the VTA and projects to the prefrontal cortex, nucleus accumbens, amygdala, and the hippocampus. Of note, recent evidence also suggests the locus coeruleus (LC) to be a source of DA innervation in the hippocampus(Kempadoo et al., 2016; Takeuchi et al., 2016).

DA binds to five G-protein coupled receptors (GPCR, D1-D5), classified in two subclasses, namely D1R-like and D2R-like protein families, that display opposite signaling patways (figure 11). D1R-like protein family, composed by D1R and D5R, are coupled to Gs cytosolic proteins that stimulate the enzyme adenylate cyclace (AC), which produces cyclic adenosine monophosphate (cAMP). The latter activates the protein kinase A (PKA), which in turn activates the DA and cAMP-regulated phosphoprotein (DARPP-32) as well as cAMP response element binding protein (CREB). When phosphorylated by PKA, DARPP-32 amplifies PKA signaling by inhibiting protein phosphatase-1 (PP1). On the other hand, D2R-like receptor family comprises D2R, D3R, D4R that are coupled to Gi proteins. They inhibit PKA-mediated signaling pathways by both inhibiting AC and activating PP1.

DAR and in particular D1R and D2R are broadly expressed within the CNS, including in hippocampal and cortical regions (Bergson et al., 1995; Callier et al., 2003; Gangarossa et al., 2012; Goldman-

Rakic et al., 1989; Ladepeche et al., 2013; Levey et al., 1993; Puighermanal et al., 2017; Wei et al., 2018). In rodent frontal cortex, D1-like family receptors expression appears during embryonic development and steadily increases during brain development, with higher levels of D1R than D5R (Araki et al., 2007; Sillivan and Konradi, 2011); see also Annex 1, extracted from (Van Oostrum et al., 2020). In the human hippocampus, D1R is already expressed in neonates, and its expression steadily increases during development, reaching maximum levels in adulthood (Rothmond et al., 2012). D2R is mainly expressed in the dentate girus in mossy cells whereas D1R expression is widespread, and is expressed in interneurons (GAD67) as well as pyramidal neurons (Gangarossa et al., 2012).

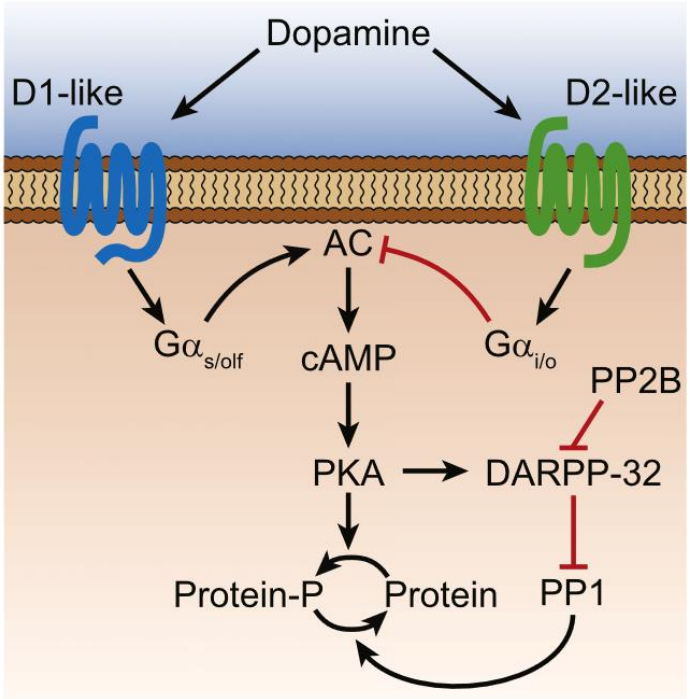

Figure 11. Canonical D1R-like and D2R-like signaling pathways. *D1R activation triggers the activation of PKA and DARPP-32 while D2R activation triggers their inhibition. Adapted from (Tritsch and Sabatini, 2012).*

It is accepted that DA, through its action on D1Rs, potentiate NMDAR signaling (Cepeda et al., 1993, 1992; Cepeda and Levine, 2012; Chen et al., 2007; Otmakhova and Lisman, 1996; Varela et al., 2009). The D1R activation enhances the surface expression of NMDAR as well as their function (Dudman et al., 2003; Hallett et al., 2006; Hu et al., 2010; Lau and Zukin, 2007; Li et al., 2010;

Tingley et al., 1997), favoring the NMDAR-dependent LTP of excitatory glutamate synapses (Otmakhova and Lisman, 1996). Reciprocally, NMDAR activation favors D1R surface expression and signaling (Navakkode et al., 2007). This neuromodulatory-neurotransmission is thought to rely on intracellular cascades involving protein kinases, with the most proeminent being PKA and DARPP-32 that can phosphorylate the GluN1 subunit of NMDAR as well as Fyn (a member of the Src family kinases, SKF) that phosphorylates the GluN2B subunit of NMDAR. Also, D1R and NMDARs can directly interact through their CTDs, and that this interaction can modulate their surface expression, membrane trafficking, and receptors signaling independently of PKA or PKC cascades (Andrianarivelo et al., 2021; Cahill et al., 2014; Fiorentini et al., 2003; Ladepeche et al., 2013; Lee et al., 2002; Nai et al., 2010; Pei et al., 2004; Scott et al., 2002), reviewed in (Wang et al., 2012). Although D2Rs interact with the non-obligatory GluN2B subunit of NMDARs, I will focus here exclusively on the interaction between D1R and NMDARs. D1Rs interact with the obligatory GluN1 subunit and with the non-obligatory GluN2A-subunit through theirs T2 and T3 domains, respectively (figure 12). The T2 domain, that bears negative charges, interacts with the cassette C1 (D864-T900) on GluN1 CTDs which bears three arginin residues (positively charged) via electrostatic interactions (Woods et al., 2005). Furthermore, the phosphorylation of D1R-CTD at serine 397 by casein kinase 1 have been suggested to increase the interaction between GluN1 subunit and D1R (Woods et al., 2005). Of note, both the non-obligatory GluN2-subunits and D1R have been suggested to interact with PSD-95 (Bard et al., 2010; Ladepeche et al., 2013). It has been shown that both GluN1 subunit and PSD-95 interaction domain with D1R are overlapping, thus suggesting that PSD-95 limits D1R-GluN1-NMDAR interaction (Zhang et al., 2009).

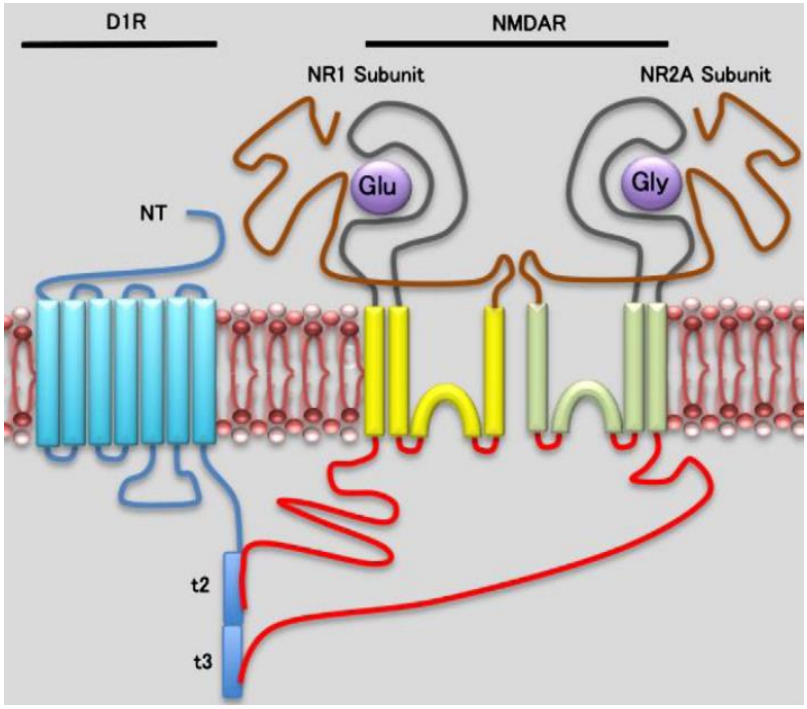

Figure 12. D1R-NMDAR interaction. *D1R interacts directly with NMDAR via electrostatic interactions involving their CTDs. The T2 domain of D1R interact with the CTD of the obligatory subunit GluN1-NMDARs and the T3 domain, located on D1R CTD, interact with non-obligatory GluN2A subunit. Adapted from (Wang et al., 2012).*

The D1R-NMDAR interaction through the T2 domain reduces NMDAR-dependent excitotoxicity via PI3-kinase signaling, independent of changes in calcium influx (i.e. a non-ionotropic regulatory mechanism), whereas D1R-NMDAR interaction through the T3 domain inhibits NMDAR currents (Lee et al., 2002). Reciprocally, in primary hippocampal culture, NMDAR-D1R interaction were shown to increase D1R surface level and activity, i.e. cAMP accumulation (Pei et al., 2004; Scott et al., 2002). Moreover, D1R-NMDAR interaction significantly alters NMDAR surface trafficking and membrane localization, favoring the retention of NMDAR at peri-/extra-synaptic locations (Ladepeche et al., 2013). They observed that activating D1R resulted in the disruption of complex, allowing NMDARs to enter synapses which resulted in an increased synaptic signaling Although this interaction was first characterized in heterologous systems (e.g. HEK cells, following the transfection of both NMDAR and D1R), it has been shown that disrupting D1R-NMDAR complexes, by infusing competing peptide directly in the hippocampus, is sufficient to selectively alter working memory in mice without affecting motor function nor motivation (Nai et al., 2010), further strengthening the hypothesis that direct interaction between membrane receptors participate in the regulation of neuronal activity. Note that discrepancies have been observed, depending on the brain regions, i.e. hippocampus or striatum, and the pathophysiological context on the D1R-NMDAR regulatory processes (Andrianarivelo et al., 2021; Cahill et al., 2014).

5.3.2.2 mGluR-GluN1-NMDAR

Metabotropic glutamate receptors (mGluR) are glutamate receptors of the GPCR family. They structurally differ from other GPCRs because of their large clamshell-like ligand binding domain (LBD) that is linked to the 7-helix transmembrane domain with a cysten-rich domain (CRD). mGluRs are widely accepted to modulate synaptic transmission and plasticity (Reiner and Levitz, 2018). mGluRs are divided in three groups based on sequence homology, second messengers and pharmacological properties (Ferraguti and Shigemoto, 2006). Type I mGluRs are composed by mGluR1 and mGluR5, type II mGluRs are composed by mGluR2 and mGluR3, and type III are composed by mGluR4 and mGluR6-8. Both type II and type III mGluRs are coupled to Gi cytosolic protein whereas type I mGluRs are coupled to Gq cytosolic proteins. Although it is accepted that mGluRs work as homodimers, recent studies have highlighted heterodimerization of mGluRs. Type I mGluRs can make heterodimers within their group whereas type II and type III mGluRs can heterodimerize between the two groups. Furthermore, it has been shown that mGluRs can heterodimerize with other GPCRs, such as dopamine type I receptors (Sebastianutto et al., 2020).

Type I mGluRs display a complementary expression profile in the brain, with mGluR5 being the predominant form in the hippocampus (Ferraguti and Shigemoto, 2006; Romano et al., 1995) (figure 13). mGluR5 are encoded by a single gene (*Grm5*), and are present in 2 isoforms, namely mGluR5a and mGluR5b. mGluR5a isoforms are highly expressed early during postnatal development whereas mGluR5b are predominant in the adult brain (Minakami et al., 1995). Type I mGluRs are considered as mainly postsynaptic while type II and type III are mainly localized presynaptically (Bodzęta et al., 2021). Type I mGluRs are localized at the vicinity of the PSD (Scheefhals et al., 2023). Type I mGluRs have been shown to directly interact with NMDARs through their CTDs, and this interaction has been proposed to be a form of homoestatic control of synaptic excitability (Moutin et al., 2012; Perroy et al., 2008). Briefly, type I mGluRs and NMDARs can also interact indirectly through scaffolding proteins (e.g. Homer). The constituively expressed long Homer isoform (Homer1b/c) contain a C-terminal coiled-coil multimerization domain that enable its coupling with other scaffolding proteins (e.g. SHANK), allowing the formation of large multiprotein assembly (Hayashi et al., 2009). However, sustained activation of NMDAR triggers the expression of Homer1a (Brakeman et al., 1997; Moutin et al., 2012), a short Homer isoform that

is lacking the multimerization domain, that lead to the disruption of the scaffolding protein complex (Aloisi et al., 2017; Moutin et al., 2012; Perroy et al., 2008) and to mGluR-NMDAR interaction, thus leading to their autoinhibition (Moutin et al., 2012; Perroy et al., 2008).

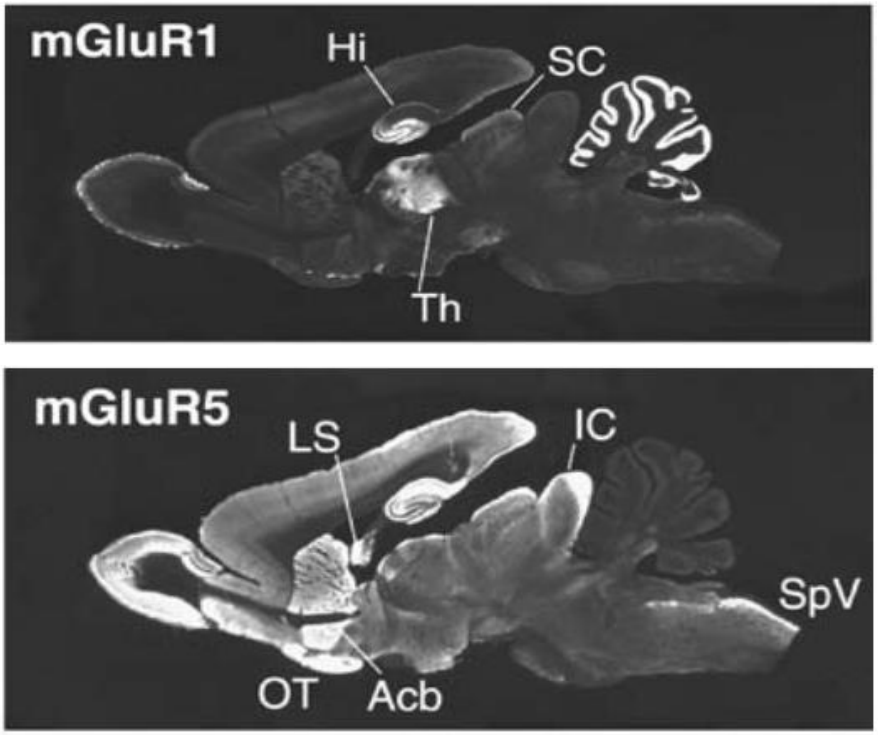

Figure 13. Distribution of the postsynaptic type I mGluRs. *mGluR1 and mGluR5 have a complementary expression profile in the brain. Main olfactory bulb (MOB), Hippocampus (Hi), superior colliculus (SC), lateral septum (LS), accumbens nucleus (Acb), inferior colliculus (IC), spinal vestibular nucleus (SpV). Adapted from (Ferraguti and Shigemoto, 2006).*

The mGluR1/5 are mainly coupled to Gq protein. Gq activates the phospholipase C that leads to the release of calcium from the intracellular stores and/or through voltage-gated calcium channels (VGCCs), and finally results in the activation of PKC (figure 14). mGluR1/5 have also been shown to activate other effectors such as PI3K-mTOR and ERK signaling, Cdk5, as well as casein kinase 1 (CK1) (Chergui et al., 2005; Hou and Klann, 2004; Liu et al., 2002, 2001). In particular, it has been shown that type I mGluR-driven intracellular calcium increase triggers the activation of Calcineurin which dephosphorylate autoinhibitory phosphate onto CK1 CTD, and leads to the transient activation of CK1 (Liu et al., 2002).

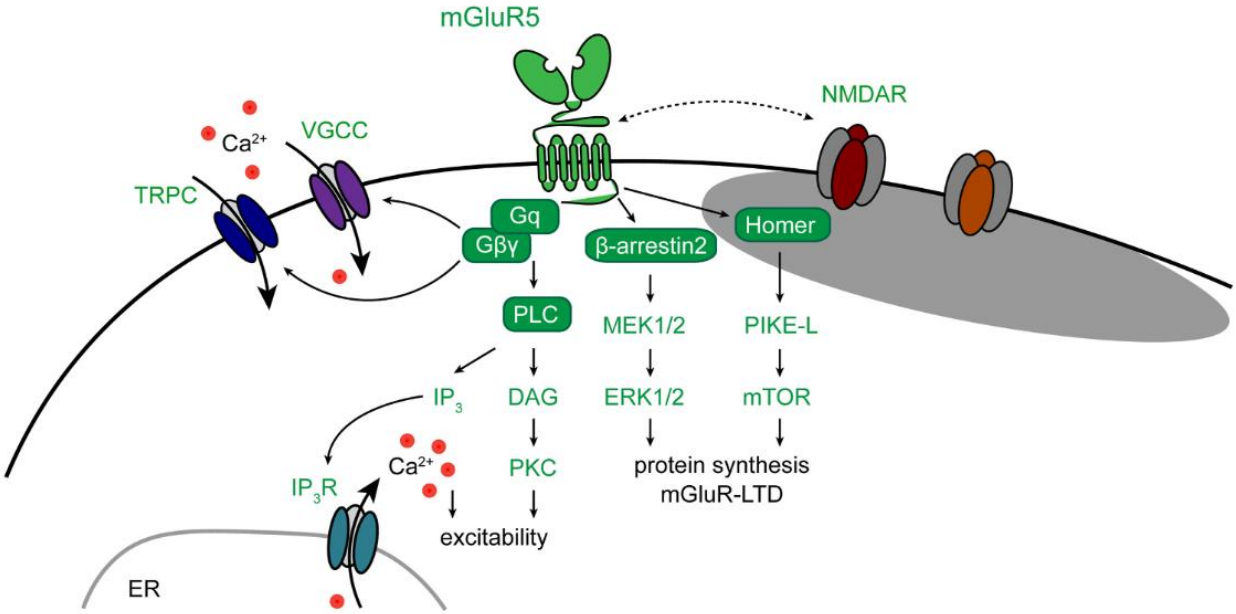

Figure 14. Main mGluR5-signaling pathways. *mGluR5 are Gq-coupled GPCR. They canonically activate the phospholipase C (PLC) and protein kinase C (PKC) that triggers an increase in the calcium concentration. mGluR5 also triggers signaling pathways through arrestin and homer that activate ERK and mTOR-signaling pathways, respectively. Adapted from (Bodzęta et al., 2021).*

mGluR1/5 are well-known for enhancing postsynaptic excitability, and in particular ion channels as well as NMDAR-evoked responses. Moreover, mGluRs have been implicated in different forms of plasticity. mGluR5s are involved in NMDAR-dependent LTP, either by priming the induction of LTP or by supporting LTP by favoring protein synthesis (Balschun and Wetzel, 2002; Bashir et al., 1993a; Neyman and Manahan-Vaughan, 2008). On the other hand, selective stimulation of mGluRs, or low frequency stimulation, is sufficient to induce NMDAR-independent LTD (Bashir et al., 1993b; Lüscher and Huber, 2010).

6. Methods to investigate protein-protein interactions (PPI).

6.1 Biochemical approaches

6.1.1 Co-immunoprecipitation

Co-immunoprecipitation (coIP) was originally adapted from affinity chromatography, a technique traditionally used in protein purification. CoIP relies on the interaction between a matrix-bound molecule (in this case, an antibody coupled to agarose or sepharose beads) and a target protein present in a protein homogenate or cell lysate (Kaboord and Perr, 2008; Lin et al., 2024). Nonspecifically bound proteins are washed away using detergents and/or appropriate salt concentrations. Finally, the proteins of interest are eluted and further analyzed, typically using Western blot or mass spectrometry. The combination of coIP and mass spectrometry is a powerful tool for discovering new putative interactions (Larance and Lamond, 2015; Trinkle-Mulcahy et al., 2008; Yang et al., 2008). However, interactions detected by coIP may result from either direct binding or indirect interactions mediated by cofactors. Additionally, weak and/or transient interactions, such as those typically occurring between surface receptors, are difficult to detect using coIP (Kusumi et al., 2012).

6.1.2 Proximity-dependent labeling approaches

Proximity-dependent labeling strategies use enzymes that are fused to a protein of interest (bait), to produce reactive molecules that covalently bind to neighboring proteins (putative interactors) (Roux et al., 2012). Alternatively, fusing the enzyme to a minimal targeting motif (such as a GPI anchor) can be employed to map the protein population in a specific compartment (Rhee et al., 2013). Labeled candidate interactors can then be purified using coIP/affinity chromatography and analyzed by Western blot or mass spectrometry. These approaches enable the targeting/biotinylation of endogenous proteins. However, they rely on the expression of a recombinant protein fused to the enzyme, which may affect the localization, surface trafficking, and/or function of the protein of interest. Notably, these technologies provide a snapshot of potential protein-protein interactions (PPI) but cannot be used to study the dynamics of PPIs. BioID / TurboID methods are based on a promiscuous biotinylation of protein (on lysine residues) by a

mutated BirA within a range of ~10 nm. The biotinylation kinetics of these enzymes is slow (ranging from minutes to hours), which limits their usefulness in discovering binding partners (Kim and Roux, 2016). Split-TurboID have been used to map the surface proteome at the neuron/astrocytes interface in vivo (Takano et al., 2020). Peroxidase-based method (engineered ascorbate peroxidase, APEX and horse radish peroxidase, HRP) are based on a promiscuous biotinylation of proteins (on tryptophan and tyrosine residues) in presence of tyramine derivatives and hydrogen peroxide (H_2O_2), within a radius of 20 – 40 nm (Kim and Roux, 2016). These two methods are best suited for investigating surface proteins due to the low membrane permeability of tyramide (e.g. non-permeant tyramide) (Shuster et al., 2022). The biotinylation kinetics of those enzymes is high (~sec to min). However, the use of hydrogen peroxide makes their application *in vivo* challenging. This strategy has been recently used to investigate the surface nano-organization of NMDAR-surface "proximitome" in primary hippocampal neurons (Jamet et al., 2024). They uncovered that the surface organization of NMDAR interactome, referred as surface protein interactome of NMDAR, was greatly altered after incubation of aNMDAR-AAb at both synaptic and extasynaptic compartments (Jamet et al., 2024).

6.2 Fluroescence imaging approaches

Fluorescence imaging approaches allow to visualize PPI in real time and in living samples, thus enabling to determine where and when PPIs are occurring.

6.2.1 Resonance Energy Transfert (RET) techniques

The principle of resonance energy transfert (RET) consists in a non-radiative transfer of energy from a donor, that is in an excited state, to an acceptor (figure 15) (Jones and Bradshaw, 2019). The donor and the acceptor can either be fluorescent proteins (fluorescence RET, FRET) or the donor is an enzyme that catalyzes a substrate that becomes bioluminescent (bioluminescence RET, BRET) (Wu and Jiang, 2022). When the donor and the acceptor interact, because of the distance-dependent energy transfert, the emission of the donor reduces whereas the one of the acceptor increases. Importantly, the energy transfert between the donor and the acceptor is inversely proportional to the sixth power of the distance between them, and typically occurs when

they are less than 10 nm apart. Because of its high dependency to the distance between the donor and the acceptor, which largely exceeds the diffraction limits in conventional microscopy (200 – 300 nm), RET have been described and used as a molecular nanoruler (Anton et al., 2022). However, both FRET and BRET generally requires the overexpression of recombinant proteins that are fused to donor or acceptor molecules, usually within the C or N-terminal regions. It is important to consider that both the trafficking and activity of the proteins of interest can be significantly affected by the grafting of donor/acceptor molecules and by overexpression.

6.2.1.1 FRET

In FRET the donor and the acceptor are fluorescent proteins. Beside the distance between the donor and the acceptor (figure 15), several parameters must be filled for FRET to occur: (1) the degree of spectral overlap between the donor and the acceptor i.e. the emission spectra of the donor fluorescent protein must overlap with the excitation spectra of the acceptor fluorescent protein (figure 15), (2) the dipole orientation angle between the donor and the acceptor (ideally, there are parallel to one another), (3) the quantum yields of the donor i.e. the ratio of photos emitted per photons absorbed. Typical FRET couples are CFP (λ peak excitation = 430, λ peak emission = 475) with YFP (λ peak excitation = 513, λ peak emission = 527), or GFP (λ peak excitation = 488, λ peak emission = 507) with mCherry (λ peak excitation = 587, λ peak emission = 610) (Algar et al., 2019; Bajar et al., 2016; Greenwald et al., 2018) (figure 15).

Several methods can be used to measure FRET, including the acceptor/donor emission ratio, fluorescence recovery after photobleaching of the acceptor, and fluorescence lifetime imaging (FLIM) (Algar et al., 2019). Briefly, acceptor/donor emission ratio consists in measuring the fluorescence intensity of the acceptor when exciting the donor. This method is however largely limited by spectral bleed through (excitation of the acceptor when exciting the donor due to the wideness of the emission and excitation spectrum of the fluorescent molecules) and is highly concentration dependent. Fluorecence recovery after photobleaching of the acceptor consists in measuring the increase in fluorescence intensity of the donor as a result of the bleaching of the acceptor. This method is limited by the cell damages, and bleaching of the donor iself can occur. Furthermore, the temporal resolution of this technique is low. On the other hand, FLIM

measurements are not affected by spectral bleed through, differences in concentration, nor variance in intensity excitation. The fluorescence lifetime is the time a molecule resides in the excitate state S1 before relaxing to the ground state S0 through the emission of photon. When FRET occurs, the fluorescence lifetime of the donor is reduced.

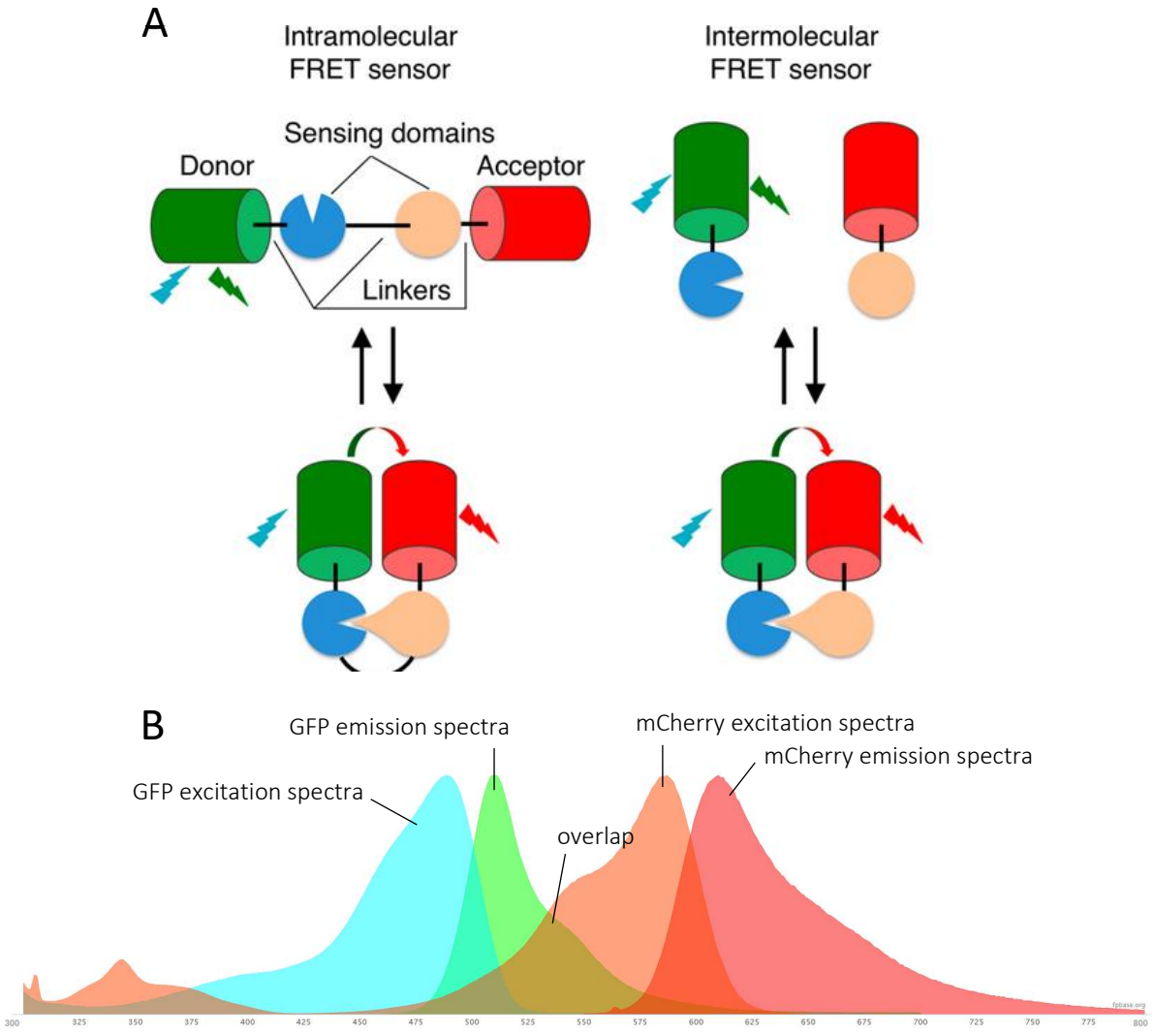

Figure 15. Föster resonance energy transfer (FRET) principle. *FRET imaging is one the main techniques to investigate protein-protein interaction in live cells. The proteins of interest are fused to a donor (e.g. GFP) and acceptor (e.g. mCherry) in the case of intermolecular FRET, or they are fused onto the same molecules (intramolecular FRET, e.g. activity sensor, for example). During FRET, the donor is excited and if an acceptor is its close proximity (within 10 nm radius), a transfert of energy might occur. Adapted from (Bajar et al., 2016). B. The emission spectrum of the donor and the excitation spectrum of acceptor must overlap, as shown for GFP and mCherry, for FRET to occur (created with fpbase).*

6.2.1.1 BRET

BRET involves an enzyme as donor, e.g. luciferase, that catalyzes the oxidation of a substrate that become bioluminescent (Pfleger et al., 2006). When the acceptor molecule is in close proximity (within 10 nm), energy transfer to the acceptor (a fluorescent protein, e.g. YFP or GFP) can occur. The substrates used in BRET are classicaly hydrophobic compounds that can cross biological membranes, thus allowing to use BRET in live cells (Borroto-Escuela et al., 2013).

6.2.2 Protein Fragment Complementation or bimolecular fragment complementation

Bimolecular fragment complementation (BiFC) was first described in *Escherichia coli* based on the observation that fluorescent proteins, such as GFP, can be fragmented into two non-fluorescent N- and C-terminal fragments that can re-fuse and become fluorescent again (Ghosh et al., 2000). However, BiFC is irreversible (i.e. the fused fragments cannot be fragmented again) and therefore, BiFC cannot be used to study interaction dynamics. Furthermore, the splitted fragments easily reassociate, easily generating false positives when the concentrations of the proteins are high. BiFC have been successfully used to identify specific synaptic connections (e.g. GRASP system) between individual neurons in culture as well as *in vivo* (Choi and Kaang, 2022; Choi et al., 2018; Druckmann et al., 2014; Feinberg et al., 2008; Kim et al., 2012).

6.3 Proximity ligation assay

Proximity ligation assay (PLA) is an antibody-based method, and follow the same principle (e.g. incubation with primary antibodies directed against the proteins of interest followed by the incubation with secondary antibodies). Secondary antibodies are conjugated to complementary oligonucleotides. If the two secondary antibodies are in close contact (within 16 nm), a circle-forming DNA oligonucleotide, known as PLA secondary probe, can hybridize and be ligated. The nucleotides are then amplified and finally labeled with a detection probe (Söderberg et al., 2008, 2006) (figure 16). PLA have been used to investigate PPIs in cell culture and slices, including D1R-GluN1-NMDAR complexes (Andrianarivelo et al., 2021; Cahill et al., 2014) (figure 16). Importantly,

the performance of PLA critically relies on the quality of primary antibodies, which is notoriously very low for extracellular-targeting of both the endogenous GluN1 subunit of NMDAR and D1R. Consequently, PLA-based investigations of D1R-GluN1-NMDAR interaction have been performed on fixed and permeabilized samples. Furthermore, PLA does not enable to investigate surface specific and dynamic interactions between D1R-GluN1-NMDAR.

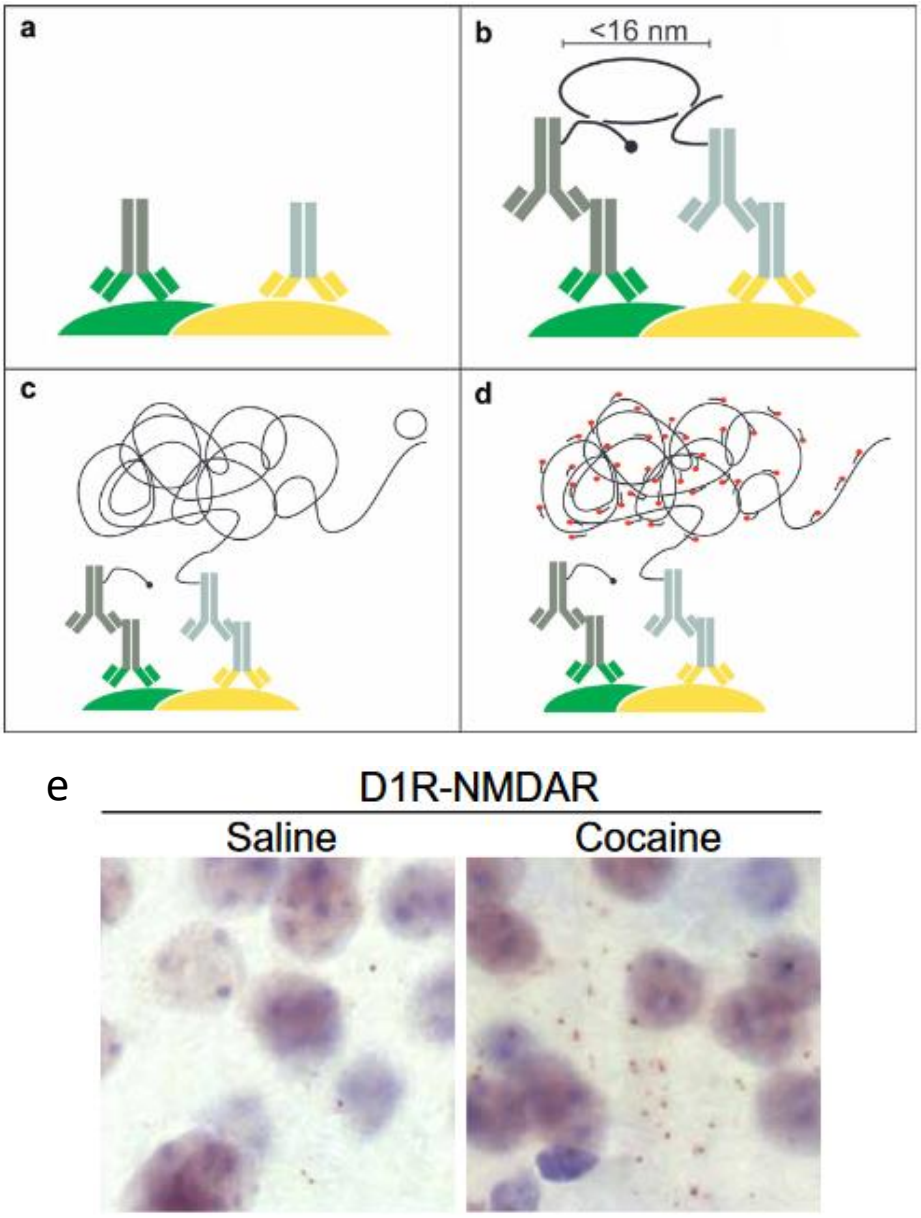

Figure 16. proximity ligation assay (PLA) allowed to investigate the interaction between GluN1-NMDAR and D1R. *(A-D) Experimental workflow. PLA is an antibody-based method. The first steps are similar to conventional immunohistochemistry experiments e.g. incubation. B. Following the incubation with*

secondary antibodies, which are conjugated with a short DNA strand, a PLA secondary probes is added e.g. a DNA strand that can hybridize ans ligate the short DNA strands of the secondary antibodies if they are closer than ~ 16 nm. (C) The resulting circle-forming DNA nucleotides is amplified by a DNA polymerase and then (D) labeled. E. PLA have been used to investigate the interaction between D1R and GluN1-NMDAR in both cultures and tissues. Indeed, using PLA (Andrianarivelo et al., 2021) have clearly demonstrated that D1R-GluN1-NMDAR is quantatitevly increased in the striatum in mice following exposure to cocaine. Adapted from Adapted from (Andrianarivelo et al., 2021; Trifilieff et al., 2011).

6.4 Single Particle tracking (SPT)

The propensity of receptors to form complexes have been mainly obtained with biochemical approaches, proximity ligation assay, and live imaging approaches such as RET (FRET, and BRET) which, in comparison with the other mentioned methods, have the advantage of analyzing receptor oligomerization in live cells (Dorsch et al., 2009; Milligan and Bouvier, 2005; Petit-Pedrol and Groc, 2021). These methods usually require high expression levels of protein, which could interfere with the surface trafficking of the protein, and are based on average measurements of entire population of receptors, thus limiting our understanding of the occurrence, stability, and dynamics of PPI at single molecule/receptor level. The possibility to target surface interactions in native environment is highly limited. Thus, despite extensive evidence supporting the formation of surface receptor oligomers in heterologous cell system using mainly biochemical approaches, the existence of such protein complexes have remained controversial (Frederick et al., 2015; Pin et al., 2007).

To resolve controversies on the existence of weak and low-affinity receptor oligomerization, extensive efforts have been made in the field, over the past decade, to directly monitore receptor-receptor interaction and fully characterize monomer-dimer equilibrium under physiological conditions. The random collision between two receptors results in the formation of a very short-lived encounter complex, which can either dissociate or convert into a productive complex upon “true” interaction. The latter is associated with molecular rearrangements and the formation of non-covalent chemical bonds between the two receptors (Tam et al., 2022; Waugh, 1954). Thanks to the development of SPT imaging techniques which allow to track the movement of single receptors at the cell surface (see also Chapter 1.5.2.3), it has been possible to directly observe events where receptors get in close proximity (e.g. within an interacting range) through either

intensity or distance measurements. Pioneer studies using fluorescent ligands as receptor-labeling strategy have been able to directly observe association and dissociation events of homodimers of GPCR at the surface of CHO cells, thus highlighting the dynamic and stochastic nature of receptor oligomerization (Hern et al., 2010; Kasai et al., 2011). Highly diffusive receptors were associating in dimers, with a lifetime of interaction varying between 91 ms for N-formyl peptide receptor (FPR, 37 °C) to 700 ms for muscarinic M1 receptor (21 °C), and dissociating continuously, with only a fraction of receptors (30 – 40 %) involved in homodimer complexes at a given time (Hern et al., 2010; Kasai et al., 2011). Importantly, the estimated average lifetime was, in both conditions, longer than the lifetime of random collision, strengthening the view of transient specific oligomerization events. Such methodology is however not easily exportable to all surface receptors and, more importantly, the use of modified ligands could interfere with both the biology as well as the trafficking of the receptors. Moreover, such approach only allowed to study receptor homodimerization in ligand-free receptors. Some of the above-mentioned limitations have been overcome by the development of SPT imaging approach using SNAP-tag technology (Calebiro et al., 2013; Tabor et al., 2016). In this system, surface exogeneous receptor containing a SNAP-tag (20 kDa) are covalently labeled with an impermeant organic fluorophore and tracked at the cell surface (Gautier et al., 2008). They further confirmed the highly dynamic nature of the membrane interactions. GPCRs were highly dynamics, associating and disassociating at high rates (figure 17). The propensity in forming oligomers was receptor-dependent. Around 80% of the β1-adrenergic receptors were in a monomeric state whereas it falled down to 20% of the receptors when imaging β2-adrenergic receptors (Calebiro et al., 2013). The use of single-particle tracking (SPT) to investigate protein-protein interactions (PPI) faces however several limitations. To achieve a deeper understanding of receptor dynamics, it is crucial to monitor receptors over extended periods. However, this is often impeded by the limited stability of organic fluorophores, which are susceptible to photobleaching. Recent advancements in techniques such as DNA-PAINT have shown promise in extending molecular tracking (Niederauer et al., 2023). Previously, dynamic studies of PPIs have primarily focused on single-color imaging (Calebiro et al., 2013; Hern et al., 2010; Kasai et al., 2011; Tabor et al., 2016), thus limiting investigations to homodimerization. It is now possible to simultaneously track two distinct protein species -such as a GPCR and its associated G-protein- within live cells (Sungkaworn et al., 2017). This breakthrough paves the way for exploring receptor heterodimerization in real-time. It can be noted that low labeling density is

a prerequisite for SPT (*see also chapter 1.5.2.3*). However, the ability to observe interaction events, highly depends on the density of labeling. Increasing the number of labeled receptors can dramatically impair the quality of the reconstruction whereas reducing the degree of labeling improves the localization and tracking but reduces the probability in observing oligomerization events (Scarselli et al., 2016). Subsequently, these approaches have been limited to simplistic cell model, e.g. heterologous cell lines such as chinese hamster ovary (CHO) cells that display a rather flat shape and are easy to manipulate i.e. where the experimentators can "easily" control the concentration of receptors per cell area.

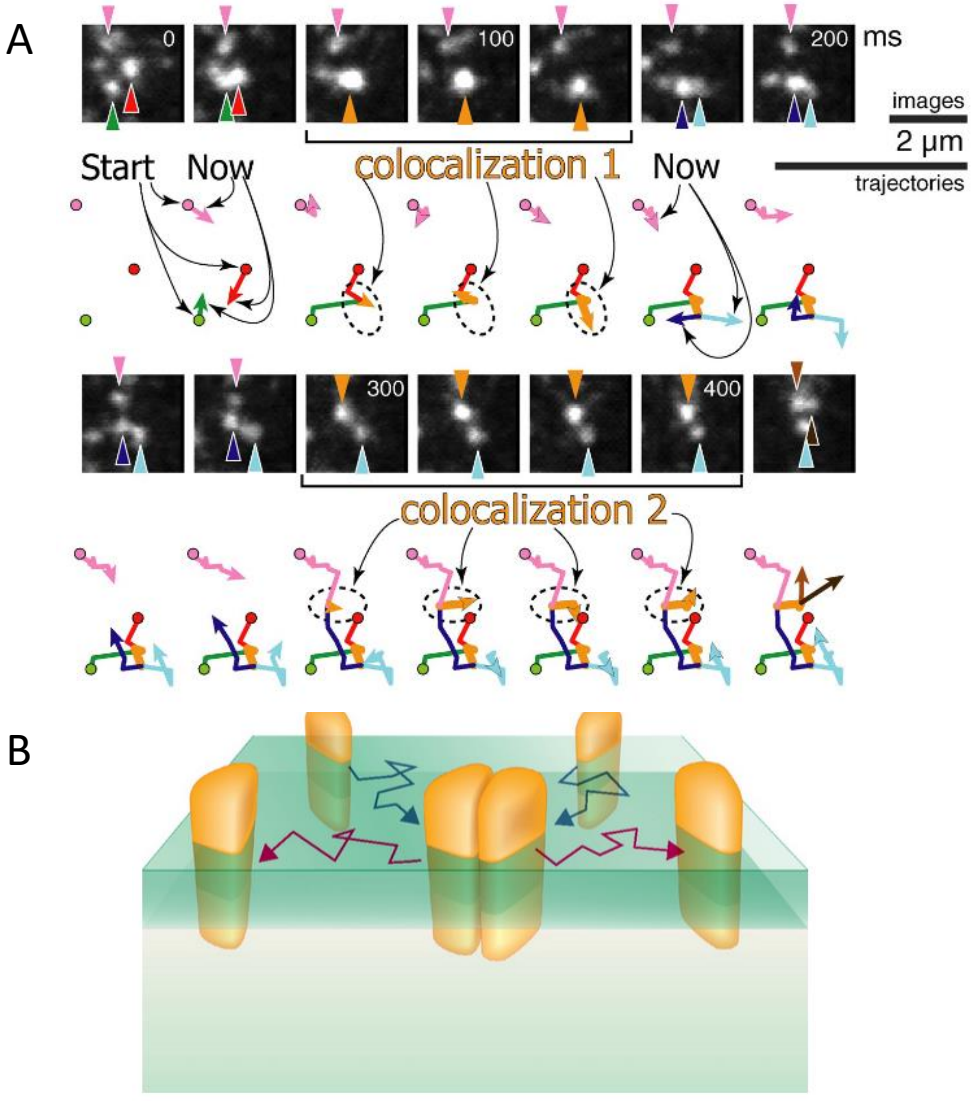

Figure 17. SPT-based investigation of GPCR membrane dynamics. *A-B. GPCRs have long been proposed to form oligomers at the cell surface. Thanks to the development of single particle tracking methods, it has*

been observed that surface GPCRs, herein the N-formyl peptide receptors, are highly mobile at the cell surface. It has been confirmed that GPCRs associate and dissociate continuously, in a ON and OFF manner. Adapted from (Kasai et al., 2011; Scarselli et al., 2016).

.

Chapter 2. The chemical synapse

Glutamatergic synapses are asymmetric intercellular junctions between a neuronal presynaptic terminal and a postsynaptic compartment that allow to transfer signals from the pre- to the postsynaptic side through the synaptic cleft (~20 nm). In vertebrates, the formation of synapses or synaptogenesis occurs during a protracted period. Synaptogenesis starts in the embryo and extend during the postnatal period to the adult period. Synapse turn over (i.e. formation and elimination) also occurs in the adult brain at high rates (Attardo et al., 2015; Pfeiffer et al., 2018).

1. Synapse organization

1.1 The presynaptic compartment

The presynaptic compartment is a specialized region of the neuronal axon, either localized at the axon terminal, known as a terminal bouton, or along the axonal shaft and known as *en passant* bouton. The presynaptic compartment is made by three main blocks: (1) synaptic cell adhesion molecules (sCAMs) that link the pre- and post-synaptic compartments together, (2) an active zone (AZ) cytomatrix, made of scaffold proteins that trap voltage-gated calcium channels (Cavs) and synaptic vesicles (SVs), and (3) the machinery for neurotransmitter release (figure 18).

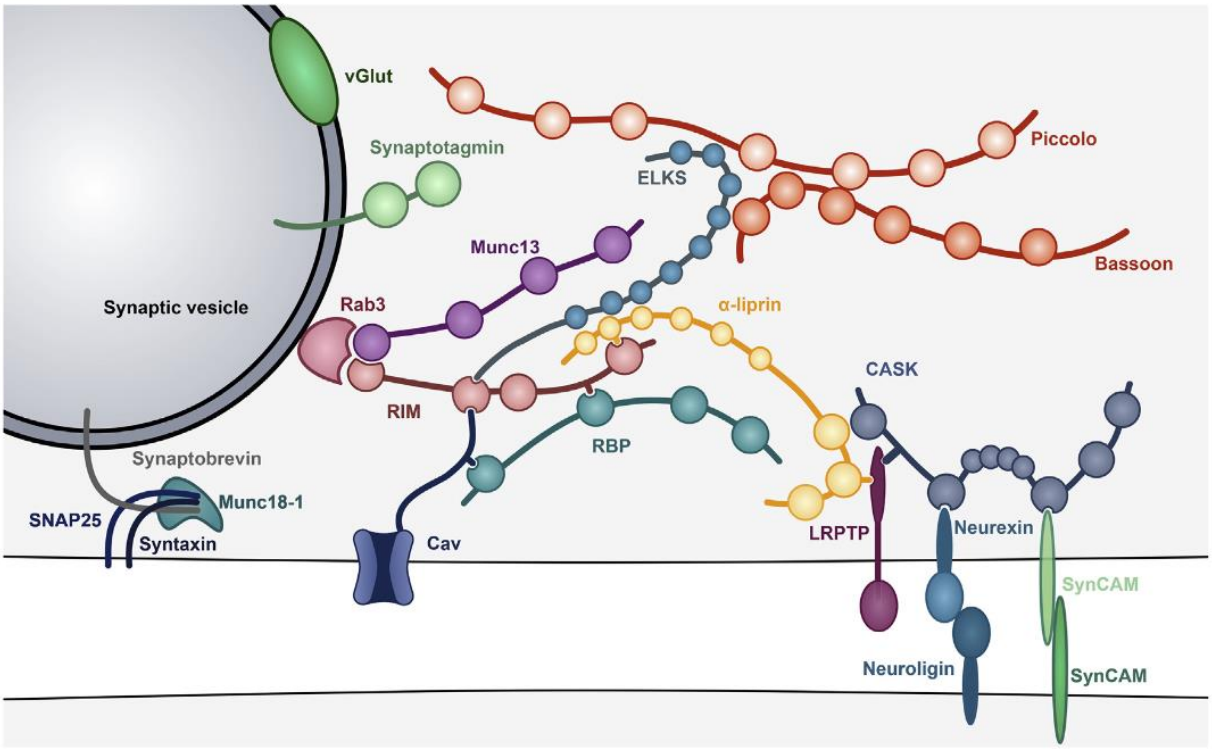

Figure 18. Basic composition of the presynaptic compartment. *The presynaptic compartment is, schematically, made of three blocks: a synaptic cell adhesion molecules (sCAMs) that link the pre- and post-synaptic compartments together (e.g. synCAM, Neurexin / Neuroligin, LRPTP), an active zone (AZ) cytomatrix, made of scaffold proteins (e.g. RIM, RBP, α-liprin, CASK, ELKS, Munc-13, Bassoon, Piccolo) that trap voltage-gated calcium channels (Cavs) and synaptic vesicles (SVs) within the active zone, and the machinery required for the release of neurotransmitter into the synaptic cleft (e.g. SNAP25, syntaxin, Munc18-1). Adapted from (Rizalar et al., 2021).*

1.1.1 Synaptic cell adhesion molecules (sCAMs)

The sCAMs are transmembrane proteins of multiple families that bridges the pre- and post-synaptic compartments, favoring the formation (e.g. synaptic specificity and synaptogenesis), maturation, maintenance as well as plasticity of synapses (Rizalar et al., 2021; Sanes and Zipursky, 2020; Südhof, 2018, 2017) (Figure 10). They can form either homophilic complexes, when both partners belong to the same family, and/or heterophilic complexes, when the partners are from different adhesion molecule family (figure 19).

For clarity, and to avoid redundancy, I will detail in this section both pre- and post-synaptic CAMs.

Neurexins and their ligands. Neurexins are a large family of adhesion molecules encoded by three genes (*Nrxn1-3*) generating each α-, β-, and γ-neurexins which lead to the formation of more than 12,000 expressed isoforms due to alternative splicing. Although *Nrxn-1* mRNA has been detected in glial cells, Neurexins are considered as primarily expressed in neuronal cells where they are localized at synapses. Neurexins are considered as a central regulator of the synaptic activity as the genetic deletion of neurexin 1α has been shown to decrease the spontaneous activity of excitatory synapses whereas triple α-neurexin 1-3 knock-out affected both excitatory and inhibitory synaptic activity as well as calcium-dependent neurotransmitter release. The neurexin, by interacting with AZ scaffold proteins, promotes the proper organization of the neurotransmitter release machinery (Rizalar et al., 2021). Moreover, Neurexins binds to several other trans-synaptic ligands, including Nlg, Cerebellins and C1qls that links neurexins to GluD and GluK2 receptors, respectively, as well as LRRTMs (leucine-rich repeat transmembrane), GABA receptors, or Latrophilins (Südhof, 2021, 2018). Nlg are expressed by four genes (*Nlg1-4*) with Nlg-1 being localized at excitatory synapses.

Latrophilins. Latrophilins are adhesion GPCRs i.e. they contain a typical 7-transmembrane region and two extracellular adhesion domains. They are encoded by three genes (Latrophilins 1-3; gene symbols *Adgrl1-Adgrl3*). They form transcellular junctions by interacting with neurexins, teneurins, as well as fibronectin leucine-rich transmembrane proteins (FLRTs) (Figure 11). In the hippocampus in vivo, it has been shown that latrophilin-2 is targeted to the distal region of the dendritic tree of CA1 neurons

LAR (Leukocyte-associated receptor)-type receptor phospho-tyrosine phosphatases (LRPTPs). There are three types of LRPTPs in mammals, namely PTPRD, PTPRF, and PTPRS, with the latter isoform being the most predominant form in the brain. They interact with a large number of postsynaptic ligands such as TrkC, SALMs, SliTrks, IL-1RAPs, and Netrin-G Ligands 3 (Figure 11). They role, however, is not clear as it has been shown that the deletion of PTPRS produces little effects on synapses (Horn et al., 2012) but, impaired NMDAR-mediated responses without changing the overall content nor the subunit composition of synaptic NMDARs (Sclip and Südhof, 2020).

Cadherins. Cadherins are a large family of more than 100 members, that mediate calcium-mediated homophilic cis- and trans-interactions in all tissues, including the brain. Although cadherins have been shown to control spine morphology (Elia et al., 2006; Togashi et al., 2002), they are not considered as synaptogenic (Südhof, 2018).

Immunoglobulin superfamily. The immunoglobulin (Ig) superfamily comprises the glycoproteins synCAMs, Nectin as well as N-CAM. By directly or indirectly interacting to the cell cytoskeleton (e.g. spectrin-β1), some member of the Ig-superfamily have been shown to regulate the morphology of dendritic spines (Cheadle and Biederer, 2012; Leshchyns'ka et al., 2003). Similarly, the deletion of synCAM decreases the size and the number of synapses (Fowler et al., 2017). The synCAMs are localized at the vicinity of the PSD (Perez de Arce et al., 2015) where they contribute to synaptic plasticity mechanisms (Robbins et al., 2010).

Ephrins ligands and Eph receptors. Ephrin (Eph receptor-interacting protein) ligands and Eph (erythropoietin-producing hepatocellular carcinoma) receptors (also known as Eph receptor tyrosine kinases) (Figure 11) constitute a large family involved in synapse formation and synapse maturation (reviewed in (Hruska and Dalva, 2012). The Eph receptors family can be divided in two sub-families, namely EphA (A1-5) and EphB (B1-3). Ephrin A ligands are tethered to the cell membrane through GPI anchors while EphB ligands are transmembrane proteins with a conserved cytoplasmic tail composed by a sterile alpha motif (SAM) and a PDZ-binding domain. Importantly, EphB2 are localized with the PSD (Perez de Arce et al., 2015).

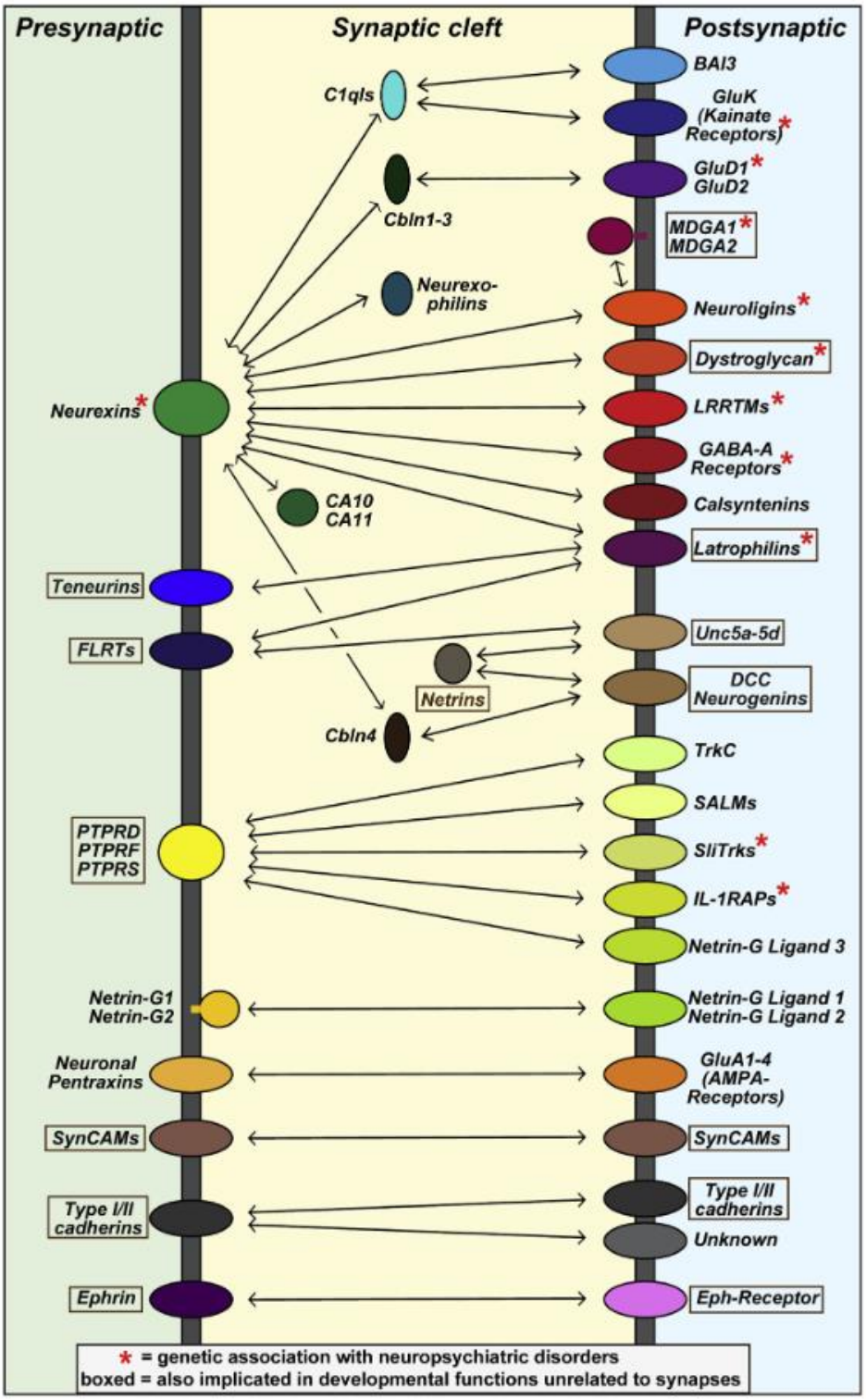

Figure 19. Trans-synaptic cell adhesion molecule (CAM) interactors. *Trans-synaptic interaction between CAM bridges the pre-synaptic compartment together with the post-synaptic compartment. Adapted from (Südhof, 2018).*

1.1.2 Active zone (AZ) cytomatrix proteins

The AZ machinery provides a platform for the correct positioning of SVs and Cavs in regards to the pre- / post- synaptic nanocolumn (Figure 10). It is composed by several scaffolding proteins, in particular the protein families Rab3-Interacting Molecules (RIM), RIM-binding proteins (RBP), α-liprin, CASK, ELKS, Munc-13, Piccolo, and Bassoon (Rizalar et al., 2021), that form an interconnected molecular node (Wang et al., 2009) (Figure 10). RIM and RBP are accepted to be at the core, and redundant, of the organization of the AZ. Indeed, it was shown that only the combined loss of RIM and RBP remove Cavs and abolishes SVs tethering from the AZ (Acuna et al., 2016).

1.1.3 Other molecules of the presynaptic compartment

The number of molecules present in the presynaptic terminal is vast and reviewed in (Rizalar et al., 2021; Simms and Zamponi, 2014). I here would like to mention, the calcium channels that are very important for the action potential-induced vesicle fusion and synaptic vesicle proteins. Ca_vs are voltage-gated calcium channels that couple the action-potential driven membrane depolarization of the presynaptic neuron with the release of neurotransmitters into the synaptic cleft. There are two categories of channels, known as high voltage-activated (HVA) and low voltage-activated (LVA), depending on the required voltage change for the channel to open; reviewed in (Simms and Zamponi, 2014). HVA are formed by the pore-forming $Ca_v\alpha1$ subunit together with $Ca_v\beta$ and $Ca_v\alpha2\delta$ while LVA are formed by the sole $Ca_v\alpha1$ subunit. There are three families of $Ca_v\alpha1$: Ca_v1, Ca_v2, and Ca_v3. The Ca_v1 is composed by the L-type channels $Ca_v1.2$, 1.3, and 1.4. The Ca_v2 family is composed by $Ca_v2.1$, which can give rise to P- and Q- type $Ca_v2.1$, $Ca_v2.2$ (N-type channels), and $Ca_v2.3$ (R-type channels). The Ca_v3 family is composed by the T-type calcium channels $Ca_v3.1$, $Ca_v3.2$, and $Ca_v3.3$.

The synaptic vesicle (VS) proteins are composed by membrane proteins such as VAMP/synaptobrevin, Synaptotagmin, Synaptophysin, and neurotransmitter transporter such as the vesicular glutamate transporter (vGLUT), and SV-associated proteins such as Rab proteins and synapsins (Figure 10), which together allow for the correct trafficking and positioning of the SVs (Takamori et al., 2006). SVs are spatially organized within the presynaptic terminals / AZ. Indeed,

a subset of SVs are docked thanks to the interaction between the SV proteins Rabs and the AZ cytomatrix proteins RIM/Munc-13. Moreover, it has been shown that Munc-13 renders the SVs fusion competent by promoting the link between the SVs and the membrane SNARE complex (Figure 10).

1.2 The postsynaptic compartment

The postsynaptic compartment, but more generally excitatory terminals are commonly located within dendritic protrusions, also known as dendritic spines. They contain a protein-rich zone, known as PSD, located underneath the postsynaptic membrane and aligned to the presynaptic AZ (figure 20). The postsynaptic terminal can be pictured as in layers: (1) the first layer is composed by receptors and adhesion molecules, (2) the second layer is the one of protein scaffold which interact with membrane receptors of layer 1 as well as with elements of (3) the cell cytoskeleton, and (4) enzymes and signaling molecules. It is widely accepted that the efficacy of the synaptic transmission primarily depends on the amount of neurotransmitter released within the synaptic cleft as well as the number of postsynaptic receptors. Recent studies have further strengthened this notion by demonstrating a linear relationship between the synaptic strength and the size of the PSD (Holler et al., 2021).

1.2.1 Neurotransmitter receptors

At excitatory synapses, the effect of the neurotransmitter glutamate is mainly mediated by the ionotropic glutamate receptors NMDAR, AMPAR as well as the metabotropic glutamate receptors mGluRs. Glutamate receptors are not homogeneously distributed in the PSD but highly segregated in regards of the neurotransmitter release site. Both AMPAR and NMDAR are enriched at the center of the PSD, where they are organized in nanodomains (Kellermayer et al., 2018; MacGillavry et al., 2013; Nair et al., 2013; Tang et al., 2016) (figure 20). On the other hand, mGluRs are enriched at the vicinity of the PSD (e.g. perisynaptic domain), away from the neurotransmitter release site (Scheefhals et al., 2023) (Figure 12). Although localized at the core of the PSD, AMPAR and NMDAR are poorly overlapping. In fact, NMDAR are surrounded by AMPAR nanodomains (Hosokawa et al., 2021). Thanks to the trans-synaptic CAM Nlg-1 (Haas et al., 2018), it is accepted that AMPAR

nanodomains are aligned with presynaptic neurotransmitter release sites (Tang et al., 2016), forming so-called nanocolumns. It has been shown that disrupting this alignment by 100 nm is sufficient to dramatically impair the efficacy of the synaptic transmission (Haas et al., 2018).

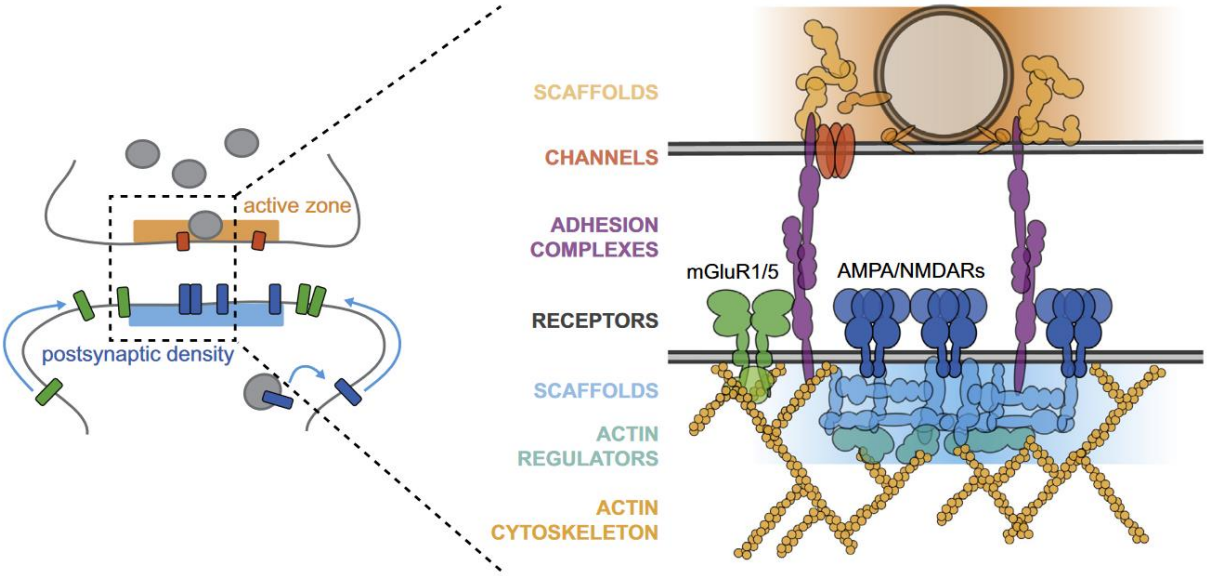

Figure 20. Schematic of a glutamatergic synapse – focus on the post-synaptic compartment. *Type I mGluR (mGluR1/5) are organized perisynaptically whereas AMPAR and NMDAR are at the center of the PSD. The organization of snaptic receptors depends on their interaction with both protein scaffolds and CAMs.*

1.2.2 Postsynaptic scaffolds

Scaffold proteins regulate the synaptic organization of the membrane receptors, and constitute a platform that shape downstream cell signaling pathways (Good et al., 2011; Scheefhals and MacGillavry, 2018). Schematically, we can segregate the postsynaptic scaffolds into layers. The top layer is composed by the family of MAGUK proteins which interact with glutamate receptors (Rasmussen et al., 2017; Scheefhals and MacGillavry, 2018). The middle layer is composed synapse-associated protein 90 (SAP-90)/PSD-95-associated proteins (SAPAPs) which are connected to the third layer, composed by SRC homology 3 (SH3) and multiple ankyrin repeat domains protein (SHANK, *Shank 1-3*) proteins (Rasmussen et al., 2017; Scheefhals and MacGillavry, 2018; Zieger and Choquet, 2021), and finally the actin cytoskeleton (Figure 12). Below, I just describe 3 families of those scaffold proteins, although many more exist and have been described.

1.2.2.1 MAGUK

MAGUK proteins comprises the PSD-95, PSD-93, SAP-97, and SAP-102; reviewed in (Zhu et al., 2016). All MAGUKs have an invariable C-terminal domain containing a PDZ domain which allow for their binding to glutamate receptors, either directly in the case of NMDARs or indirectly through adaptors proteins (e.g. stargazin and transmembrane AMPAR regulating proteins, TARPs) in the case of AMPARs. PSD-95 is considered as the main PSD scaffold and is the most abundant (Cheng et al., 2006). PSD-95 is tethered to the cell membrane after palmitoylation of the N-terminal group and is organized perpendicularly to the PSD (Zhu et al., 2016).

1.2.2.2 Homer

The homer family consists of 3 subtypes (Homer 1-3, each encoded by a single gene) with various isoforms. Within the PSD, homer interacts with both type I mGluRs and the protein scaffolds SHANK, thus linking them together (Rasmussen et al., 2017). Homer is thus considered as regulating the synaptic clustering of type I mGluRs.

1.2.2.3 SHANK

The SHANK protein family is composed by 3 subtypes, known as SHANK1-3 and each encoded by a single gene. By their binding to other scaffold proteins and the actin cytoskeleton, SHANK proteins build network between gluatamate receptors. Shank proteins are highly expressed within the PSD where they are important for glutamatergic signaling, homeostatic plastitcity as well as neuronal development and the maturation of the PSD; in human, mutation in *SHANK* has been linked to autism (Bourgeron, 2015; Monteiro and Feng, 2017).

2. Synapse formation

Most of synapses present in the brain are formed early in postnatal development. Initially, an over-abundance of synapses is produced, and these synapses are later refined through activity-

dependent stabilization or elimination, also known as synaptic pruning. In the mouse brain, the density of synapses rapidly increases during the first month before remaining stable (Cizeron et al., 2020). In human, synapses are formed during the postnatal period with a density of synapses in the cerebral cortex peaking during late-childhood (Petanjek et al., 2011). Schematically, the process of synapse formation can be divided in three critical steps: (1) axon guidance during which axons migrate to targeted areas, (2) synaptic specificity that relates to the interaction between axon and dendrites in order to build putative synaptic partners, and (3) synaptogenesis per se that relates to the coordinated assembly of protein complexes and membrane domains for the formation of functional synapses (Ahmari and Smith, 2002; Biederer and Stagi, 2008; Chou et al., 2020; McAllister, 2007; Südhof, 2021, 2018; Washbourne, 2015). Here, I will focus on the synaptogenesis process.

2.1 Recruitment of synaptic proteins

Synaptogenesis is a process through which pre- and postsynaptic molecule assembly form a stable complex that allow transmission. The question of whether the pre- or postsynaptic site forms first and attract the other or whether their assembly is correlated remains still a vivid debate. Here, I will describe the pre- and postsynaptic molecular scenario that have been proposed.

2.1.1 Recruitment of presynaptic components

In immature neurons, presynaptic components are predominantly synthetized in the soma and transported within vesicles along the axon to nascent presynaptic sites; reviewed in (Emperador-Melero and Kaeser, 2020; Rizalar et al., 2021). In mature neurons, local protein translation within presynaptic sites have been demonstrated (Hafner et al., 2019). Whether local protein synthesis occurs during synapse formation remains unclear. Presynaptic assembly requires the delivery of SVs together with scaffolding proteins. It remains unclear whether AZC proteins and SVs are transported within the same organelle to the site of nascent synapses. It was shown that the AZC proteins Piccolo and Bassoon were transported unitarily, i.e. without SVs, early to the site of nascent synapse (Fejtova et al., 2009; Shapira et al., 2003). Recent work has however showed that SVs and AZC proteins are co-transported (Vukoja et al., 2018). Once at the presynaptic site, AZC

proteins ans can form protein condensates by liquid-liquid phase separation (LLPS) (Wu et al., 2019). Surprisingly, none of the AZC proteins that accumulate early at the nascent synapse are anchored to the plasma membrane, raising the question of whether the formation of the AZ can occur at any site within the neuronal axon or is limited to specific locations (Burlingham et al., 2022). The precise alignement between the pre- and the post-synaptic terminals is however required for synaptic transmission (Tang et al., 2016), and a misalignment of 100 nm is sufficient to decrease the efficacy of synaptic transmission (Haas et al., 2018). Considering that sCAM (e.g. Neurexins, LRPTPs) alone can induce the formation of pre-synapses (Südhof, 2018, 2017; Um and Ko, 2013), it has been hypothesized that sCAM have an instructive role for the formation of presynaptic sites. This question remains largely debated since removing in mice all forms of LRPTP (Emperador-Melero et al., 2021) or Neurexins (Varoqueaux et al., 2006) failed to alter the number of synapses.

2.1.2 Recruitment of postsynaptic components

Components of the postsynapse, including scaffolding proteins and glutamate receptors, are expressed before synapses are made (Gerrow et al., 2006; Washbourne et al., 2004, 2002). NMDAR are among the first post-synaptic receptors to be detected at nascent synapses (Groc et al., 2006a; Pagano et al., 2021; Petralia et al., 1999). In fact, NMDARs are recruited within minutes after presynaptic contact (Washbourne et al., 2004, 2002). It is still unknown whether post-synaptic components, including NMDARs, are vesicularly transported in pre-formed “transport packets” directly to the protosynapses (Washbourne et al., 2004, 2002) or if receptors are recruited from diffuse pools by gradual accumulation (Bresler et al., 2004; Chen et al., 2024)) through lateral diffusion within the plasma membrane plane (Groc et al., 2006b, 2006a). For the NMDARs, for instance, both the presence of extrasynaptic NMDARs on the surface of immature neurons (Petralia et al., 2010; Rao and Craig, 1997; Schmidt-Salzmann et al., 2014; Tovar and Westbrook, 1999), and the absence of intracellular vacuoles containing NMDARs near NMDA receptor islands support the hypothesis that NMDARs cluster at nascent postsynapses from diffusive surface pools (Tao-Cheng et al., 2015).

What are the mechanisms that cluster NMDAR early during development?

It is known that synaptic NMDAR can be clustered through their anchoring to PSD intracellular scaffolds (e.g. the MAGUKs SAP-102) as well as sCAMs (e.g. EphB2R). It has been suggested that NMDARs can be transported at nascent synapses together with SAP-102, but no PSD-95 (McAllister, 2007; Washbourne et al., 2004). It is accepted that PSD-95 is recruited later during synapse maturation while SAP-102, which belong to the same protein family, regulate NMDAR trafficking at immature synapses (Elias et al., 2008; Sans et al., 2000; Washbourne et al., 2004). PSD-95 appear secondarily, following NMDAR activation (Yoshii and Constantine-Paton, 2007), and is involved in synapse maturation later on (El-Husseini et al., 2000). Recent work has highlighted differences depending on the brain region. In particular, SAP-102 and PSD-95 expression peaks concomitantly at 3 postnatal weeks in both mice hippocampus and cortex (Cizeron et al., 2020) (figure 21). Following depolarization-induced NMDAR extrasynaptic islands, that mimick early NMDAR clusters at nascent synapses (more enriched in NMDAR than AMPAR, and in SAP-102 than PSD-95), SAP-102 was detected only in 35 – 45% of these structures whereas both NMDAR and CaMKII are detected in all of them (Tao-Cheng et al., 2015). The latter being consistent with other observation that young immature synapses display high levels of GluN1- and GluN2B-containing NMDARs as well as CaMKII (Swulius et al., 2010). In a recent paper, it has been shown that CaMKII accumulation is rapidly triggered (within 1 min) by NMDA-mediated calcium influx and is followed by the clustering of AMPAR (within 2 – 5 min). They also showed that blocking the interaction between NMDAR and MAGUK were sufficient to inhibit the induced clustering of the NMDARs (Chen et al., 2024).

The sCAMs, and in particular EphB2 and Nlg-1, regulate NMDAR clustering at synapses (Budreck et al., 2013; Dalva et al., 2000). Activating endogenous EphB2 significantly increased the GluN2B-containing NMDAR synaptic content in mature neurons (DIV 14 and 21) but not in immature neurons (DIV 7) (Nolt et al., 2011). Mice lacking EphB2 show no defect in the number nor the structure of spines compared to littermates (Henderson et al., 2001). Similarly, Nlg-1 has been shown to promote NMDAR clustering via direct interaction (Budreck et al., 2013). However this interaction was not confirmed by other studies (Elegheert et al., 2017). Although it has been suggested that both NMDAR and Nlg-1 would accumulate at nascent synapses before recruiting PSD scaffold proteins (Barrow et al., 2009). Yet, the authors observed that, unlike PSD-95,

NMDARs fail to accumulate at Nlg-1 sites (Barrow et al., 2009). Altogether, these data show that the several molecules can play a role in the early clustering of NMDAR at nascent postsynaptic sites.

To trigger synaptic formation, NMDAR activation likely comes from extrasynaptic glutamate spillover and co-agonist (D-serine or glycine) release by astrocytes. It has long been known that immature neurons can spontaneously release neurotransmitters from growing growth cones or even axons before establishing synaptic contact (Dai and Peng, 1996; Kraszewski et al., 1995; Matteoli et al., 1992; Sabo et al., 2006; Young and Poo, 1983; Zakharenko et al., 1999). Upon activation, NMDAR triggers a calcium influx and subsequent calcium-mediated pathways, including the recruitment of AMPARs and the assembly of a robust scaffold apparatus. Once synaptic precursors have reached the protosynapse, they need to organize into the highly segregated structure that forms the PSD. Evidence that postsynaptic scaffolding proteins can form condensates through LLPS, and that these protein condensates recruit synaptic glutamatergic receptors, SynGAP and trans-synaptic proteins suggests that LLPS could also serve as a synaptic-building platform during neuronal development (Chen et al., 2020; Hosokawa et al., 2021; Zeng et al., 2018, 2016). Similarly, it has been shown that activated CaMKII can undergo LLPS with NMDAR and AMPAR, and form protein condensates that recapitulate the synaptic segregation between AMPAR and NMDAR observed in neuronal cells (Hosokawa et al., 2021). Thus, considering that, as in the *in vitro* condensates, PSD are not enclosed by a membrane but rather solely composed by a dense mixture of thousands of proteins, one could hypothesize that synapses may form during development by phase separation (Chen et al., 2020).

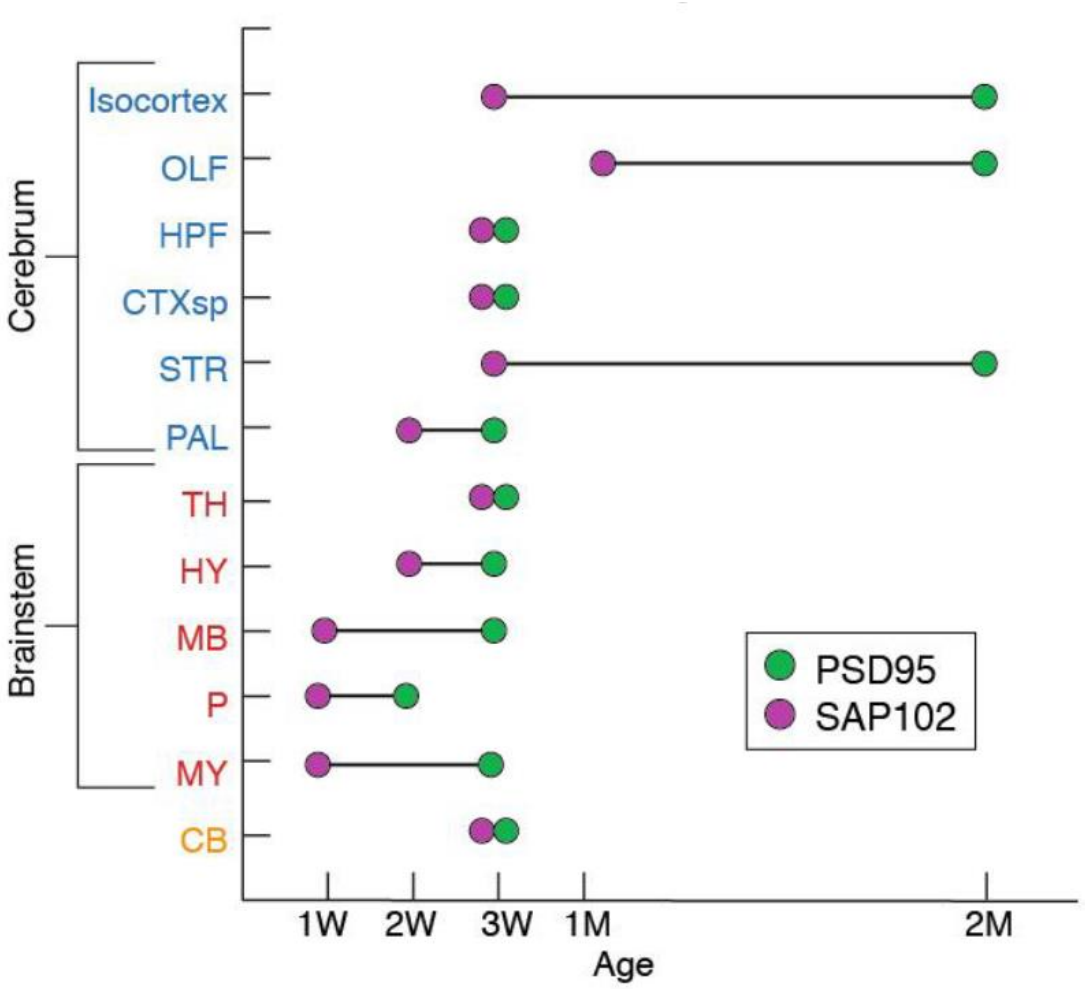

Figure 21. Age of the peak value for the density of the MAGUK proteins PSD-95 and SAP-102. *The postsynaptic scaffolding protein SAP-102 peaks before PSD-95, in most brain region, during brain development in mice. Regions: isocortex, olfactory areas (OLF), hippocampal formation (HPF), cortical subplate (CTXsp), striatum (STR), pallidum (PAL), thalamus (TH), hypothalamus (HY), midbrain (MY), pons (P), medulla (MY), cerebellum (CB). Adapted from (Cizeron et al., 2020).*

2.2 Synapse maturation

The immature brain is characterized by a high turnover of synapses, with continuous formation and elimination of immature synapses. It is believed that synapses are first produced in over-abundance and are then either stabilized or eliminated in an activity-dependent manner. Synapse maturation is classically characterized by an increase in the strength of AMPAR-mediated postsynaptic currents and a switch in the subunit composition of NMDARs, from mainly expressing GluN2B- and GluN3A-containing NMDARs to GluN2A-containing NMDARs.

2.2.1 Increase in the strength of AMPAR-mediated synaptic current

At nascent and immature synapses, AMPAR and NMDAR are rarely found together in a stable manner (Groc et al., 2006a; Hanse et al., 2013; Isaac et al., 1995). Nascent synapses have thus been considered "silent", i.e. containing NMDAR but no AMPAR, or AMPAR-labile, i.e. containing both AMPAR and NMDAR but with a highly unstable AMPAR transmission (Xiao et al., 2004). AMPARs are acquired later as a result of NMDAR activity and subsequent rise in calcium concentration (Durand et al., 1996; Wu et al., 1996) or stabilized by activity (Abrahamsson et al., 2008, 2007; Xiao et al., 2004). It has also been suggested that NMDAR activation blocks the recruitment of AMPARs at silent synapses (Adesnik et al., 2008). In line with the hypothesis that NMDAR activity recruit AMPARs, it has been shown that blocking NMDAR activity increases the number of silent synapses (Liao et al., 1999; Zhu and Malinow, 2002). Although short-term blockade of NMDAR activity increases the number of silent synapse (Zhu and Malinow, 2002), chronic silencing of NMDAR, either pharmacological or genetic, unsilence synapses (Gray et al., 2011; Zhu and Malinow, 2002) due to possible NMDAR-independent compensatory mechanisms. Recently, it further emerges that a large proportion of silent/labile synapses are present in filopodia-like protrusions in the adult mouse cortex (Vardalaki et al., 2022).

2.2.2 Shift in NMDAR composition

2.2.2.1 GluN2B/GluN2A-NMDAR shift

In hippocampal and cortical glutamatergic synapses, GluN2B-containing NMDARs are the main synaptic NMDARs early in development. As brain development proceeds, there is an activity-dependent substitution of non-obligatory GluN2-subunits from GluN2B-rich NMDARs to GluN2A-rich NMDARs at maturing synapses (Barria and Malinow, 2002; Bellone and Nicoll, 2007; Liu et al., 2004). This is characterized by a faster kinetics and a lesser sensitivity towards the GluN2B-subunit-specific antagonist ifenprodil of NMDAR EPSCs (Bellone and Nicoll, 2007). Furthermore, in comparison with GluN2B-, GluN2A-containing NMDARs are characterized by a lower surface mobility at synapses (Groc et al., 2006b) and decreased endocytosis (Lavezzari et al., 2004; Roche et al., 2001), which altogether fuel a model in which GluN2A-containing NMDAR are more "stable" at mature synapses. The fact that GluN2B-containing NMDARs are predominant during

synaptogenesis and that the developmental shift is concommittant to synapse maturation has led the hypothesis that NMDAR subunit composition may regulate synapse maturation. It has been shown that overexpressing GluN2A-subunit early during development decreases synapse formation (Gambrill and Barria, 2011). However, the overexpression of a chimeric form of GluN2A subunit, that contains the CTD of GluN2B and in particular the interaction domain for CaMKII, were sufficient to allow synapse formation (Gambrill and Barria, 2011). In fact, it has been shown that AMPAR synaptic transmission requires CaMKIIα (Incontro et al., 2018). It is important to note that other studies that have used knock-in strategies, and not overexpression systems, showed neurons expressing chimeric GluN2B subunit with GluN2 CTD or GluN2B subunit lacking CaMKII-binding site develops normally, and synapse formation and maturation were unaffected (Halt et al., 2012; McKay et al., 2018; Ryan et al., 2013). Altogether, these data strongly ponderate the role of GluN2 subtype-specific CTD in regulating the shift in NMDAR composition, that is likely due by changes in levels of expression (McKay et al., 2018). Yet, type I mGluRs signaling pathways, through PLC and PKC-dependent signaling pathaways, are directly involved in the developmental NMDAR shift as it is prevented in mGluR5-null animals (Matta et al., 2011).

The developmental NMDAR shift is also involved in the development-associated change in spine morphology (see also Chapter 2.3 on dendritic spine). The actin-mediated motility of filopodia (e.g. appearance, retraction, and extension of filopodium) is initially high in immature neurons before decreasing as the neurons mature (Dunaevsky et al., 1999; Gambrill and Barria, 2011). NMDAR are well-known to regulate filopodia motility, and therefore synapse formation. In immature neuron, which are enriched in GluN2B-containing NMDAR, the activity of GluN2B-containing NMDAR increases the motility of membrane protrusions in a CaMKII-dependent manner (Gambrill and Barria, 2011). Knocking-down GluN2B subunit greatly impairs the formation of globular actin and the formation of dendritic spines in vivo (Akashi et al., 2009). The expression of GluN2A subunit, which is low in immature neuron and enriched in mature neurons, has opposite effects, reducing both spine motility and number upon early expression (Gambrill and Barria, 2011).

2.2.2.2 GluN3A-NMDARs

GluN3A-containing NMDARs are glycine (and D-serine)-gated NMDARs since they are not activated by glutamate. Their expression peaks during the first postnatal weeks, during synaptogenesis and synaptic pruning, and then rapidly decreases (Grand et al., 2018; Pérez-Otaño et al., 2016; Stroebel et al., 2021). GluN3A-containing NMDARs are highly mobile at the neuronal membrane in comparison to both GluN2B- and GluN2A-containing NMDARs with no/few synaptic anchoring (González-González et al., 2023; Pérez-Otaño et al., 2016). It is accepted that GluN3A-NMDARs are a dominant-negative form of NMDARs that antagonize GluN2-containing NMDARs and thus favor synapse elimination during brain development. Indeed, knocking-out GRIN3A subunit resulted in an increased number of spines as well as enhanced synaptic maturation (Das et al., 1998; Henson et al., 2012) whereas over-expressing GRIN3A subunits favored synaptic pruning (Kehoe et al., 2014). The mechanisms of action are however not clear and several putative mechanisms can explain GluN3A-containing NMDARs actions. First, GluN3A-containing NMDAR can compete with GluN2-containing NMDARs for the anchoring at PSDs. However, this hypothesis is weakened by the fact that GluN3A CTDs are lacking PDZ domains. Second, GluN3A subunits can co-assemble with GluN2-subunits in a triheterotetrameric form (GluN1-GluN2-GluN3-containing NMDARs. Third, GluN3A-containing NMDARs can actively destabilize synaptic NMDAR through non-ionotropic signaling pathways; reviewed in (Pérez-Otaño et al., 2016). GluN3A subunit specifically alters GluN2A-, but no GluN2B-, containing NMDARs lateral diffusion, by preventing them from stabilizing at the post-synapses. GluN3A subunit prevents the interaction of GluN2A-containing NMDARs with the sCAM EphB2R, which is known to extracellularly interact with NMDARs, decreasing their synaptic anchoring (González-González et al., 2023).

3. Dendritic spine morphogenesis

3.1 Spines morphological categories

In mature brains, most excitatory synapses are located onto dendritic spines. Dendritic spines are traditionally classified in four categories: thin, mushroom, stubby, and filopodia; reviewed in (Berry and Nedivi, 2017) (figure 22). Most of the dendritic spines fall into the first two categories. They are characterized by a spine head of ~200 nm to 1 µm in diameter that is attached to the dendritic shaft by a neck of ~100 – 200 nm in diameter. It has been shown that the spine head volume correlated to the PSD volumes which linearly correlates with the synaptic transmission strength (Holler et al., 2021). Spines are considered as highly dynamic. They can undergo actin-dependent structural remodeling during brain development as well as upon neuronal activity and thus, change/adapt their functions (Holler et al., 2021; Hotulainen and Hoogenraad, 2010). Early during development, stubby spines (i.e. lacking spine neck) and filopodia are more common whereas, in the mature brain, mushroom and mainly thin spines are common. Indeed, during neuronal development, it is accepted that most synapses are first located onto the dendritic shaft or within filopodia-type protrusions (Fiala et al., 1998; Papa et al., 1995; Ziv and Smith, 1996) and then, as the brain matures, onto dendritic spines.

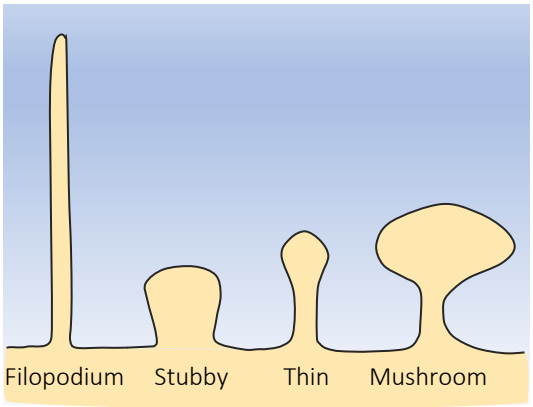

Figure 22. Morphology of dendritic spines. *Schematic drawing of spines morphologies. Adapted from (Hering and Sheng, 2001).*

3.2 Model of spinogenesis

The formation of spine and the temporal mechanism are not fully understood, with several different, non-mutually exclusive, models that exist today (figure 23) (García-López et al., 2010;

Yuste and Bonhoeffer, 2004). Dendritic spines germinate from shaft synapse following shaft synaptic formation and stabilization (model 1). In this model, the formation of the presynaptic terminals preceeds, or triggers, the formation of the postsynaptic terminal. This model is supported, for instance, by the fact a majority of axodendritic synapses are located within the dendritic shaft immature neurons whereas they are located in spines in mature neurons (Fiala et al., 1998) as well as the observation that spine outgrowth and synapse maturation are correlated (Zito et al., 2009). On the other hand, dendritic filipodia-like membrane protrusions initiate axodendritic contact and synapse formation (Calabrese et al., 2006). Filopodia are highly motile structures. They transiently extend from the dendritic shaft and retract rapidly, within a rage of ~10 min (Ziv and Smith, 1996). One hypothesis is that dendritic filopodia-like protrusions increase the chance of encounter with a developing axon. In this model, spines first enter in contact with presynaptic boutons before forming synapses (Nägerl et al., 2007). The actin-binding protein drebrin, which organization is regulated by NMDARs, accumulate at filopodia-like protrusion and recruit postsynaptic components (Sekino et al., 2006; Takahashi et al., 2003). Following axodendritic contact and synapse formation, the local increase in intracellular calcium stabilizes the axodendritic connection (Lohmann and Bonhoeffer, 2008). In line with this, the actin-mediated motility of filopodia (e.g. appearance, retraction, and extension of filopodium) is initially high in immature neurons before decreasing as the neurons mature (Dunaevsky et al., 1999; Gambrill and Barria, 2011).

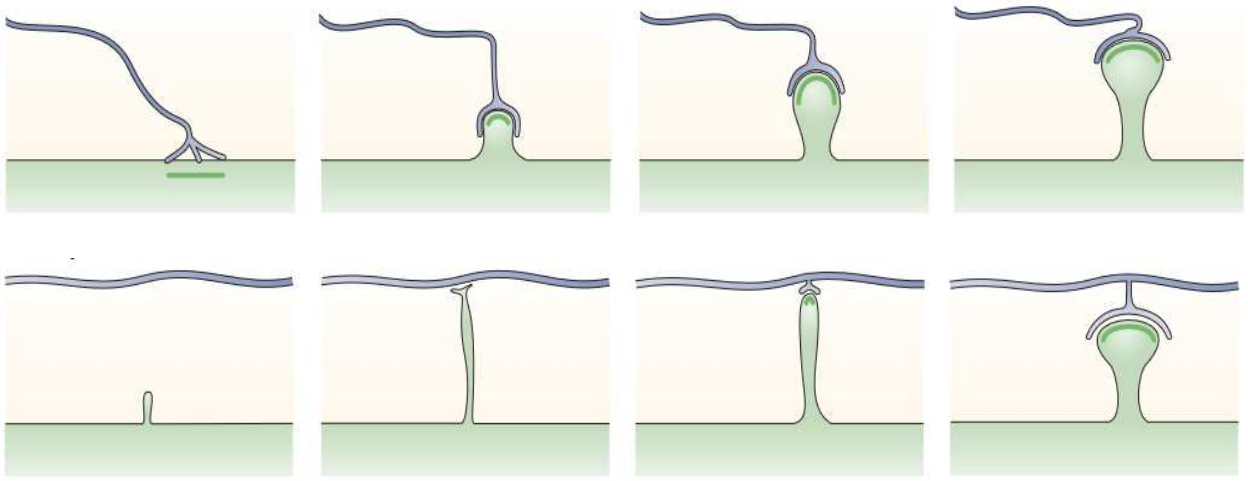

Figure 23. Models of spinogenesis. *(top) In this first model, spines arise from shaft synapses while in the second model (bottom), dendritic-filopodia initiate the axodendritic contact which lead to synapse formation. A third model (not shown) where the postsynaptic compartment develops independently from the presynaptic compartment have also been proposed. This model rely, for instance, on the observation of naked spines (i.e. spines with no presynapse) in Purkinje cells of glycine-gated GluD2 knock-out mice (Südhof, 2018). Adapted from (Yuste and Bonhoeffer, 2004).*

4. Regulators of synapse formation

4.1 Role of neuronal activity

The role of neuronal activity (e.g. neurotransmitter release) in synaptic development is a highly debated and controversial topic. Although it is commonly accepted that synapse formation is regulated by neuronal activity, it has been shown that synapse formation can occur without neuronal activity (e.g. neurotransmitter release) (Andreae and Burrone, 2018, 2015, 2014; Harms and Craig, 2005; Kwon and Sabatini, 2011; Okawa et al., 2014; Sando et al., 2017; Sigler et al., 2017; Verhage et al., 2000). Indeed, neuronal culture chronically incubated with tetrodotoxin (which blocks action potential firing) develop normally in comparison with untreated cultures (Harms and Craig, 2005). Similarly, transgenic animals in which the neurotransmitter release is absent can form glutamatergic synapses to similar levels than wild-type animals (Sando et al., 2017; Sigler et al., 2017; Verhage et al., 2000).). Evoked neurotransmitter release is triggered by an action potential-driven depolarization of the presynaptic membrane which induces calcium

influx through the opening of the voltage-gated calcium channel and finally, result in the exocytosis of the neurotransmitter glutamate within the synaptic cleft. Spontaneous release of neurotransmitter occurs when a synaptic vesicle spontaneously fuse with the presynaptic membrane and a quantum of neurotransmitters is released. Interestingly, both evoked and spontaneous release are developmentally regulated. It has been suggested that the rate of spontaneous release is maximum early during brain development whereas evoked release is maximal early in immature neurons and then decreases (Andreae et al., 2012). Increasing the frequency of spontaneous release at the neuromuscular junction of the Drosophila significantly increased the number of presynapses (Choi et al., 2014) while its early blocking altered development of hippocampal neurons (Andreae and Burrone, 2015). Although the precise mechanisms explaining the above-mentioned differences in the effect of glutamate between spontaneous and evoked release are unclear, some studies have suggested that each mode of release can activate, within the same synapse, different subsets of NMDARs (Atasoy et al., 2008; Reese and Kavalali, 2016) and/or AMPARs (Sara et al., 2011); reviewed in (Kavalali, 2015).

4.2 Role of astrocytes

Astrocytes are closely associated with neurons as well as synapses, forming the tripartite synapse e.g. a complex composed by the pre- and postsynaptic terminal as well as glia processes. Astrocytes regulate multiple aspect of neuronal and synaptic function, including synapse formation (Allen, 2014; Chung et al., 2024). The role of astrocytes in synaptogenesis has been difficult to test initially, as astrocytes are crucial for neuron survival (Banker, 1980). This issue was overcome with the development of retinal ganglion cell (RGC) cultures, extracted from postnatal retinas, which can be grown without astrocytes. When cultured alone, RGCs survive and develop neurites but form few synapses; however, the presence of astrocytes and/or the addition of astrocyte-conditioned media is sufficient to promote synapse formation (Pfrieger and Barres, 1997; Ullian et al., 2001) This issue was overcome with the development of retinal ganglion cell (RGC) cultures, extracted from postnatal retinas, which can be grown without astrocytes. When cultured alone, RGCs survive and develop neurites but form few synapses; however, the presence of astrocytes and/or the addition of astrocyte-conditioned media is sufficient to promote synapse formation (Hama et al., 2004) as well as their stability and morphology (Nishida and Okabe, 2007).

Collectively, these molecules are known as synaptogenic or as synaptic organizers. They are classified into two categories: cell-adhesion molecules (contact factors) and secreted factors. The latter can be further divided in extracellular scaffolding molecules and diffusible factors. This part will be further detailed in the *chapter 3-4.3* on synaptogenic molecules.

4.3 Excitatory synaptogenic molecules

Synaptogenic molecules (or synaptic organizers) are expressed by both glia and neuronal cells (Yuzaki, 2018). They regulate the assembly of the pre- and postsynaptic terminal and therefore, synaptogenesis. Importantly, I will emphasize molecules that have been shown to promote synapses formation (i.e. synaptogenic) and not the molecules that promote synapse maturation.

4.3.1 Secreted factors

4.3.1.1 Extracellular scaffolding proteins

Thrombospondins protein family (produced by glia cells). Thrombospondins (TSPs), and in particular TSP-1 and -2, are proteins of the extracellular matrix (ECM) that are known to induce the formation of synaptically silent synapses (i.e. containing NMDARs but not AMPARs) (Christopherson et al., 2005; Eroglu et al., 2009). The addition of purified TSP to culture media is sufficient to increase the number of synapses while double knock-out animals, for both TSP-1 and -2, displayed a reduced number of synapses (Christopherson et al., 2005). At the molecular level, TSP acts on the postsynaptic calcium channel α2δ1, also known as gabapentin receptor that activates Rho GTPase Rac1 (Eroglu et al., 2009; Risher et al., 2018). Also, TSP1 can act by directly binding to the postsynaptic adhesion molecule Nlg-1 (Xu et al., 2010). It is important to note that structural studies have however failed to reproduce the interaction between TSP1 and Nlg-1 (Elegheert et al., 2017).

Glypican-4 and -6 (produced by glia cells). Glypicans are a family of heparan sulfate proteoglycans with 6 isoforms (GPC1-6). Specifically, GPC-4 and -6, which expression peaks around the second postnatal week in mouse brain e.g. at the peak of synaptogenesis, promote the formation of

synaptically active (containing AMPARs) synapses (Allen et al., 2012; Farhy-Tselnicker et al., 2021). In fact, GPC-4 and -6 promote the recruitment of synaptic GluA1-AMPARs, but no GluA2 nor GluA3 (Allen et al., 2012).). Of note, GPCs are heparan sulfate proteoglycans (HSPGs) that are tethered to plasma membrane via a GPI anchor and thus, requires to be cleaved by proteases to be in a soluble form (Huang and Park, 2021). At the molecular level, GPCs activates a protein tyrosine phosphatase receptor (PTPRD), which is localized presynaptically. The activation of PTPR by GPC triggers the release by the presynaptic terminal of the AMPA clustering factor neuronal pentraxin-1 which directly binds to AMPARs (Farhy-Tselnicker et al., 2017).

Pentraxin (produced by both glia and neurons). Neuronal pentraxin consists of pentraxin-1, pentraxin-2, and pentraxin-r whereas pentraxin-3 is expressed by glia cells (Chung et al., 2024; Yuzaki, 2018). Pentraxin-1/2/3 are secreted in a soluble form whereas pentraxin-r is a transmembrane protein that can be released in soluble form following its cleavage (also known as ectodomain shedding, see *Chapter 2.4.4*) by the matrix metalloproteinase tumor necrosis factor α-converting enzyme (TACE). In rodents, both pentraxin-1 and prentraxin-r are expressed in the hippocampus, cortex and cerebellum. Pentraxins form homo- and heteromeric complexes and thus exist in hexamers. It is hypothesized that pentraxin-1/2/3 are anchored at synapses by binding to pentraxin-r. They bind to the ATD of AMPARs and trigger its clustering, thus favoring synapse formation (S.-J. Lee et al., 2017). Activation of TACE (e.g. during type I mGluR-dependent LTD) has been proposed to promote AMPAR clustering and subsequent internalization It has been shown that glial pentraxin-3, which is highly expressed in the developing brain, promotes synaptic AMPAR clustering (Fossati et al., 2019). Similarly, the immediate early gene and member of the pentraxin family neuronal – activity regulated pentraxin (Narp) have also been shown to promote AMPAR clustering (O'Brien et al., 2002, 1999; Tsui et al., 1996; Xu et al., 2003).

SPARCL1 (produced by glia cells). Secreted protein acidic and rich in cysteine (SPARC) – like 1 (SPARCL1), also known as Hevin, is a glycoprotein of the SPARC family. SPARCL1 was initially identified as synaptogenic as it has been shown sufficient to induce the formation of synapses in RGC (Kucukdereli et al., 2011) and in neurons derived from human embryonic stem cells (Gan and

Südhof, 2019) as well as increasing NMDAR-dependent synaptic transmission (Gan and Südhof, 2020). SPARCL1 mechanism of action is however not clear. SPARCL1 may bridge presynaptic and postsynaptic compartments by linking the usually non-interaction presynaptic neurexin-1α with the postsynaptic neuroligin-1B (Singh et al., 2016). Another group observed that SPARCL1 synaptogenic effect were conserved in knock-out animals for the three and four isoforms of neurexins and neuroligins, respectively, and observed that SPARCL1 promotes spontaneous excitatory synaptic transmission (Gan and Südhof, 2020), and similarly as for TSP-1, structural studies failed to reproduce the interaction between Nlg-1 and SPARCL1 (Elegheert et al., 2017).

Precerebellin and C1q-like (produced by neuronal cells). Precerebellin (Cbln) family is composed by four subtypes (Cbln1-4) and are majoritarily expressed in the cerebellum. Cbln are organized in hexamer. Cbln1, for instance, induces excitatory spine formation by linking presynaptic neurexin to postsynaptic GluD receptors, herein GluD2, as well as inducing their clustering (Ito-Ishida et al., 2008). Application or overexpression of Cbln1/2/4 have been shown to triggers synapse formation, both excitatory an inhibitory. It has been shown that humans have a higher expression of Cbln2 in the prefrontal cortex (PFC) compared to macaques, and humanized mice that reproduce this phenotype display increased density in dendritic spines (Shibata et al., 2021). C1q-like proteins (C1ql1-C1ql4) are highly expressed in the climbing fibers to Purkinje cells. As for Cbln, C1q-like proteins link presynaptic terminal with postsynaptic receptors (Yuzaki, 2018).

Leucin-rich glioma inactivated (Lgi) protein 1 (produced by neuronal cells). Lgi family are secreted glycoproteins, composed of four members (Lgi1-Lgi4). They bind to the extracellular region of disintegrin and metalloproteinase (Adam) transmembrane proteins that are lacking any catalytic activity (e.g. Adam22, Adam23, Adam11) (Kegel et al., 2013). A splice variant of Adam22 that contains a PDZ domain within its CTD allows the recruitment of PSD-95, TARP/stargazin, and AMPARs (Fukata et al., 2006; Kegel et al., 2013).

4.3.1.1 Diffusible factors

Extracellular vesicles released by astrocytes. Extracellular vesicles can be released by both neuron and glia cells, and provide molecular cues during brain development (Forero et al., 2024; Pipicelli et al., 2023; Sharma et al., 2019). Particularly, astrocytes have been shown to secrete extracellular vesicles (also known as exosomes)-containing the synaptogenic protein Fibulin-2 (Patel and Weaver, 2021).

Wnts (produced by neurons). The glycoproteins wingless-type (Wnts), and in particular Wnt-7a and Wnt-5a, have been shown to have, depending on the studies, pre- and/or postynaptogenic actions (Cerpa et al., 2008; Farías et al., 2009; Sahores et al., 2010; Varela-Nallar et al., 2010) and Wnt-5a were shown to specifically upregulate NMDAR currents (Cerpa et al., 2011). Wnt-7a were shown to promote the clustering of presynaptic terminal as well as of postsynaptic terminals in hippocampal neurons in vitro, although some studies failed to reproduce Wnt-7A synaptogenic effect on the postsynaptic compartment (Cerpa et al., 2008). Exogenous application of Wnt-7a were shown to promote dendritic spines growth and PSD-95 clustering in a Dvl-1 and CaMKII-dependent manner (Ciani et al., 2011). Knock-out animals for either Dvl1 or Wnt7a show reduced number of spines in hippocampal neurons in both *commu ammonis* (CA) 1 and 3 (Ciani et al., 2011).

Fibroblast growth factors (produced by neurons). The glycoproteins FGFs are well-known to play a role in various aspect of development, including a presynaptic organizer role. In particular, FGF-22 and FGF-7 are highly expressed in the hippocampus early durin brain development. The overexpression or exogenous application of FGF-22 promote presynaptic clustering (e.g. increased number of vGLUT clusters) in hippocampal neurons in vitro (Dabrowski et al., 2015).

Semaphorins (produced by neurons). Semaphorins are a class of membrane and secreted glycoproteins. The class 3 of secreted semaphorins composed by 8 subtypes (Sema3A-G), which bind to the receptors neuropilin and plexin, have been shown to have a synaptogenic action (Tran

et al., 2009; Yamashita et al., 2007). The application of exogenous sema3a increase the number of excitatory synapses in primary cortical neuronal cultures through the collapsing response mediator protein 1 (crmp1). Both crmp1 and sema3a knowck-out animals showed a defect in the number of spines (Yamashita et al., 2007). However, another study failed to reproduce sema3A synaptogenic effect but observed a synaptogenic action for sema3F (Tran et al., 2009).

4.3.2 Cell-adhesion molecules (CAM)

Neuroligin (expressed by both glia and neurons). Nlg1-3 are expressed at similar levels by both neurons (postsynapse) and astrocytes. Consistent with the notion that the contact of an astrocyte is sufficient to promote synapse formation (Hama et al., 2004), impairing the expression of Nlg by the astrocytes have been shown to reduce the number of synapses only within the astrocyte territory (Stogsdill et al., 2017). The synaptogenic action of neuroligins, and in particular Nlg-1, is subject to controversies (Gan and Südhof, 2020; Südhof, 2021, 2018, 2017). Nlg-1 was first considered as synaptogenic as its overexpression in heterologous cells is sufficient to promote the formation of synaptic contacts (Scheiffele et al., 2000). However, triple knock-out mice for the three neuroligin subtypes (*Nlg1-3*) did not show a reduction in the number of synapses (Varoqueaux et al., 2006). Yet, Nlgs appear to be required for some aspects of synaptic maturation. It has been shown that Nlg1 activity on synapse formation/maturation depends on the activity of NMDAR (Chubykin et al., 2007), to which they bind directly as well as indirectly through the common binding partner PSD-95 (Mondin et al., 2011). The transsynaptic and synaptogenic CAM Nlg-1 have been shown to organize AMPARs in front of the neurotransmitter release site. Disruption of the interaction between Nlg-1 and postsynaptic scaffold PSD-95 were sufficient to misalign AMPARs from the neurotransmitter release site, which affected the synaptic transmission (Haas et al., 2018). The role of Nlg-1 as trans-synaptic organizer and thus on synaptic transmission has been strengthened by the observation that disruption in Nlg functions induces autism-spectrum disorder and neurodevelopmental disorders (Nakanishi et al., 2017; Nguyen et al., 2020).

Latrophilins (expressed in the neuronal post-synaptic compartment). Latrophilin are postsynaptic CAMs that are specifically expressed in the distal dendritic segment of CA1 pyramidal neurons, in the S. moleculare-lacunosum (Anderson et al., 2017; Südhof, 2018). Latrophilin is considered as the sCAM whom deletion lead to the most severe phenotype (Südhof, 2018). Deleting latrophilin-2, which is located postsynaptically, dramatically impaired the number of synapses, thus suggesting that latrophilin-2 triggers synapse formation and/or maintenance (Anderson et al., 2017).

Ephrin ligands and Eph receptors (expressed by both neurons and glia cells). Ephrin ligands and Eph receptor tyrosine kinase) constitute a large family involved in synapse formation and synapse maturation (Hruska and Dalva, 2012). The Eph receptors family can be divided in two sub-families, namely EphA (A1-5) and EphB (B1-3). Binding of Ephrin ligand B to EphB triggers the activation of the kinase domain on EphB CTD as well as the phosphorylation of the CTL of Ephrin ligand B. Both EphA and EphB have been shown to play a role on excitatory synaptogenesis. It has been shown that EphA4 and EphBs (1/2/3) regulate the formation of dendritic spines and synapses, respectively. Moreover, EphB2 have been proposed to trigger the clustering of the presynaptic machinery as transfecting heterologous cells with EphB2 were sufficient to trigger presynaptic clustering in contacting axons (Kayser et al., 2006). At the postsynaptic site, it is suggested they regulate NMDAR clustering, localization and function in mature but not immature neurons (Dalva et al., 2000; Nolt et al., 2011; Takasu et al., 2002; Washburn et al., 2020). EphB2 expression gradually increases in the mouse hippocampus and cortex during postnatal development (Henderson et al., 2001). EphBs (1/2/3) are required for both spine formation and morphogenesis (Henkemeyer et al., 2003; Kayser et al., 2006). However, mice lacking EphB2 show no defects in dendrite or axonal outgrowth, spine number, or ultrastructure (Henderson et al., 2001). Altogether, these data indicate EphB2 is required for the synaptic clustering of NMDAR in mature neurons.

4.4 Ectodomain shedding

Ectodomain shedding is considered as post-transaltional protein modification. It consists in the cleavage of the extracellular portion of a transmembrane protein or GPI-anchored protein, just before the TM domain, by a protease (also known as sheddase). The transmembrane portion can be further cleaved by a transmembrane protease (Martín-de-Saavedra et al., 2022b). The main known CNS sheddases are the soluble matrix metalloproteases (MMPs, which belongs to the ECM), as well as the membrane anchored a disintegrin and metalloproteases (ADAMs), and β-site amyloid precursor protein cleaving enzymes (BACE1 and BACE2, localized in endosomes and Trans-Golgi network) protease families (Lichtenthaler et al., 2018). Ectodomain shedding plays a key role in synaptic formation and maintenance, as well as in the regulation of synaptic activity. Several synaptic transmembrane proteins (e.g. CAMs) have been shown to undergo ectodomain shedding (Martín-de-Saavedra et al., 2022b). It is the case for Nlg-1 (Peixoto et al., 2012; Suzuki et al., 2012), neurexins (Martín-de-Saavedra et al., 2022a), as well as Ephrins and Eph receptors (Hruska and Dalva, 2012). Ectodomain shedding can result in the termination of activity of the cleaved protein, as well as it can trigger new signaling pathways. Indeed, the shed soluble fragment can itself trigger autocrine and paracrine signaling pathways (Martín-de-Saavedra et al., 2022a). For many synaptic CAMs ectodomain shedding causes the termination from the weakening of the adhesion between the pre- and the postsynaptic terminal. As an example, preventing neuronal activity-regulated Nlg-1 ectodomain shedding results in an increased number of dendritic spines (Peixoto et al., 2012; Suzuki et al., 2012).

4.5 Synapse limiting molecules

Synapse limiting molecules are molecules that either trigger synapse elimination (out of the scope if this introduction) or limit the formation of synapse during brain development. For example, it has been shown that the transcription factor MEF2 suppress the formation of spines in an activity-dependent manner during brain development (Flavell et al., 2006; Shalizi et al., 2006). The rise of neuronal activity in developing neurons induces the activation of calcineurin, which triggers the dephosphorylation and subsequent activation of the transcription factor MEF2 that in turn restrict the number of synapses (Flavell et al., 2006; Shalizi et al., 2006). Another example is SPARC. SPARC

is produced by astrocytes and is an inhibitor of SPARCL1/hevin. SPARC expression rapidly increase early during postnatal development (maximum around postnatal day 20) whereas it is expressed at low levels in the mature brain (López-Murcia et al., 2015).

Chapter 3. The extracellular matrix

The space between cells is known as the extracellular space (ECS). The ECS occupies about 20% of total brain volume in adult mammals. Within the brain parenchyma, the ECS is composed by both the interstitial fluid (ISF) and an extracellular matrix (ECM) (figure 24), a hygroscopic meshwork of long-chain macromolecules, many of which are tethered to cell membranes and serves as scaffolds and signaling units (Toole, 2004). The ECS appears to be rather dynamic depending on the several physiological parameters. For instance, brain's ECS increases by 60% during sleep, allowing metabolites clearance (Xie et al., 2013). The ECS constitutes a reservoir of extracellular ions that are necessary for neuronal electrical activity, mediates chemical signaling, and forms a vehicle for substances to move from blood vessels to cells, and vice-versa (Syková and Nicholson, 2008). More generally, all intercellular signaling (excepting the ones mediated by gap junctions) diffuse through the ECS. The ECS appears therefore critical for all brain functions. Diffusion is the dominant mechanism of molecular transport within the ECS, and is primarily constrained by the geometry of the ECS (Syková and Nicholson, 2008). However, diffusion of macromolecules is further modified by specific physicochemical characteristics such as electrochemical gradients, binding to surface proteins such as receptors, and the viscosity of the ISF which includes interaction with the ECM components (Syková and Nicholson, 2008).

1. ECM composition

The ECM is produced by both neuronal and glia cells. Brain ECM is mostly composed by negatively-charged glycosaminoglycans (GAG), e.g. hyaluronan or hyaluronic acid (HA), the glycoprotein tenascin (Tn), proteoglycans and fibrous proteins such as collagen, laminin, and fibronectin. Proteoglycans are mainly composed by the secreted chondroitin sulfate proteoglycans (CSPG) and the membrane-bound heparan sulfate proteoglycans (HSPG). The main CSPGs are aggrecan, versican, brevican, and neurocan which are collectively known as lecticans. Altogether they form a meshwork of variable composition depending on the brain region (Dauth et al., 2016).

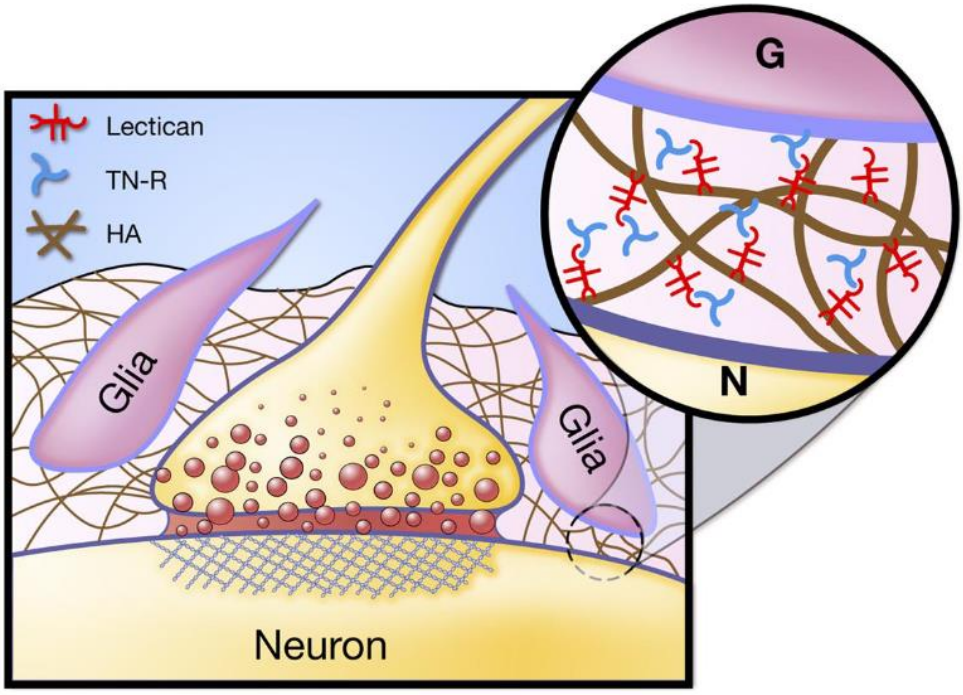

Figure 24. The brain interstitial ECM. *The ECM surrounds every cell and occupies around 20 % of the volume of the brain. Adapted from (Syková and Nicholson, 2008)*

1.1 Hyaluronic acid

HA is a non-sulfated GAG and is one of the major components of the ECM. It is a linear, negatively charged, polysaccharide chain of the disaccharide unit D-glucoronic acid and N-acetyl-D-glucosamine (Toole, 2004, 2001). HA is produced by the enzyme hyaluronan synthases (HAS), a group of transmembrane glycosyltransferases, whose catalytic sites is located at the cytosolic site (Weigel et al., 1997). HA is synthetized within the cell and extruded to the ECS while being produced (Toole, 2004, 2001). There are three identified isoforms of the HAS (HAS1-3), each encoded by a single gene located in a different chromosome (Vigetti et al., 2014; Weigel et al., 1997). The expression of HAS isoenzymes is tissue-, cell-, and time-specific. Importantly, each HAS isoenzyme produces a HA polymer of a different size. HAS3 produces a polymer of 1 to 2 x 10^5 Da while HAS1 and HAS2 produce the longest, from 2 x 10^5 to 2 x 10^6 and > 2 x 10^6 Da, respectively (Zakusilo et al., 2021). HA degradation is achieved by two mechanisms, either by specific enzymatic degradation by hyaluronidases (HYAL) or unspecific oxidative damage by reactive oxygen species (ROS) (Berdiaki et al., 2023). HYAL are endoglycosidases that cleave glycosidic bonds of the HA

polysaccharidic chain. HYAL are encoded by 6 genes, HYAL1, HYAL2, HYAL3, HYAL4, PH20/SPAM1, and HYAL-P1 pseudogenes (Csoka et al., 2001). HYAL1 and HYAL2 are the most characterized one. HYAL2, which is located at the plasma membrane, degrades large HA polymers that are then endocytosed and further degraded by HYAL1 in lysosomes (Bourguignon and Flamion, 2016). Although HA acts as a backbone for the interstitial ECM, a portion of it remains tethered to the cell surface, forming an extra- or pericellular coat, either by a sustained interaction with the synthases or by binding to specific HA-receptor as CD44 and receptor for hyaluronic-acid-mediated motility (RHAMM) (Evanko et al., 2007; Toole, 2001) (figure 25). At physiological pH, the negative charge HA is balanced with cations (e.g. Na^+, Ca^+, Mg^{2+}, K^+), which confers to HA a high hydrophilicity. Such high-water retention stabilizes the secondary structure of HA into a single-stranded left-handed helix with two disaccharide residues per turn (two-fold helix) (Heatley and Scott, 1988). In aqueous solution, HA two-fold helix will also form intermolecular hydrophobic interactions, which allow for the aggregation of HA polymer chains into coil structures (Fallacara et al., 2018). HA is considered as a space filling molecule and it is likely that the characterisitics of HA meshwork (e.g. viscosity and viscoelasticity) varies depending on both the molecular weight (MW) and concentration of HA.

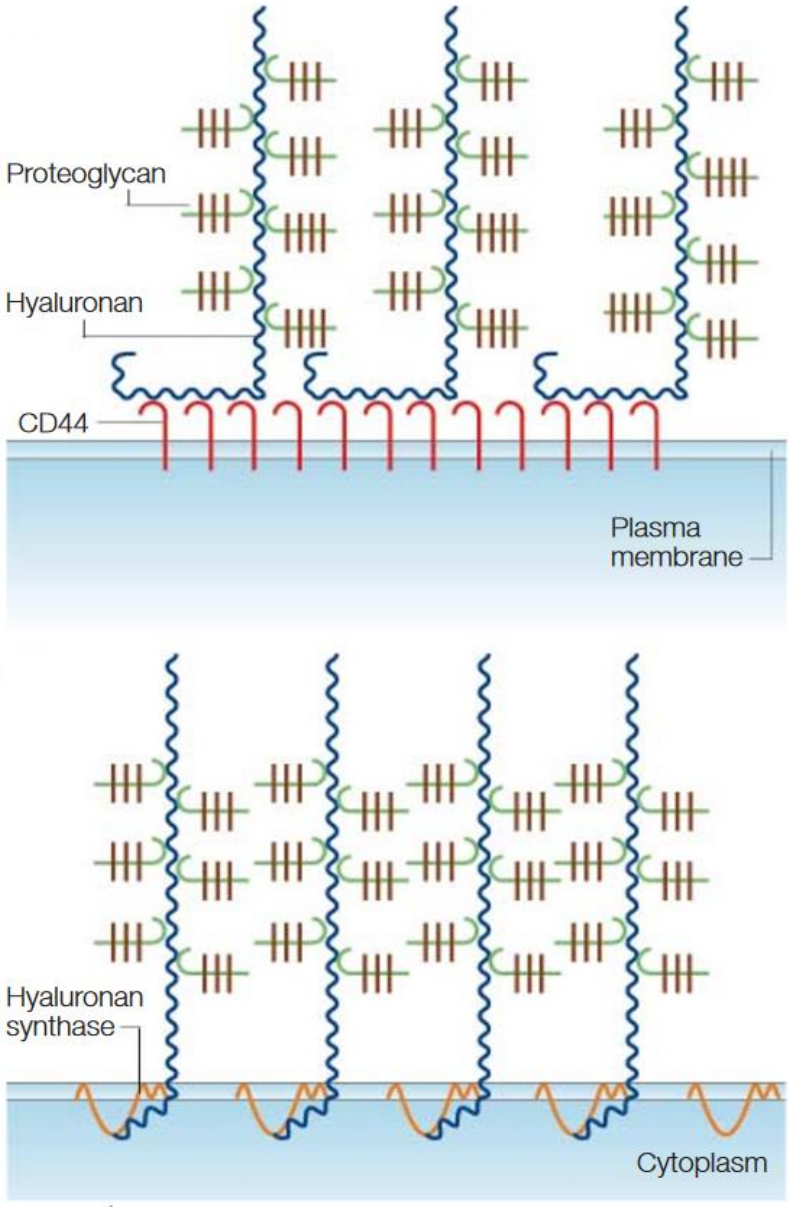

Figure 25. Model of interaction between HA and cell surfaces. *HA is tethered to cell membrane e.g. forming a pericellular coat, through the interaction with HA-receptors such as CD44 and/or producing enzymes (HAS1-3). Adapted from (Toole, 2004)*

1.1.1 HA signaling

HA has several receptors which are collectively known as hyaladherins e.g. CD44, RHAMM, LYVE1, TLR2, and TLR4 (Vigetti et al., 2014; Zakusilo et al., 2021). They modulate biological processes such as cell adhesion and migration, tumorigenesis, cell survival, apoptosis, and inflammation (Zakusilo

et al., 2021). On the size of the HA polymers, considered either as low molecular weight (LMW, below 500 kDa) or high molecular weight (HMW, above 1000 kDa), depends the signaling outcome (Zakusilo et al., 2021). LMW-HA signaling is immunostimulatory, pro-inflammatory, and angiogenic while HMW-HA signaling would be immunosuppressive, anti-inflammatory, and anti-angiogenic (Berdiaki et al., 2023; Vigetti et al., 2014; Zakusilo et al., 2021). The main hypotheses for this size-dependent signaling pathways are that both structures of the HA chain (e.g. rod-to-coil transition at the ~250 kDa range) (Weigel and Baggenstoss, 2017) and the ability to cluster receptors vary depending on the size of the polymer (Jiang et al., 2005; Ooki et al., 2019; Yang et al., 2012). HMW-HA can be fragmented by HYAL enzymes, classically HYAL2 and HYAL1 which are working sequentially. After cleavage by HYAL2, the HA-fragments (up to 200 kDa) are internalized in a CD44-dependent manner and further degraded into up to 800 Da fragments by HYAL1 (Vigetti et al., 2014). In the case of HA-fragmentation by ROS, which are classically formed upon injuries or inflammation, fragmented HA can accumulate in the ECS (Berdiaki et al., 2023; Donelan et al., 2022).

1.1.2 Lecticans

Lecticans, namely aggrecan, versican, brevican, and neurocan, are a family of CSPGs. All four lecticans are expressed in the CNS (Milev et al., 1998). Although the expression of brevican and neurocan is restricted to the CNS, aggrecan and versican are also expressed in connective tissues (Zimmermann and Dours-Zimmermann, 2008). They are formed by a core protein, that is covalently bound to GAGs side chains, and two globular domains at the N- and C-terminals, known as G1 and G3, respectively. Of note, aggrecan display an additional domain, known as G2 domain (Yamaguchi, 2000). Their central domain display variable length and sequence, as well as a different number of putative GAG attachment sites depending on the lectican (Yamaguchi, 2000; Zimmermann and Dours-Zimmermann, 2008). For example, aggrecan has the longest central domain and the most GAG attachment sites while brevican is the shortest and has the less attachment sites for GAGs. The lecticans can be found as CSPGs or as simple glycoproteins, lacking GAGs (Yamaguchi, 2000). All lecticans have been shown to undergo proteolytic cleavage of the central protein by various MMPs and/or a disintegrin and metalloproteinase with thrombospondin motifs (ADAMTS) activity such as aggrecanase (Ferrer-Ferrer and Dityatev, 2018; Howell and

Gottschall, 2012). The lecticans are attached to HA through their N-terminal domain and to the polymeric glycoprotein Tn through their C-terminal domain (Yamaguchi, 2000).

1.1.3 Tenascin (Tn)

Tn are a family of large oligomeric glycoproteins containing 5 members in mammals, namely TnC, TnR, TnX, TnN (or TnW), and TnY. Among them, TnR and TnC are predominantly expressed in the CNS, with TnR being the sole expression (Jakovcevski et al., 2013; Joester and Faissner, 2001). TnR expression persists in the adult brain while the expression TnC decreases with brain development (Ferhat et al., 1996; Nörenberg et al., 1996). All Tn glycoproteins follow the same prototypical structure. It is composed a Tn assembly domain at the N-terminus, followed by epidermal growth factor-like repeats and a variable number of fibronectin type III repeats, and a fibrinogen-like domain at the C-terminus (Joester and Faissner, 2001). Through oligomerization of their N-terminal domains, TnC and TnR form, in native conditions, hexamer and trimer, respectively (Jones and Jones, 2000; Nörenberg et al., 1996). Tn bind to several cell surface components such as integrins, HSPGs (e.g. syndecans and lypicans), cell adhesion molecules of the immunoglobulin family, but also to components of the ECM, and more particularly to lecticans (Yamaguchi, 2000). Notably, the interaction between the G3 domain of lecticans and the fibronectin type III repeats 3-5 domains of the hexameric TnC and tetrameric TnR mediates the crosslinking of lecticans (Lundell et al., 2004). TnR is an essential component of the perineural net (PNN), a highly condensed ECM lattice enriched in lecticans and link proteins that surrounds somata, primary dendrites and the axon initial segment (AIS) of paravalbumin-expressing interneurons (Dityatev et al., 2007; Suttkus et al., 2014).

1.1.4 Link proteins

Hyaluronan and proteoglycans binding link protein (HAPLN) are stabilizing proteins. They consist in 4 members (HAPLN1-4). Their structure is similar to the one of the globular G1 domain of the lecticans. Their role is to reinforce the interaction between HA and the lecticans. This functional relationship between the lecticans and the link protein is reflected genetically as each of the HAPLN-encoding gene shares the same locus with one of the four lectican gene. They form 4

HAPLN-CSPG pairs of genes: HAPLN1-versican, HAPLN2-brevican, HAPLN3-aggrecan, and HAPLN4-neurocan (Spicer et al., 2003). However, this configuration is most likely the result of genetic duplications events that occurred during evolution, and does not imply co-expression or binding preferences (Spicer et al., 2003; Zimmermann and Dours-Zimmermann, 2008).

1.2 Architecture of the interstitial matrix: the HLT model

The interaction of the different components of the ECM leads to the formation of a meshwork where HA acts as a backbone. Following the hyaluronan-lectican-tenascin (HLT) model proposed by (Yamaguchi, 2000), the growing HA chain is extruded from the cell into the ECS where it associates with lecticans and link proteins, with the latter stabilizing the HA-lectican complexes (figure 26). Furthermore, the lectican interacts with one of the subunits of the tenascin oligomers. A single tenascin oligomer will be able to bridge up to 3 (TnR) or 6 (TnC) HA/lecticans complexes, leading thus to the formation of a ternary complex and an ECM lattice. Following the HLT model, changes in one of the components (e.g. length of the lectican core protein, tenascin subtype, etc.) will change the density of the ECM lattice. Additionally, changes in the lectican subtype or in HA-MW will modify the amount of attracted water and subsequently changes the properties of the ECM lattice.

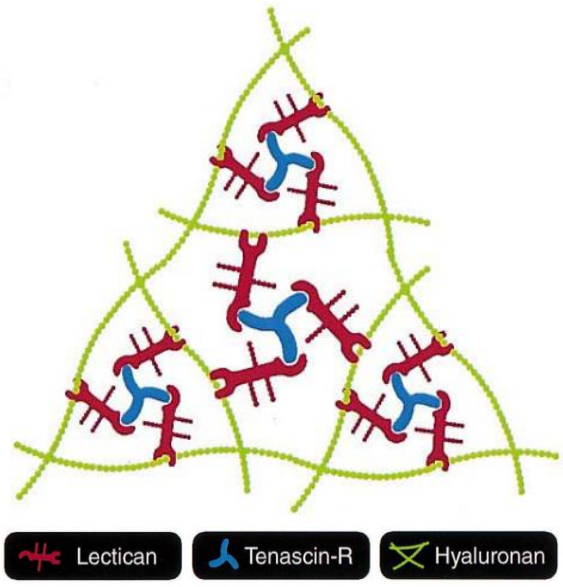

Figure 26. The HLT model. *Components of the ECM (hyaluronan or HA, tenascin, and lectican) form a ternary complex and en ECM lattice. Adapted from (Yamaguchi, 2000)*

2. ECM in brain development

2.1 ECM composition during brain development

The ECS occupies, in average, 40 % of the P2-P3 rat brain, and progressively decreases to reach adult level (~ 20 %) at P23 (Lehmenkühler et al., 1993). This initially large ECS fraction in the immature brain may be secondary to its structural immaturity, with few both dendritic arborizations and glia processes, and thus more matrix to maintain the structural integrity of the brain. Over the course of brain development, starting around the second postnatal weeks in rodent, changes in the composition of the ECM have been observed (Zimmermann and Dours-Zimmermann, 2008). The juvenile CNS, enriched in HMW-HA, the lecticans neurocan and versican V1 splice variants, TnC as well as the link protein HAPLN1 are being replaced by a mature type of matrix enriched in the homologous set of proteins brevican, versican V2 splice variant, TnR and HAPLN2 and 4 (Rauch, 2004; Zimmermann and Dours-Zimmermann, 2008). In the rat brain, the amount of HA increase during the early stages of development to reach a maximum around 7 days after birth, and then slowly decline to adult levels (Jenkins and Bachelard, 1988; Margolis et al., 1975; Polansky et al., 1974; Takechi et al., 2020) (figure 27). The HA content will then remain constant during adulthood before increasing in old brains (Cargill et al., 2012; Reed et al., 2018). Similar to changes in HA quantity, the size of HA chain is also developmentally regulated (figure 27). The expression pattern of the HAS isoforms is not homogeneous and will depends on both the CNS region and the developmental stage. In rat cortical areas, HAS3 is highly expressed during embryonic development while HAS2, which produce the longest HA chain, peaks around birth when the HA content is the highest. On the other hand, the expression of HAS1 steadily increases during the postnatal period (Takechi et al., 2020). It can thus be hypothesized that HA of different sizes play different roles in development. This is supported by evidences that HAS2 global knockout is lethal at embryonic stage whereas the loss of either HAS1 and HAS3 is viable, with no obvious developmental defects (Arranz et al., 2014; Camenisch et al., 2000; Kessler et al., 2015). It is however possible that the loss of one HAS isoform is compensated by the others (Hayashi et al., 2019). Although all 3 HAS isoforms are expressed in the neocortex, it is only the loss of either HAS3

and HAS2 that reduces the HA content in both the hippocampus and cortex and resulted in seizures (Arranz et al., 2014). Importantly, this differential expression of the different components of the ECM is conserved in vitro in cortical cultures. Indeed, both CSPGs and HA are found at the earliest stages of brain development *in vivo*, and are detected in cortical cultures around cell bodies and neurites before the formation of PNN (Deepa, 2006; Fowke et al., 2017), and the differential expression of the HAS isoforms during development is also conserved in culture (Fowke et al., 2017)

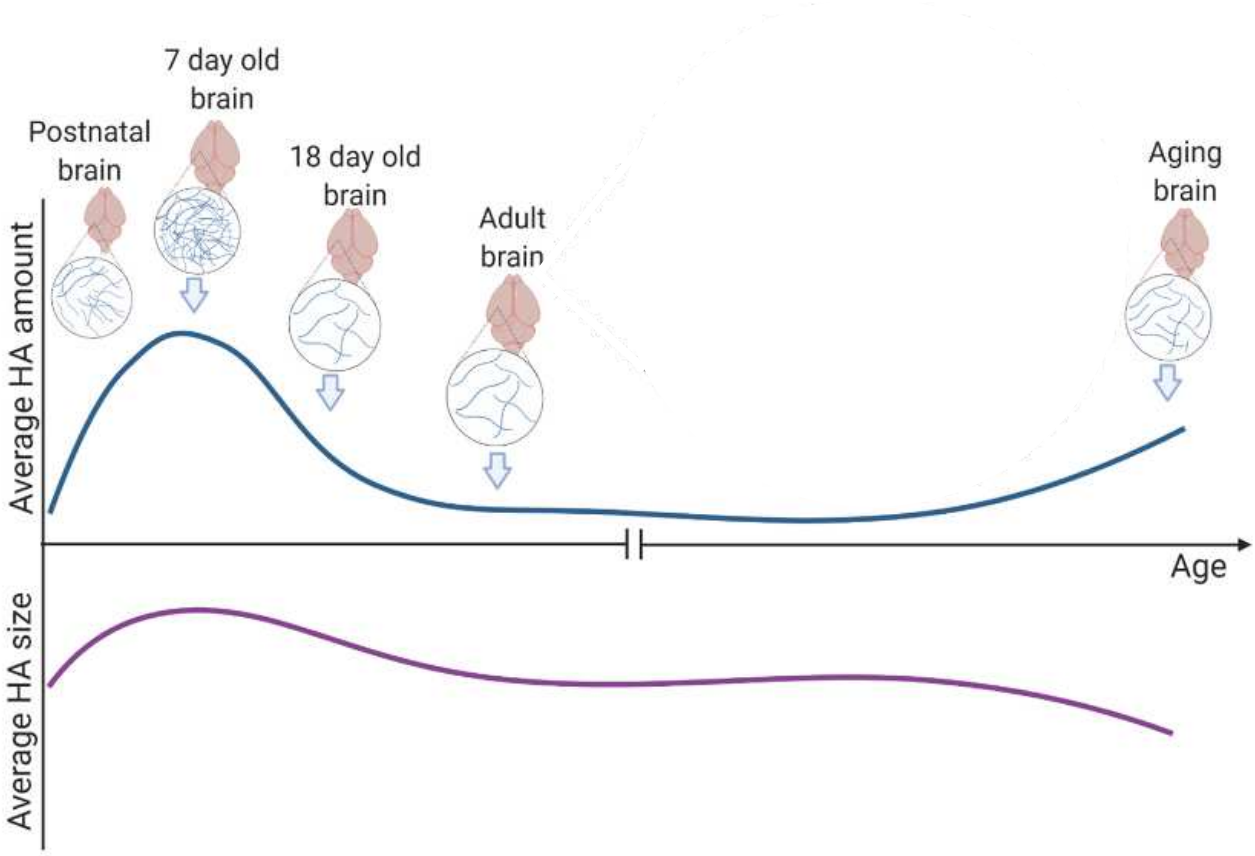

Figure 27. HA amount and size during rodent brain development and aging. *Both the average size and amount of hyaluronic acid (HA) are maximal early during brain development. Adapted from (Zakusilo et al., 2021)*

2.2 PNN formation and closure of the critical periods of brain development

It is widely accepted that the initial and relatively loose juvenile matrix will be replaced by a firmer mature form of meshwork that will be maintained during adulthood (Zimmermann and Dours-

Zimmermann, 2008). One classical example for such remodeling is the formation, between the second and the fifth week after birth in rodent, of the well-studied PNN which appearance coincides with the closure of the critical brain plastic window (Carulli and Verhaagen, 2021). Interestingly, the timeline of maturation of PNN, which is dependent on neuronal activity, as well as its composition (e.g. HA, TnR and lecticans) are conserved in vitro in neuronal culture (Carulli et al., 2006; Dityatev et al., 2007). It is well accepted that the formation of this condensed ECM structure, that surrounds the somata, primary dendrites and the AIS of GABAergic interneurons, acts as a developmental brake on synaptic plasticity. In particular, this was suggested by evidences that injection in the adut brain of chondroitinase ABC, which degrades CSPGs, can restore or enhance plasticity to the levels of juvenile animals (Pizzorusso et al., 2006, 2002), and that it could allow for regeneration mechanisms following brain or spinal cord injury (Bradbury et al., 2002; Moon et al., 2001). Similar mechanisms have been shown in the amygdala where the maturation of PNN is responsible for closing a developmental window during which fear memories can be erased (Gogolla et al., 2009). Complementarily, mice lacking PNN (e.g. obtained by knocking-out either the link protein HAPLN1 or the lectican aggrecan) display a protracted critical plasticity window (Carulli et al., 2010; Rowlands et al., 2018).

2.3 Progenitor proliferation and differentiation

Several components of the ECM, and in particular laminins, lecticans and HSPGs (e.g. glypicans, syndecans, and perlecans), can modulate or promote progenitor proliferation either directly or through integrins-mediated signaling (Long and Huttner, 2019). Furthermore, changes in the ECM have been proposed to have participated in the greater expansion of the human neocortex during evolution (Fietz et al., 2012). Even if the role of HA in regulating ECM brain stiffness is not clearly understood, changes in the quantity and size of the HA chains would affect the viscoelasticity properties of the brain matrix (Tønnesen et al., 2023). Modulating in vitro, through hydrogels, the stiffness of the matrix affects progenitor cell fate and cell morphology (Engler et al., 2006; Georges et al., 2006; Seidlits et al., 2010). In a loose hydrogel matrix, that mimics the one of developing immature brain, progenitor preferably differentiate into neurons and display a branched morphology while increasing the matrix stiffness lead to decreased branching and more glia cells (Georges et al., 2006; Seidlits et al., 2010).

2.4 Neurite outgrowth and axon guidance

The activation or inhibition of neurite outgrowth is dependent on the composition of the ECM (e.g. presence of GAGs) and on the cell type. Laminins, through their adhesion to integrins and subsequent induction of intracellular signaling, are considered as one of the strongest promoters of neurite growth (Letourneau et al., 1992; Long and Huttner, 2019; Myers, et al., 2011). Furthermore, laminin substrates provide guidance cues for growing axons *in vitro* (Myers, et al., 2011). All four lecticans are widely accepted to inhibit neurite sprouting (Yamaguchi, 2000). HA, which is part of the interstitial ECM and can also form a pericellular coat (Evanko et al., 2007) promotes neurite extension (Kultti et al., 2006; Rilla et al., 2008; Takechi et al., 2020). The synthesis of HA alone promotes, in non-neuronal cell types, the formation of membrane protrusions or villi (Kultti et al., 2006; Rilla et al., 2008). Inhibiting the activity of the HAS impairs neurite outgrowth in cortical neurons *in vitro* (Takechi et al., 2020). It is thus possible that such coating is also present around neuronal cells where it promotes growth cone formation and extension. HA can act directly or indirectly by inducing receptor-mediated signaling (e.g. through CD44 and RHAMM). CD44 and/or RHAMM have been identified as mediating the roles of HA on plasma membrane protrusion (Oliferenko et al., 2000) and dendrite development (Nagy et al., 1995; Skupien et al., 2014), synapse morphology (Roszkowska et al., 2016) as well as astrocyte branching (Konopka et al., 2016). Thus, ECM participate in axon guidance and growth cones would retract from the lectican-containing zones (Schmalfeldt et al., 2000) whereas other regions, rich in laminins for example, could be attractive. The glycoprotein reelin plays a critical role on brain development, and in particular on growth cone motility (Leemhuis et al., 2010). The role of reelin have been highlighted in the *Reeler* mouse, whom is lacking expression of reelin, and display lamination defects due to defects in cell migration and a disorganized architecture in the cerebellum, cortex, and hippocampus as well as defective dendritic development (Ferrer-Ferrer and Dityatev, 2018; Niu et al., 2004).

2.5 Synapse formation and post-synaptic maturation

For the molecules thrombospondins, glypicans, SPARCL1, pentraxins, Cbln and C1q-like, and Lgi1 , please refer to chapter 2.

Agrin. Agrin is a HSPG whom cleavage has been proposed to serve as coincidence detector of pre- and postsynaptic activation (Matsumoto-Miyai et al., 2009). Indeed, upon synaptic activation, the presynaptic terminal releases the protease neurotrypsin that cleaves Agrin into a 90 (agrin-90) and a 22 kDa (agrin-22) fragment. The agrin-22 fragment has been shown to promote the formation of postsynaptic filopodia in a NMDAR-dependent manner. Interestingly, a link can be made with a polysialylated form of neural cell adhesion molecule (NCAM), which is known to promote synaptogenesis and synapse stabilization during development, as its activity is mediated by the binding of HSPG in a NMDAR-dependent manner (Dityatev et al., 2004).

Laminins and their receptor integrins. Laminins are glycoproteins that formed heterotrimeric chains of laminin-α, -β, and -γ. Laminins have been shown to regulate brain development, including progenitor proliferation (Long and Huttner, 2019). Laminins have been shown to stabilize spines. Indeed, knocking-out laminin-α5 expression in hippocampal neurons have been shown to reduce the number of dendritic spines (Omar et al., 2017).

Reelin. The glycoprotein reelin, which is produced by GABAergic interneurons (Campo et al., 2009), stimulates the formation of spines. Indeed, null mice (or *reeler* mice) display a reduced number of spines (Niu et al., 2008) whereas mimicking the action of reelin, that was obtained by overexpressing one of its receptor, had an opposite effect (Dumanis et al., 2011). Interestingly, it has been shown that the synaptic content in reelin increases during development. During neuronal maturation, reelin favors the development-associated shift in NMDAR (Groc et al., 2007a) as well as the insertion of AMPAR in the adult hippocampus (Qiu et al., 2006), leading to an hypertrophy of the dendritic spines and an enhanced LTP (Pujadas et al., 2010).

Hyaluronic acid (HA). HA have been shown to affect both the number and morphology of excitatory synapses. It has been shown that treating neuronal spheroids with exogeneous hyaluronidase increase the number of excitatory synapses, while the number of inhibitory remained unchanged, resulting in neural network hyperactivity *in vitro* (Wilson et al., 2020). On the other hand, downregulating CD44, one of the receptor of HA, alters the morphology of dendritic spines which were shown to be thinner and longer (Roszkowska et al., 2016). Lastly, digesting HA has been shown to increase the excitatory synaptic content in GluN2B-containing NMDAR (Schweitzer et al., 2017). Collectively, these results suggest that HA is important for the maturation and the structural integrity of dendritic spines.

3. Local diffusion

Diffusion, defined as the random movement of molecules driven by Brownian motion, is the primary mechanism governing the movement of molecules in aqueous solutions, including synaptic ECS (Syková and Nicholson, 2008; Tønnesen et al., 2023). As a result, the regulation of diffusion is critical for neural function and brain development. Four key factors regulate diffusion: (1) the geometry of the ECS, (2) the viscosity of the ISF and interactions with ECM components, (3) interactions with membrane components, and (4) electrochemical gradients (Syková and Nicholson, 2008; Tønnesen et al., 2023). In this discussion, I will focus on the role of the ECM in regulating diffusion. The interstitial ECM, particularly HA, plays a significant role in brain diffusion. HA is anchored to cell membranes and can also be released into the surrounding medium (ECS), modifying its viscosity (Tian et al., 2013; Toole, 2004, 2001; Zhao et al., 2023). Additionally, HA's negative charge allows it to potentially interact with positively charged soluble molecules and membrane components (Toole, 2004, 2001). Studies in HAS3 knock-out animals have shown that diffusion is substantially altered despite normal PNN formation (Arranz et al., 2014). Several studies have corroborated this by demonstrating changes in diffusion and viscosity after hyaluronidase treatment (Godin et al., 2017; Grassi et al., 2023; Soria et al., 2020). This highlights the role of the ECM and its local composition as a key regulator of the movement of molecules, including synaptogenic factors, secreted into the ECS. These molecules diffuse through the ECS

until they reach their targets or are sequestered by the ECM. It remains unclear whether the ECM density and structure are uniformly distributed throughout the brain or are locally regulated in specific regions, such as the synaptic cleft as suggested by (Paviolo et al., 2022). They observed higher diffusivity within a 500 nm radius from synapses in comparison to the "extrasynaptic" compartment (Paviolo et al., 2022). Yet, it has been shown that the synaptic organizer pentraxin-3, secreted by astrocytes into the ECS, must bind locally to the ECM to cluster AMPA receptors and promote synapse formation (Fossati et al., 2019). Digestion of the ECM by hyaluronidase is sufficient to disrupt the effects of pentraxin-3 (Fossati et al., 2019).

4. ECM and neuronal activity

The active participation of astrocytes has leaded to the widely accepted concept of tripartite synapse, which includes the pre- and postsynaptic terminals as well as astrocytes that make intimate contacts with the synaptic structures and shape synaptic activity (Allen, 2014; Chung et al., 2024). An extension of this concept toward the "tetrapartite" synapse, which includes the ECM, have been proposed based on the action of the various ECM components in shaping synaptic plasticity (Dityatev et al., 2010; Dityatev and Rusakov, 2011; Dityatev and Schachner, 2003; Ferrer-Ferrer and Dityatev, 2018). This model is based on the role of the ECM on synaptic biology. In particular, the ECM is critical for the formation and stabilization of synapses either directly or through their receptor (e.g. integrins) which are coupled to the cytoskeleton. The ECM also interacts with surface neurotransmitter receptors and ion channels, tuning their dynamics and organization (Frischknecht et al., 2009; Schweitzer et al., 2017). This space-filling meshwork imposes constraints both on receptor surface diffusion and the structure of dendritic spines (Frischknecht et al., 2009; Roszkowska et al., 2016; Schweitzer et al., 2017; Yang et al., 2012). Furthermore, the ECM appears highly dynamic, undergoing permanent activity-dependent remodeling, which involves cleavage by proteolytic enzymes or direct recycling, which together allow for synaptic plasticity (Dankovich et al., 2021; Ferrer-Ferrer and Dityatev, 2018).

5. Naked-mole rat and naked mole rat hyaluronic acid

Naked mole rats (NMR) (figure 28), *heterocephalus glaber,* are rodents native to the regions of northeast Africa (Ethiopia, Somalia, and Kenya). They are eusocial mammals that live in large colonies (up to 300 members) of overlapping litters in which typically one female and up to 4 males breed whereas the rest are non-breeding helpers maintaining and protecting the colony (Buffenstein et al., 2012). NMR are strictly subterranean, inhabiting underground sealed mazes of tunnels and chambers. Such subterranean lifestyle protects NMR from predation but constitutes, on the other hand, a very challenging environment as the atmosphere is considered as both hypoxic (10 – 15 % oxygen) and hypercapnic (~ 5 – 10 % CO_2)(Buffenstein et al., 2012). To overcome the challenges of subterranean lifestyle, the NMR have evolved unique adaptations. NMR are well-known for their lifespan and healthspan. Indeed, they live approximatively 30 years in captivity which is 5 times longer than predicted for a ~40 g rodent and around 9 times longer than a mouse of a similar size (Buffenstein, 2008; Buffenstein and Jarvis, 2002). They show attenuated age-associated physiological decline and no age-associated increase in mortality risk (Buffenstein, 2008; Ruby et al., 2018). Furthermore, cancer and degeneration are very rare in NMR (Edrey et al., 2013).

Figure 28. The African Naked Mole Rat. *Photograph of a colony of naked mole rat. Adapted from (Buffenstein et al., 2012)*

One of the possible explanations is that NMRs are among the few neotenous mammal species. Neoteny, or retention of juvenile features, has first been mentioned for the NMR based on the resistance of NMR adult hippocampal neurons to anoxia in comparison to other rodents where it drastically decreases with age (Skulachev et al., 2017). One of the reason of this resistance is the retention, in the adult NMR brain, of high level of the GluN2D-NMDAR subtype whereas GluN2D-

NMDAR expression decreases in mice with brain development (Peterson et al., 2012). Furthermore, NMR brain development is largely protracted (Orr et al., 2016; Penz et al., 2015). The maturation of the hippocampus is completed in adults of 8 – 10 years of age (Penz et al., 2015). Such extension of the developmental period may further permit resilience to degeneration. The molecular mechanisms responsible for these properties are however still unclear. Among the few possible explanations, it has been hypothesized that the underground habitat of the NMR generate HA with very high molecular weight (vHMW-HA) (Tian et al., 2013). It is accepted that producing vHMW-HA modifies the elasticity and flexibility of the NMR skin, allowing them to move in narrow tunnels. Although there are discrepancies in the measured size of NMR-HA polymer depending on the methodology, the observed size of NMR-HA was systematically higher than in mouse and/or guinea pig tissues (Del Marmol et al., 2021; Tian et al., 2013), including in the brain (Tian et al., 2013). The formation of vHMW-HA is due to two point mutations (N178S and N301S) in the active site of the HAS2 enzyme (Tian et al., 2013), which already produce the longest HA chain. A recent report showed that the formation of vHMW-HA is a common feature of underground rodents which therefore suggest such properties has evolved with a subterranean lifestyle (Zhao et al., 2023). Importantly, all this underground rodent species share the mutation at the 301 residues (Faulkes et al., 2015). vHMW-HA is characterized by an increased size and viscosity (Kulaberoglu et al., 2019; Zhao et al., 2023). HA extracted from NMR brain form voluminous cloud-like supercoiled structures (Kulaberoglu et al., 2019). Both the volume fraction and diffusion permeability to macromolecules, but not of small molecules, are reduced in NMR compared to rat brain in normoxic conditions which therefore suggest higher diffusion hindrance in the NMR ECS (Thevalingam et al., 2021). Importantly, the expression of vHMW-HA promotes the cancer resistance and longevity properties of NMR and its sole expression is sufficient to export both NMR properties into another rodent (Tian et al., 2013; Zhang et al., 2023). Similarly, reproducing the NMR brain ECM by injecting hydrogel were shown to be sufficient to reduce the load of Aβ and to improve the cognitive functions in a mouse model of Alzheimer disease (Zhao et al., 2022).

Objectives of the thesis

NMDAR strongly contributes to the synaptogenesis phase. They are among the first receptors to accumulate at the site of axodendritic contact, forming the so-called “silent” synapses that contain no/few labile AMPAR. Thanks to the development of super-resolution imaging techniques, it is well accepted that glutamate receptors, including NMDAR, must be “at the good place at the good time”. In mature neurons, once inserted at the plasma membrane laterally diffuse within the membrane plane and eventually enter synapses where they are organized into nanodomains. On the other hand, in immature neurons receptors are highly “unstable”. They are both constantly cycling between intracellular and membrane compartments and highly diffusive within the membrane plane. While it is well accepted that NMDAR’ organization at synaptic contacts is dependent on their transient anchoring to scaffolding proteins, the mechanisms allowing for their organization at immature ones, which are not yet equipped with strong scaffold apparatus, remain unclear. Since surface diffusion of surface molecules is modulated by reversible binding to intracellular, transmembrane, or extracellular components we set-out to investigate the role of the transmembrane (part 1) and extracellular components (part 2) in this context, focusing on the early mechanisms allowing for the surface organization and clustering of NMDAR.

Part 1 Evidence that NMDAR can also interact with other surface macromolecules, including receptors, and that those interactions can shape the surface diffusion and the organization of NMDAR has promoted the possibility that surface protein-protein interaction (PPI) represents a potent way to cluster NMDAR. We therefore set out to investigate the role of PPI, taking the prototypic D1R and GluN1-NMDAR couple as model, in the organization of NMDAR during neuronal maturation. To this end, we used a combination of confocal and super-resolution microscopy approaches to explore the regulation of the D1R-GluN1-NMDAR interaction itself in developing hippocampal neuronal cultures and the roles of the interaction on both GluN1-NMDAR organization and glutamatergic synaptogenesis. In particular, we focused on several questions:

Can we directly observe the interaction between D1R-GluN1-NMDAR in live hippocampal neurons? We collaborated with the team of Dr. Jean-Baptiste Sibarita to develop a super-resolution imaging, namely multidimensional spectral single localization

microscopy (MS-SMLM), approach to directly observe D1R-GluN1-NMDAR oligomerization and hence, resolve its kinetics and stability.

Is D1R-GluN1-NMDAR interaction developmentally regulated? MS-SMLM as well confocal imaging were used at two developmental stages, referred as immature and mature, to resolve the stability of D1R-GluN1-NMDAR interaction.

What are the intracellular regulatory mechanisms involved in mediating D1R-GluN1-NMDAR interaction? We investigated the role of neuronal activity and of potential intra-cellular signaling molecules (e.g. kinases) on D1R-GluN1-NMDAR interaction.

Is D1R-GluN1-NMDAR interaction shaping the functional (nano)-organization of NMDAR? To this end, we used different strategies to modulate, both positively and negatively, the interaction between D1R and GluN1-NMDAR. We used previously available techniques to disrupt the interaction and developed a strategy aiming at increasing the interaction between D1R-GluN1-NMDAR. Using these approaches, we evaluated the effects of the interaction on GluN1-NMDAR functional clustering using confocal and super-resolution imaging as well as calcium imaging.

Is D1R-GluN1-NMDAR interaction important for glutamatergic synaptogenesis? We chronically modulated, either preventing or enhancing, for several days, the interaction between D1R and GluN1-NMDAR at different developmental time windows and assessed the number of glutamatergic post-synapses.

Part 2 The ECM, a hygroscopic meshwork of macromolecules that surrounds every cell, and in particular the HA, is well known to hinder the surface diffusion and clustering of membrane macromolecules. Moreover, the fact that HA, which is a major component of the interstitial ECM but also tethered to cell membranes, is enriched early during brain development leaded to the hypothesis leaded to the hypothesis that HA could shape the organization of NMDAR during development. However, classical approaches, including in vitro, have focused on degrading the matrix through the addition of exogenous hyaluronidase. Herein, we set out to investigate the role of HA on the surface organization of NMDAR by both reducing and enhancing its content. In particular, we focused on several questions:

Can we modulate HA content and size? To this end, we aimed at both decreasing, through exogenous hyaluronidase, or increasing the ECM content in HA as well as to modulate the length of the polymer. To enhance HA both content and size, we developed plasmids that encode for the rat HAS2 (which produces HMW-HA), either in its wild-type form or bearing the two mutations that have been described as responsible for the production of vHMW-HA in the NMR.

Is HA important for NMDAR (nano)-organization and lateral diffusion? We used confocal as well as dSTORM and PALM imaging to assessed the role of HA on the organization and surface trafficking of GluN1-NMDAR following HA acute digestion or long-term enhancement.

Is HA important for neuronal development and maturation? We assessed the development of both spines and the dendritic arbor after enhancing the content and size in HA.

Result 1. Non-canonical interplay between D1R and GluN1-NMDAR tunes synaptogenesis

Detailed author contributions with respect to the other co-first authors, in addition to the author contributions outlined on page 19 of the paper.

Nathan Bénac, *co-first author*, performed and analyzed the data of the following experiments:

MS-SMLM experiments presented in fig. 2c-f together with Ezequiel G. Saraceno (G.E.S) and in fig. 3d-e together with G.E.S. and Mar Petit-Pedrol (M.P.P.).

Immunocytochemistry experiments presented in fig. 2b, fig. 3a, b, f, fig. 4a-g, fig. 5a, b, g, fig. 6g-h, supplementary fig. 3, supplementary fig. 4a, b, c, g, h, supplementary fig. 6a, b, d, supplementary fig. 7a, b, c, supplementary fig. 8c, d.

Immunohistochemistry experiment presented in fig. 6i

Microfluidic culture presented in fig. 6j-n and supplementary fig. 8e-g.

FLIM-FRET experiments presented in supplementary fig. 2c-f and supplementary fig. 3d-f.

Western-Blots from neuronal cultures or hippocampi homogenates presented in supplementary fig. 2a-b, supplementary fig. 5a-b.

dSTORM experiments presented in fig. 5c, d, e, f, h and supplementary fig. 6c.

Calcium imaging experiments presented in fig. 5i-k.

Corey Butler, *co-first author*, built the SM-SMLM microscope together with Remi Galland (R.G.) and Jean-Baptiste Sibarita (J-B.S.) and helped in designing the analysis pipeline. The original publication is (Butler et al., 2022).

Gustavo Ezequiel Saraceno, *co-first author*, performed and analyzed the data of the following experiments:

MS-SMLM experiments presented in fig. 2c-f together with N.B. and in fig. 3d-e together with N.B. and M.P.P.

Quantification presented in fig. 3g while the images in fig. 3f were acquired by N.B.

IHC experiments presented fig. 6a-f.

Other:

The experiments presented fig. 7 were entirely performed by our collaborators Nahoko Kuga, Yuya Nishimura, Taiki Yokoi, Takuya Sasaki, and Yuji Ikegaya.

The experiments presented **fig. 3h-i** were entirely performed by our collaborators Ping Su and Fang Liu.

nature communications

Article

https://doi.org/10.1038/s41467-023-44301-z

Non-canonical interplay between glutamatergic NMDA and dopamine receptors shapes synaptogenesis

Received: 25 March 2023

Accepted: 7 December 2023

Published online: 02 January 2024

Check for updates

Nathan Bénac[1,7], G. Ezequiel Saraceno[1,7], Corey Butler[1,7], Nahoko Kuga[2,3], Yuya Nishimura[2], Taiki Yokoi[3], Ping Su[4], Takuya Sasaki[2,3], Mar Petit-Pedrol[1], Rémi Galland[1], Vincent Studer[1], Fang Liu[4], Yuji Ikegaya[2,5,6], Jean-Baptiste Sibarita[1] & Laurent Groc[1]

Direct interactions between receptors at the neuronal surface have long been proposed to tune signaling cascades and neuronal communication in health and disease. Yet, the lack of direct investigation methods to measure, in live neurons, the interaction between different membrane receptors at the single molecule level has raised unanswered questions on the biophysical properties and biological roles of such receptor interactome. Using a multidimensional spectral single molecule-localization microscopy (MS-SMLM) approach, we monitored the interaction between two membrane receptors, i.e. glutamatergic NMDA (NMDAR) and G protein-coupled dopamine D1 (D1R) receptors. The transient interaction was randomly observed along the dendritic tree of hippocampal neurons. It was higher early in development, promoting the formation of NMDAR-D1R complexes in an mGluR5- and CK1-dependent manner, favoring NMDAR clusters and synaptogenesis in a dopamine receptor signaling-independent manner. Preventing the interaction in the neonate, and not adult, brain alters in vivo spontaneous neuronal network activity pattern in male mice. Thus, a weak and transient interaction between NMDAR and D1R plays a structural and functional role in the developing brain.

Understanding how developing neurons form functional networks underlying brain functions remains a central question in neuroscience. The vast majority of excitatory glutamatergic synapses are formed early in development during the synaptogenesis period. The glutamatergic NMDA receptor (NMDAR) strongly contributes to the early and late phase of synaptogenesis[1,2]. NMDARs are ionotropic glutamate receptor composed of two dimers of subunits, i.e. obligatory GluN1 subunits associated with GluN2 or 3 subunits, that are activated by agonist (glutamate) and co-agonists (glycine or D-serine)[2]. At developing synapses, NMDARs are among the first glutamatergic receptors to be detected, forming the so-called "silent" synapses that contain no/few labile AMPA receptors[3]. The NMDAR clustering constitutes thus an essential nucleation step for the early formation of synaptic sites[4]. Upon their activation at these immature unstable synaptic sites, NMDARs would flux calcium, activate signaling cascades, and stabilize AMPARs and scaffolding proteins. Other signaling molecules, such as

[1]Univ. Bordeaux, CNRS, IINS, UMR 5297, F-33000 Bordeaux, France. [2]Laboratory of Chemical Pharmacology, Graduate School of Pharmaceutical Sciences, The University of Tokyo, 7-3-1 Hongo Bunkyo-ku, Tokyo 113-0033, Japan. [3]Department of Pharmacology, Graduate School of Pharmaceutical Sciences, Tohoku University, 6-3 Aramaki-aoba, Sendai, Miyagi 980-8578, Japan. [4]Campbell Family Mental Health Research Institute, Centre for Addiction and Mental Health, University of Toronto, Toronto, Canada. [5]Center for Information and Neural Networks, Suita City, Osaka 565-0871, Japan. [6]Institute for AI and Beyond, The University of Tokyo, Tokyo 113-0033, Japan. [7]These authors contributed equally: Nathan Bénac, G. Ezequiel Saraceno, Corey Butler.
e-mail: laurent.groc@u-bordeaux.fr

adhesion receptors and gliomediators, have also been identified and investigated for their role in early synaptic assembly, maturation and maintenance[5–9]. Yet, the mechanism underpinning the very early clustering of essential synaptic membrane proteins, such as the NMDAR, remain however rather enigmatic.

The proteins present at the neuronal surface, i.e. the surfaceome, change over the course of brain development, with a high diversity at early stages[10]. Neurotransmitter receptors expressed at the plasma membrane of immature neurons are highly diffusive and poorly confined when compared to mature neurons[3,11,12]. Their cycling between intracellular and membrane pools is also upregulated at early stages[13]. Clustering the highly-diffusive NMDARs at early synaptic contacts would thus require some active and potent processes. Since early synaptic contacts are not yet equipped with intracellular postsynaptic scaffold apparatus[14,15], additional mechanisms are likely to contribute to the NMDAR early clustering. Besides their stabilization by intracellular proteins, NMDARs can directly interact with other surface proteins, including neurotransmitter and neuromodulatory receptors[16]. These surface protein-protein interactions stabilize and cluster NMDARs[16], promoting the possibility that such interactions play a role in synaptogenesis. Some of these interactors have been related to synaptogenesis and synaptic maturation processes, such as dopamine, Ephrin, and neuroligin receptors[17–19]. The dopamine receptor type I (D1R) and NMDAR interact through amino acid sequences located in their respective intracellular C-tails[20,21], and such an interaction strongly control the surface dynamics and distribution of both receptors[22–25]. However, even if the interaction between NMDAR and D1R have been extensively investigated for its functional role[20,23,26–30], precise biophysical characterization of the interaction in native condition is still lacking. Imaging techniques allowing both direct visualization and characterization of protein-protein interactions have been developed in heterologous cells[31–39] but no observation has yet been made in live neurons. Therefore, fundamental questions about their stability, their occurrence and regulation mechanisms must be answered to gain access to their biological roles. To address this key question, we here developed a multidimensional spectral single molecule localization microscopy approach (MS-SMLM) to directly visualize and biophysically characterize the interactions between NMDAR and D1R at the neuronal surface. We specifically investigated whether such putative interaction tunes NMDAR clustering during the period of synaptogenesis.

Results

Direct visualization and quantification of surface receptor-receptor interaction events in live neurons using MS-SMLM

Quantum dots (Qds)-based single nanoparticle experiments have been widely used to track the surface diffusion of receptors because of the pointing accuracy of the single molecule imaging and nanoparticle photostability[40]. We took advantage of these properties to concomitantly investigate the surface dynamics of dopamine receptor 1 (D1R) and GluN1 subunit-containing NMDAR (GluN1-NMDAR) after their labeling with Qds of different wavelengths onto cultured hippocampal neurons (Fig. 1a). We set a custom spectral microscope with a 4Pi configuration for versatile (2D + t + λ) MS-SMLM (Fig. 1b, c). Schematically, it is composed of two inverted microscope bodies precisely aligned one on top of the other: i) the bottom microscope performs state-of-the-art (2D + t) SMLM (here referred as “spatial”) equipped with an azimuthal TIRF/HiLo illumination device, and ii) an upper microscope for spectral (λ) characterization using photons usually lost in traditional mono-objective configurations. The two microscopes were precisely aligned by translating the bottom microscope using a (x, y, θ, φ) stage placed below the bottom microscope. Such a geometry allows to perform 2D-localization using all photons collected by one high numerical aperture (NA) TIRF objective (×100 Oil, NA1.49) and determine the spectral signature of the detected fluorophores using a second high-NA objective (×60, Water Dipping NA1) without compromising the localization performances. Two synchronized sensitive EMCCDs cameras allow the tracking of the bright Qds across the entire field of view of the EMCCDs (nearly 80 μm × 80 μm @ 30 Hz) using conventional filter sets and dichroic mirrors[41] (Fig. 1b). The precise localization (below the diffraction limit ~200 nm) of overlapping single emitters of each receptor (each receptor-Qd complexes were set at equivalent density) was determined using spectrally-informed multi-Gaussian fitting (Supplementary Fig. 1). This fitting allow us to estimate the lowest as possible distance between different emitters with a multi-fit error of 56 nm[41]. However, since we used a complex of antibody and Qd to track receptors, we arbitrarily set the search distance for putative interaction using the common cut-off of 100 nm (Fig. 1a)[34].

Transient events in which surface GluN1-NMDAR and D1R closely confine (i.e. below our search distance of 100 nm) were repetitively observed over time throughout the dendritic tree (Fig. 1d; Supplementary Fig. 1). These events were tracked over time and isolated (Fig. 1d, e). To define whether such an event was based on random colocalizations or specific interactions, we monitored the behavior of GluN1-NMDAR with either D1R wild-type (D1R-wt) or a truncated D1R in which the T2 sequence involved in the interaction was genetically deleted (Fig. 2a) as we expected both the occurrence and the duration of the events to be affected upon true interaction. Moreover, the reduced colocalization of D1R-dT2 and GluN1-NMDAR (defined as the fraction of GluN1 cluster area that overlap with D1R cluster) was also confirmed in hippocampal neurons through live surface immunostaining (Fig. 2b). The occurrence of interacting event in presence of D1R-dT2 was significantly reduced. In the control condition, 30% of the receptor localizations were interacting whereas it was decreased to 19% for GluN1-D1R-dT2. Furthermore, the average lifetime of the GluN1-NMDAR-D1R-dT2 interaction was significantly lower whereas the estimated dissociation rate or K_{off} was significantly increased (Fig. 2c–f). However, the observed lifetime of the non-interacting tracks i.e. monomers remained unaltered in all conditions (Fig. 2d). The mean lifetime and estimated K_{off} of GluN1 homodimers were also not altered by the presence of either D1R-wt or D1R-dT2 (Fig. 2d–f). These data indicated that our MS-SMLM approach is able to probe interactions between surface receptors in live neurons. The average lifetime of GluN1-NMDAR/D1R was 130 ± 0.01 ms and the estimated K_{off} was 13 ± 0.7 s^{-1}. Spatially, D1R-GluN1-NMDAR interactions were highly labile and seem to occur randomly onto the dendritic shaft with no evidence of dedicated interaction hot spots (Supplementary Fig. 1d), therefore highlighting the stochastic nature of the interaction.

Because the GluN2A subunit also interact with the D1R C-tail through the T3 sequence (GluN2A-NMDAR::D1R)[20], we tested the putative role of such sequence on the GluN1-NMDAR-D1R interaction. For this, we used Förster Resonance Energy Transfer (FRET) imaging on COS-7 cells that express either GluN1-GluN2A (T2 and T3 domains) or GluN1-GluN2B (T2 only) subunits. We observe no differences in the GluN1-NMDAR-D1R FRET signals between these conditions, suggesting that the T3 domain has a negligible role (Supplementary Fig. 2). Furthermore, the TAT-T2 competing peptide disrupted the interaction between GluN1-NMDAR and D1R[20,23] whereas the TAT-T3 competing peptide failed to do so when compared to the TAT-non sense sequence (TAT-NS) (Supplementary Fig. 2). Thus, it appears that the T2 sequence plays a major and dominant role in the NMDAR-D1R interaction.

GluN1-D1R interaction is increased in immature neurons in a CK1- and mGluR5-dependent process

Synaptogenesis is an intense and rapid phase that starts during the second week in cultured hippocampal neurons and during the first postnatal weeks in rodents. We defined two time-windows based on the developmental stages, i.e. the number of synapses, of hippocampal neurons, referred as “immature” and “mature”: the immature window

https://doi.org/10.1038/s41467-023-44301-z

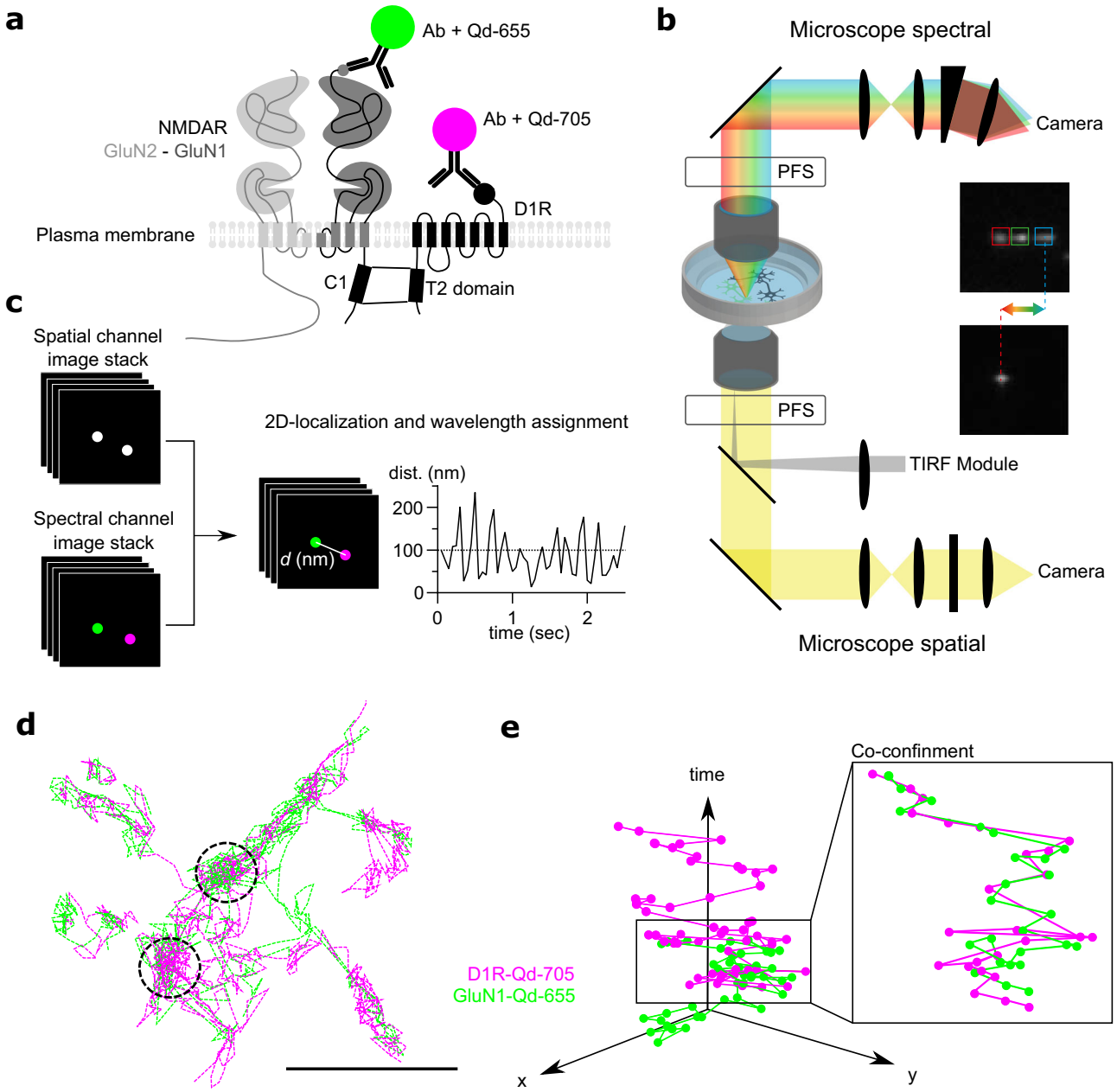

Fig. 1 | Multidimensional spectral single molecule localization microscopy (MS-SMLM) principle. a Experimental design of the single Qd tracking. Receptors were labeled with antibodies directed against extracellular tags. Qd-655 and Qd-705 were used to distinguish receptor types. The interaction between receptors occurs intracellularly at the T2 domain (C1 cassette of the GluN1 subunit). **b** Microscopy setting to perform MS-SMLM using two microscopes and cameras. PFS: perfect focus system. **c** SM-SMLM principle. **d** Representative reconstruction of GuN1-NMDAR and D1R surface diffusion, scale bar, 1 μm. **e** Example trajectories of one GluN1-NMDAR and one D1R laterally diffusing (x, y) onto the neuronal surface over time.

corresponds to days in vitro (DIV) 7 to 9 at the beginning of the synaptogenic period whereas the mature one (DIV 15 and above) corresponds to the end of the period (Fig. 3a, b). Both MS-SMLM imaging and immunocytochemical labeling demonstrated both qualitative and quantitative changes in the interaction properties between GluN1-NMDAR and D1R across development. The observed average lifetime of D1R-GluN1-NMDAR heteromers was significantly decreased at the mature stage compared to the immature one and the estimated K_{off} were significantly higher at the mature stage when compared to the immature one. However, the observed average lifetime of the non-interacting tracks or monomers remained unchanged (Fig. 3d), highlighting the specificity of the interaction change. This observation at the single receptor level was confirmed by the immunolabelling of surface D1R and GluN1-NMDAR since they highly colocalized at immature stage but rarely at mature one (Fig. 3f). We further ascertained this observation by measuring the in vivo level of D1R-NMDAR complex using co-immunoprecipitation assay with an efficient antibody directed against the GluN2A subunit (no current efficient antibody against GluN1 subunit for such Co-IP) (Fig. 3h). The level of co-immunoprecipitated D1R-GluN2A subunit complex in the rat hippocampus was twice higher at postnatal day (P) 8 when compared to P36 animals. This change was specific to the D1R-NMDAR complex as the previously defined D2R-GluN2B-NMDAR[42] complex level was unchanged across development (Fig. 3i). Collectively, these data indicate the surface interactions between GluN1-NMDAR and D1R are differentially regulated during neuronal development. This increased interplay was

https://doi.org/10.1038/s41467-023-44301-z

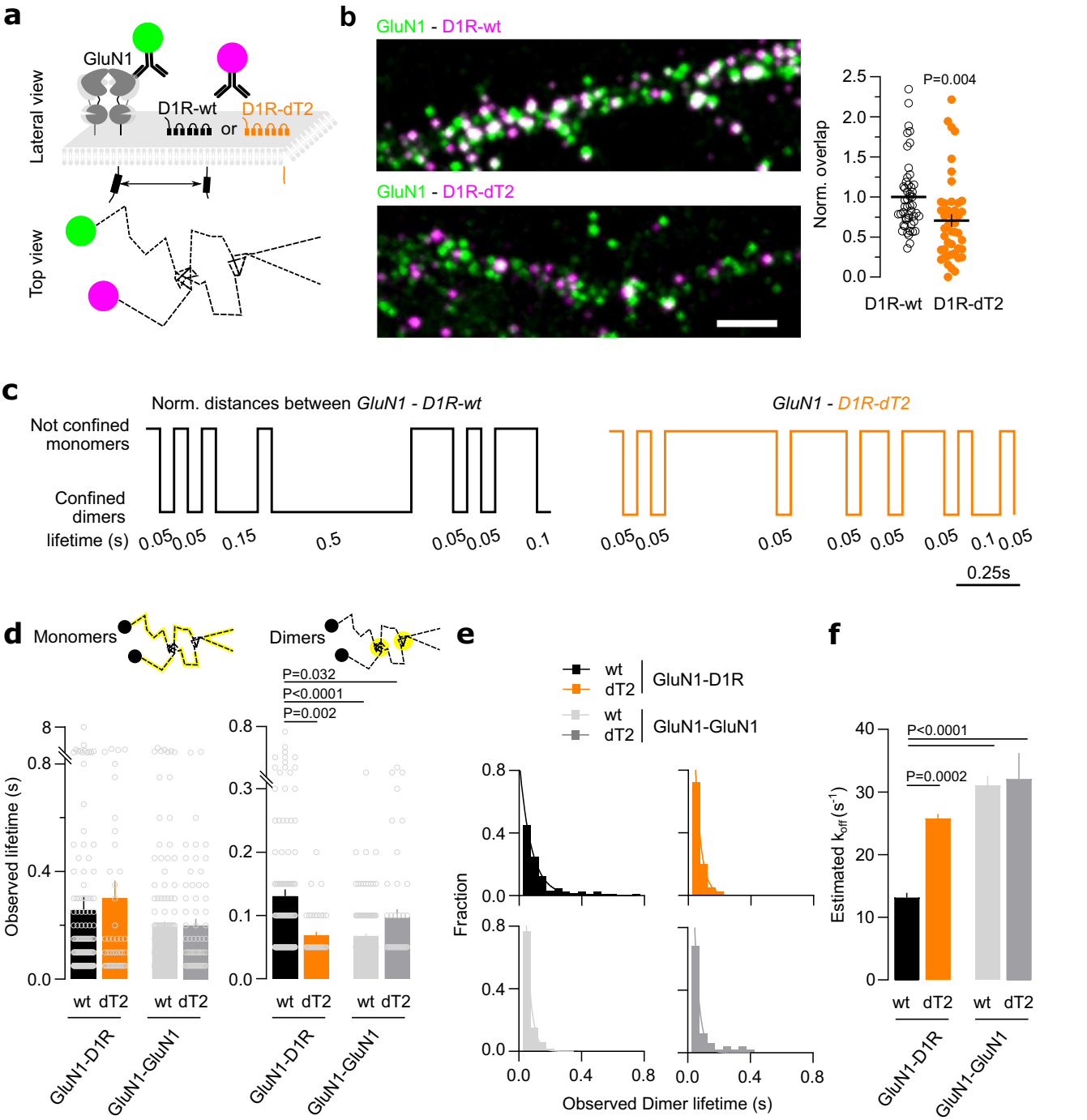

Fig. 2 | MS-SMLM allows for the direct visualization and qualitative investigation of surface receptor-receptor interaction events in live neurons. **a** Experimental design of the surface single Qd tracking of NMDAR and D1R. **b** Representative images with quantification of the normalized overlap between GluN1-NMDAR-D1R-wt ($n = 50$ neuronal fields) and GluN1-NMDAR-D1R-dT2 ($n = 44$ neuronal fields; two-tailed unpaired t-test). Data are presented as mean +/- SEM. Scale bar, 5 μm. **c** Representative normalized timeline of the distances separating one GluN1 from one D1R-wt or one GluN1 from one D1R-dT2. **d** Comparison of the average observed lifetime of the receptors (*left*) in non-confined space (monomeric state) for GluN1-D1R-wt ($n = 168$ events), GluN1-D1R-dT2 ($n = 45$), GluN1-GluN1 with D1R-wt ($n = 165$) or D1R-dT2 ($n = 65$); (*right*) in a co-confined space (dimeric state) between GluN1 and D1R-wt ($n = 138$), GluN1 and D1R-dT2 ($n = 40$), GluN1 and GluN1 expressed with D1R-wt ($n = 159$) or D1R-dT2 ($n = 50$; Kruskal-Wallis with Dunn's multiple comparisons test). Data are presented as mean +/- SEM. **e** Distribution and one exponential fit of the interaction events. **f** Comparison of the estimated K_{off}, i.e. dissociation rate (One-way ANOVA with Tukey's multiple comparisons test). Data are presented as mean +/- SEM. Source data are provided as a Source Data file.

also observed in cultured cortical neurons suggesting a shared mechanism for glutamatergic neurons (Supplementary Fig. 3).

We therefore investigated the mechanisms underpinning the surface interactions between GluN1-NMDAR and D1R in immature hippocampal neurons. As neuronal activity in the developing brain can tune synaptic maturation, neuronal activity was either up- or down-regulated by bath application of glutamate or tetrodotoxin (TTX), respectively. Silencing neuronal activity decreased GluN1-NMDAR-D1R co-localization whereas global activation of glutamate receptors increased it (Fig. 4a). Surprisingly, depolarizing neurons with KCl

https://doi.org/10.1038/s41467-023-44301-z

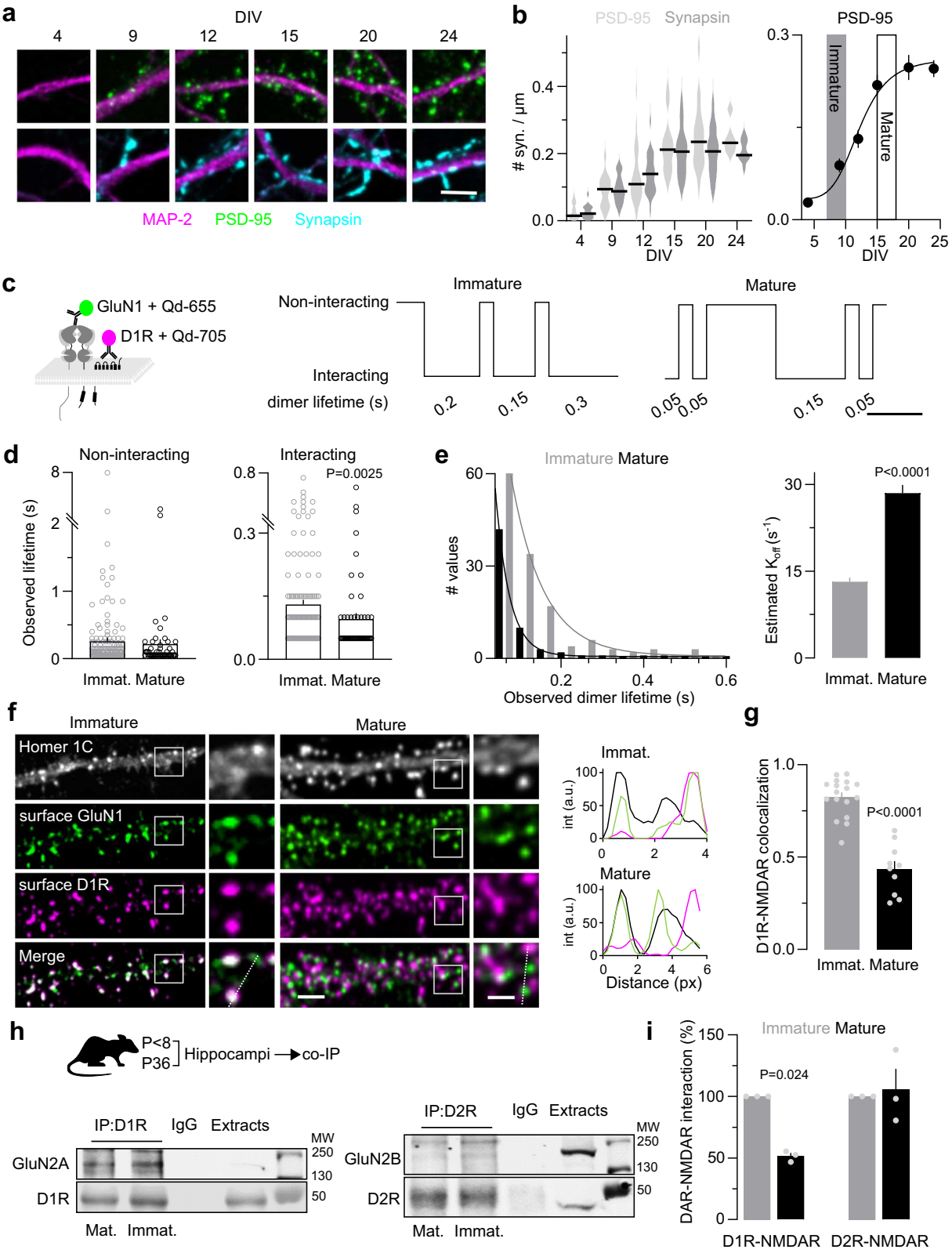

(50 mM), which increase neuronal firing, did not change GluN1-NMDAR-D1R co-localization (Fig. 4b). In fact, the glutamate-induced increase in GluN1-NMDAR-D1R colocalization was prevented by a mGluR inhibitor (LY341495) but not with antagonists of the AMPAR/kainate receptors (NBQX) or NMDAR (AP-5) (Fig. 4c), nor by co-applying NBQX and AP-5 together (Supplementary Fig. 4). The role of mGluR was evidenced by using the mGluR5 antagonist (MTEP), which decreased GluN1-NMDAR-D1R colocalization (Supplementary Fig. 4). In addition, we could mimic the effect of ambient glutamate with the mGluR1/5 agonist DHPG (Fig. 4d). These data indicate that the GluN1-NMDAR-D1R interaction is regulated by neuronal activity and involve mGluR-dependent signaling processes.

To identify this pathway we focused on the interaction domain of the D1R with GluN1-NMDAR, the T2 domain[20]. The domain bears highly

Fig. 3 | Increased dopamine-NMDA receptor interaction in immature neurons. **a** Representative image of hippocampal dendrites over in vitro development. Dendrites were labeled with MAP-2 (magenta), postsynaptic densities with PSD-95 (green), and presynaptic terminals with synapsin (blue). Scale bar, 5 μm. **b** (left) Quantification of the number of post-synapses (PSD-95) and pre-synapses (synapsin) at 4 DIV ($n = 18$ fields for both PSD-95 and synapsin), 9 DIV ($n = 17$ fields for both PSD-95 and synapsin), 12 DIV ($n = 30$ fields for PSD-95 and 29 for synapsin), 15 DIV ($n = 21$ for PSD-95 and 20 for synapsin), 21 DIV ($n = 21$ for PSD-95 and 20 for synapsin), 24 DIV ($n = 11$ for both PSD-95 and synapsin). Error bars represent the mean values; (right) non-linear fitting of the number of post-synapses over time, inflection point is at ~12 DIV. Data are presented as mean +/- SEM. **c** (left) Experimental design. (right) Representative normalized timeline of the distance separating one GluN1 from one D1R in immature and mature neurons. **d** Comparison of the observed mean lifetime of (left) non-interacting GluN1-NMDAR-D1R in immature ($n = 168$ events) and mature ($n = 55$) neurons, (right) individual interacting events between GluN1 and D1R in immature ($n = 138$) and mature neurons ($n = 61$; two-tailed Mann-Whitney U test). Data are presented as mean +/- SEM. **e** Distribution and one exponential fit of the interaction events between GluN1-D1R in immature and mature neurons with estimated K_{off} (two-tailed unpaired t-test). Data are presented as mean +/- SEM. **f** Representative images of hippocampal dendrites on which surface GluN1-NMDAR (green), D1R (magenta), and Homer 1 C (white) were imaged in immature and mature neurons alongside corresponding intensity plots. Scale bar, 5 and 2 μm. **g** Quantification of the colocalization between D1R and GluN1-NMDAR in immature ($n = 17$ cells) and mature ($n = 10$ cells) neurons (two-tailed unpaired t-test). Data are presented as mean +/- SEM. **h** Experimental set-up and immunoblots. **i** Densitometric analysis of the levels of GluN2A and GluN2B co-immunoprecipitated by antibody directed towards D1R or D2R, respectively. The levels of D1R-NMDAR interaction were considered as the ratio of NMDAR co-IP with D1R-IP. Results are normalized to P8, 3 animals per condition (One-way ANOVA with Tukey's post hoc test). Data are presented as mean +/- SEM. Source data are provided as a Source Data file.

conserved sequences that are involved in the formation of non-covalent complexes through electrostatic interaction. Particularly, it contains a serine residue at the position 397 that can be phosphorylated by Casein Kinase 1 (CK1) which would lead to an increased interaction between D1R-GluN1-NMDAR[25,43] (Fig. 4e). We thus predicted that rising neuronal activity in immature neurons induces post-translational changes of the T2 domain in a CK1-dependent manner, modifying the interaction properties between D1R and GluN1-NMDAR. We first demonstrated the role for CK1 in regulating the interaction between D1R-GluN1-NMDAR in hippocampal glutamatergic neurons. To do so, we specifically inhibited CK1 as well as other protein kinases targeting other sites on the D1R and GluN1 C-termini, e.g. Casein Kinase 2 (CK2) and Calcium/Calmodulin-dependent Kinase II (CaMKII). CK1 inhibition disrupted GluN1-NMDAR-D1R co-localization whereas the inhibition of PKA, PKC, CK2, CaMKII or GRK2 had no effect (Fig. 4f). The role of CK1 was further confirmed by using another antagonist, i.e. IC-261, which also disrupted GluN1-NMDAR-D1R co-localization (Supplementary Fig. 4). To confirm that such unique post-translational modification of D1R could indeed strengthen the interaction between GluN1 and D1R, we generated a phosphomimic form of D1R, i.e. D1R-S397D. Both FRET on COS-7 cells and surface immunostaining on hippocampal neurons demonstrated an increased GluN1-NMDAR-D1R interaction with the phosphomimic form of D1R when compared to D1R-WT (Supplementary Fig. 4), a process that was activity-independent (Supplementary Figure 4). Together, these data support the view that D1R-GluN1-NMDAR clustering is tuned by changes in D1R-phosphorylation barcode in a CK1-dependent manner. An inhibition of CK1 (through CKI-7) together with the activation mGluRs (through DHPG) were sufficient to abolish the positive effect of DHPG on the interaction (Fig. 4g). Consistent with the prominent effect in immature neurons, the relative protein level of the subunit alpha of CK1, which is highly enriched within the hippocampus[44], was significantly increased at early stage, *i.e.* at the peak of D1R-GluN1-NMDAR interaction, in both hippocampal cultures and in the hippocampus in vivo (Supplementary Fig. 5). Collectively, these data show that D1R-GluN1-NMDAR interaction is favored during neuronal development by modification of D1R C-tail phosphorylation barcode by CK1 in a mGluR-dependent manner.

GluN1-D1R interaction controls GluN1 surface organization

We next investigated the putative function of this increased interaction between GluN1-NMDAR and D1R onto immature neurons. Because it has been suggested that the interaction between GluN1 and D1R modulates their surface trafficking properties[23], we first tested whether the GluN1-NMDAR surface distribution is regulated by the receptor-receptor interaction. In these immature neurons, the prediction is that the receptor interaction favors the clustering of surface NMDARs, likely outside already formed early synaptic sites. First, we measured the areas of surface clusters of GluN1-NMDAR and tested whether bigger NMDAR clusters were associated with a high content of D1R. In D1R-wt condition, GluN1-NMDAR cluster area positively correlates with the GluN1-NMDAR-D1R content (considered as the percentage of overlap between GluN1 and D1R) (Fig. 5a,b). Interestingly, the correlation was further increased in presence of phosphomimic D1R-S397D (Fig. 5b), whereas it was lost upon disruption of the interaction with D1R-dT2 (Fig. 5b). As D1R-dT2 is expressed for several days, we used a complementary approach to acutely disrupt GluN1-NMDAR-D1R interaction using a TAT-competing peptide that contains the T2 amino acid sequence (TAT-T2) or TAT-NS (control). Note that this peptide could partly interfere with the controversial D1R-D2R interaction that has been reported only in the striatum[45,46]. The competing peptide efficiently decreased the GluN1-NMDAR-D1R content (Supplementary Fig. 6). The inhibition of CK1 by CKI-7 produced a similar outcome (Supplementary Fig. 6). To better characterize this process, we used direct stochastic optical reconstruction microscopy (dSTORM) to probe the nanoscale organization of GluN1-NMDAR (Fig. 5c) as surface NMDARs are organized within nanodomains of 50-100 nm diameter[47]. To that extend, we co-expressed the GluN1 subunit with either D1R-wt, D1R-dT2 (no interaction) or D1R-S397D (strengthened interaction) (Fig. 5d, e). Although the number of nanodomains per clusters were not changed (Supplementary Fig. 6), the surface organization of GluN1-NMDARs between synaptic and extra-synaptic compartments were drastically impaired. GluN1-NMDARs are in the majority concentrated within the post-synaptic compartment with approximately one-third of the surface receptor pool being located extra-synaptically. As expected, in control condition surface GluN1-NMDARs were highly enriched at synapses (based on Homer 1 C) as demonstrated by a higher density of localization (number of localizations per nm^2) in synaptic areas (Fig. 5d–f). This synaptic/extrasynaptic repartition was lost in presence of D1R-dT2 that equalized NMDAR nanodomain density (Fig. 5d–f). Remarkably, in presence of the phosphomimic D1R-S397D, the NMDAR distribution was shifted toward a higher extrasynaptic content (Fig. 5d–f). These data indicate that the interaction between NMDAR and D1R, which is located outside synapses (Fig. 5g)[23,48], regulate NMDAR nanoscale organization at extrasynaptic location (Fig. 5h).

We finally tested whether these clusters were functional and eventually recruited in early synaptic contact. For this, we co-expressed the calcium (Ca^{2+}) indicator GCaMP6f together with D1R-WT, D1R-dT2, or D1R-S397D and monitored the frequency of the NMDAR-mediated spontaneous Ca^{2+} events in protrusions and onto the dendritic shaft of DIV 12 hippocampal neurons (Fig. 5i–k). At this stage, glutamatergic synapses are prominently located in protrusions (e.g. filopodia-like, spine; Supplementary Fig. 6). As expected, in the D1R-wt condition, the frequency of calcium transients was higher in protrusions than on dendrites (Fig. 5j, k), consistent with a higher amount of functional glutamatergic synapses in protrusions than

https://doi.org/10.1038/s41467-023-44301-z

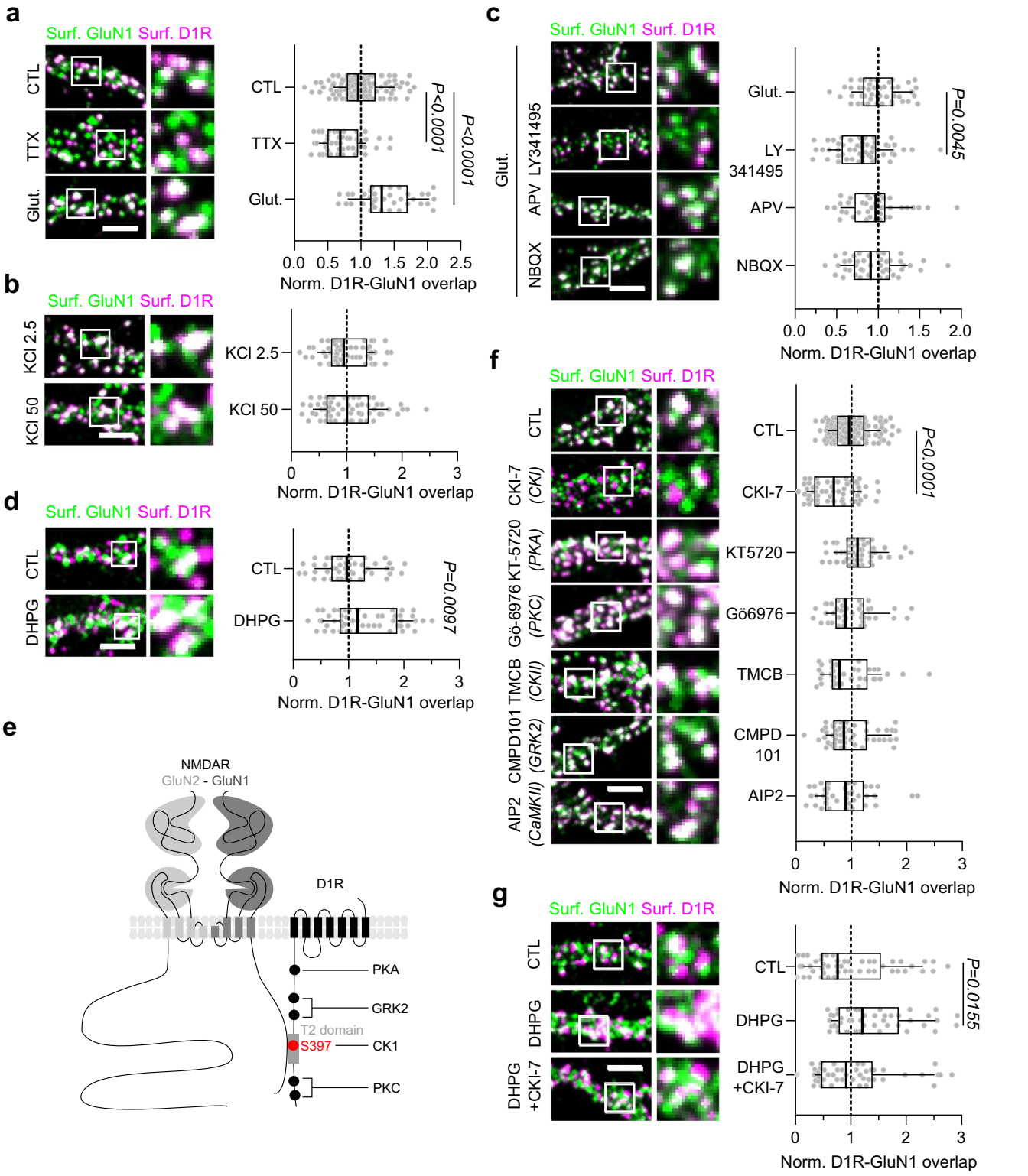

dendritic shaft. However, in the presence of the phosphomimic D1R-S397D, the frequency of transients swapped and became higher on the dendrites than in protrusions (Fig. 5j, k). In the presence of D1R-dT2, the higher frequency of events in protrusions was not observed, with equal event detection between protrusions and dendritic shafts (Fig. 5j, k). Altogether, these data indicate that the interaction between NMDAR and D1R favors the functional clustering of NMDARs in dendritic shaft of immature neurons, possibly reflecting a pro-synaptogenic effect.

Early in development, GluN1-D1R interaction tunes synaptogenesis

To directly address this possibility, we chronically disrupted D1R-GluN1-NMDAR interaction by using TAT-based control (TAT-NS) or competing (T2) peptides (see[23], Supplementary Fig. 2) during either an early or late phase of synaptogenesis (Fig. 6a–d). Upon early chronic disruption of the interaction with the TAT-T2 peptides, the number of excitatory synapses (represented as the number of Homer 1 C cluster) was significantly reduced by 15% (TAT-NS) whereas disruption of the

Fig. 4 | GluN1-D1R interaction is activity-dependent and increased by the phosphorylation of D1R by casein kinase 1 (CK1). a–d Representative images of hippocampal dendrites on which surface GluN1-NMDAR (green) and D1R (magenta) were labeled after exposures to various pharmacological treatments with respective quantification of D1R-GluN1-NMDAR mean overlap, (**a**) Buffer (CTL, $n = 105$ fields), TTX (1 μM, $n = 49$) and glutamate (50 μM, $n = 37$); (**b**) KCl 2.5 mM (CTL, $n = 55$) or KCl 50 mM ($n = 60$); (**d**) Buffer (CTL, $n = 47$) or DHPG (50 μM, $n = 51$); (**c**) glutamate alone ($n = 47$) or together with APV (50 μM, $n = 40$), LY-341495 (100 μM, $n = 52$) or NBQX (2 μM, $n = 43$) (**a**, **c** One-way ANOVA with Dunnett's post hoc test; b-d, two-tailed unpaired t-test). Scale bar, 5 μm. Results are normalized to CTL (**a**, **b**, **d**) or glutamate (**c**). **e** Cartoon illustrating putative D1R phosphorylation sites. **f** Representative images of hippocampal dendrites on which surface GluN1-NMDAR (green) and D1R (magenta) were labeled after exposures to various kinase inhibitors with respective quantification of the normalized GluN1-NMDAR-D1R mean overlap in control (CTL) condition ($n = 126$ fields) or following acute treatment with CKI-7 (100 μM, $n = 57$), KT-5720 (25 μM, $n = 49$), Gö−6976 (1 μM, $n = 41$), TMCB (5 μM, $n = 37$), CMPD101 (1 μM, $n = 50$) and AIP2 (1 μM, $n = 40$; One-way ANOVA with Dunnett's post-hoc test). Scale bar, 5 μm. **g** Representative images of hippocampal dendrites on which surface GluN1-NMDAR (green) and D1R (magenta) were labeled after treatment with buffer (CTL, $n = 48$ fields), DHPG alone (50 μM, $n = 44$) or together with CKI-7 (100 μM, $n = 45$) with respective quantification of D1R-GluN1-NMDAR mean overlap (One-way ANOVA with Dunnett's post-hoc test). Scale bar, 5 μm. Data are presented as box-and-whisker plots: line at median, IQR in box, whiskers represent 10–90 percentile. Source data are provided as a Source Data file.

interaction at the end of the synaptogenic period did not alter the number of excitatory synapses (Fig. 6b–e). Because synapses are more stable in mature neurons than in immature ones, we tested whether a longer exposition with the competing peptide modify the number of synapses in mature neurons. Yet, this number was not altered even after 8 days of treatment with control or competing peptide (Supplementary Fig. 7), therefore suggesting that the interaction is required for synaptogenesis only early in development. Consistently with an instrumental role, the strengthening of the interaction (obtained through the expression of the phosphomimic D1R-S397D) during that early stage significantly increased the number of glutamatergic synapses (Fig. 6g, h). Another hallmark of the maturation of glutamatergic synapses is the GluN2A/GluN2B subunit ratio that increases during development. We measured the synaptic content of GluN2A and GluN2B subunits in our experimental conditions. After an early disruption of the interaction, a premature high level of synaptic GluN2A-NMDAR and low level of GluN2B-NMDAR were observed, suggesting that the NMDAR-D1R interaction favors surface GluN2B-NMDAR functions (Fig. 6c–f). Altogether, these data indicate that D1R-GluN1-NMDAR interaction is necessary and sufficient at an early developmental stage to tune the formation and maturation of glutamatergic synapses.

An intriguing aspect of these observations comes from the fact that they were performed in hippocampal neuronal networks devoid of dopamine signaling. In this line, the level of dopamine in the developing hippocampus, i.e. the first two postnatal weeks, is extremely low. We confirmed this by immunolabelling tyrosine hydroxylase-positive (TH +) fibers in the CA1 area of P5 hippocampi. Fibers could be detected to a very low level when compared to other structures (e.g. striatum) and later stages (not shown) (Fig. 6i), indicating a low level of dopamine and noradrenaline. Since dopamine is present at low level in the neonate hippocampus, we investigated whether the synaptogenic role of the NMDAR-D1R interaction was preserved in developing hippocampal networks exposed to low level of dopaminergic fibers. To this end, we co-cultured hippocampal neurons with either hippocampal glutamatergic neurons (control, h-h) or dopaminergic-containing midbrain neurons (m-h) using microfluidic chip devices (Fig. 6j). We clarified the phenotype of cultured mesencephalic neurons originating from the ventral mesencephalon by immunolabeling with TH and dopamine hydroxylase (DBH), which convert dopamine to noradrenaline. We confirmed that the vast majority (90%) of our TH+ mesencephalic neurons are negative for DBH staining, thereby dopaminergic (Supplementary Fig. 8). Axons from TH+ dopaminergic neurons from chamber 1 were able to propagate into the hippocampal chamber (chamber 2) where they intermingled with glutamatergic neurons (Fig. 6j). Consistent the well-documented trophic effect of dopamine[17], hippocampal neurons co-cultured with dopaminergic neurons (m-h) exhibited higher dendritic arborization and complexity (Supplementary Fig. 8). After 12 days of hippocampal-mesencephalic co-culturing, the glutamatergic neurons that develop alongside dopaminergic fibers had higher synaptic density compared to control (Fig. 6k, l), as expected from the well-established role of dopamine in network formation[17,49]. Yet, early disruption of the NMDAR-D1R interaction significantly decreased the number of excitatory synapses by 35%, a similar extent than in hippocampal neuronal network only (Fig. 6m, n). Collectively, these data demonstrate that in immature hippocampal networks the surface interaction between NMDAR and D1R tunes synaptogenesis in a dopamine signaling-independent manner.

GluN1-D1R interaction is required for in vivo early hippocampal network activity

We next tested the role of this interaction in vivo in the developing hippocampus. Since the D1R-GluN1-NMDAR interaction is necessary and sufficient for the development of excitatory synapses, we predicted that the D1R-GluN1-NMDAR interaction contributes to the fine-tuning of early hippocampal network activity. First, the D1R-GluN1-NMDAR interaction was chronically disrupted in mice by intraperitoneal injections[50] of competing (TAT-T2) or control (TAT-NS) peptide at early stage (before postnatal day (P) 10) during the synaptogenesis window (Fig. 7). Hippocampal local field potential (LFP) activity was then recorded 1-2 days after the last peptide injection. Consistent with previous observations from the mouse cortex at postnatal transition[51], the hippocampus in non-anesthetized P7 head-fixed control mice spontaneously exhibited giant depolarizing potentials (GDPs), with an event frequency of 18 ± 0.15 per min. The chronic administration of competing TAT-T2 peptide, but not TAT-NS peptide, significantly reduced the GDP frequency (Fig. 7a, b). Note that there was no statistical difference between TAT-T2 and TAT-NS groups, due to the high variability of the TAT-NS mice. To complement this observation, we chronically disrupted the interaction during a similar postnatal period (P7-10) and recorded spontaneous hippocampal activity in urethane-anesthetized mice (P12). The control group spontaneously exhibited large-amplitude burst events (LB), with an event frequency of 1.8 ± 0.26 burst/min (Fig. 7c–e). In TAT-T2 mice, LB event frequency was significantly reduced and the inter-event intervals were significantly increased as shown by the rightward shift in the distribution (Fig. 7d). Thus, the D1R-GluN1-NMDAR interaction regulates some features of the spontaneous activity in the developing hippocampus. We then performed a similar series of experiments at the young adult stage (P30-35). At P35, LFP oscillatory patterns, and sharp wave and fast oscillatory ripples were detected in control freely-moving mice (Fig. 7f, g). The chronic administration of competing peptides had no effect on either LFP oscillatory pattern, or sharp wave and fast oscillatory ripple (Fig. 7f–i). Note that the hippocampal spontaneous activities at early (P7-12) and late (P35) stages were completely different and likely supported by different neuronal populations and processes. Yet, these results indicate that the D1R-GluN1-NMDAR interaction contributes to the fine-tuning of spontaneous hippocampal neuronal network activity early in development, with no detectable effect on the adult hippocampal spontaneous activity.

https://doi.org/10.1038/s41467-023-44301-z

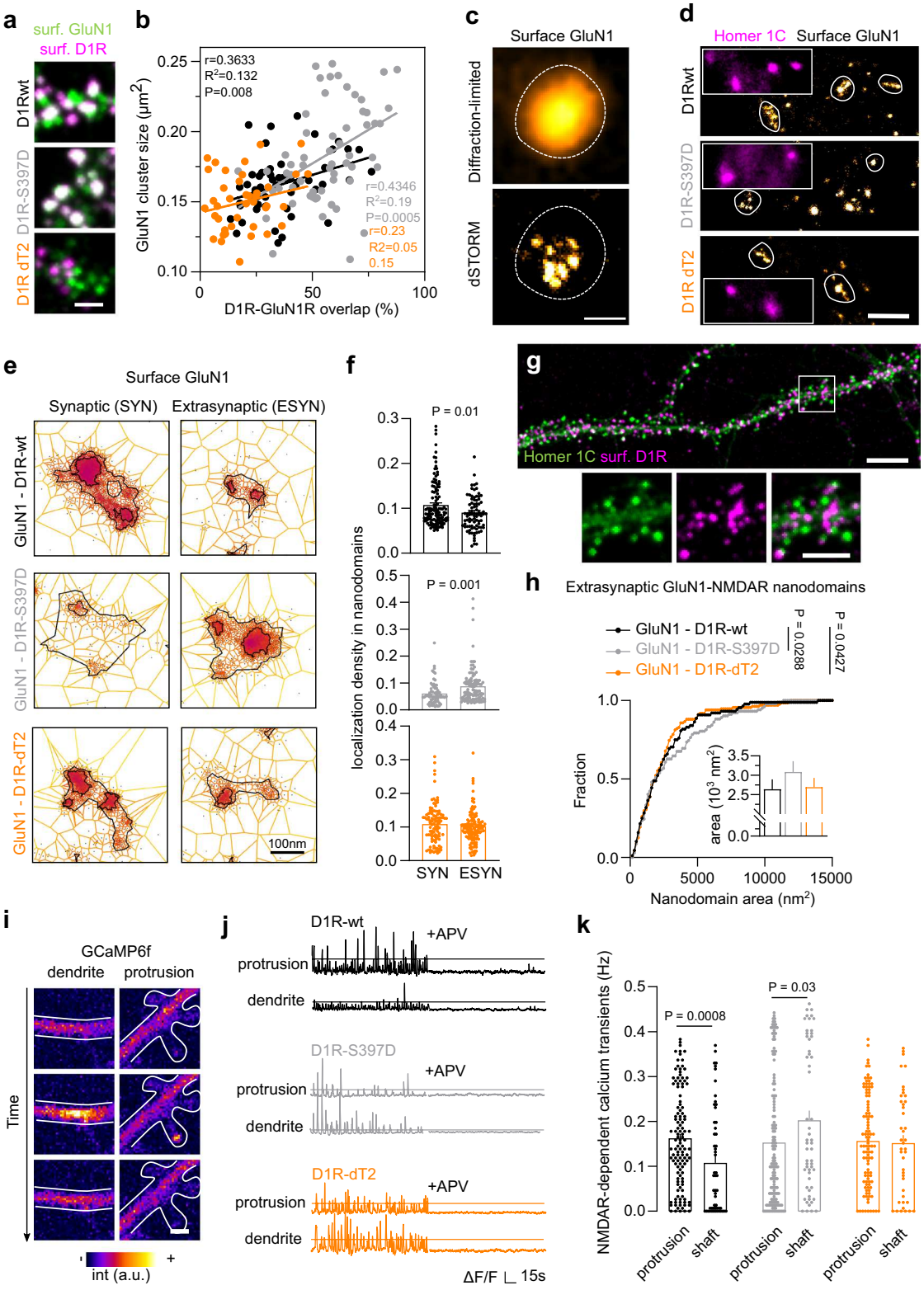

Discussion

The development of imaging approaches such as single molecule-based microscopy, has unveiled with unprecedented spatio-temporal resolution, the dynamics and organization of receptors at the plasma membrane[52,53]. We provide the characterization of the membrane interaction between two prototypical and key receptors, i.e. the NMDAR and G-coupled dopamine D1R. At the surface of hippocampal neurons, their interaction lasts on average ~130 ms and occurs along the dendritic tree, consistent with the stochastic surface dynamics of both receptors[12,23,54–56]. The interaction was qualitatively higher early in development, promoting the formation of NMDAR-D1R complexes in a mGluR5- and CK1-dependent manner. In immature hippocampal neurons, this interaction is stronger and favors membrane NMDAR clustering and synaptogenesis in a dopamine receptor signaling-independent manner. Thus, we unveil a non-canonical interplay between NMDAR and D1R, demonstrating that a weak and transient

Fig. 5 | Surface interaction with D1R shapes GluN1 nano-organization and clustering. a Representative image of hippocampal dendrites on which surface GluN1-NMDAR (green) and D1R (magenta) were labeled from D1R-wt, D1R-S397D (grey), or D1R-dT2 (orange) expressing neurons from 3 independent experiments. Scale bar, 2 μm. **b** Correlation between the size of GluN1-NMDAR cluster and the overlap between GluN1-NMDAR and D1R when co-expressed with D1R-wt, D1R-S397D or D1R-dT2. P-value were calculated using a two-sided *t*-test. **c** Example of diffraction-limited and super-resolution images of surface GluN1-NMDAR. Scale bar, 300 nm. **d** Representative images of super-resolved surface GluN1-NMDAR and diffraction-limited Homer 1 C staining. Scale bar, 1 μm. **c**, **d** Representative images from 4 independent experiments. **e** Representative clustering images obtained with SR-Tesseler software. Scale bar, 100 nm. **f** Comparison of the density of localizations per nanodomains inside and outside synapses when GluN1 is co-transfected with either D1R-WT ($n = 7$ cells), D1R-dT2 ($n = 7$) or D1R-S397D ($n = 6$; two-tailed Mann-Whitney U test). Data are presented as mean +/- SEM. **g** Representative immunofluorescence image of surface D1R (magenta) and Homer 1 C (green) from 3 independent experiments. Scale bar, 10 and 5 μm. **h** Cumulative distribution of the area in nm^2 of extra-synaptic GluN1-NMDAR nanodomains synapses when GluN1 is co-transfected with either D1R-WT ($n = 88$ nanodomains), D1R-dT2 ($n = 136$ nanodomains) or D1R-S397D ($n = 102$ nanodomains; two-tailed Kolmogorov-Smirnov test). Bar graphs represent mean +/- SEM. **i** Representative GCaMP6f-fluorescence images from 3 independent experiments. Scale bar, 2 μm. **j** Representative NMDAR-mediated Ca^{2+} signals, scale is 0.05 (D1R-WT and -dT2) or 0.2 (D1R-397D) ΔF/F. **k** Comparison of the NMDAR-mediated Ca^{2+}-transient frequency in protrusions and dendrite when GluN1 is expressed together with D1R-wt ($n = 153$ spines and 54 shaft), D1R-S397D ($n = 145$ spines, 56 shafts) or D1R-dT2 ($n = 105$ spines, 45 shafts; two-tailed Mann–Whitney U test). Data are presented as mean +/- SEM. Source data are provided as a Source Data file.

interaction between receptors can have a major structural and functional role for synaptogenesis in the developing hippocampus. As a consequence, the interaction modulates in vivo some features of the neonate spontaneous hippocampal network activity. The lack of effect on the adult spontaneous hippocampal activity does not preclude a functional role of the interaction in other network activities, specific tasks, and behaviors. Future studies will likely tackle these important questions.

Defining the properties of protein-protein interaction at the surface of living neurons has proven to be technically challenging. Commonly used methods to investigate receptor complexes in the brain, such as co-immunoprecipitation and proximity ligation assay (PLA), provide valuable information on the overall amount of hetero-receptor complexes present in a given structure at a given time but lack insights on the qualitative nature of the interaction between different receptors (for review, see[16]). For instance, critical parameters such as their occurrence or duration in the native environment have remained unknown. On the side note, the existence of membrane receptor heterocomplexes is still vividly debated (e.g. D1/D2 complex[45,46]). Thanks to the development of a custom MS-SMLM we were in the position to provide the first characterization of the interaction between surface GluN1-NMDAR and D1R at the single molecule level with nanoscale resolution in live neurons. The observed average lifetime of the GluN1-NMDAR-D1R interaction was 130 ± 0.01 ms, with a dissociation rate of 13 ± 0.7 s^{-1}. These values are in a similar range to the ones defined from surface GPCR homomers in heterologous cells[31–33,35,36]. Finally, the D1R-NMDAR interactions were detected whole along the dendritic tree between receptors that stochastically cross each other since we didn't observe directed motion, or attraction, between receptors before/after the interaction. When single diffusing NMDAR and D1R get closer than 1 μm we observed that, on average, 30% of their localizations fall into the interaction area. At first glance, interactions do not appear to be clustered in specific areas, although we cannot rule out that specific membrane and/or intracellular subdomains favor the likelihood of interactions.

The strength of the interaction is finely regulated during development. Quite strikingly, we observed that during a rather limited developmental time window (DIV 10 to 15; doubling of glutamate synapse numbers) the GluN1-NMDAR-D1R interaction was twice stronger at the early time point, suggesting that important molecular cascade change during the synaptogenesis period. We identified on the D1R C-terminus a serine residue at position 397 that is regulated by CK1 and regulates the receptor interaction. Although weak and transient, the NMDAR-D1R interaction plays an instrumental role in clustering membrane NMDAR and promoting synaptogenesis in a mGluR-dependent process. Together with previous evidence showing that mGluRs are required for the experience- and activity-dependent changes in NMDAR transmission (i.e. GluN2A/GluN2B ratio) during development[57], our data fuel thus a developmental model in which ambient glutamate activates mGluRs that will locally favor NMDAR-D1R interaction, NMDAR clustering, calcium influx, synaptogenesis, and synaptic maturation through regulation of the GluN2A/GluN2B ratio. In the absence of D1R (D1R knock-out mice), synaptogenesis and spinogenesis are expectedly strongly reduced[58]. The NMDAR-D1R interaction occurs early in development when the dopaminergic innervation of the hippocampus is rather scarce[59] supporting a preponderant role of protein-protein interaction independent of the presence of dopamine. The classical dopamine intracellular signaling cascade likely becomes prominent at adulthood when dopamine signaling controls hippocampal synaptic plasticity and cognitive functions[60–70]. The low level of dopamine in the neonate hippocampus further strengthens the NMDAR-D1R interaction because dopamine receptor activation drastically reduces this interaction[20,23]. In non-physiological conditions, an upregulation of dopamine levels early in development could thus strongly impact synaptogenesis and network formation. Consistently, in the brain of dopamine transporter knock-out mice the upregulated level of dopamine reduces the formation of synapses and spines[71]. The synaptic maturation of the GluN2A/GluN2B ratio is also corrupted in the brain of pups with elevated dopamine levels following mother exposition to cocaine, a deficit that could be rescued by positive modulation of mGluR[72]. Thus, low dopamine levels likely favor dopamine-NMDAR crosstalk and its function whereas high levels of dopamine activate dopamine receptors and classical GPRC signaling but shut-off the dopamine-NMDAR direct crosstalk.

Surface NMDAR interacts with other neuromodulatory GPCRs, such as cholinergic, adrenergic, or histaminergic ones[16] that may be involved in the newly-described protein-protein interplay. The size and composition extent of the described protein-protein complex is thus possibly larger. In addition to other monoamine receptors, NMDARs can interact with, for instance, ion channels (e.g. BK, TRPM[73–75]; and adhesion receptors, providing an additional layer of complexity on the composition of such a putative complex, while also highlighting its broad and strategic potential for regulating of G-protein signaling, protein kinase/phosphatase, agonist-induced ionotropic transmission, potassium currents and dendritic excitability. Furthermore, we demonstrate that the D1R-NMDAR direct crosstalk at early stage occurs in absence of dopamine, consistent with its low level in the hippocampus. Such non-canonical process echoes previous evidences demonstrating the non-canonical and functional interplay between the ghrelin receptor (GHSR1a) and D1R, which are both present in hippocampal neurons[76], but operate in a ghrelin-independent manner since ghrelin, the agonist of GHSR1a, is not present in the hippocampus. It further supports the view that receptor-receptor interaction, in an agonist-independent manner, can regulate key functions of glutamate synapses and associated behavior in mice. Since signaling molecules related to GPCR can be spatially structured down to the nanoscale level to ensure specificity for GPCRs[77], it further supports the view that protein-protein interaction structures the receptor nanoscale organization, downstream signaling, and essential synaptic plasticity functions. Furthermore, changes in the NMDAR membrane interactome

https://doi.org/10.1038/s41467-023-44301-z

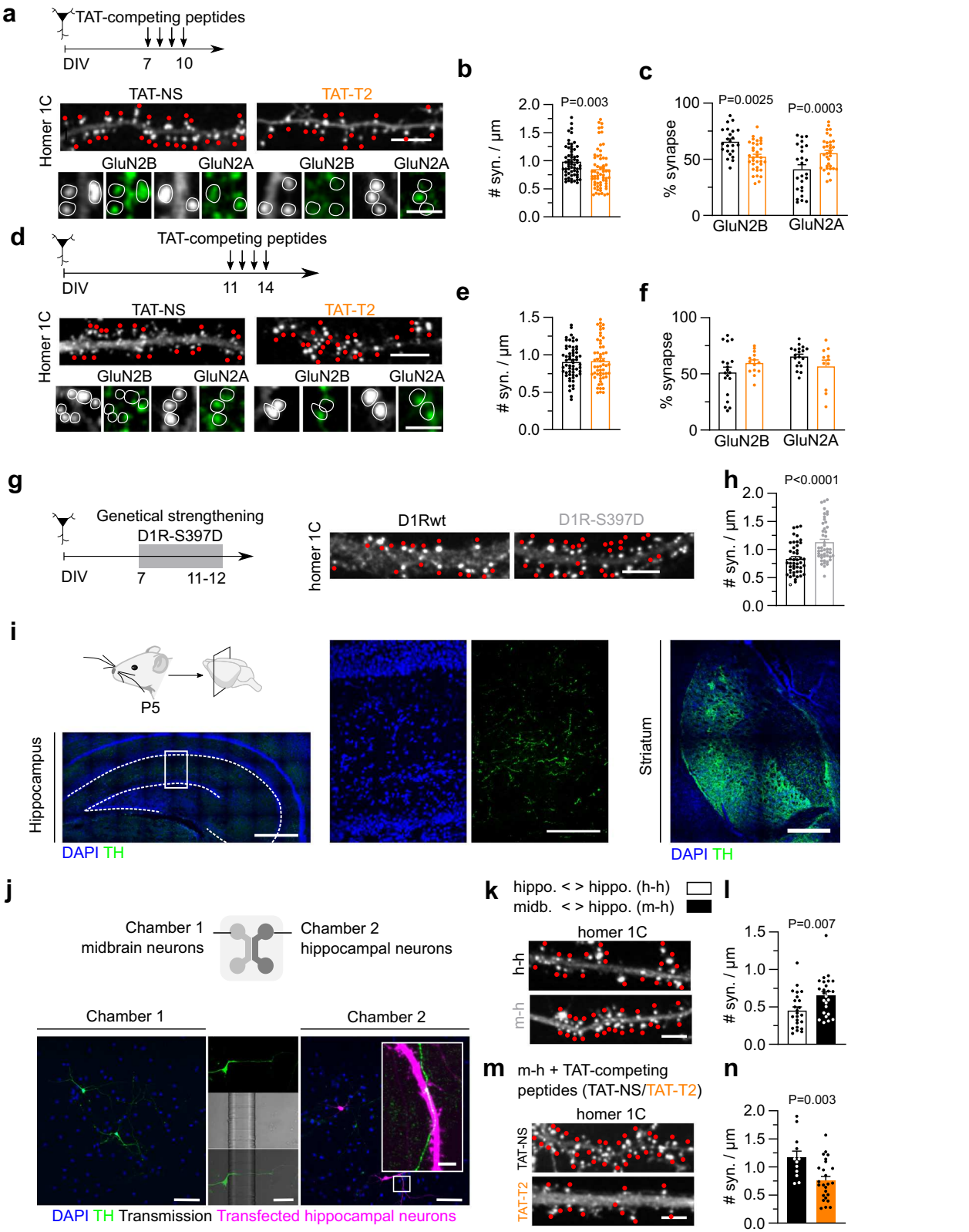

alone have been associated to the emergence of psychotic disorders[78], and more broadly receptor hetero-complexes to understand their roles in health and major brain neuropsychiatric disorders[79–84].

As a limit, our approach provides an unprecedented resolution in defining the membrane interaction between different receptors at video rate. Yet, further improving the spatial and temporal resolutions will likely shed additional lights on the protein-protein interaction. Beyond these resolution aspects, performing these measurements with more than 2-colors will allow us to image and quantify the formation of possible heterocomplexes[41]. It also remains unknown whether NMDAR interacts in the same condition with other membrane receptors. For instance, whether mGluR5, NMDAR, and D1R form a protein complex at the surface of developing neurons is an interesting question, particularly because mGluR5 and NMDAR can directly

Fig. 6 | GluN1-D1R interaction is necessary for synaptogenesis. a Experimental design of the TAT-competing peptide challenge in developing immature neurons with representative images of hippocampal dendrites on which Homer 1 C cluster (synapses), GluN2A subunit, or GluN2B subunit were labeled in the presence of TAT-NS or TAT-T2 competing peptides. Scale bar, 5 and 1 μm. **b** Comparison of the number of synapses (e.g. number of Homer 1 C clusters per μm of dendrite) after treatment with TAT-NS ($n = 60$ fields) or TAT-T2 ($n = 62$) and (**c**) the percentage of synapses that are positive for GluN2B (TAT-NS, $n = 23$; TAT-T2, $n = 34$) and/or GluN2A (TAT-NS, $n = 25$, TAT-T2, $n = 33$; two-tailed Unpaired t-test). Data are presented as mean +/- SEM. Scale bar, 5 and 1 μm. **d** Experimental design alongside representative images of hippocampal dendrites on which Homer 1 C cluster (synapses), GluN2A subunit, or GluN2B subunit were labeled in the presence of TAT-NS or TAT-T2 competing peptides. Scale bar, 5 and 1 μm. **e** Comparison of the number of synapses after treatment with TAT-NS ($n = 59$ fields) or TAT-T2 ($n = 55$) and (**f**) the percentage of synapses that are positive for GluN2B (TAT-NS, $n = 19$; TAT-T2, $n = 11$) and/or GluN2A (TAT-NS, $n = 19$; TAT-T2, $n = 14$; two-tailed unpaired t-test). Data are presented as mean +/- SEM. **g** Experimental set-up with representative images and (**h**) corresponding comparison of the number of synapses following expression of D1R-WT ($n = 44$ fields) or D1R-S397D ($n = 41$; two-tailed unpaired t-test). Data are presented as mean +/- SEM. Scale bar, 5 μm. **i** Representative images of TH immunostaining. Scale bar, (i) 500 μm and 100 μm. **j** Experimental setup with representative fluorescence images from 4 independent experiments. Scale bar, 100 μm and 5 μm. **k** Representative Homer 1 C images. **l** comparison of the synaptic density in hippocampal neurons co-cultured with hippocampal (h-h, $n = 24$ fields) or midbrain neurons (m-h, $n = 25$; two-tailed unpaired t-test). Data are presented as mean +/- SEM. Scale bar, 5 μm. **m** Representative images and (**n**) comparison of the synaptic density in hippocampal neurons co-cultured with midbrain neurons and chronically treated with competing peptides, either TAT-NS ($n = 12$ fields) or TAT-T2 ($n = 25$; two-tailed unpaired t-test). Data are presented as mean +/- SEM. Scale bar, 5 μm. Source data are provided as a Source Data file.

interact[85]. Such a large and diverse complex with ionotropic and GPCR receptors may help to confine intracellular signaling pathways to nanoscale domains[77] and integrate diverse molecular information. Technological breakthroughs that will permit to test the claim that physical interactions between various membrane receptors form a mosaic of signaling "hubs" that structure synapse formation and plasticity will thus be of prime interest.

Methods

Cell cultures

Cultures were kept at 37 °C – 5% CO_2.

Primary neuronal cultures. Tissue for dissociated hippocampal cultures was harvested from embryos of an unascertained mixture of sexes prevenient from gestant Sprague-Dawley rats at the age of 9–12 weeks old purchased weekly from Janvier Labs (Saint-Berthevin, France). Hippocampal cultures were prepared from embryonic stage (E18) rats. Briefly, hippocampi were dissected and collected in HBSS containing Penicillin-Streptomycin (PS) and HEPES and dissociated with Trypsin-EDTA/PS/HEPES. Cells were plated either at a density of 250 000 per 60 mm petri-dishes onto 1 mg/ml poly-L-lysine pre-coated 18 mm coverslips or at 40 000 cells per microfluidic chambers. Regarding midbrain cultures, ventral mesencephalons were dissected from E14 rats, collected in Leibovitz L-15 medium (Gibco, # 11415056), and dissociated with Trypsin-EDTA/PS/HEPES. Cells were plated at a density of 40,000 cells per chambers. Neuronal cells were maintained in Neurobasal Plus medium (Gibco, A3585911) supplemented with GlutaMAX™ (Gibco, #35050-038), B-27™ Plus (Gibco, A3653401).

Heterologous cell culture. COS-7 cell-line came directly from commercial sources that state for their authenticity (https://www.sigmaaldrich.com/FR/fr/product/sigma/cb_87021302). We did not perform in-house identification. All cell lines were tested negative for mycoplasma contamination. Mycoplasma testing was performed by a third-party (Eurofins) via qPCR from cell culture media. COS-7 cells were kept in Dubelcco's Modified Eagles's Medium (DMEM) supplemented with 10% fetal calf serum, 1% pyruvate and 2 mM GlutaMAX.

Cell transfection

Primary cultures. Hippocampal neurons were transfected either at 7 or 10 DIV using the calcium-phosphate coprecipitation method. DNA plasmids were diluted in TE buffer (1 mM Tris-HCl pH 7.3, 1 mM EDTA) and a final concentration of 250 mM of CaCl2 (2.5 M CaCl2 in 10 mM HEPES, pH 7.2) were added. This mix was added dropwise to 2X HEPES-buffered saline (in mM: 12 dextrose, 50 HEPES, 10 KCl, 280 NaCl and 1.5 Na2HPO4 • 2H2O, pH 7.2). Coverslips were transferred to 12-well plate containing 250 μl/well of conditioned culture medium supplemented with 2 mM kynurenic acid. 50 μl of the precipitate solution was added to each well and incubated for 1 h at 37 °C. Cells were then washed with non-supplemented Neurobasal medium containing 2 mM kynurenic acid and moved back to the culture dish. To prevent excitotoxicity, 50 μM of D-2-amino-5-phosphonovalerate (D-AP5) was added to the culture medium when transfecting with GluN1-NMDAR. Hippocampal neurons in co-culture with midbrain neurons through microfluidic chips were transfected using lipofectamine-2000 (Invitrogen) according to the manufacturer's recommendations. Where indicated, cells were incubated chronically with competing peptides, namely TAT-NS (YGRKKRRQRRRGSSEVILDQPVIAKPLIPALSVALSVKEEA), TAT-T2 (YGRKKRRQRRRLVYLIPHAVGSSEDLKKEEAGGIAKPLEKL) and TAT-T3 (YGRKKRRQRRRSPALSVILDYALSVVSLEKIQPVTHSGQHST) at a final concentration of 1 μM for four consecutive days or at 10 μM for 10 to 25 min.

COS-7 cells. Transfection with X-tremeGENE HP DNA (Roche) was done 1 day after plating. 200 μM of D-AP5 were added to the culture media when transfecting with GluN1-NMDAR. Cells were imaged 20-24 hours after transfection.

Animals

This study was conducted in accordance with both the NIH and European Community guidelines (Directive 2010/63/EU) for the care and use of animals. Every effort was made to minimize the number of animals used and their suffering. All animals were housed and maintained on a 12-h cycle at room temperature (22 °C) and 40–70% (typically 60%) humidity with ad libitum access to food and water.

C57BL/6 J mice. The protocol was approved by the Experimental Animal Ethics Committee of the University of Tokyo (approval number: P29-14). A total of 18, 14 and 11 male C57BL/6 J mice at postnatal day 4, 7 and 29 with preoperative weights of 5–7 g and 20–30 g, respectively, were used in this study.

Sprague-Dawley rats. The protocol was approved by the Animal Care Committee of the Centre for Addiction and Mental Health (approval number: #824) of the University of Toronto as well as by the local Bordeaux Ethics Committee (APAFIS#21727-2019010918359887). A total of twice 3 male Sprague-Dawley rats at post-natal day 7 and 36 were used in this study (co-IP), and gestant Sprague-Dawley rats at the age of 9–12 weeks old were purchased from Janvier Labs, and P5 ($n = 4$), P10 ($n = 3$) and P25 ($n = 3$) animals were randomly chosen for the experimentation.

Multi-dimensional spectral single molecule localization microscopy

Neurons were first incubated for 10 min with a mix of rabbit anti-GFP and mouse anti-Flag primary antibodies, washed and incubated for

https://doi.org/10.1038/s41467-023-44301-z

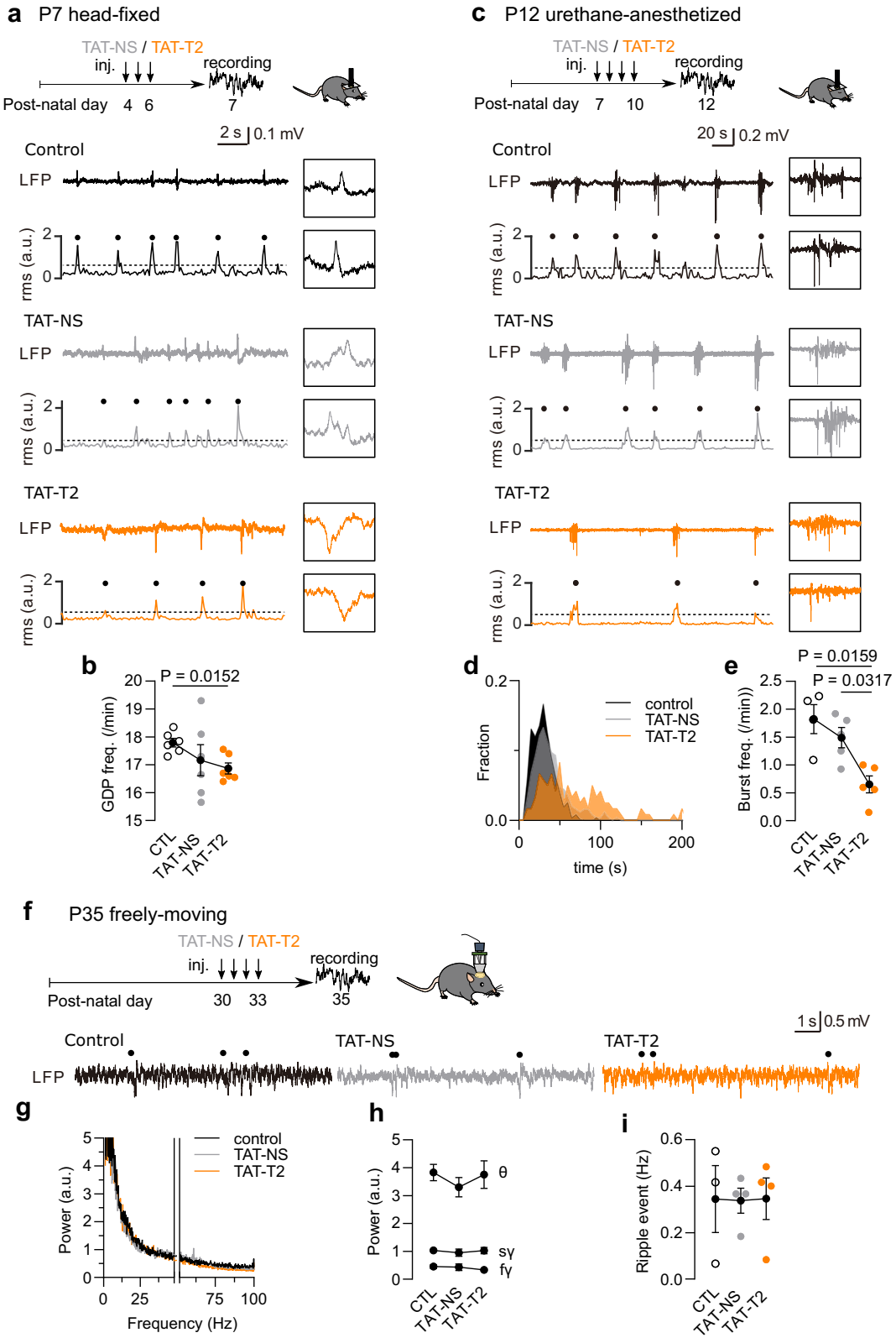

10 min with F(ab')2-Goat anti-Rabbit IgG (H + L) Secondary Antibody, Qdot 705, F(ab')2-Goat anti-Mouse IgG (H + L) Secondary Antibody, Qdot 655, and nanodiamond (Adamas Nano). All incubations were done in conditioned 1% BSA-Tyrode solution (in mM: 105 NaCl, 5 KCl, 2 MgCl2, 12 D-glucose, 25 HEPES, pH 7.4). Surface receptors diffusion were imaged for 1000 consecutive frames with an acquisition time of 50 ms (20 Hz).

Microscopy set-up. Our spectral microscope uses a 4Pi configuration composed of two commercially inverted microscope bodies (Nikon TiE) precisely aligned one on top of the other thanks to a (x, y, θ, φ) stage (UMS, Scientifica). The lower microscope is equipped with a high NA TIRF objective (100X Oil NA1.49, Nikon), an azimuthal TIRF/HiLo illumination device (iLAS2, Gataca Systems), a Quad band filter set (F66-04TN, AHF) and an astigmatism-based kit (manual N-STORM kit,

Fig. 7 | GluN1-D1R interaction is required for early basal network activity in vivo. a Experimental timeline for P7 head-fixed mice with representative LFP traces and the corresponding root mean square (RMS) in control (CTL), TAT-NS and TAT-T2 injected mice. **b** Comparison of the frequency of GDP events ($n = 6$ mice per group; two-tailed Mann–Whitney U test). Data are presented as mean +/- SEM. **c** Experimental timeline for P12 urethane-anesthetized mice with representative LFP traces and the corresponding root mean square (RMS) in control (CTL), TAT-NS, and TAT-T2-injected mice. **d** Distributions of inter-LB intervals. **e** Comparison of the frequency of LB events ($n = 4$-5 mice per group; two-tailed Mann–Whitney U test). Data are presented as mean +/- SEM. **f** Experimental timeline for P35 freely moving mice and representative LFP traces in control, TAT-NS and TAT-T2-injected mice. Hippocampal ripple events are indicated by black dots (above the traces). **g, h** Comparison of fast Fourier Transform (FFT) plots of LFP activity at 1–100 Hz bands excluding 48-52 Hz, ($n = 3$–4 mice per group). Data are presented as mean +/- SEM. **i** Comparison of the frequency of ripple events ($n = 3$–4 mice per group; two-tailed Mann-Whitney U test). Data are presented as mean +/- SEM. Source data are provided as a Source Data file.

Nikon) which altogether enable to perform state-of-the-art 3D SMLM. The upper microscope is equipped with a high NA water dipping objective (60X, Water Dipping NA1, Nikon) and a spectral detection arm for spectral (λ) characterization of the detected single molecules. The spectral detection arm is composed of a low dispersive prism (10° edge prism, PS814-A, Thorlabs) placed in the Fourier plane of a 4 f imaging relay to convert each emitter's wavelength into a spatial displacement, laterally shifting the localization of the single emitter linearly with respect to its mean spectral emission, and a triple laser lines rejection filter (ZET 405/488/561, F67-408, AHF) to reject excitation laser light. It also integrates a ~ 1.5x zoom to optically match the lower (spatial) and upper (spectral) FOVs as closely as possible. Two synchronized sensitive EMCCDs (Photometrics EVOLVE 512B), one for each detection path, allow the microscope to track single emitters across 80 μm x 80 μm field-of-views. Finally, the whole 4Pi microscope is caged in a custom plexiglass heated at 37 °C (Life Imaging System) and driven by the MetaMorph software (Molecular Devices).

Single Molecule Localization analysis. We used PALMTracer, a custom-made software operating as a plugin of MetaMorph software, to analyze and represent the multi-dimensional (x, y, t, λ) SMLM data. It uses a combination of wavelet decomposition and 2D Gaussian fitting[86,87] to perform state-of-the-art astigmatism-based 3D single-molecule localization. Once localized, molecule trajectories are computed from the molecular coordinates of the spatial channel using a simulated annealing algorithm[88]. Files are automatically analyzed using an integrated batch engine.

Spectrally displaced localization analysis. The spectral determination of each localized molecule has been described here[41]. It is based (1) on the pairing of single emitter's localizations obtained on both spatial and spectral channels, and (2) on measuring the spatial shift induced by the prism inserted in the spectral detection arm. From a spectral shift calibration process, it is then possible to retrieve the mean emission wavelength of the detected single molecule. Briefly, a field transformation of the spatial localizations (lower channel) is first applied to superposed both field-of-views. Then, the localizations in the spatial and the spectral channels are paired thanks to a linear search in a pair search zone defined around the transformed spatial localization from an a-priori knowledge of the prism-induced spatial dispersion and molecules emission wavelength. The pair distance d is finally measured enabling to assignment an emission wavelength to the spatial localization thanks to a spectral calibration of the spectral detection arm (Supplementary Fig. 1b). The spectral calibration was performed using multicolor diffraction limited microbeads (100 nm) with well-defined fluorescence spectra, simultaneously detected on both channels. The spatial shift induced by the dispersive element inserted into the spectral detection arm is then computed measuring the distance of the localization of each emission peaks on the spectral channel from the fiducial localizations on the spatial channel after field transformation. This calibration leaded to a computed spectral shift of -8.1 ± 0.1 nm/pixel (Supplementary Fig. 1c). Lastly, independent lateral drifts in either of the channels were compensated on each path separately by tracking fiducials markers of known emission spectra to ensure robust spectrally displaced localization analysis along the entire acquisition time.

Spectrally-informed multi-Gaussian fitting. In order to distinguish overlapping single molecule signals, i.e. occurring when single emitters are separated by less than ~200 nm, we devised a multi-emitter fitting approach that take advantage of the localization information in the spectral channel[41] (Supplementary Fig. 1d). by increasing the robustness and accuracy of the multi-gaussian fitting process, such parameters initialization allows for monitoring receptors of different species that are simultaneously exploring the same nanoscopic environment.

Analysis of particle-particle interactions. A computational algorithm was developed to extract the distances separating each receptor couple in our recordings. Receptors were considered as interacting when their distance fell within the confined threshold. This threshold was set at 100 nm.

Immunohistochemistry

Live surface staining (15 min at 37 °C) was followed by 15 min fixation in 4% paraformaldehyde (PFA) / 4% sucrose in PBS at room temperature (RT). The cells were then incubated for 15 min in PBS with 50 mM NH4Cl and blocked in PBS-1% bovine serum albumin (BSA) for 1 hour at RT. For intracellular staining, cells were fixed, permeabilized with 0.1% Triton X-100/PBS for 5 min and blocked 30 min in PBS-1% BSA. Alternatively, cells were fixed and permeabilized with ice-cold methanol. The secondary antibodies were prepared in blocking solution and incubated for 1 hour at RT. Coverslips were mounted in Fluoromount media and kept at 4 °C until imaging.

When needed, cells were, prior to fixation, co-incubated for 25 min at 37 °C with primary antibodies and various inhibitors or 5 min with 50 μM of glutamate or KCl (at 50 mM or 2.5 mM).

Microfluidic devices production

Microfluidic molds were fabricated on glass by soft lithography with the UV-curable adhesive NOA81 (Thorlabs) which resulted in a positive relief pattern of the microfluidic chip. A mixture of PDMS (Sylgard 184) with curing agent (10 to 1 ratio) was poured onto the positive replicate, degassed under vacuum before reticulated over-night at 70 °C. The resulting negative replica-polymer was detached, punched to create four reservoirs, cleaned and dried in sterile conditions. Finally, the polymer print was bonded onto a 1 mg/ml poly-L-lysine coated glass coverslip and stored at 37 °C until cell seeding.

Epifluorescence confocal image acquisition and analysis

Spinning disk. Images were acquired using a high-speed spinning disk confocal unit equipped with an electron multiplying charge-coupled device (EMCCD) camera (Photometrics QuantEM 512SC) through either a 20x objective (Leica, HC PLAN APO, 0.7 NA) and/or a 63x oil objective (Leica, HCX HPL APO CS, 1.4-0.6 NA). Hardware was controlled with MetaMorph software (Molecular Devices). All images were analyzed with ImageJ 1.53c (National Institute of Health, USA). For the Sholl Analysis, hippocampal neurons were transfected with a GFP-encoding plasmid at DIV 7, and hippocampal dendritic trees were

reconstructed using the ImageJ' plugin "SNT". The overlap between D1R and GluN1-NMDAR was defined as the fraction of GluN1 cluster area that overlap with D1R cluster.

Calcium imaging. Neuronal cells were transfected with GCaMP6f together with either D1R-wt, D1R-dT2 or D1R-S397D at DIV 7 and imaged 2-3 days post-transfection. For isolation of NMDAR-dependent Ca^{2+} transients, neurons were incubated in Mg^{2+}-free Tyrode's solution containing 5 μM nifedipine and 5 μM bicuculline for 15 min before imaging. Two time-lapse images of 3000 frames were acquired at 20 Hz, one before and one 5 min after incubation with D-AP-5 at 50 μM. Calcium activity was analyzed as previously described[89]. Briefly, mean normalized fluorescence i.e. ΔF/F was calculated by subtracting each value with the mean of the previous 5-s values lower than P_{50} (μ) and dividing the result by μ. ΔF/F traces were smoothened by convoluting the raw signal with a 10-s squared kernel and positive calcium transients were automatically defined based on a threshold set at 5*SD of the AP-5 trace.

dSTORM

Images were acquired using a Nikon Ti eclipse system equipped with a Perfect Focus System (PFS), an azimuthal TIRF arm (Gataca Systems, Massy, France), and an Apo TIRF 100x NA1.49 oil-immersion objective and an Evolve EMCCD camera (Photometrics, Tucson, USA) with a final pixel size of 65 nm. This system is equipped with a Ti-S-ER motorized stage controlled by MetaMorph software (Molecular Device, USA). Samples were illuminated in TIRF mode and images were obtained with an exposure time of 20 ms with up to 40,000 consecutive frames. Imaging was carried out at room temperature in a closed Ludin chamber (Life Imaging Services, Switzerland) using a pH-adjusted extracellular solution containing oxygen scavengers and reducing agents. Multicolor fluorescent microspheres (Tetraspeck, Life Technologies) were used for lateral drift correction. Super-resolution images were reconstructed with PALMTracer and protein-clustering into nano-size clusters i.e. nanodomains was obtained using the SR-Tesseler method[90]. Segmentations of the clusters were performed by applying a threshold of twice the average density δ of the whole dataset, with a minimum area of 7 and a minimum number of localizations of 5. Clusters' nanodomains were identified by applying a threshold of one time the average density of each cluster (0.4 minimum area, 25 minimum number of localizations). To analyze GluN1 enrichment at post-synapses (considered as homer 1 C puncta), the average density of detections was divided by the average density of extra-synaptic detections.

Frequency-domain-based FRET-FLIM microscopy

COS-7 cells were co-transfected with carboxyl terminally tagged GluN1-GFP together with HA-GluN2A and with the carboxyl terminally tagged D1R (WT or S397D)-mCherry in a proportion of 1:1:1, unless stated otherwise. mCherry alone was used as a FRET-negative control. Cells were imaged with an HCX PL Apo 63x oil NA 1.4 objective using an appropriate GFP filter set. Cells were excited using a sinusoidally modulated 3 W 478 nm LED (light-emitting diode) at 36 MHz under wild-field illumination. Emission was collected using an intensified CCD LI2CAM camera (Lambert Instrument BV, Groningen, The Netherlands). Lifetimes were calibrated using a solution of erythrosin B that was set at 0.086 ns. The lifetime of the sample is determined from the fluorescence phase-shift between the sample and the reference from a set of 12 phase settings using the manufacturer's LI-FLIM software.

In vivo electrophyisological recording

Peptide administration. TAT-NS and TAT-T2 peptides (3 mg/kg, i.p.) were daily administered for 3–4 consecutive days. For P4 mice, peptide administration was performed for 3 days and an electrophysiological recording was performed under a head-fixed condition at P7 (termed P7 head-fixed). For P7 mice, peptide administration was performed for 4 days and an electrophysiological recording was performed under a urethane-anesthetized. For P29 mice, an electrode assembly was first implanted into the hippocampus and peptide administration was performed for 4 days from P30 and recordings were obtained at P12 (termed P35 freely moving). Control mice were not injected with any drugs.

Surgery and electrophysiological recording. For electrophysiological recording from P7 head-fixed mice, the mice were anesthetized with isoflurane gas (0.5–2.5%) and restrained with their head held in place by a metal plate. A craniotomy was performed to create a rectangular hole (3.0 × 1.0 mm^2) centered at 1.5 mm posterior and 1.5 mm lateral to the bregma using a metal cutter, and the dura was surgically removed. Two 32-gauge needles were implanted in the bone above the cerebellum to serve as ground and reference electrodes. A silicon probe that consisted of 64 recording sites (Buzsaki 64, NeuroNexus) was inserted into the brain at a speed of 5μm/s so that the final depth of the electrode tip in the brain was 1300 μm. The electrodes were allowed to stabilize at their final position for 10 min before recording began. To aid in the reconstruction of the tracks left by the probe, the backside of the probe was coated with a DiI solution (80 mg/ml, Invitrogen).

For electrophysiological recording from P12 urethane-anesthetized mice, the mice were anesthetized with urethane (1.5 g/kg, i.p.) and the same procedures applied to the P7 head-fixed mice were performed with a craniotomy centered at 1.8 mm posterior and 1.7 mm lateral to the bregma and the final depth of the electrode tip in the brain ranged from 1500 to 1800μm.

For electrophysiological recording from P35 freely moving mice, the mice were implanted with an electrode assembly at P29. For electrode implantation, the mice were anesthetized with isoflurane gas (1–2%). A craniotomy with a diameter of ~2 mm was performed using a high-speed drill, and the dura was surgically removed. Two stainless-steel screws were implanted in the bone above the cerebellum to serve as ground and reference electrodes. An electrode assembly that consisted of 4 tetrodes, which was created using a 3D printer (Form 2, Formlabs), was stereotaxically implanted above the right hippocampus (1.8 mm posterior and 1.5 mm lateral to bregma). The tip of the electrode bundle was lowered to the cortical surface, and the electrodes were inserted 1.8–2.0 mm into the brain at the end of surgery. The electrodes were constructed from 17-μm-wide polyimide-coated platinum-iridium (90/10%) wire (California Fine Wire), and the electrode tips were plated with platinum to lower electrode impedances to 150–300 kΩ at 1 kHz. Electrophysiological data were sampled at 2 kHz and filtered between 0.1 and 500 Hz for at least 15 min using a Cereplex direct recording system (Blackrock).

Histological analysis to confirm electrode locations. At the end of the recording in P12 mice, the silicon probe stained with DiI was carefully removed from the brain. All mice were perfused intracardially with cold 4% PFA in 25 mM PBS and decapitated. After dissection, the brains were fixed overnight in 4% PFA. For P12 mice, the brains were rinsed in PBS and coronally sectioned at a thickness of 100 μm by a vibratome. For P35 mice, the brains were equilibrated with 30% sucrose in PBS, coronally sectioned at a thickness of 50 μm by a microtome, and counterstained with cresyl violet. The positions of electrodes were confirmed by identifying the corresponding electrode tracks in histological tissue. When electrode positions were not clearly visible, electrodes showing apparent LB events at P12 or ripple events at P35 were considered as electrodes located inside the hippocampus.

LFP data analysis. For LFP recording data from P7 head-fixed mice, the 20-min LFP traces were band-pass filtered at 1–50 Hz and the root

mean square (RMS) was computed with a bin size of 100 ms and giant depolarizing potentials (GDPs) were detected when the RMS exceeded 3 standard deviations above the mean. The minimum intervals between neighboring GDPs were set to be 1 s.

For LFP recording data from P12 urethane-anesthetized mice, to reduce 50-Hz humming noise, a 40-60 Hz notch filter was applied to the LFP data. The RMS of the 60-min LFP traces was computed with a bin size of 1 s and large-amplitude burst (LB) events were detected if the RMS exceeded a threshold of 1 mV/s.

For LFP recording data from P35 freely moving mice, the power spectra of LFP traces during 60-s quiescent periods at a moving speed of less than 2 cm/s were calculated by fast Fourier transformation at frequencies ranging from 1 to 100 Hz. The power of LFPs in the following sub-frequency bands were calculated: theta (6–10 Hz), slow gamma (20–40 Hz), and fast gamma (60–100 Hz). For the detection of ripples, LFP signals were band-pass filtered at 150–250 Hz and the RMS was calculated in the ripple-band with a bin size of 20 ms. Ripple events were detected when the RMS exceeded 3 standard deviations above the mean.

Tissue preparation

P5 animals were anesthetized with pentobarbital (300 mg/kg) and transcardially perfused with 4% PFA. Whole brains were removed and fixed overnight in 4% PFA, cryoprotected by immersion in 30% sucrose solution and sliced into 20 μm thick coronal sections on a microtome-cryostat (Leica CM3050S).

Biochemistry

Western Blot. Brain samples were snap-frozen in liquid nitrogen and stored at −80 °C. Neuronal cultures and brain samples were homogenized with TET buffer (20 mM Tris pH 8 – 1 mM EDTA –1.3% Triton X-100) complemented with proteases inhibitors), incubated on ice 10 min and centrifuge 10 min at 10,000 *g* to remove debris. The protein concentration of all samples was simultaneously determined using Pierce BCA Protein Assay Kit (Thermo Fisher Scientific). Either 4 or 10 μg of protein was loaded in 4-20 % precast SDS-polyacrylamide gel electrophoresis and transferred to a nitrocellulose membrane (Bio-Rad, Hercules, USA). The membrane was blocked in 5% non-fat milk Tris-buffer saline (TBS)/0.1% Tween-20 (TBST) at R.T. for 1 hour. Primary antibodies were diluted in 0.5 % milk TBST and incubated O.N. at 4 °C under agitation. Incubation with corresponding secondary antibody was performed for 1 h at R.T. Specific protein stain was revealed with SuperSignal West Femto Maximum Sensitivity Substrate detection kit (Pierce, Thermo Fisher Scientific Inc., Cambridge, UK) and total membranes were scanned using a Li-COR Odyssey-Sc imaging system. Quantification of band intensity was performed using Odyssey software and it was normalized to tubuline staining. Full scan blots are available in the Source Data file.

Co-immunoprecipitation. The co-immunoprecipitation assay was performed as previously described[50]. Briefly, rat brain tissues were homogenized in lysis buffer (50 mM Tris-HCl, 150 mM NaCl, 2 mM EDTA, 0.5% sodium deoxycholate, 1% NP-40, 1% Triton X-100, 0.1% SDS, Protease inhibitor cocktail (Sigma-Aldrich, 1:100, pH 7.4) on ice. Then the samples were gently shaken at 4 °C for 1 hour and centrifuged at 10,000 *g* for 10 min. The supernatant was collected as the protein extract. The concentration of samples was measured using Pierce BCA Protein Assay. For co-immunoprecipitation experiments, 500 – 700 μg protein extract was incubated with protein A/G plus agarose (25 μl per sample; Santa Cruz Biotechnology, catalog number: sc-2003) at 4 °C for 1 hour, and then the supernatant was incubated together with new protein A/G plus agarose in the presence of primary antibodies against D1R (2 μg) or D2R (2 μg) or control IgG (1–2 μg) at 4 °C for 12 hours with gentle shaking. Pellets were washed, boiled for 5 min in SDS sample buffer and 2-Mercaptoethanol and subjected to SDS-PAGE. A total of 50-100 μg of protein extract was used as a control in each experiment. Full scan blots are available in the Source Data file.

Antibodies

Reference		Provider	Dilution
Primary antibodies			
rabbit polyclonal anti-GFP	#A-6455	ThermoFisher Sc.	1/500 or 1/10 000
mouse monoclonal anti-Flag	#F1804	Sigma-Aldrich	1/500 or 1/10 000
mouse monoclonal anti-TH	#MAB318	Merck Millipore	1/1000
mouse anti-CK1 alpha	#sc-75582	Santa Cruz	1/1000
mouse monoclonal anti-beta-tubulin	TUB2.1	Sigma-Aldrich	1/5000
Rabbit anti-GluN2A	Clone A12W	Merck Millipore	1/1000 (WB)
rabbit anti-GluN2A	custom-made	Agrobio	1/200 (IF)
rabbit anti-GluN2B	custom-made	Agrobio	1/200 (IF), 1/1000 (WB)
rabbit anti-D1R	17934-1-AP	Proteintech	2 μg
rabbit anti-D2R	55084-1-AP	Proteintech	2 μg
rabbit anti-NR2A	NB300-105	Novus Biologicals	1/1000
rabbit anti-NR2B	ab65783	Abcam	1/1000
Chicken anti-MAP2	ab5392	Abcam	1/5000
Mouse anti-synapsin 1	#106011	Synaptic System	1/1000
Mouse anti-PSD95	MA1-046	ThermoFisher Sc.	1/500 (IF), 1/1000 (WB)
Rabbit anti-DBH	ab209487	Abcam	1/2000
Secondary antibodies:			
goat anti-mouse alexa fluor 488	#A11001	ThermoFisher Sc.	1/1000
Donkey anti-mouse alexa fluor 647	#A31571	ThermoFisher Sc.	1/1000
goat anti-rabbit alexa fluor 647	#A21244	ThermoFisher Sc.	1/1000
Goat anti-chicken 488	#A11039	ThermoFisher Sc.	1/1000
anti-mouse H + L HRP	#715-035-150	Jackson Immunoresearch	1/5000
goat-anti-rabbit IgG (H + L) highly cross-absorbed secondary antibody Alexa Fluor Plus 800	#A32735	ThermoFisher Sc.	1/5000
Alexa Fluor 790 AffiniPure Goat-anti-Rat IgG (light chain specific)	#112-655-175	Jackson ImmunoResearch	1/1000
Alexa Fluor 790 AffiniPure Goat-anti-Rabbit IgG (light chain specific)	#115-655-174	Jackson ImmunoResearch	1/1000
Quantum Dots:			
F (ab')2-Goat anti-Rabbit IgG-coupled Qdot655	#Q11422MP	ThermoFisher Sc.	1/50000
F (ab')2-Goat anti-Rabbit IgG-coupledQdot705	#Q11461MP	ThermoFisher Sc.	1/50000

Statistical analysis

No statistical methods were used to predetermine sample size. Sample size was based on previous publications with similar models and experiments. To ensure replicability, results are derived from at least

three independent experiments. No data were excluded from the analysis. All statistical tests were performed using GraphPad Prism. Datasets were analyzed for normality and parametric or non-parametric statistical test (two-tailed) were used accordingly. Test details and statistical outcomes are reported in the relevant figure and figure legends.

Reporting summary

Further information on research design is available in the Nature Portfolio Reporting Summary linked to this article.

Data availability

Data and resources are available on request from the corresponding author. Source data are provided as a Source Data file. Source data are provided with this paper.

Code availability

Codes used for this paper are available on request from the corresponding author.

References

1. Lau, C. G. & Zukin, R. S. NMDA receptor trafficking in synaptic plasticity and neuropsychiatric disorders. *Nat. Rev. Neurosci.* **8**, 413–426 (2007).
2. Paoletti, P., Bellone, C. & Zhou, Q. NMDA receptor subunit diversity: Impact on receptor properties, synaptic plasticity and disease. *Nat. Rev. Neurosci.* **14**, 383–400 (2013).
3. Groc, L., Gustafsson, B. & Hanse, E. AMPA signalling in nascent glutamatergic synapses: There and not there! *Trends Neurosci* **29**, 132–139 (2006).
4. Washbourne, P., Bennett, J. E. & McAllister, A. K. Rapid recruitment of NMDA receptor transport packets to nascent synapses. *Nat. Neurosci.* **5**, 751–759 (2002).
5. Tan, C. X. & Eroglu, C. Cell adhesion molecules regulating astrocyte–neuron interactions. *Curr. Opin. Neurobiol.* **69**, 170–177 (2021).
6. Wilton, D. K., Dissing-Olesen, L. & Stevens, B. Neuron-glia signaling in synapse elimination. *Annu. Rev. Neurosci.* **42**, 107–127 (2019).
7. Allen, N. J. & Lyons, D. A. System formation and function. *Science (80-.).* **185**, 181–185 (2018).
8. Cameron, S. & McAllister, A. K. Immunoglobulin-like receptors and their impact on wiring of brain synapses. *Annu. Rev. Genet.* **52**, 567–590 (2018).
9. Südhof, T. C. Towards an understanding of synapse formation. *Neuron* **100**, 276–293 (2018).
10. van Oostrum, M. et al. Surfaceome dynamics reveal proteostasis-independent reorganization of neuronal surface proteins during development and synaptic plasticity. *Nat. Commun.* **11**, 1–16 (2020).
11. Borgdorff, A. J. & Choquet, D. Regulation of AMPA receptor lateral movements. *Nature* **417**, 649–653 (2002).
12. Groc, L. et al. NMDA receptor surface mobility depends on NR2A-2B subunits. *Proc. Natl. Acad. Sci. USA.* **103**, 18769–18774 (2006).
13. Lavezzari, G., McCallum, J., Dewey, C. M. & Roche, K. W. Subunit-specific regulation of NMDA receptor endocytosis. *J. Neurosci.* **24**, 6383–6391 (2004).
14. Washbourne, P., Liu, X. B., Jones, E. G. & McAllister, A. K. Cycling of NMDA receptors during trafficking in neurons before synapse formation. *J. Neurosci.* **24**, 8253–8264 (2004).
15. Friedman, H. V., Bresler, T., Garner, C. C. & Ziv, N. E. Assembly of new individual excitatory synapses: Time course and temporal order of synaptic molecule recruitment. *Neuron* **27**, 57–69 (2000).
16. Petit-Pedrol, M. & Groc, L. Regulation of membrane NMDA receptors by dynamics and protein interactions. *J. Cell Biol.* **220**, 1–15 (2021).
17. Money, K. M. & Stanwood, G. D. Developmental origins of brain disorders: roles for dopamine. *Front. Cell. Neurosci.* **7**, 1–14 (2013).
18. Washburn, H. R., Chander, P., Srikanth, K. D. & Dalva, M. B. Trans-synaptic signaling of Ephs in synaptic development, plasticity, and disease. *Neuroscience* **5537**, 127–133 (2022).
19. Bemben, M. A., Shipman, S. L., Nicoll, R. A. & Roche, K. W. The cellular and molecular landscape of neuroligins. *Trends Neurosci* **38**, 496–505 (2015).
20. Lee, F. J. S. et al. Dual regulation of NMDA receptor functions by direct protein-protein interactions with the dopamine D1 receptor. *Cell* **111**, 219–230 (2002).
21. Fiorentini, C., Gardoni, F., Spano, P. F., Di Luca, M. & Missale, C. Regulation of dopamine D1 receptor trafficking and desensitization by oligomerization with glutamate N-methyl-D-aspartate. *receptors. J. Biol. Chem.* **278**, 20196–20202 (2003).
22. Cepeda, C. & Levine, M. S. Where do you think you are going? The NMDA-D1 receptor trap. *Sci. STKE* **2006**, 1–6 (2006).
23. Ladepeche, L. et al. Single-molecule imaging of the functional crosstalk between surface NMDA and dopamine D1 receptors. *Proc. Natl. Acad. Sci. USA.* **110**, 18005–18010 (2013).
24. Li, Y. C., Liu, G., Hu, J. L., Gao, W. J. & Huang, Y. Q. Dopamine D1 receptor-mediated enhancement of NMDA receptor trafficking requires rapid PKC-dependent synaptic insertion in the prefrontal neurons. *J. Neurochem.* **114**, 62–73 (2010).
25. Scott, L. et al. Allosteric changes of the NMDA receptor trap diffusible dopamine 1 receptors in spines. *Proc. Natl. Acad. Sci. USA.* **103**, 762–767 (2006).
26. Pei, L., Lee, F. J. S., Moszczynska, A., Vukusic, B. & Liu, F. Regulation of dopamine D1 receptor function by physical interaction with the NMDA receptors. *J. Neurosci.* **24**, 1149–1158 (2004).
27. Nai, Q. et al. Uncoupling the D1-N-methyl-D-aspartate (NMDA) receptor complex promotes NMDA-dependent long-term potentiation and working memory. *Biol. Psychiatry* **67**, 246–254 (2010).
28. Cahill, E. et al. D1R/GluN1 complexes in the striatum integrate dopamine and glutamate signalling to control synaptic plasticity and cocaine-induced responses. *Mol. Psychiatry* **19**, 1295–1304 (2014).
29. Andrianarivelo, A. et al. Disrupting D1-NMDA or D2-NMDA receptor heteromerization prevents cocaine's rewarding effects but preserves natural reward processing. *Sci. Adv.* **7**, eabg5970 (2021).
30. Gréa, H. et al. Human autoantibodies against n-methyl-d-aspartate receptor modestly alter dopamine d1 receptor surface dynamics. *Front. Psychiatry* **10**, 1–7 (2019).
31. Kasai, R. S., Ito, S. V., Awane, R. M., Fujiwara, T. K. & Kusumi, A. The class-a gpcr dopamine d2 receptor forms transient dimers stabilized by agonists: detection by single-molecule tracking. *Cell Biochem. Biophys.* **76**, 29–37 (2018).
32. Kasai, R. S. et al. Full characterization of GPCR monomer-dimer dynamic equilibrium by single molecule imaging. *J. Cell Biol.* **192**, 463–480 (2011).
33. Calebiro, D. et al. Single-molecule analysis of fluorescently labeled G-protein-coupled receptors reveals complexes with distinct dynamics and organization. *Proc. Natl. Acad. Sci. USA.* **110**, 743–748 (2013).
34. Sungkaworn, T. et al. Single-molecule imaging reveals receptor-G protein interactions at cell surface hot spots. *Nature* **550**, 543–547 (2017).
35. Hern, J. A. et al. Formation and dissociation of M1 muscarinic receptor dimers seen by total internal reflection fluorescence imaging of single molecules. *Proc. Natl. Acad. Sci. USA.* **107**, 2693–2698 (2010).
36. Tabor, A. et al. Visualization and ligand-induced modulation of dopamine receptor dimerization at the single molecule level. *Sci. Rep.* **6**, 1–16 (2016).

37. Asher, W. B. et al. Single-molecule FRET imaging of GPCR dimers in living cells. *Nat. Methods* **18**, 397–405 (2021).
38. Graham, T. G. W., Ferrie, J. J., Dailey, G. M., Tjian, R. & Darzacq, X. Detecting molecular interactions in live-cell single-molecule imaging with proximity-assisted photoactivation (PAPA). *Elife* **11**, 1–46 (2022).
39. Low-Nam, S. T. et al. ErbB1 dimerization is promoted by domain co-confinement and stabilized by ligand binding. *Nat. Struct. Mol. Biol.* **18**, 1244–1249 (2011).
40. Groc, L. & Choquet, D. Linking glutamate receptor movements and synapse function. *Science (80-.)* **368**, eaay4631 (2020).
41. Butler, C. et al. Multi-dimensional spectral single molecule localization microscopy. *Front. Bioinforma.* **2**, 1–14 (2022).
42. Liu, X. Y. et al. Modulation of D2R-NR2B interactions in response to cocaine. *Neuron* **52**, 897–909 (2006).
43. Woods, A. S. et al. Role of electrostatic interaction in receptor-receptor heteromerization. *J. Mol. Neurosci.* **26**, 125–132 (2005).
44. Chergui, K., Svenningsson, P. & Greengard, P. Physiological role for casein kinase 1 in glutamatergic synaptic transmission. *J. Neurosci.* **25**, 6601–6609 (2005).
45. Perreault, M. L. et al. Disruption of a dopamine receptor complex amplifies the actions of cocaine. *Eur. Neuropsychopharmacol.* **26**, 1366–1377 (2016).
46. Frederick, A. L. et al. Evidence against dopamine D1/D2 receptor heteromers. *Mol. Psychiatry* **20**, 1373–1385 (2015).
47. Kellermayer, B. et al. Differential nanoscale topography and functional role of glun2-nmda receptor subtypes at glutamatergic synapses. *Neuron* **100**, 106–119.e7 (2018).
48. Uchigashima, M., Ohtsuka, T., Kobayashi, K. & Watanabe, M. Dopamine synapse is a neuroligin-2-mediated contact between dopaminergic presynaptic and GABAergic postsynaptic structures. *Proc. Natl. Acad. Sci. USA.* **113**, 4206–4211 (2016).
49. Tritsch, N. X. & Sabatini, B. L. Dopaminergic modulation of synaptic transmission in cortex and striatum. *Neuron* **76**, 33–50 (2012).
50. Su, P. et al. A dopamine D2 receptor-DISC1 protein complex may contribute to antipsychotic-like effects. *Neuron* **84**, 1302–1316 (2014).
51. Colonnese, M. T. & Khazipov, R. 'Slow activity transients' in infant rat visual cortex: A spreading synchronous oscillation patterned by retinal waves. *J. Neurosci.* **30**, 4325–4337 (2010).
52. Werner, C., Sauer, M. & Geis, C. Super-resolving microscopy in neuroscience. *Chem. Rev.* **121**, 11971–12015 (2021).
53. Calebiro, D., Koszegi, Z., Lanoiseléee, Y., Miljus, T. & O'brien, S. G protein-coupled receptor-g protein interactions: a single-molecule perspective. *Physiol. Rev.* **101**, 857–906 (2021).
54. Papouin, T. et al. Synaptic and extrasynaptic NMDA receptors are gated by different endogenous coagonists. *Cell* **150**, 633–646 (2012).
55. Dupuis, J. P. et al. Surface dynamics of GluN2B-NMDA receptors controls plasticity of maturing glutamate synapses. *EMBO J* **33**, 842–861 (2014).
56. Bard, L. et al. Dynamic and specific interaction between synaptic NR2-NMDA receptor and PDZ proteins. *Proc. Natl. Acad. Sci. USA.* **107**, 19561–19566 (2010).
57. Matta, J. A., Ashby, M. C., Sanz-Clemente, A., Roche, K. W. & Isaac, J. T. R. MGluR5 and NMDA receptors drive the experience- and activity-dependent nmda receptor nr2b to nr2a subunit switch. *Neuron* **70**, 339–351 (2011).
58. Wang, H. D., Stanwood, G. D., Grandy, D. K. & Deutch, A. Y. Dystrophic dendrites in prefrontal cortical pyramidal cells of dopamine D1 and D2 but not D4 receptor knockout mice. *Brain Res* **1300**, 58–64 (2009).
59. Verney, C. et al. Morphological evidence for a dopaminergic terminal field in the hippocampal formation of young and adult rat. *Neuroscience* **14**, 1039–1052 (1985).
60. Azevedo, E. P. et al. A role of Drd2 hippocampal neurons in context-dependent food intake. *Neuron* **102**, 873–886.e5 (2019).
61. Lee, J. Y. et al. Dopamine facilitates associative memory encoding in the entorhinal cortex. *Nature* **598**, 321–326 (2021).
62. McNamara, C. G., Tejero-Cantero, Á., Trouche, S., Campo-Urriza, N. & Dupret, D. Dopaminergic neurons promote hippocampal reactivation and spatial memory persistence. *Nat. Neurosci.* **17**, 1658–1660 (2014).
63. Rosen, Z. B., Cheung, S. & Siegelbaum, S. A. Midbrain dopamine neurons bidirectionally regulate CA3-CA1 synaptic drive. *Nat. Neurosci.* **18**, 1763–1771 (2015).
64. Rossato, J. I., Bevilaqua, L. R. M., Izquierdo, I., Jorge, H. & Medina, C., M. Dopamine Controls Persistence of Long-Term Memory Storage. *Science (80-.).* **325**, 2–5 (2009).
65. Tsetsenis, T. et al. Midbrain dopaminergic innervation of the hippocampus is sufficient to modulate formation of aversive memories. *Proc. Natl. Acad. Sci. USA.* **118**, 1–10 (2021).
66. Takeuchi, T. et al. Locus coeruleus and dopaminergic consolidation of everyday memory. *Nature* **537**, 357–362 (2016).
67. Gálvez-Márquez, D. K. et al. Spatial contextual recognition memory updating is modulated by dopamine release in the dorsal hippocampus from the locus coeruleus. *Proc. Natl. Acad. Sci. USA* **119**, 2017 (2022).
68. Fuchsberger, T. et al. Postsynaptic burst reactivation of hippocampal neurons enables associative plasticity of temporally discontiguous inputs. *Elife* **11**, 1–23 (2022).
69. Chowdhury, A. et al. A locus coeruleus-dorsal CA1 dopaminergic circuit modulates memory linking. *Neuron* **110**, 3374–3388 (2022).
70. Smith, W. B., Starck, S. R., Roberts, R. W. & Schuman, E. M. Dopaminergic stimulation of local protein synthesis enhances surface expression of GluR1 and synaptic transmission in hippocampal neurons. *Neuron* **45**, 765–779 (2005).
71. Berlanga, M. L. et al. Multiscale imaging characterization of dopamine transporter knockout mice reveals regional alterations in spine density of medium spiny neurons. *Brain Res* **1390**, 41–49 (2011).
72. Bellone, C., Mameli, M. & Lüscher, C. In utero exposure to cocaine delays postnatal synaptic maturation of glutamatergic transmission in the VTA. *Nat. Neurosci.* **14**, 1439–1446 (2011).
73. Zong, P. et al. Functional coupling of TRPM2 and extrasynaptic NMDARs exacerbates excitotoxicity in ischemic brain injury. *Neuron* **110**, 1–15, https://doi.org/10.1016/j.neuron.2022.03.021 (2022).
74. Yan, J., Peter Bengtson, C., Buchthal, B., Hagenston, A. M. & Bading, H. Coupling of NMDA receptors and TRPM4 guides discovery of unconventional neuroprotectants. *Science (80-.)* **370**, eaay3302 (2020).
75. Gómez, R. et al. NMDA receptor-BK channel coupling regulates synaptic plasticity in the barrel cortex. *Proc. Natl. Acad. Sci. USA.* **118**, 1–12 (2021).
76. Kern, A. et al. Hippocampal dopamine/DRD1 signaling dependent on the ghrelin receptor. *Cell* **163**, 1176–1190 (2015).
77. Anton, S. E. et al. Receptor-associated independent cAMP nanodomains mediate spatiotemporal specificity of GPCR signaling. *Cell* **185**, 1130–1142 (2022).
78. Jézéquel, J., Johansson, E. M., Leboyer, M. & Groc, L. Pathogenicity of antibodies against nmda receptor: molecular insights into autoimmune psychosis. *Trends Neurosci* **41**, 502–511 (2018).
79. Fribourg, M. et al. Decoding the signaling of a GPCR heteromeric complex reveals a unifying mechanism of action of antipsychotic drugs. *Cell* **147**, 1011–1023 (2011).
80. Moreno, J. L. et al. Allosteric signaling through an mGlu2 and 5-HT2A heteromeric receptor complex and its potential contribution to schizophrenia. *Sci. Signal.* **9**, 1–19 (2016).
81. González-Maeso, J. et al. Identification of a serotonin/glutamate receptor complex implicated in psychosis. *Nature* **452**, 93–97 (2008).

82. Borroto-Escuela, D. O., Wydra, K., Filip, M. & Fuxe, K. A2AR-D2R heteroreceptor complexes in cocaine reward and addiction. *Trends Pharmacol. Sci.* **39**, 1008–1020 (2018).
83. Ellaithy, A., Younkin, J., González-Maeso, J. & Logothetis, D. E. Positive allosteric modulators of metabotropic glutamate 2 receptors in schizophrenia treatment. *Trends Neurosci* **38**, 506–516 (2015).
84. George, S. R., Kern, A., Smith, R. G. & Franco, R. *Dopamine receptor heteromeric complexes and their emerging functions*. *Progress in Brain Research* vol. 211 (Elsevier B.V., 2014).
85. Perroy, J. et al. Direct interaction enables cross-talk between ionotropic and group I metabotropic glutamate receptors. *J. Biol. Chem.* **283**, 6799–6805 (2008).
86. Izeddin, I. et al. Wavelet analysis for single molecule localization microscopy. *Opt. Express* **20**, 2081–2095 (2012).
87. Kechkar, A., Nair, D., Heilemann, M., Choquet, D. & Sibarita, J.-B. Real-time analysis and visualization for single-molecule based super-resolution microscopy. *PLoS One* **8**, e62918 (2013).
88. Racine, V. et al. Multiple-target tracking of 3D fluorescent objects based on simulated annealing. *3rd IEEE Int. Symp. Biomed. Imaging From Nano to Macro - Proc.* 1020–1023 (2006).
89. Johansson, E. M. et al. Human endogenous retroviral protein triggers deficit in glutamate synapse maturation and behaviors associated with psychosis. *Sci. Adv.* **6**, eabc0708 (2020).
90. Levet, F. et al. SR-Tesseler: a method to segment and quantify localization-based super-resolution microscopy data. *Nat. Methods* **12**, 1065–1071 (2015).

Acknowledgements

We thank Julien Dupuis, François Maingret, and Olivier Nicole for insightful discussions, Hélène Gréa for training on microfluidic device, the Bordeaux Imaging Center for support in microscopy and in particular Christel Poujol and Magalie Mondin for advice and discussions, the IINS in vivo facility for animal housing. We would also like to thank the Cell Biology Facility, especially Delphine Bouchet, Constance Manso, Elodie Cougouilles, Morgane Meras, Léa Villetelle, Emeline Verdier, Christelle Breillat, and Rémi Sterling, for molecular and cellular tool productions and general cell biology activity management. This work was supported by The National Center for Scientific Research (CNRS), Agence Nationale de la Recherche (Projects DynHippo and DopamineHub to L.G.; NanoPlanSyn and soLIVE to J.B.S), Human Frontier Science Program (RGP0019/2016 to L.G., Y.I., F.L.), Fondation pour la Recherche Médicale, European Research Council Synergy grant (ENSEMBLE, #951294 to L.G.). We also acknowledge France-BioImaging infrastructure supported by the French National Research Agency (ANR-10-INBS-04 to L.G. and J-B.S.).

Author contributions

N.B., C.B., G.E.S., N.K., Y.N., T.S., T.Y., P.S., and M.P-P. conducted the experiments and collected the data. C.B., R.G., J-B.S. developed the MS-SMLM. P.S. and F.L. performed co-immunoprecipitation experiments. V.S. supervised microfluidic experiments. N.B., C.B., G.E.S., N.K., Y.N., T.Y., P.S., and M.P-P. analyzed the data. N.B., G.E.S., T.S., Y.I., and L.G. designed the study and experiments. N.B. and L.G. wrote the paper, which all authors helped to revised.

Competing interests

The authors declare no competing interests.

Additional information

Supplementary information The online version contains supplementary material available at https://doi.org/10.1038/s41467-023-44301-z.

Correspondence and requests for materials should be addressed to Laurent Groc.

Peer review information *Nature Communications* thanks the anonymous reviewers for their contribution to the peer review of this work. A peer review file is available.

Supplemental materials for

Non-canonical interplay between glutamatergic NMDA and dopamine receptors shapes synaptogenesis

Nathan Bénac[1§], G. Ezequiel Saraceno[1§], Corey Butler[1§], Nahoko Kuga[2,7], Yuya Nishimura[2], Taiki Yokoi[6], Ping Su[3], Takuya Sasaki[2,6], Mar Petit-Pedrol[1], Rémi Galland[1], Vincent Studer[1], Fang Liu[3], Yuji Ikegaya[2,4,5], Jean-Baptiste Sibarita[1], Laurent Groc[1*]

[1] Univ. Bordeaux, CNRS, IINS, UMR 5297, F-33000 Bordeaux, France

[2]Laboratory of Chemical Pharmacology, Graduate School of Pharmaceutical Sciences, The University of Tokyo, 7-3-1 Hongo Bunkyo-ku, Tokyo, 113-0033, Japan

[3]Campbell Family Mental Health Research Institute, Centre for Addiction and Mental Health, University of Toronto, Toronto, Canada

[4]Center for Information and Neural Networks, Suita City, Osaka, 565-0871, Japan

[5]Institute for AI and Beyond, The University of Tokyo, Tokyo 113-0033, Japan

[6]Department of Pharmacology, Graduate School of Pharmaceutical Sciences, Tohoku University, 6-3 Aramaki-aoba, Sendai, Miyagi, 980-8578, Japan

[§] These authors equally contributed

* Email: laurent.groc@u-bordeaux.fr

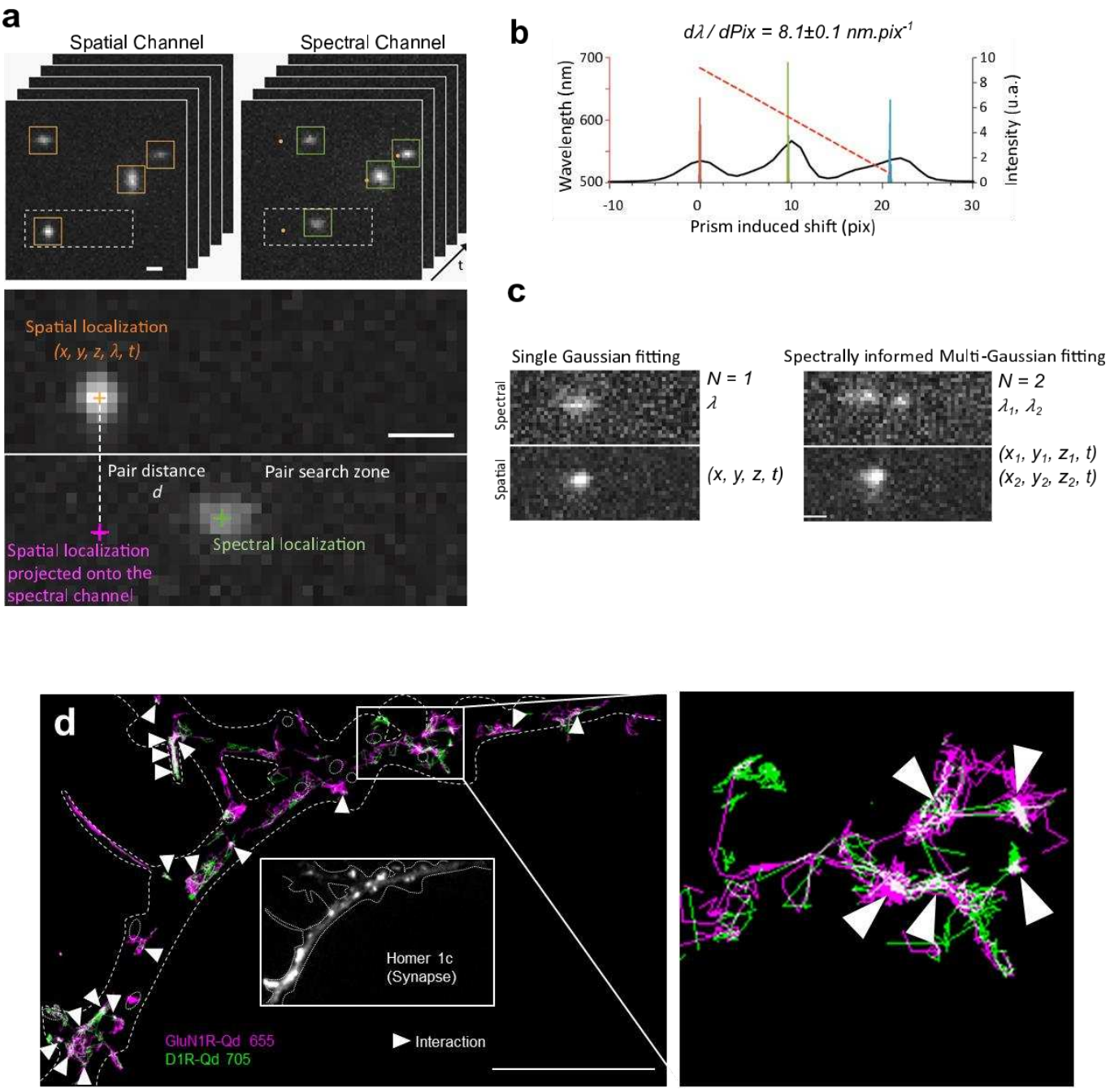

Supplementary Fig. 1 MS-SMLM method.

a Spectrally displaced localization principle. b Calibration of the prism-induced shift in the spectral channel. c, Spectrally informed multi-gaussian fitting principle. d Representative reconstruction of GuN1-NMDAR and D1R surface diffusion. The white arrows represent the locations of the interacting events. Scale bar, 10 µm.

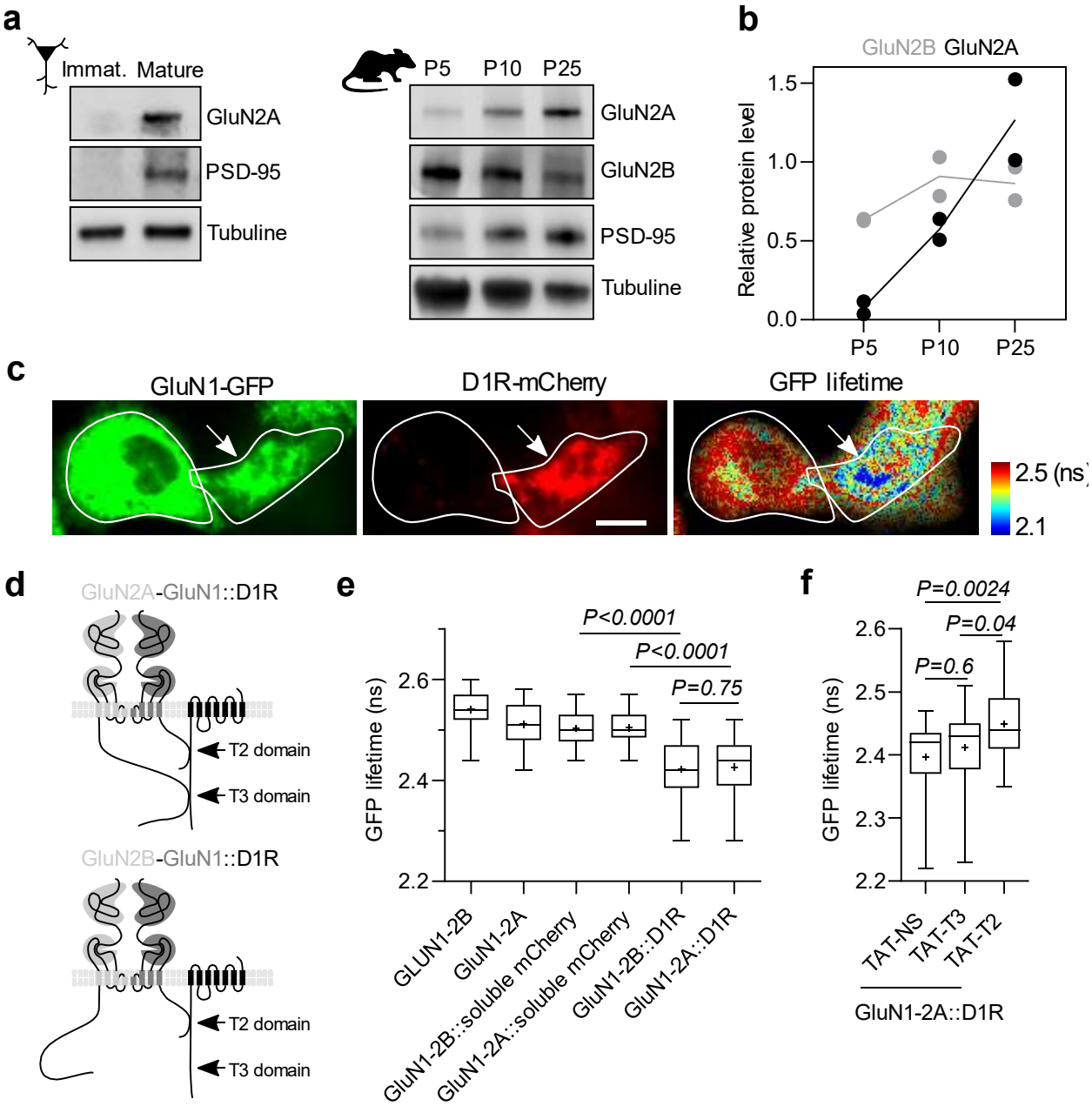

Supplementary Fig. 2 Role of the GluN2A/B subunit in the GluN1-NMDAR-D1R interaction.

a Representative immunoblots with **b** corresponding quantification of the protein level (relative to tubuline) of the GluN2A and GluN2B subunits in the hippocampus of P5, P10 and P25 animals. N = 2 animals per group. **c** Representative fluorescence and color-coded GFP lifetime images. Scale bar, 50 µm. **d** Experimental set-up. **e** Quantification of the GluN1-GFP lifetime when GluN1-NMDAR is co-expressed, in COS-7 cells, either with the GluN2B (GluN1-2B, n = 31 cells) or GluN2A (GluN1-2A, n = 31 cells) subunits alone or together with soluble mCherry (acceptor control, GluN1-2B::soluble mCherry, n = 26 cells; GluN1-2A::soluble mCherry, n = 17 cells) or D1R-mCherry

(GluN1-2B::D1R, n = 41 cells; GluN1-2A::D1R, n = 41 cells). Two-tailed unpaired t-test. **f** Quantification of the GluN1-GFP lifetime in the GluN1-GFP-GluN2A::D1RmCherry configuration after incubation with either a control competing TAT-peptide (TAT-NS, n = 29 cells), or targeting either the T2 domain (between GluN1-NMDAR and D1R; TAT-T2, n = 28 cells) or the T3 domain (between GluN2A-NMDAR and D1R; TAT-T3, n = 30 cells). One-way ANOVA with Tukey's post-hoc test. Dots represent the mean.

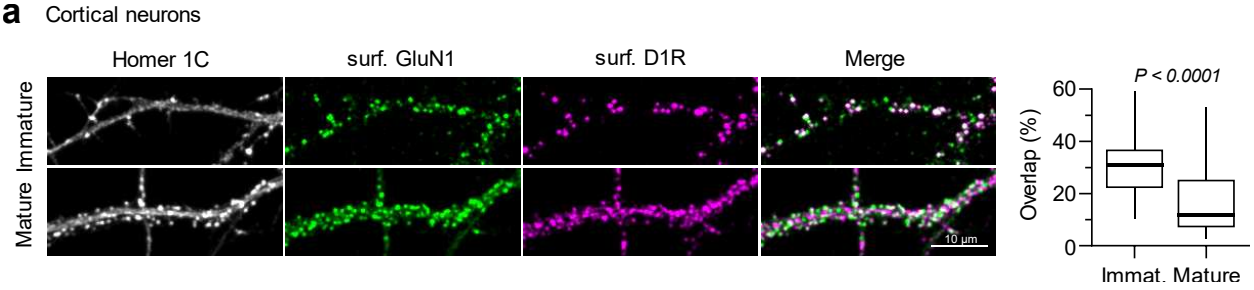

Supplementary Fig. 3 GluN1-NMDAR-D1R interaction paradigm is conserved in cortical culture.

a Representative immunofluorescence images with quantification of GluN1-NMDAR-D1R overlap in immature (9 DIV, n = 25 cells) and mature (>15 DIV, n = 28 cells) cortical neurons. Two-tailed unpaired t-test. Scale bar, 10 µm.

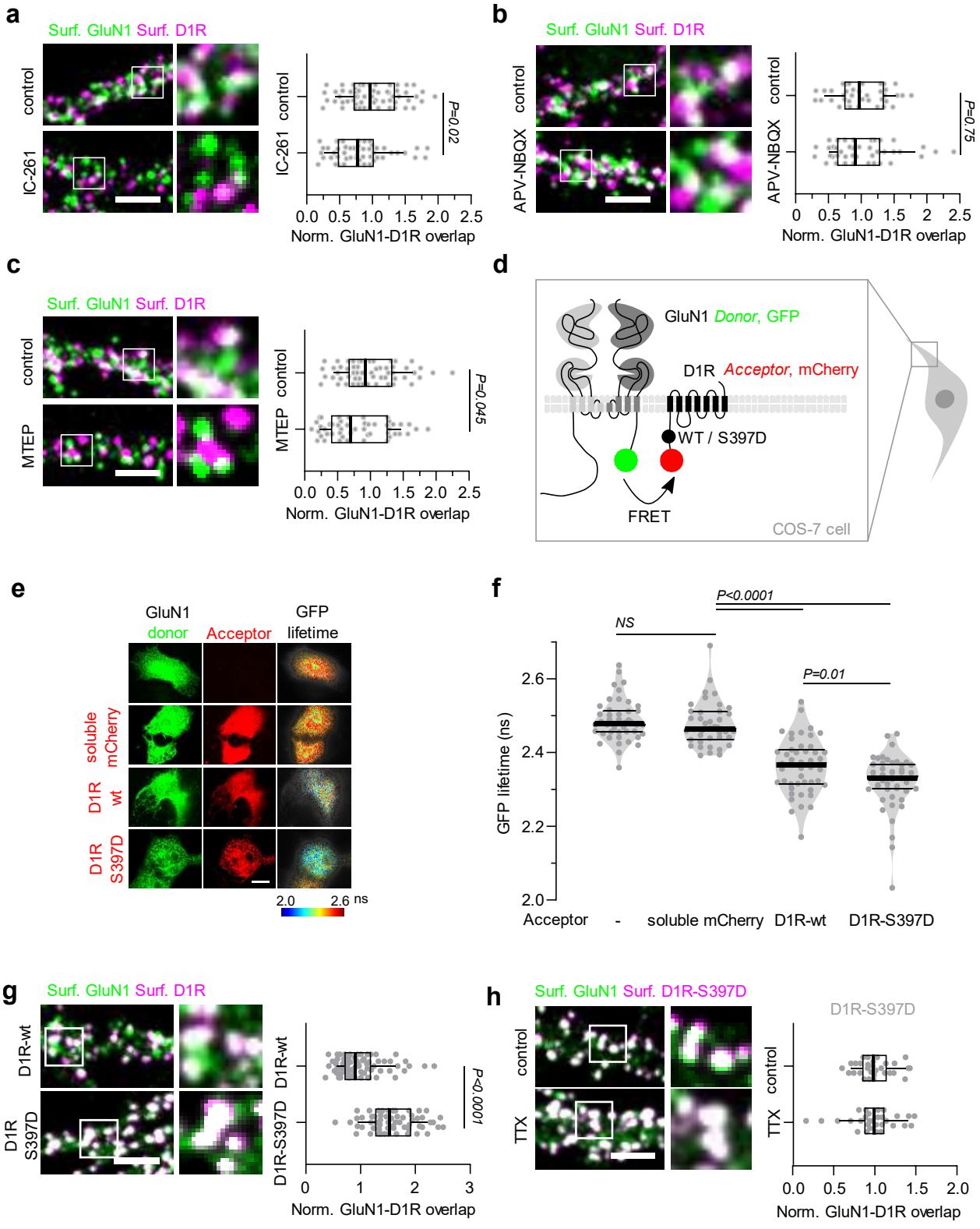

Supplementary Fig. 4 GluN1-NMDAR-D1R is regulated in a CK1 and mGluR5-dependent manner.

a-c Representative images of hippocampal dendrites on which surface GluN1-NMDAR (green) and D1R (magenta) were labelled after exposure to (a) control (buffer; n = 59 fields) or IC-261 (CK1 inhibitor, 50 µM; n = 51 fields); (b) buffer (control; n = 38 fields) or AP-V and NBQX (50 µM and 2µM, respectively; n = 42 fields); (c) buffer (control, n = 56 fields) or MTEP (mGluR inhibitor, 10 µM; n = 49 fields). Two-tailed unpaired t-test. **d** Experimental set-up. **e** Representative fluorescence and color-coded GFP lifetime images. Scale bar, 20 µm. **f** Measure of GFP-fluorescence lifetime when GluN1-GFP is expressed alone (n = 46 cells) or together with soluble mCherry (control condition, n = 40 cells), D1R-wt-mCherry (n = 48 cells) or D1R-S397D-mCherry (47 cells), one-way ANOVA with Tukey's post-hoc test. **g** Representative images of hippocampal dendrites on which surface GluN1-NMDAR (green) and D1R (WT or S397D, magenta) were labelled alongside quantification of the overlap between GluN1-NMDAR and D1R-wt (n = 25 cells, 52 fields) or D1R-S397D (n = 30 cells, 60 fields), Two-tailed unpaired t-test. Scale bar, 5 µm. **h** (left) Representative images of hippocampal dendrites on which surface GluN1-NMDAR (green) and D1R-S397D (magenta) were labelled after exposure to TTX; (right) quantifications of the overlap between GluN1-NMDAR and D1R-S397D following application of either buffer (CTL, n = 30 cells, 59 fields) or TTX (n = 30 cells, 53 fields). Two-tailed unpaired t-test. Scale bar, 5 µm.

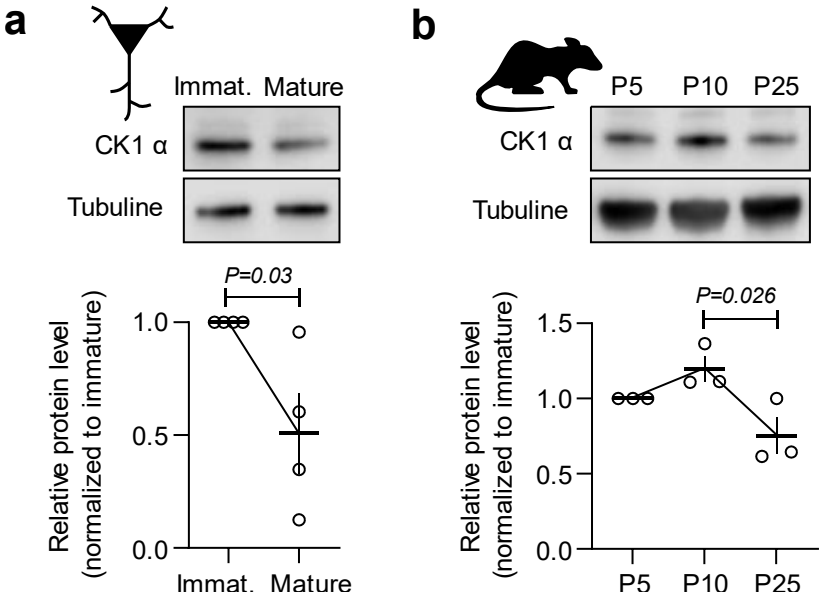

Supplementary Fig. 5 CK1α is differentially expressed over neuronal development both *in vitro* and *in vivo*.

a Representative immunoblots with corresponding quantification of the relative protein level of CK1-alpha in immature (n=4) and mature (n=4) hippocampal cultures. The results are normalized to immature. Unpaired t-test. **b** Representative immunoblots with quantification of the relative protein level of CK1-alpha in hippocampi from P5, P10 and P25 animals. N = 3 animals per group. The results are normalized to P5. One-way ANOVA with Tukey's post-hoc test.

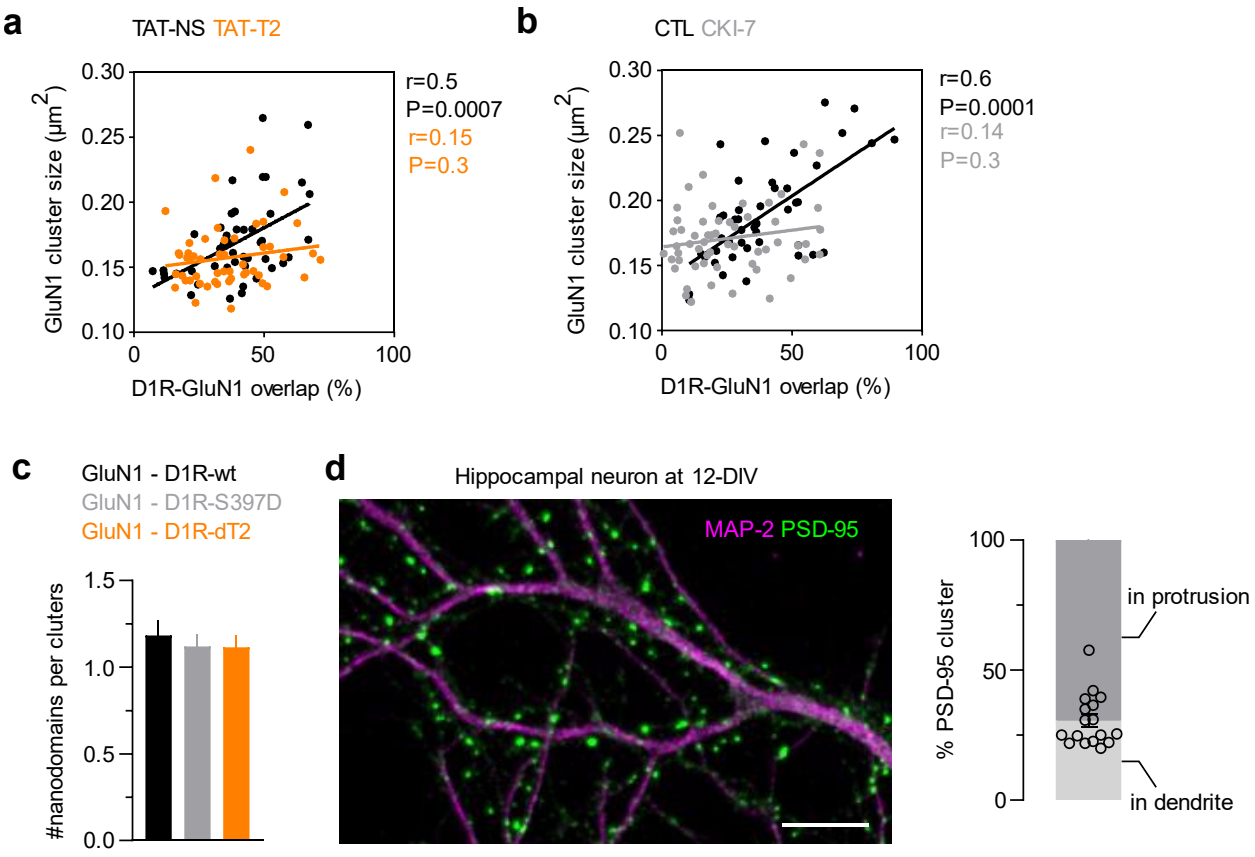

Supplementary Fig. 6 **The interaction between GluN1 and D1R controls the organization of GluN1 at the neuronal surface.**

a-b Correlation between the size of GluN1-NMDAR cluster and the overlap between GluN1-NMDAR and D1R in control condition or after disruption of the interaction through competing peptides (a) or CKI-7 (b) incubation. **c** Quantification the number of GluN1 nanodomains per clusters when GluN1 is co-expressed with D1R-wt (n = 7 cells, 186 clusters and 214 nanodomains), D1R-dT2 (n = 7 cells, 217 clusters and 242 nanodomains) or D1R-S397D (n = 6 cells, 151 clusters and 169 nanodomains). **d** (left) Representative image of hippocampal dendrites at 12 days in vitro (DIV). Dendrites were labelled with MAP-2 (magenta) and postsynaptic densities with PSD-95 (green). Scale bar, 10 µm. (right) Percentage of post-synaptic densities i.e. PSD-95 puncta located in protrusion or onto the dendrite in DIV 12 hippocampal neurons (n = 17 neurons).

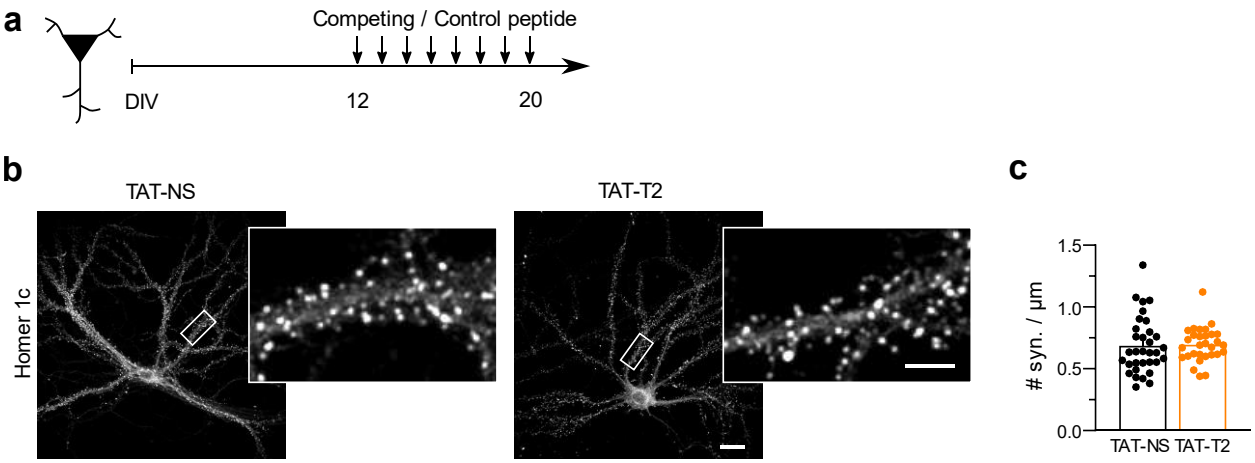

Supplementary Fig. 7 Longer incubation of mature neurons with TAT-competing peptides does not alter the number of post-synapses in vitro.

a Experimental set-up. **b** Representative images of Homer 1c staining. Scale bar, 20 and 5 µm. **c** Quantification of the number of synapses in mature neurons treated for 8 consecutive days with control (TAT-NS, n = 33 cells) or competing peptides (TAT-T2, n = 30 cells). Two-sided unpaired t-test.

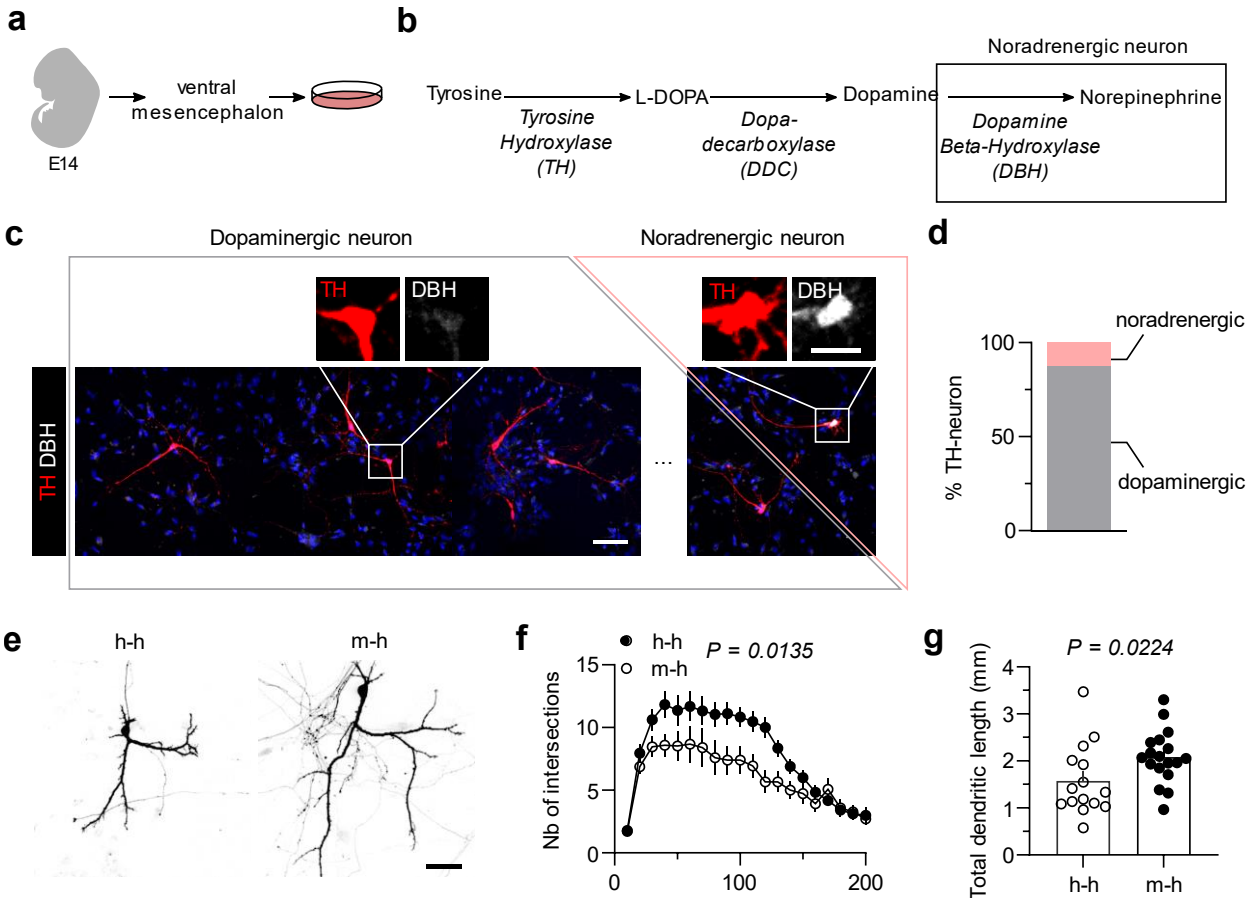

Supplementary Fig. 8 Characterization of the primary neuronal culture from the midbrain.

a Experimental set-up. **b** Catecholamines synthesis pathway. **c** Representative fluorescence images of TH (red) and DBH (gray) staining. Scale bar, 50 and 20 µm. **d** Quantification of the percentage of dopaminergic (DBH negative, TH positive) and noradrenergic (DBH positive, TH positive) neurons. **e** Representative fluorescence images of hippocampal neurons co-cultured with hippocampal neurons (h-h) or dopaminergic-containing midbrain neurons (m-h). Scale bar, 50 µm; **f** Sholl Analysis (step size of 10 µm). Two-tailed Kolmogorov-Smirnov test. **g** Total dendritic size of hippocampal neurons co-cultured with hippocampal neurons (h-h n = 15 cells) or with midbrain neurons (m-h, n = 18 cells). Two-tailed unpaired t-test.

Discussion and perspectives

1. Protein-protein interactions (PPI) between surface receptors: beyond the controversy

Commonly used method to investigate protein-protein interaction, including biochemical strategies such co-immunoprecipitation (co-IP) or imaging approaches such as proximity ligation assay (PLA), and live imaging approaches such as RET (resonance energy transfer; FRET, fluorescence energy transfer and BRET, bioluminescence resonance energy transfer) and fluorescence recovery after photobleaching (FRAP), have been used to resolved the propensity of macromolecules to form heteromeric complexes (Dorsch et al., 2009; Milligan and Bouvier, 2005; Petit-Pedrol and Groc, 2021). Even if the data generated have supported the presence of such complexes, controversies concerning the prevalence and the role of such putative weak PPI (e.g. interactions between surface receptors), which typically are short-lasting and concern a limited fraction of receptors at a given time, have emerged. The above-mentioned techniques are bulk (e.g. intracellular and membrane), averaging measurement of populations of macromolecules, preventing thus to resolve oligomers' kinetics and stability. Some of these limitations have been overcome thanks to the development of single particle tracking (SPT) techniques that permit to follow, at the cellular membrane, the diffusion of single receptors and allow to directly observe transient dimerization events. Such methods have been efficiently used to assess GPCR dimerization in heterologous cell cultures (e.g. CHO cells) following their labeling with fluorescent ligands or the exogeneous expression of recombinant receptors (SNAP-/ CLIP-tag technologies) (Asher et al., 2021; Calebiro et al., 2013; Hern et al., 2010; Kasai et al., 2011). However, they have been mainly used to track one, sometime two, populations of receptors in flat membranes and for limited periods of time due to both the low-fluorescence and photobleaching of fluorophores.

Herein, we used a custom MS-SMLM approach developed by (Butler et al., 2022) to resolve the surface interaction between D1R and NMDAR at the membrane of hippocampal neurons after their sparse indirect co-immunolabeling with primary antibodies and Fab-coupled quantum-dots (QD) (~ secondary antibody) of different wavelengths (emitting at 655 and 705 nm). QDs are extremely bright and photostable nanoparticle that have been a prime choice to track the surface diffusion of membrane receptor, for extended periods of time, at the surface of neurons both in

culture and in slices *ex vivo* (Biermann et al., 2014; Varela et al., 2016). The interaction between D1R-GluN1-NMDAR were transient, repeatedly occurring in an ON/OFF manner between highly diffusing receptors and with on average 30% of their localizations falling into the interaction zone. In average, D1R-GluN1-NMDAR interaction lasted 130 ± 0.01 ms with an apparent dissociation rate (or K_{off}) of 13 ± 0.7 s^{-1}.

In my PhD work, we arbitrarily defined the cut-off distance between receptors to consider interacting versus non-interacting receptors at 100 nm. This was due to i) labeling strategy (indirect immunolabeling), ii) the size of the coated QDs (~ 20 nm in average), and iii) the size of the extracellular domain of the recombinant GluN1-NMDA and D1 receptors. Exogenous GluN1-NMDAR were fused to a FLAG tag while D1R were fused to the green fluorescent protein (GFP) at their N-terminal domains. Future developments aiming for smaller probes (e.g. through direct immunolabeling with either primary antibody, Fab fragments or nanobodies (Choquet et al., 2021) directly coupled with QDs) as well as smaller fluorescent proteins could further lower this threshold distance of 100 nm. Furthermore, alternative approaches to the transfection of exogeneous receptors could provide a better physiological setting. Although our MS-SMLM approach allow to specifically track endogenous receptors, there is nowadays no commercially-available primary antibody that allow to specifically target both D1R and GluN1-NMDAR at the neuronal membrane in live cells. Secondly, even if several CRISPR – Cas9 editing strategies have been extensively developed to modify surface neurotransmitter receptors in primary neurons in culture (Fang et al., 2021; Willems et al., 2020), their use is however limited due to low rates of efficiency making near-impossible of finding double knock-in neurons. On a side note, it has been shown that the size of the fluorescent protein / QD can limit the capacity of tagged-neurotransmitter receptor to enter inside synaptic clefts, which are ~ 20 nm wide in average (Choquet et al., 2021; Groc et al., 2007b; S. H. Lee et al., 2017). It is however important to consider that D1R are mainly located extrasynaptically (Uchigashima et al., 2016) as well as the interaction between D1R-GluN1-NMDAR (Ladepeche et al., 2013), limiting this negative impact.

2. PPI: membrane receptor organizers in immature neurons

2.1 D1R-GluN1-NMDAR interaction over the course of neuronal development

We observed that the strength of the interaction was differentially regulated during neuronal maturation, which was defined by two time points, referred as “immature” and “mature”, between which the number of excitatory synapses doubled. The D1R-GluN1-NMDAR interaction were drastically reduced in this time window both *in vitro* and *in vivo*. This developmental regulation of the D1R-GluN1-NMDAR interaction that were observed in hippocampal neurons was conserved in glutamatergic cortical neuronal cultures. At the immature stage, interactions between D1R-GluN1-NMDAR were promoted by ambient glutamate through the recruitment of metabotropic glutamate receptors mGluR. We showed that mGluR activate the protein kinase Casein Kinase 1 (CK1), leading to the phosphorylation of D1R C-tail at the serine 397 (i.e. located inside the interaction domain, known as T2 domain, of D1R with GluN1-NMDAR) which is sufficient to increase the interaction between D1R-GluN1-NMDAR. Noteworthy, we unveil that CK1-subunit α content decreased by half over development (*in vitro* and *ex vivo*), consistent with the above scenario.

It is well accepted that PPI is a multi-step process. Random collisions occur between diffusing surface receptors, leading to the formation of very short-lived encounter complex that can convert into a productive complex upon “true” interaction. The formation of a longer-lived encounter complex is associated with molecular rearrangements of the protomers and formation of non-covalent bonds. Thus, changes in membrane diffusion, receptor expression levels, and/or interaction avidity can impact the likelihood of having an interaction as well as its properties. The observed changes in the occurrence of the interaction between immature and mature neurons can be associated to the high instability of the immature neuronal membrane (e.g. high membrane diffusion) (Borgdorff and Choquet, 2002; Groc et al., 2006a, 2004). Indeed, such high surface diffusion would increase the likelihood of random collisions and thus of formation of encounter complexes. Such high lateral dynamics could also compensate for the initially relatively low amount of surface D1R in immature compare to mature neurons (annex 1). We showed a mGluR- and CK1-dependent post-translational modification of D1R at the 397 residues. This phosphorylation increases the number of negative charges in D1R C-tail, therefore strengthening its electrostatic bond with GluN1-NMDAR cassette C1 which in turn carry positive charges,

encompassing for the observed qualitative changes in the interaction properties. In addition, the GluN2-subunit composition of the NMDAR could influence the biophysical properties of the interaction since D1R can also interact with the CTD of GluN2A, which is enriched in mature neurons, through its T3 domain (Lee et al., 2002). Although we did not test the role of the T2 and T3 domains on the biophysical properties of D1R-GluN1-NMDAR interaction with our MS-SMLM approach, FRET experiments carried on heterologous cell systems showed that, in comparison to the T2 domain, the T3 domain had a negligible role on the interaction. Lastly, even if the interactions between surface receptors are considered as stochastic (Scarselli et al., 2016) and that we did not observe any indications towards interaction hot-spots, we cannot rule out the existence of membrane (sub)-domains that will favor the interaction. In fact, presence of such hot-spots would dramatically increase the likelihood of interaction between highly diffusing receptors. Surely, assessing the presence of interaction hot-spots by combining MS-SMLM with other super-resolution microscopy approaches will feed our understanding on the development-dependent regulation of the D1R-GluN1-NMDAR interaction.

2.2 D1R-GluN1-NMDAR favors the functional clustering of NMDAR and promote excitatory synaptogenesis

Surface GluN1-NMDAR start to cluster when the interaction with D1R are possible, thus supporting the hypothesis that D1R-GluN1-NMDAR interaction seed NMDAR clusters in immature neurons. Indeed, D1R are able to aggregate GluN1-NMDAR within large clusters, enriched in the extrasynaptic membrane. When the interaction was prevented, D1R were unable to aggregate GluN1-NMDAR at this early stage. The interaction-dependent increase in the clustering of NMDAR was sufficient to promote excitatory synaptogenesis. Indeed, the chronic disruption of the interaction, at a time of a strong D1R-GluN1-NMDAR interaction, dramatically reduced the number of excitatory synapses. Promoting the interaction increased the number of excitatory post-synapses. On the other hand, competing with the interaction at later stages, when the interaction was reduced, had no effect on the number of synapses.

Herein, we reported a positive correlation between D1R-GluN1-NMDAR interaction with the surface nano-organization of GluN1-NMDAR. Upon collision, diffusing receptors oligomerize,

which leads to their trapping and local clustering. Considering the 1:1 valency of the interaction and the fact that the surface organization of GluN1-NMDAR is perturbed but not lost upon disruption of the interaction, one could hypothesize additional regulatory mechanisms allowing the extrasynaptic organization and aggregation of NMDAR. First, as exposed earlier, we cannot exclude the existence of membrane and/or cytosplasmic subdomains that will favor the clustering, and thus the interaction, of both D1R and GluN1-NMDAR. Of note, it has been shown that the surface nano-organization and diffusion of the GPCR $GABA_B$ were dependent on their interaction with cortical actin filaments (Jobin et al., 2023). Secondly, the NMDAR interactome is very large and include several neuromodulator and neurotransmitter receptors, including mGluR, as well as adhesion molecules (Petit-Pedrol and Groc, 2021). We thus cannot dismiss the possibility of having the existence of hubs that are formed by different type of surface macromolecules, including neurotransmitter receptors. This would allow multimerization and lead to the aggregation and clustering of receptors. Answering to those questions will be essential to understand the mechanisms responsible for the regulation of the interactions *per se* as well as the positive effects of those interaction on excitatory synaptogenesis.

We showed that the interaction between D1R and GluN1-NMDAR were necessary and sufficient at early stages for synaptogenesis. One can wonder whether the interaction between D1R-GluN1-NMDAR preferentially occurs at axodendritic contact. The release of ambient glutamate will locally stabilize D1R-NMDAR, which in turn will flux calcium and recruits other synaptic and scaffold proteins leading locally to the formation and/or the stabilization of a synaptic contact. It is not clear however if D1R-GluN1-NMDAR heteromers activate specific signaling pathways and/or if the sole clustering of NMDAR, that could be obtained through extracellular cross-linking for instance, is sufficient to promote excitatory synaptogenesis. Alternatively, one could hypothesize the formation of a seed or hub of different receptors and associated signaling molecules (herein, the formation of spatially structured D1R-GluN1-NMDAR-mGluR-CK1 macro-complexes). The latter hypothesis is supported by the fact that mGluR activity, but not NMDAR, is involved in the regulation of the interaction, and that mGluR directly interact with GluN1-NMDAR (Perroy et al., 2008). Future experiments aiming at assessing the existence of surface protein macro-complexes through proximity-dependent biotinylation labelling followed by proteomic profiling as well as multicolor MS-SMLM will be critical in the near future.

3. Role of dopamine (DA) in the regulation of D1R-GluN1-NMDAR interaction and the D1R-GluN1-NMDAR-mediated synaptogenic effect

We observed that the synaptogenic effect of D1R-GluN1-NMDAR interaction is conserved in reconstructed networks that were composed by midbrain-containing dopaminergic neurons in co-culture with hippocampal glutamatergic neurons. This result was however surprising considering the negative effect of DA, or its agonists, on D1R-GluN1-NMDAR interaction in hippocampal neurons (annex 2 and (Ladepeche et al., 2013)). Based on the scarce dopaminergic innervation of the hippocampus in the neonate in comparison to adults (Bénac et al., 2024; Verney et al., 1985), one could hypothesize two different development-dependent periods for the regulation of the interactions between D1R and GluN1-NMDAR, with an early "dopamine-independent" and late "dopamine-dependent" period. Following this view, the interaction between D1R-GluN1-NMDAR regulates NMDAR surface nano-organization, and allows for its functional clustering in the neonate brain. Later on, upon dopaminergic innervation of the hippocampus, the interaction will participate in the neuromodulation-neurotransmission interplay. For instance, it has been shown that disruption of the D1R-GluN1-NMDAR heteromers redistribute NMDAR from their extrasynaptic to the synaptic pools, therefore facilitating the synaptic transmission (Ladepeche et al., 2013).

It is important to consider that different regulation mechanisms of the interaction have been suggested, depending on the brain region and the pathological condition. Indeed, it is well accepted that cocaine consumption increases the extracellular levels of dopamine, which leads, in the striatum, to an increase level of interaction between D1R-GluN1-NMDAR in mice but also in postmortem human samples (Andrianarivelo et al., 2021; Cahill et al., 2014). It was shown that such increased interaction between D1R-GluN1-NMDAR act as a key player in the addiction mechanism by inducing long-term molecular changes (such as an increased number of dendritic spines) and disrupting the interaction prevented them (Andrianarivelo et al., 2021). The molecular mechanisms involved are however not clear. It will be interesting to understand the molecular mechanisms underlying the above-mentioned brain region- and pathological-dependent regulation mechanisms of the interaction, and if whether they are due to changes in the

biophysical properties of the interaction or to the presence of different region-specific players (e.g. second messenger, surface interactor, etc.).

Result 2. The extracellular matrix tunes glutamatergic receptor surface organization in hippocampal neurons

The extracellular matrix tunes glutamatergic receptor surface organization in hippocampal neurons

Nathan Bénac[1], Zoë Jamet[1], Camille Mergaux[1], Carlos Cação[1], Laurent Groc[1,*]

Affiliations

[1] Univ. Bordeaux, CNRS, IINS, UMR 5297, F-33000 Bordeaux, France

[*] Email: laurent.groc@u-bordeaux.fr

Abstract

The extracellular matrix (ECM) is an essential structure of the brain that tune cell communication and many other neuronal and glial processes. For instance, the ECM can modulate synaptic transmission, synaptogenesis, and long-term synaptic plasticity through molecular mechanisms that still remain to be fully uncovered. Here, we explore the molecular interplay between the ECM and membrane glutamatergic receptors that are essential in the glutamatergic synaptic transmission. Using a combination of superresolution imaging, pharmacological and genetic interventions to either decrease or increase the ECM content in hyaluronic acid (HA) in cultured hippocampal neurons and astrocytes, we provide evidence that HA and the ECM regulates the organization and lateral diffusion of membrane macromolecules. Surprisingly, the ECM differently affect glutamatergic receptors, i.e. NMDA and AMPA receptors, and membrane molecules. In addition, the extrasynaptic membrane compartment appears to be the prime target of the ECM changes. Together, these data strengthen the instrumental role of the ECM in tuning membrane receptor distribution at the extrasynaptic and synaptic compartments.

Introduction

Brain excitatory neurotransmission is primarily mediated by glutamatergic synapses, and changes in their strength, also known as synaptic plasticity, are considered the foundation for learning and memory. This process often requires the activation of ionotropic glutamate receptors that are located within the post-synaptic membrane, such as the N-Methyl-D-Aspartate receptors (NMDAR). NMDAR are obligate heterotetramers composed by two dimers of subunits, i.e. obligatory GluN1 subunits associated with GluN2 or 3 subunits, that are activated by co-agonist (glycine or D-serine) and agonist (glutamate), respectively (Paoletti et al., 2013; Stroebel and Paoletti, 2021). Synaptic activation and plasticity rely on the precise localization of the glutamate receptors which are constantly diffusing between synaptic and extrasynaptic compartments following thermally-driven Brownian motion (Dupuis et al., 2023; Groc and Choquet, 2020; Kellermayer et al., 2018; Tang et al., 2016). The extracellular matrix (ECM), a soluble meshwork of macromolecules that surrounds every cell and fills the extracellular space (ECS), has long been known to modulate the surface trafficking of membrane proteins, including receptors (Frischknecht et al., 2009; Jacobson et al., 2019; Schweitzer et al., 2017). The ECM consists of hyaluronic acid (HA), chrondroitin sulfate proteoglycans (CSPG) and glycoproteins such as tenascin (Zimmermann and Dours-Zimmermann, 2008). The ECM is well known to modulate the development of the brain, including progenitor proliferation and differentiation as well as synaptogenesis and neurite/axonal growth, but also brain activity and plasticity (Long and Huttner, 2019). In fact, the ECM is considered as an integral part of the tetrapartite synapse, which comprises the pre- and post-synaptic compartments, glia cell and ECM components (Dityatev et al., 2010; Dityatev and Rusakov, 2011; Ferrer-Ferrer and Dityatev, 2018). In the naked mole rat (NMR), a subterranean African rodent species characterized by long lifespan and healthspan, prolonged development, and resistance to cancer and neurodegeneration (Buffenstein et al., 2012; Buffenstein and Jarvis, 2002), HA display a very high molecular weight HA (vHMW-HA, > 6,000 kDa) (Tian et al., 2013). The expression of vHMW-HA in mice is sufficient to transfer some cellular properties of the NMR (Zhang et al., 2023), further supporting the key role of the ECM on brain and other organ physiology. Yet, the molecular mechanisms underlying the modulation of the surface trafficking and their subsequent consequences on the neuronal membrane organization remain enigmatic. Using a combination of superresolution imaging, pharmacological

and genetic interventions to either decrease or increase the ECM content in HA in cultured hippocampal neurons and astrocytes, we provide evidence that HA, one of the main components of the ECM, regulates the organization and lateral diffusion of membrane macromolecules.

Material and Methods

1. Cultures

Hippocampal tissues were harvested from embryonic stage (E18) embryos of an unascertained mixture of sexes prevenient from gestant Sprague-Dawley rat at the age of 9–12 weeks old, and purchased from Janvier Labs. Hippocampi were collected in HBSS containing Penicillin-Streptomycin (PS) and HEPES and dissociated with Trypsin-EDTA/PS/HEPES. Dissociated cells were plated at a density of 275 000 per 60 mm petri-dishes onto 1 mg/ml poly-L-lysine pre-coated 18 mm coverslips and were maintained in Neurobasal Plus medium (Gibco, A3585911) supplemented with GlutaMAX™ (Gibco, #35050-038), B-27™ Plus (Gibco, A3653401) and 1.5 % horse serum (ThermoFisher Scientific, #26050088). Hippocampal cultures were kept at 37 °C in 5 % CO_2. Cell culture media were replaced with Neurobasal Plus/GlutaMAX/B-27-containing media after 3-days in vitro (DIV). HEK293T cells were plated at a density of 100 000 onto 0.1 mg/ml poly-L-lysine pre-coated 18 mm coverslips in 12-well plate and kept in Dubelcco's Modified Eagle's Medium (DMEM) supplemented with 10% fetal calf serum, 1% pyruvate and 2 mM GlutaMAX.

4. HAS2-encoding plasmids

cDNA encoding for hyaluronidase synthase 2 (HAS2) from *rattus norvegicus* were purchased from Origene (NM_013153). The HAS2-N178S-N301S, herein referenced as HAS2-NMR, was obtained by performing site-directed mutagenesis, using Quickchange II XL Site-Directed Mutagenesis kit (Agilent), of the *rattus norvegicus* HAS2 cDNA with the following primers:

Forward-N178S: 5'- CCAATTGGTCTTGTCTAGCAAGAGTATTTGCATC – 3'

Forward N301S: 5' – GTGGAAGACTGGTACAGTCAGGAATTCATGGG – 3'

Reverse-N178S: 5'- GATGCAAATACTCTTGCTAGACAAGACCAATTGG – 3'

Reverse N301S: 5' – CCCATGAATTCCTGACTGTACCAGTCTTCCAC – 3'

5. Transfection

Hippocampal neurons were transfected between 7 and 10 DIV using the calcium-phosphate coprecipitation method. Briefly, DNA plasmids were diluted in TE buffer (1mM Tris-HCl pH 7.3, 1mM EDTA) and a final concentration of 250mM of CaCl2 (2.5M $CaCl_2$ in 10 mM HEPES, pH 7.2) were added. This mix was added dropwise to 2X HEPES-buffered saline (in mM: 12 dextrose, 50 HEPES, 10 KCl, 280 NaCl and 1.5 Na2HPO4·2H2O, pH 7.2). Coverslips were transferred to 12-well plate containing 250 µl/well of conditioned culture medium supplemented with 2mM kynurenic acid. 50 µl of the precipitate solution was added to each well and incubated for 1h at 37°C. Cells were then washed with non-supplemented Neurobasal medium containing 2 mM kynurenic acid and moved back to the culture dish. To prevent excitotoxicity, 50mM of D-2-amino-5-phosphonovalerate (D-AP5) was added to the culture medium when transfecting with GluN1-NMDAR.

HEK293T cells were transfected with X-tremeGENE HP DNA (Roche) 1 day after plating as per manufacturer instructions.

6. Immunofluorescence

For live surface staining, cells were incubated with primary antibodies diluted in cell culture media for 15 min at 37 °C and fixed for 15 min with 4 % paraformaldehyde (PFA) / 4 % sucrose in PBS at room temperature (RT). The cells were then incubated for 15 min in PBS containing 50 mM NH4Cl at RT and blocked for 30 min in 1 % BSA in PBS at RT. For intracellular staining, cells were fixed and permeabilized with 0.25 % Triton X-100/PBS for 5 min at RT before blocking. For non-live surface staining, cells were fixed then washed in PBS/NH_4Cl before incubating with primaries antibodies, diluted in blocking solution and incubated overnight (ON) at 4 °C. Secondary antibodies were prepared in blocking solution and incubated for 1 hour at RT. For confocal microscopy, cells were then mounted in DAPI-containing Fluoromount media and kept in the dark at 4 °C until imaging. For dSTORM imaging, cells were post-fixed for 15 min with 4 % PFA / 4 % sucrose at RT, washed, and stored in PBS at 4 °C until imaging. When needed, cells were incubated with 50 units of hyaluronidase or heat-denatured hyaluronidase (10 min at 95 °C) at 37°C prior to fixation.

7. Spinning disk

Images were acquired using a spinning disk confocal unit equipped with an electron multiplying charge-coupled device (EMCCD) camera (Photometrics QuantEM 512SC) through either a 20x dry (Leica, HC PLAN APO, 0.7 NA) and/or a 63x oil-immersion (Leica, HCX HPL APO CS, 1.4-0.6 NA) objective. Hardware was controlled with MetaMorph software (Molecular Devices). All images were analyzed with ImageJ 1.53c. For the Sholl Analysis, hippocampal dendritic trees were reconstructed using the ImageJ' plugin "SNT".

8. SPT-Palm

Images were acquired using a Nikon Ti eclipse system equipped with a Perfect Focus System (PFS), an azimuthal TIRF arm (Gataca Systems) and an Apo TIRF 100X NA1.49 oil-immersion objective and an Evolve EMCCD camera (Photometrics) with a pixel size of 65 nm, and equipped with a motorized stage controlled by MetaMorph software (Molecular Device). Imaging was carried at 37 °C in an open Ludin chamber (Life Imaging Services). GluN1-mEOS3.2 was photoactivated using 405 nm laser and resulting photoconverted single molecule fluorescence was excited with a 561 nm laser. Both 405 and 561 nm lasers illuminated the samples simultaneously. Images were obtained with an exposure time of 50 ms with 4,000 consecutive frames, and a binning of 2. Trajectories were reconstructed with PalmTracer. For each single trajectory of more than 10 points, the instantaneous coefficient diffusion (D) was calculated from linear fits of the first four points of the mean square displacement (MSD) over time function using $MSD(t) \leq r2 > (t) = 4Dt$. Representative images of the trajectories were obtained using the software FluoSIM (Lagardère et al., 2020). When specified, cells were incubated with 50 units of hyaluronidase for 15 min at 37 °C before the SPT-Palm acquisitions.

9. dSTORM

Images were acquired on a commercial Leica SR GSD microscope (Leica Microsystems) equipped with a Leica HC PL Apo TIRF 160x NA1.43 oil-immersion objective and an iXion EMCCD camera (ANDOR) with a final pixel size of 100 nm. Hardware was controlled by Leica LAS software. Samples

were illuminated in TIRF mode and images were obtained with an exposure time of 20 ms with up to 95,000 to 100,000 consecutive frames. Imaging was carried out at room temperature in a closed Ludin chamber (Life Imaging Services) using a pH-adjusted extracellular solution containing oxygen scavengers and reducing agents, as detailed in (Beghin et al., 2017). Multicolor fluorescent microspheres (Tetraspeck, Life Technologies) were used for lateral drift correction. Super-resolution images were reconstructed with PALMTracer and protein-clustering into nano-size clusters i.e. nanodomains was obtained using the SR-Tesseler method (Levet et al., 2015). Segmentations of the clusters were performed by applying a threshold of twice the average density δ of the whole dataset, with a minimum area of 10,000 nm^2 and a minimum number of localizations of 5. Clusters' nanodomains were identified by applying a threshold of one time the average density of each cluster (144 nm^2 minimum area, 25 minimum number of localizations).

10. Antibodies

Primary antibodies		**Provider**	**Dilution**
mouse anti-GluN1	clone 10B11	E. Gouaux	1/10 000
chicken anti-MAP2	ab5394	Abcam	1/5 000
rabbit anti-PSD95	124008	Synaptic System	1/1 000
HABP-biotin	AMS.HKD-BC41	AMSBIO	1/1 000
Secondary Antibodies			
Donkey anti-mouse alexafluor 647	A31571	ThermoFisher Sc.	1/1 000
Goat anti-chicken alexafluor 488	A11039	ThermoFisher Sc.	1/1 000
Mouse anti-rabbit alexafluor 568	A10042	ThermoFisher Sc.	1/1 000
Streptavidin-647	AS32357	ThermoFisher Sc.	1/1 000
Streptavidin-568	511226	ThermoFisher Sc.	1/1 000

11. Statistical Analyses

No statistical methods were used to predetermine sample size. Sample size was based on previous publications with similar models and experiments. To ensure replicability, results are derived from at least three independent experiments. All statistical tests were performed using GraphPad Prism. Datasets were analyzed for normality and parametric or non-parametric statistical test (two-tailed) were used accordingly. Test details and statistical outcomes are reported in relevant figure legends.

12. Author contributions

N.B., designed and validated the HAS2 and HAS2-NMR constructs, performed the experiments on neuronal development and on HEK cells.

N.B., Z.J. performed Palm experiments on GluN1-NMDAR and analyzed the data.

C.M. performed the Palm experiments on GPI-mEOS3.2 and C.M. and N.B. analyzed the data.

C.C. performed the immunofluorescence and dSTORM imaging experiments on GluN1-NMDAR under N.B. supervision.

N.B. and L.G. designed the study.

N.B. and L.G. wrote the paper.

Results

1. GluN1-NMDAR surface nano-organization is disrupted upon acute HA degradation

We first assessed whether the surface organization of NMDAR was regulated by the ECM. We acutely incubated hippocampal cultures between 14 to 17 days in vitro (DIV) with hyaluronidase. We confirmed that the acute (15 min) hyaluronidase incubation was indeed sufficient to fully digest HA (supplementary fig. 1). Using confocal microscopy, we observed that the number and the size of GluN1-NMDAR clusters were not altered, both inside and outside synapses, upon removal of the HA (fig. 1a-c). However, is it important to consider that the resolution (~ 200 nm) of conventional microscopy techniques is limited, mainly due to the diffraction of light, and does not allow to fully resolved the organization of NMDAR which are known to form nanodomains of ~ 60 nm (Kellermayer et al., 2018). To this end, we used direct stochastic optical reconstruction microscopy (dSTORM) which allowed us to resolve the nano-organization of surface GluN1-NMDAR (fig. 1d-e). Upon digestion of the matrix, the nano-organization of NMDAR were disrupted both inside and outside synapses (fig. 1f-g). At synaptic sites, GluN1-NMDAR nanodomains were smaller and denser as suggested by the increase in the density of localization (fig. 1f). However, the number of synaptic nanodomains per clusters, the number of localizations per nanodomain (fig. 1f) as well as the number and the size of PSD95 clusters were at control levels (supplementary fig. 2), suggesting a slight reorganization of surface GluN1-NMDAR without modification of the global synaptic organization. On the other hand, the extrasynaptic organization of GluN1-NMDAR was severely altered. In addition to the decrease in size and increase in density which were shared within both compartments, extrasynaptic GluN1-NMDAR nanodomains were increased in number and each nanodomain showed a slight reduction in the absolute number of localizations, possibly indicating a fragmentation of the extrasynaptic membrane (fig. 1h). Collectively, these data indicate GluN1-NMDAR nano-organization is regulated by the ECM.

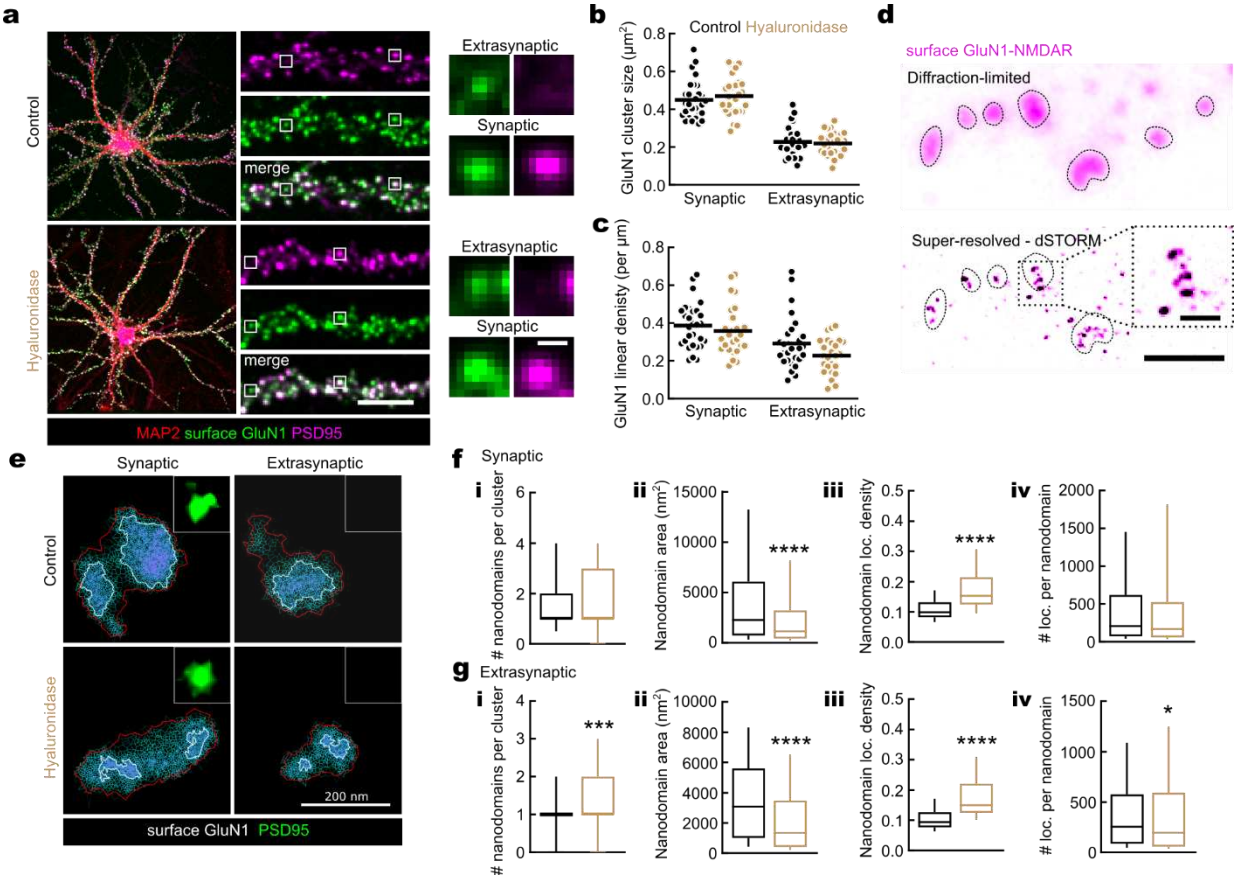

Figure 1. GluN1-NMDAR surface nano-organization is disrupted upon acute HA degradation

a, Representative fluorescence images of the dendritic marker MAP2 (red) alongside surface GluN1-NMDAR (green) and the post-synaptic marker PSD95 (magenta). Scale bars, 5 and 0.5 µm. Synaptic GluN1-NMDAR clusters were identified based on their co-clustering with PSD95. **b**, Quantification of mean size and (c) linear density (# clusters per µm of dendrite) of GluN1-NMDAR clusters in control (n = 29 neurons) or upon digestion of the ECM with hyaluronidase (n = 26 neurons). **d**, Example of diffraction-limited and corresponding super-resolved images of surface GluN1-NMDAR. Scale bar, 2 and 0.4 µm. **e**, Representative clustering images obtained with SR-Tesseler software. Synaptic or extrasynaptic NMDAR were identified based on the synaptic marker PSD95 (green). (**f**-**g**), Comparison of the number of (i) nanodomains per clusters as well as the (ii) nanodomains area, (iii) density of localization, and (iv) number of localizations in control (n = 7 cells) and following ECM digestion (n = 8 cells) both (f) inside (control, n = 335 nanodomains; hyaluronidase, n = 381 nanodomains) and (g) outside synapses (control, n = 310 nanodomains; hyaluronidase, n = 362 nanodomains). (b, c, f, g) Two-tailed Mann-Whitney U test, * $p < 0.05$, *** $p < 0.001$, **** $p < 0.0001$

2. HA regulates GluN1-NMDAR organization at the neuronal membrane

To upregulate the ECM, we acted on HA which is a large linear and hydrophilic polysaccharide composed by repeating glucuronic acid and N-acetylglucosamine linked by β (1,4) and β (1,3) glycosidic bonds, and a major component of the interstitial ECM. HA is synthetized at the inner side of the plasma membrane by transmembrane glycosyltransferase known as hyaluronan synthase (HAS) 1-3 and extruded to the ECS where, depending on its size and concentration, it modulates both the viscosity and viscoelasticity of the ECM (Toole, 2004, 2001; Weigel et al., 1997). Each HAS isoenzyme will produce a polymer of different length, with HAS2 producing the longest chain, known as high molecular weight HA (HMW-HA). While it is well accepted that HAS2-coding sequence is highly conserved across species (Faulkes et al., 2015; Tian et al., 2013), two point-mutations (N178S and N301S) were described in the sequence encoding the active site of HAS2 in the naked mole rat (NMR) as being responsible for the production of very high molecular weight HA (vHMW-HA) (Tian et al., 2013). Therefore, we subcloned the HAS2-coding cDNA sequence of rat into a bidirectional promoter (pBi) vector constitutively expressing zsGreen (transfection marker), either in its wild-type form (HAS2) or bearing the two point-mutations described in the NMR (HAS2-N178S-N301S and referred as HAS2-NMR) (Fig. 1a). We then tested whether the over-expression of HAS2 and HAS2-NMR were able to increase the content in HA in hippocampal cultures. To this end, we transfected E18-hippocampal cultures at 7-days in vitro (DIV) with control or HAS2/HAS2-NMR-encoding plasmid for 7-days before labeling for HA (Fig. 1a). Both HAS2 and HAS2-NMR constructs efficiently increased the local HA content by two-fold in transfected neurons compared to neighboring non-transfected cells (from 20 to 300 µm). Together, it suggested a local increase in the production of HA by the transfected neurons without diffusion mechanisms to other non-transfected neighboring neurons (Fig. 1b, c).

We next applied our strategies to confirm the role of the ECM on the surface organization of GluN1-NMDAR. To this end, we transfected E18-hippocampal neurons at 7 DIV with control, HAS2 or HAS2-NMR plasmids and performed live surface immunolabeling for the endogenous obligatory GluN1 subunit of the NMDAR (fig. 2a). As expected, whereas the global macroscopic organization of the NMDAR (e.g. number of clusters) were not changed (Fig. 2d-f), increasing the local HA content by over-expressing HAS2-NMR, which produces vHMW-HA, enhanced GluN1-NMDAR

clustering (Fig. 2e). Altogether, these results indicate HA regulate the organization of NMDAR at the membrane of cultured hippocampal neurons.

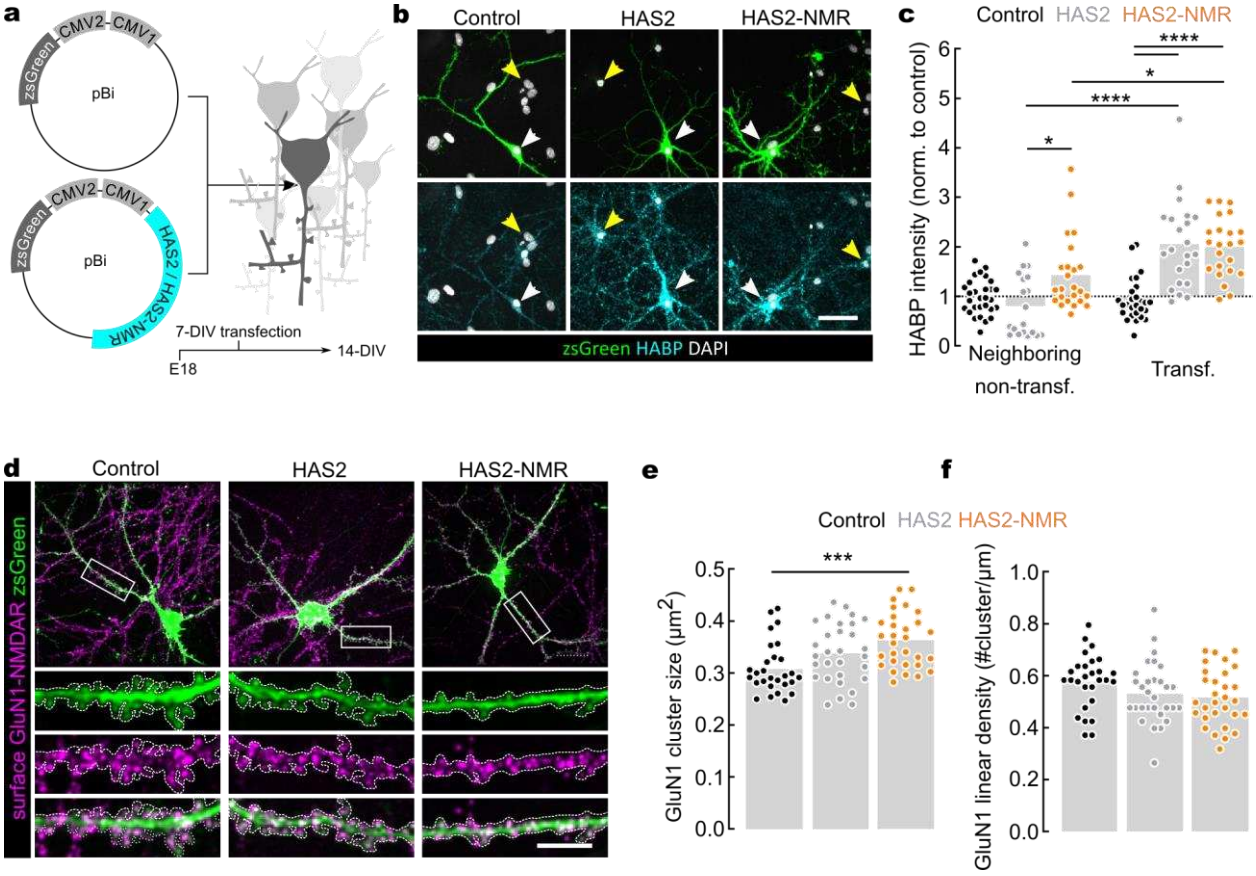

Figure 2. HA controls GluN1-NMDAR organization at the neuronal membrane

a, Experimental set-up. **b**, Representative immunofluorescence images of HABP (cyan), zsGreen (transfection marker, green), and DAPI (grey). White arrows indicate transfected neurons while yellow arrows show neighboring non-transfected cells. Scale bar, 50 µm. **c**, Relative HABP intensity following expression of either control (non-transfected n = 29 cells, transfected n = 27 cells), HAS2 (non-transfected n = 19 cells, transfected n = 22 cells) or HAS2-NMR (non-transfected n = 24 cells, transfected n = 23 cells)-encoding plasmids. Results are normalized to non-transfected control condition. Two-way ANOVA with Tukey's post-hoc test, * $p < 0.05$, **** $p < 0.0001$. **d**, Representative fluorescence images of zsGreen (green) and live-surface endogenous GluN1-NMDAR (green). Scale bars, 25 and 10 µm. **e**, Quantification of mean size of GluN1-NMDAR clusters alongside (**c**) GluN1-NMDAR linear density in neurons transfected with either control (n =

28 cells), HAS2 (n = 30 cells) or HAS2-NMR (n = 30 cells)-encoding plasmids. (e-f) Kruskal-Wallis with Dunn's multiple comparison test. *** p = 0.0005.

3. HAS2 and HAS2-NMR expression alters neuronal development

We next investigated the consequences of over-expressing HAS for several days on the neuronal development. Because HA is known to modulate the development of neuronal cells (Kultti et al., 2006; Nagy et al., 1995; Oliferenko et al., 2000; Rilla et al., 2008; Roszkowska et al., 2016; Skupien et al., 2014; Takechi et al., 2020), we tested whether the dendritic tree and the number of dendritic spines were affected upon HAS2 and HAS2-NMR expression. Both HAS2- and HAS2-NMR transfected neurons showed defects in development (Fig. 3a-e). Transfected neurons showed a reduction in the number of dendritic spines (Fig. 3a-b) as well as in the length and complexity of the dendritic tree (Fig. 3 c-e). The latter were more profoundly affected following HAS2-NMR expression than HAS2 (Fig. 3e), supposedly reflecting a HA-polymer size-dependent effect.

Because following HA expression, a portion remains tethered to cell membrane and forms a pericellular coat, we tested whether overexpressing HAS could hinder the expansion of cells. To this end, we investigated the morphology of HEK293T cells following HAS over-expression. HEK293T cells that over-expressed HAS2 and HAS2-NMR were smaller and more circular, as defined by the increase in circularity and decrease in aspect ratio (AR) (which tended to 1 indicating an equalization between the major and minor axis) (supplementary Fig. 3). Importantly, cells that were expressing HAS2-NMR showed a significantly stronger phenotype compare to HAS2, supposedly reflecting a HA-size effect (supplementary Fig. 3). Collectively, these results suggest that HAS2 and HAS2-NMR expression prevent both dendritic outgrowth and spinogenesis by hindering cell expansion.

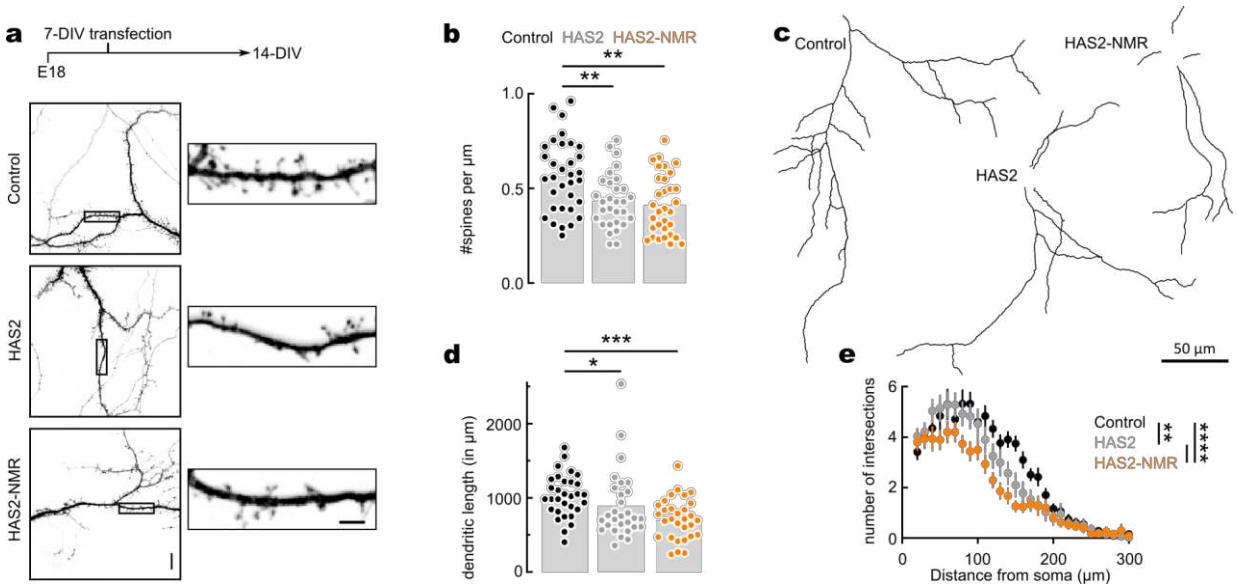

Figure 3. HAS2 and HAS2-NMR expression alters the maturation of hippocampal neurons *in vitro*

a, (top) Experimental set-up. (bottom) Representative images of hippocampal neurons transfected with either control, HAS2 or HAS2-NMR-encoding plasmid. Scale bars, 20 and 5µm. **b**, Quantification of the number of spines in control (n = 33 cells) condition or when HAS2 (n = 30 cells) and HAS2-NMR (n = 32 cells) are expressed. One-way ANOVA with Tukey's multiple comparison test. ** $p < 0.01$. **c**, Representative reconstruction of the neuronal dendritic trees. Scale bar, 50 µm. **d**, Quantification of the total dendritic length following transfection with either control (n = 31 cells), HAS2 (n = 29 cells), or HAS2-NMR (n = 30 cells)-encoding plasmid with (**e**) Sholl analysis with a step distance of 10 µm. (d) Kruskal-Wallis with Dunn's multiple comparison test. * $p < 0.05$, *** $p < 0.005$. (e) Two-way ANOVA with Tukey's multiple comparison test. ** $p < 0.01$, **** $p < 0.0001$.

4. HA hinders the diffusion of membrane macromolecules

We then tested whether the observed changes in the membrane organization of GluN1-NMDAR were due to changes in lateral diffusion. To this end, we performed single particle tracking (SPT) experiments, which allow to track the diffusion of single GluN1-NMDAR, using photoactivated localization microscopy (SPT-PALM) (Fig 4a). First, we were able to confirm, by reconstructing the images of the localization of GluN1-mEOS3.2, the dramatic changes in the overall organization of the NMDAR upon over-expression of HAS2-NMR (Fig. 4b). Indeed, while GluN1-NMDAR were present in both dendritic spines and shaft at high density in control conditions, NMDAR appeared highly aggregated in the HAS2 and HAS2-NMR conditions (fig. 4b). Furthermore, the lateral diffusion properties of GluN1-NMDAR were also altered (fig. 4b-d). Even if the median diffusion coefficients per neuron of GluN1-NMDAR were not changed, GluN1-NMDAR showed an increased confinement level, as observed by the shift in the mean square displacement (MSD) curve, in the HAS2-NMR condition compare to both HAS2 and control (fig. 4c, d). In fact, a second immobile population of NMDAR, which were absent from control neurons, we present both in the HAS2 and HAS2-NMR content, with the latter having a stronger effect (fig. 4d). To test if the effects were directly due to HA, we acutely digested the matrix by adding exogenous hyaluronidase in the bath for 15 min before performing the experiment (fig. 4e, f, supplementary fig. 4). Hyaluronidase was sufficient to revert the effects of HAS2-NMR on both the diffusion and confinement of NMDAR (fig. 4e, f). Indeed, as expected in regards of the HAS2- and HAS2-NMR-dependent effects on the spinogenesis, GluN1-NMDAR were less confined in the HAS2 and HAS2-NMR-transfected neurons (fig. 4e). Altogether, these results indicate HA directly hinders the diffusion of GluN1-NMDAR.

How much this effect is specific to NMDAR? To tackle this question, we investigated the diffusion of a smaller macromolecules, herein a GPI anchor, as well as receptor of similar size but which has been shown to be highly affected by HA (fig. 4a) (Frischknecht et al., 2009; Stroebel and Paoletti, 2021). Indeed, direct steric hindrance mechanisms imply to have different strength of effects depending on the receptor type (e.g. extracellular domain size, charges, post-translational modifications, etc.) as well as the viscosity and viscoelasticity of the matrix. Following this view playing with the size of the extracellular domain of NMDAR, or herein assessing the lateral diffusion properties of another surface macromolecules of a different size (e.g. GPI anchor) might attenuate or alternatively enhance (upon increasing the size of putative extracellular domains) the

effects of the HA on the diffusion. Although the median diffusion coefficient per neuron were not different to control levels in the HAS2 condition, the GPI anchors showed a reduced confinement level, which is likely secondary to the decrease in the number of dendritic spines (fig. 3a, b). On the other hand, expressing HAS2-NMR, which has been described to produce vHMW-HA (Tian et al., 2013), drastically altered the surface diffusion of the GPI anchors (fig. 4g-i). GPI anchors appeared highly aggregated (fig. 4g) and the median coefficient diffusion per neurons were significantly lower in the HAS2-NMR condition compared to HAS2 (fig. 4i). Furthermore, the GPI anchors showed an increased confinement compared to both control and HAS2 conditions (fig. 4h). We next tested another ionotropic glutamatergic receptor: the AMPA receptor. Over-expressing both HAS2 and HAS2-NMR greatly affected the lateral diffusion of GluA1-AMPAR (fig. 4j-l). In both conditions, GluA1-AMPAR showed an increased confinement and a reduced median coefficient diffusion (fig. 4k, l). Altogether, these data indicate the ECM, in particular HA, alters the lateral diffusion of membrane macromolecules differently depending on the macromolecule type.

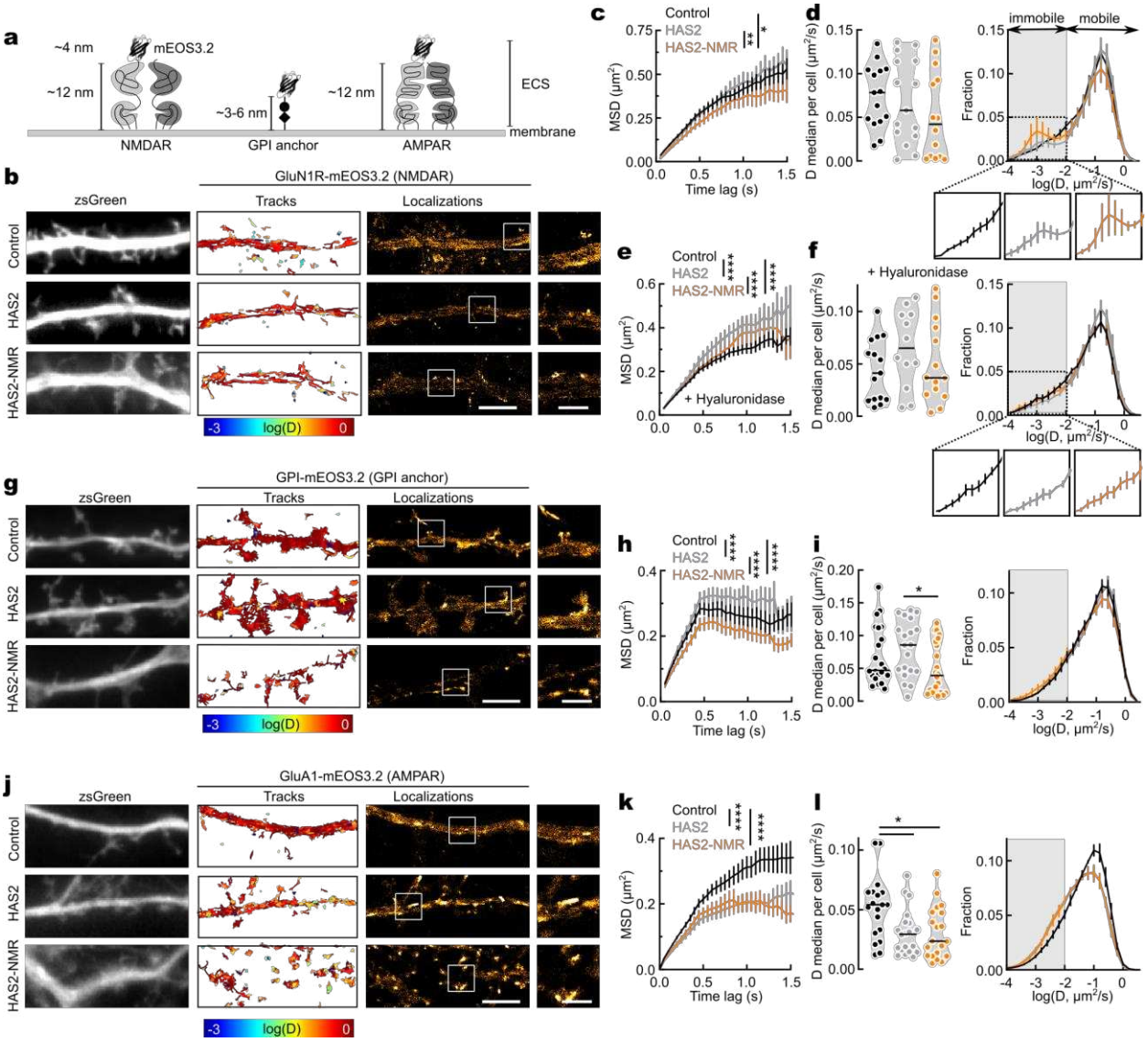

Figure 4. HA sterically hinders the lateral diffusion of macromolecules at the neuronal membrane

a, Experimental set-up. **b**, Representative fluorescence images of zsGreen (transfection marker, gray) alongside reconstructions of GluN1-mEOS3.2 diffusion-based color-coded trajectories and localizations. Scale bar, 5 and 2 µm. **c**, Mean Square Displacement curve. **d**, Median coefficient diffusion per neuron alongside corresponding semi-log plots for GluN1-NMDAR in control (n = 15 cells), HAS2 (n = 15 cells), and HAS2-NMR (n = 14 cells) conditions. **e**, Mean Square Displacement curve of GluN1-mEOS3.2 following hyaluronidase treatment. **f**, Median coefficient diffusion per neuron alongside corresponding semi-log plots of the distribution of diffusion coefficients for GluN1-NMDAR after digesting HA by incubating with hyaluronidase in control (n = 16 cells), HAS2 (n = 14 cells), and HAS2-NMR (n = 14 cells). **g**, Representative fluorescence images of zsGreen

(transfection marker, gray) alongside reconstructions of GPI-mEOS3.2 diffusion-based color-coded trajectories and localizations. Scale bar, 5 and 2 µm. **h**, Mean Square Displacement curve **i**, Median coefficient diffusion per neuron alongside corresponding semi-log plots of the distribution of diffusion coefficients for GPI anchor in control (n = 22 cells) or following over-expression of either HAS2 (n = 20 cells) or HAS2-NMR (n = 22 cells) conditions. **j**, Representative fluorescence images of zsGreen (transfection marker, gray) alongside reconstructions of GluA1-mEOS3.2 diffusion-based color-coded trajectories and localizations. Scale bar, 5 and 2 µm. **k**, Mean Square Displacement curve **i**, Median coefficient diffusion per neuron alongside corresponding semi-log plots of the distribution of diffusion coefficients for GPI anchor in control (n = 19 cells) or following over-expression of either HAS2 (n = 20 cells) or HAS2-NMR (n = 20 cells) conditions. (d, f, i, l) Kruskal-Wallis with Dunn's multiple comparison test. * $p < 0.05$. (c, d, e, k) Kolmogorov-Smirnov test. * $p < 0.05$, ** $p < 0.01$, **** $p < 0.0001$.

Supplementary Figures

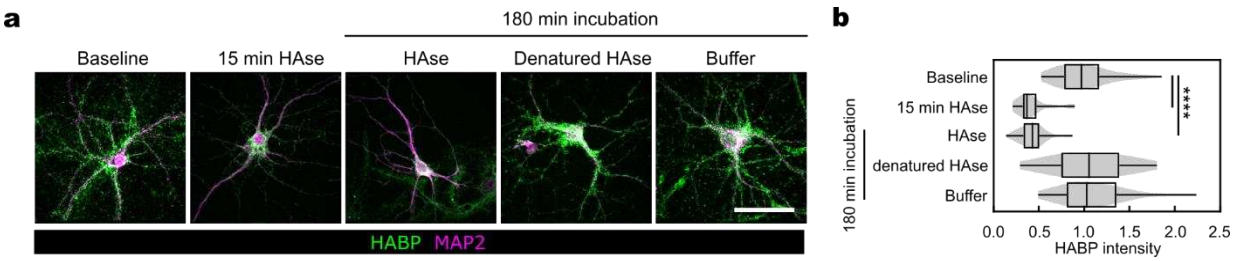

Supplementary Figure 1 (related to figure 1). HA degradation by hyaluronidase

a, Representative fluorescence images of HABP (green) and MAP2 (magenta). Scale bar, 50 µm. **b**, Quantification of HABP intensity before (baseline, n = 40 cells) and after 15 min incubation with hyaluronidase (15 min HAse, n = 30 cells) or 180 min incubation with either hyaluronidase (HAse, n = 40 cells), heat-denatured hyaluronidase (denatured HAse, n = 30 cells) or buffer (Buffer, n = 30 cells). Results are normalized to baseline. Kruskal-Wallis followed by Dunn's multiple comparison test, **** $p < 0.0001$.

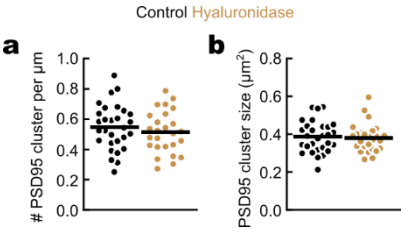

Supplementary Figure 2 (related to figure 1). Acute HA digestion does not affect PSD95 number nor size

a, Quantification of the linear density (# per µm of dendrite) as well as (b) the size of PSD95 in control condition (n = 29 neurons) or following acute HA digestion through hyaluronidase incubation (hyaluronidase, n = 26 neurons). Two-tailed Mann-Whitney U test.

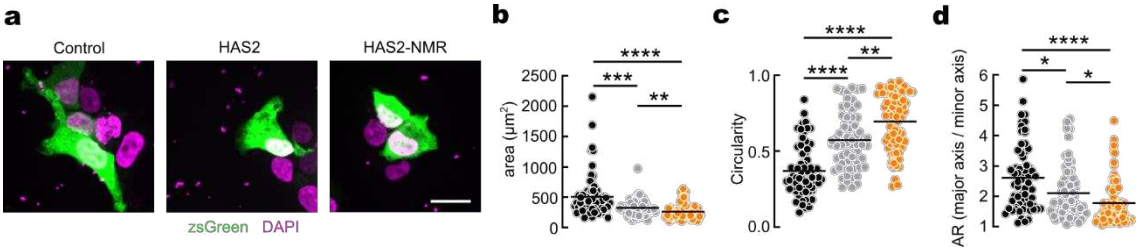

Supplementary Figure 3 (related to figure 3). HAS expression alters the morphology of HEK cells

a, Representative fluorescence images of zsGreen (transfection marker, green) and DAPI (magenta). b-d, Analysis of HEK morphology with (b) cell area in µm^2, (c) cell circularity and (d) aspect ratio (AR) defined as the product of the major axis divided by the minor axis upon transfection with control (n = 68 cells), HAS2 (n = 65 cells), and HAS2-NMR (n = 80 cells) -encoding plasmid. Kruskal-Wallis with Dunn's multiple comparison test, * $p < 0.05$, ** $p < 0.01$, *** $p < 0.005$, **** $p < 0.0001$.

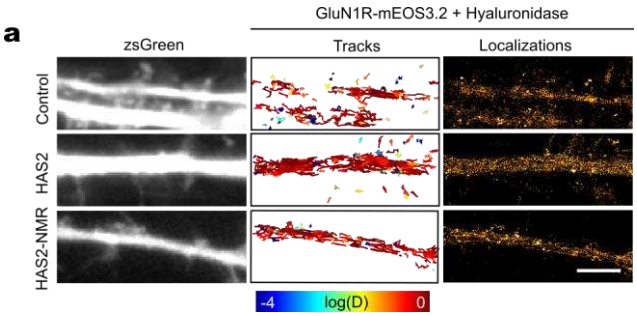

Supplementary Figure 4 (related to figure 4). Effect HA digestion with on GluN1-NMDAR lateral diffusion in control condition or following over-expression of HAS2 and HAS2-NMR

a, Representative fluorescence images of zsGreen (transfection marker, gray) alongside reconstructions of GluN1-mEOS3.2 diffusion-based color-coded trajectories and localizations following acute HA digestion with hyaluronidase. Scale bar, 5 µm.

Discussion and Perspectives

We investigated the role of HA, one of the main components of the ECM, in the membrane organization and diffusion of GluN1-NMDAR by both decreasing and increasing HA content in the ECM. Enrichment was obtained by over-expressing one synthase responsible for the production of HMW-HA in its wild-type form or bearing two mutations, namely N178S and N301S (herein referred as HAS2-NMR), described in the NMR and widely accepted to be responsible for the production of vHMW-HA. We showed that the HA promotes the clustering of membrane NMDAR through a mechanism that remain to be elucidated. I will here discuss these data and propose potential mechanism that may underpin these effects.

1. Transfecting cultured hippocampal neurons with HAS2- and HAS2-NMR increases the ECM content in HA *in vitro*

Transfecting hippocampal neurons with both HAS2 and HAS2-NMR likely increase the extracellular content in HA since HABP staining was increased at the vicinity of transfected neurons. The overexpression of theses synthases likely increases the global amount of HA in a soluble form, which will influence ECM viscosity and viscoelasticity. The changes in HABP remained, however, located to the transfected neuron with no obvious modification at the vicinity of neighboring non-transfected neurons that were even at a very close proximity (from 20 µm up to 300 µm) to the transfected neurons. This suggest that the ECM modification remains spatially constrained in this time window.

It is accepted that the formation of vHMW-HA is due to two point-mutations in the active sites of the HAS2 enzyme (Tian et al., 2013). Even if NMR HAS2 cDNA have been efficiently used to produce vHMW-HA in heterologous cell culture and in mouse *in vivo* (Tian et al., 2013; Zhang et al., 2023), there is no direct evidence that the two point-mutation within the HAS2-coding sequence are indeed responsible for mediating the production of vHMW-HA. In fact, recent studies showed that the production of vHMW-HA is an evolutionary adaptation to subterranean lifestyle and it is thus shared by all subterranean rodent species, including NMRs (Zhao et al., 2023). In fact, only one

out of the two mutations, at the 301 residue, is shared across subterranean species while the mutation at the 178 residue is present only in the NMR HAS2 (Faulkes et al., 2015). To understand whether these mutations are necessary and/or sufficient for the production of vHMW-HA, agarose gel electrophoresis or size exclusion chromatography following HA extraction and purification could be utilized. In addition, NMRs ECS shows unique properties, with smaller volume fraction and reduced diffusion (Thevalingam et al., 2021). Thus, it would be interesting to assess the complexity of the ECS, including diffusion permeability and nanoscale anatomy, using SPT (Godin et al., 2017; Grassi et al., 2023), in both organotypic and/or acute brain slices following HAS2 and HAS2-NMR expression.

2. HAS expression alters neuronal dendritic development

We reported that over-expressing HAS2 or HAS2-NMR altered the number of dendritic spines as well as the development and the complexity of the dendritic tree of cultured hippocampal neurons. The latter supposedly produced longer polymers that may further reduce dendritic outgrowth.

Previous reports have shown that treating hippocampal culture with exogenous hyaluronidase impairs neurites outgrowth (Takechi et al., 2020) while the addition of HA alone, on heterologous cells, induces the formation of membrane protrusions (Kultti et al., 2006; Nagy et al., 1995; Rilla et al., 2008; Skupien et al., 2014). At first glance, these studies and our data are contradictory. The endogenous expression of HAS2 is normally restricted to the late embryonic / early post-natal period *in vivo* and to the first days of culture *in vitro*, with a maximum at DIV 3-7 (Fowke et al., 2017; Takechi et al., 2020). In our experiments, we maintained the expression of HAS2 from DIV 7 onwards. It is likely that HAS2 expression affect the viscoelastic properties of the ECM, such as its elastic modulus (or stiffness) of the ECM which in turn will impact dendritic growth. In line with this, we observed that HAS2 and HAS2-NMR-expression altered the morphology of HEK293T cells. The brain elastic modulus (*E*) varies around 0.1 – 1 kPa, which corresponds to a fluid-like structure in opposition to other structures like cartilage (~ 25 kPa) or bone (~ 40 kPa), for instance (Engler et al., 2006; Flanagan et al., 2002; Smith et al., 2018). Knocking-down the expression of HAS2 have been shown to reduce *E* (i.e. reduction in stiffness) (Sapudom et al., 2020), suggesting that over-

expressing HAS2 will in turn increase the stiffness of the ECM. Since the number of neuronal branching is higher in soft media (Engler et al., 2006; Flanagan et al., 2002), one could subsequently hypothesize, and as we observed, that overexpressing HAS2/HAS2-NMR decreases dendritic growth. In line with this, we observed that HAS2 and HAS2-NMR altered the morphology of HEK293T cells as they appeared smaller and more circular, likely indicating defects in their ability to expand. Obviously, additional studies are necessary to decipher the mechanism underpinning these effects. For instance, investigating how HAS2/HAS-NMR alter cell elastic moduli's and ECM local properties will be of prime interest.

As HA is a highly biologically active molecule that is involved in mediating several signaling cascades, we cannot exclude that HAS2/HAS2-NMR also trigger and recruit specific intracellular signaling that restrain dendritic growth. It will thus be interesting to test the overexpression-induced changes in hippocampal neurons transcriptome. Furthermore, HA have been shown to be directly linked to mitochondria homeostasis (Zhang et al., 2024). Because changes in mitochondria dynamics and metabolism are instrumental for neuronal development, including in dictating its tempo (Iwata et al., 2023, 2020), future experiments assessing the effects of over-expressing HAS2 and HAS2-NMR on mitochondria homeostasis will feed our understanding of the effects of HA on neuronal development.

3. The ECM regulates the organization and the diffusion of NMDAR

3.1 HA controls the surface organization of NMDAR

We observed that digesting HA, through bath incubation with exogenous hyaluronidase, impairs NMDAR surface organization. The changes were detected using super-resolution imaging (dSTORM) but not with conventional fluorescence microscopy. NMDAR nanodomains were smaller and denser following hyaluronidase incubation, irrespectively of their synaptic or extrasynaptic localization. Increasing HA content or type by transfecting with HAS2-NMR-encoding plasmid increased the size of GluN1-NMDAR clusters. Thus, it emerges that HA-ECM can bi-directionally tune NMDAR surface clustering.

In conventional fluorescence microscopy approaches, the resolution, which is limited by the diffraction of light, typically lies around ~ 200 to 300 nm whereas the use of super-resolution

imaging techniques dSTORM allows to increase it by an order of magnitude (down to 20 – 30 nm). Furthermore, the sensitivity of the dSTORM technique is also increased as it is based on the detection of temporally and spatially separated single molecules. Hence, dSTORM allows, unlike conventional fluorescence microscopy, to detect changes in the organization of receptors without changes in their quantity. We observed that removing HA leads to a reorganization of the NMDAR: nanodomains were smaller and denser but with similar number of molecules.

It has been previously shown that the acute digestion of the ECM with hyaluronidase, leads to an increase in the membrane diffusion of extrasynaptic AMPA receptors whereas the synaptic ones were mainly unaffected (Frischknecht et al., 2009). One could thus hypothesize that HA preferentially target the extrasynaptic membrane and its receptors. This hypothesis is strengthened by the observations that GluN2A-NMDAR lateral diffusion, which are mainly synaptic, is unaffected upon ECM removal (Frischknecht et al., 2009) and that HABP staining, which stains for HA, poorly colocalize with postsynaptic markers such as PSD95 and Homer1 (Fowke et al., 2017; Frischknecht et al., 2009). Furthermore, the observation that the synaptic content in GluN2B-NMDAR, which are mainly present in the extrasynaptic membrane, is increased following digestion of HA (Schweitzer et al., 2017), further suggest that HA favors the extrasynaptic aggregation of the NMDAR. Upon removal, these receptors are free to diffuse and eventually translocate temporarily to synaptic sites. Herein, we observed that digesting HA massively altered the extrasynaptic nano-organization of GluN1-NMDAR. We report an increase in the number of extrasynaptic nanodomains which was associated with a decrease in the size and increase in the molecular density of the nanodomains as well as a decrease in the absolute number of molecules per nanodomains. We observed that the synaptic organization of the NMDAR was also altered with smaller and denser nanodomains. However, both the number of nanodomains per cluster and the absolute number of molecules per nanodomain were unaltered. Altogether, our data suggest an indirect effect of HA removal on synaptic NMDAR, possibly secondary to the direct action of the extrasynaptic membrane and/or to an alteration in the architecture/morphology of the dendritic spines (Dembitskaya et al., 2021; Levy et al., 2014; Roszkowska et al., 2016). Further experiments assessing the acute effects of HA removal on the nano-organization of the PSD and on the morphology of dendritic spines are necessary to shed light on this process. Similarly, understanding whether NMDAR cluster size increases preferentially at specific sites upon HAS

over-expression, and whether this changes the nano-organization of the PSD and the morphology of dendritic spines, will enlighten the roles of HA in neuronal membrane organization. Furthermore, one can explore the functional consequences of HA pro-clustering effect, especially on the extrasynaptic compartment. Indeed, an increase in extrasynaptic NMDAR have been shown to participate in triggering symptoms in Huntington's and Alzheimer's disease (Milnerwood et al., 2010; Talantova et al., 2013). Understanding how increasing HA content affects neuronal activity will be particularly interesting.

3.2 HA sterically hinders the lateral diffusion of membrane macromolecules

Increasing the ECM differentially hindered the lateral diffusion of surface macromolecules with variable levels depending on the over-expressed synthase (HAS2 or HAS2-NMR) and the type of macromolecule (GluN1-NMDAR, GPI anchor, and GluA1-AMPAR). Indeed, over-expressing HAS2 solely affected the lateral diffusion properties of GluA1-AMPAR but no GPI anchor or GluN1-NMDAR. On the other hand, over-expressing HAS2-NMR affected the lateral diffusion of all three-studied membrane macromolecules. To confirm that the observed effect was caused by a direct action of HA, we acutely digested the matrix by pre-incubating neurons with exogenous hyaluronidase before performing PALM for GluN1-NMDAR. As expected, digesting the ECM reverted the effect of over-expressing HAS2-NMR on GluN1-NMDAR lateral diffusion, which further confirmed that HA directly hinders the lateral diffusion of membrane macromolecules.

It is not clear whether the increased HA content hinders the lateral diffusion of membrane macromolecules by forming a viscous coating arounds neuron and/or by modifying the membrane compartmentalization into subdomains, as depicted by the anchored picket fence model (Jacobson et al., 2019; Kusumi et al., 2012). The anchored picket fence model has been the main model to explain the regulation of membrane lateral diffusion. Following this model, there is a continuum of connectivity between the ECM and the intracellular environment (e.g. cytoskeleton) through transmembrane proteins or "pickets" that altogether participate in creating membrane subdomains of different viscosity. While changes in the membrane compartmentalization imply equivalent effects irrespectively on the target membrane macromolecule, steric hindrance mechanisms would lead to different effects or different magnitude of effects depending on both

the target (e.g. extracellular domain height, charges, post-translational modifications, etc.) and the viscosity of the ECM, i.e. length of the HA polymer. In line with the latter hypothesis, we observed different effects depending on whether HAS2 or HAS2-NMR was over-expressed (i.e. HA polymer length) as well as the surface macromolecule (GPI anchor, GluA1-AMPAR, and GluN1-NMDAR), which altogether further indicate steric hindrance mechanisms. We observed that the lateral diffusion of GluN1-NMDAR and GluA1-AMPAR, which are of similar extracellular height, were differently affected upon matrix enhancement. GluA1-AMPAR appeared highly sensitive to any matrix enhancement as both over-expressing HAS2 and HAS2-NMR increased GluA1-AMPAR confinement to similar levels whereas GluN1-NMDAR were differently affected depending on whether HAS2 or HAS2-NMR were over-expressed. Altogether, these data suggest that the size of the extracellular domain alone does not predict the susceptibility of the macromolecule to HA. The mechanisms underlying the differences in membrane macromolecule sensitivity towards the ECM are however not clear. Considering that HA closely interact with the plasma membrane and that it is negatively charged at physiological pH, one can expect differences in extracellular domain electrostatic charges and post-translational modifications to be determinant in defining one macromolecule sensitivity towards the ECM. It will thus be interesting to investigate the roles of post-translational modifications, such as N-glycosylation which have been shown to be highly prevalent in the brain (Hanus et al., 2016; Tsai et al., 2024), as well as electrostatic charges.

We observed two different mechanisms of action of HA on GluN1-NMDAR and GluA1-AMPAR. While enhancing the HA content induced a continuous shift in the distribution of the diffusion coefficient to the left (i.e. towards slower values) for GluA1-AMPAR, we observed, in the case of GluN1-NMDAR, a specific subpopulation of highly immobile receptors. Importantly, GluN1-NMDAR display 6 amino-acids (I272, N273, T335, G336, R337, and N350) that form a positively-charged region within the ATD whereas the homologous region of GluN2B-ATD was shown to be negatively charged (Washburn et al., 2020). One can thus hypothesize direct electrostatic interaction between the negatively charged HA and the positively charged GluN1-NMDAR, accounting for the change in receptor diffusion and the immobilization of the GluN1-NMDAR. It will be interesting to investigate whether the effect of HAS2-NMR is lost upon expression of a sextuple mutant of the NMDAR that does not display the above-mentioned positively-charged pocket.

Our data support the hypothesize that the ECM not only acts as a passive and unspecific compartment but as a structure that can differentiate between membrane receptors. Collectively, these results lead to the hypothesis that the matrix, by acting on specific targets, could dramatically remodel the organization of the whole neuronal membrane. Following this view, HA not only sterically hinders the surface diffusion of membrane macromolecules but possibly directly interact with some, leading to their aggregation. This hypothesis is further supported by the fact that HMW-HA, but no LMW-HA, act as an extracellular crosslinker for one its receptor (Ooki et al., 2019; Yang et al., 2012). Defining the nanoscale organization of the ECM in parallel to that of membrane receptors will surely shed light on the molecular mechanism underpinning the instrumental role of the ECM on membrane protein organization, dynamics and functions. Furthermore, it will thus be interesting to understand how the organization of all the neuronal surface macromolecules, also known as surfaceome, as developed by (Jamet et al., 2024), is shaped by the ECM.

Annexes

Annex 1 Surface abundance of GluN1-NMDAR and D1R during in vitro cortical development

Annex 2 Effect of dopaminergic agonist SKF on D1R-GluN1-NMDAR interaction

Annex 1

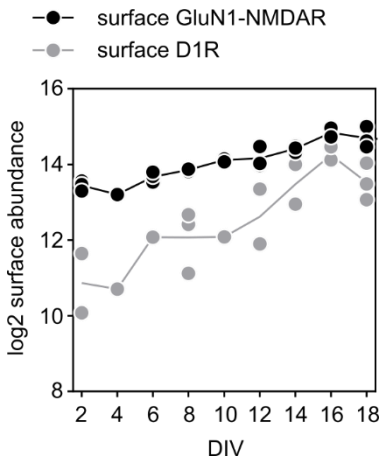

Surface abundance of GluN1-NMDAR and D1R during cortical development *in vitro*.

Data extracted from the publicly available resource http://neurosurfaceome.ethz.ch/. (Van Oostrum et al., 2020)

Annex 2

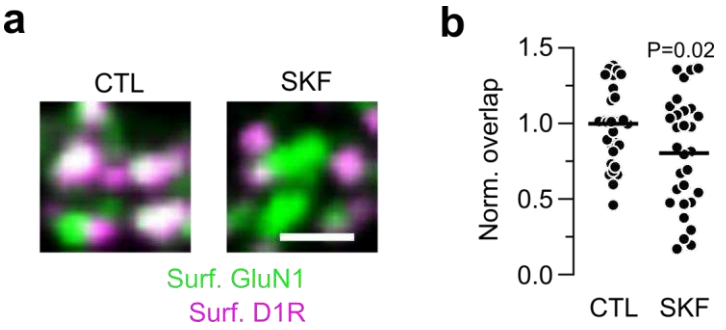

Effect of the dopaminergic agonist SKF on D1R-GluN1-NMDAR interaction.

a, Representative images of hippocampal dendrites on which surface GluN1-NMDAR (green) and D1R (magenta) were labelled after exposure to the D1/5R agonist SKF. Scale bar, 2 µm. **b**, Quantification of D1R-GluN1-NMDAR overlap after treatment with either buffer (CTL, n = 31 cells) or SKF (n = 30 cells). Unpaired t-test.

Additional publications

Additional publication 1

Accepted in Neuron (2024)

Ketamine alleviates NMDA receptor hypofunction through synaptic trapping

Frédéric Villéga[1,2#], Alexandra Fernandes[1#], Julie Jézéquel[1#], Floriane Uyttersprot[1], Nathan Benac[1], Sarra Zenagui[1], Laurine Bastardo[1], Hélène Gréa[1], Delphine Bouchet[1], Léa Villetelle[1], Olivier Nicole[1], Véronique Rogemond[3,4], Jérôme Honnorat[3,4], Julien P. Dupuis[1*], Laurent Groc[1,5*]

[1]University of Bordeaux, CNRS, Interdisciplinary Institute for Neuroscience, IINS, UMR 5297, F-33000, Bordeaux, France

[2]Department of Pediatric Neurology, CIC-1401, University Children's Hospital of Bordeaux, Bordeaux, France.

[3]Synaptopathies and Autoantibodies Team, Institut NeuroMyoGene-MeLis, INSERM U1314, CNRS UMR 5284, Université Claude Bernard Lyon1, F-69373, Lyon, France

[4]French Reference Centre on Paraneoplastic Neurological Syndromes and Autoimmune Encephalitis, Hospices Civils de Lyon, Hôpital Neurologique Pierre Wertheimer, F-69677, Bron, France

[5]Lead contact

[#] These authors contributed equally

[*]Correspondence: julien.dupuis@u-bordeaux.fr (JD), laurent.groc@u-bordeaux.fr (LG)

Summary

Activity-dependent modulations of N-methyl-D-aspartate glutamate receptor (NMDAR) trapping at synapses regulate excitatory neurotransmission and shape cognitive functions. While NMDAR synaptic destabilization has been associated with severe neurological and psychiatric conditions, tuning NMDAR synaptic trapping to assess its clinical relevance for the treatment of brain conditions remains a challenge. Here, we report that ketamine and other clinically-relevant NMDAR open channel blockers (OCBs) promote interactions between NMDAR and PDZ domain-containing scaffolding proteins and enhance NMDAR trapping at synapses. We further show that

ketamine-elicited trapping enhancement compensates for depletion in synaptic receptors triggered by autoantibodies from patients with anti-NMDAR encephalitis. Preventing synaptic depletion mitigates impairments in NMDAR-mediated CaMKII signaling and alleviates anxiety- and sensorimotor gating-related behavioral deficits provoked by autoantibodies. Altogether, these findings reveal an unexpected dimension of OCB action and stress the potential of targeting receptor anchoring in NMDAR-related synaptopathies.

Additional publication 2

Published in **EMBO Reports** (2024). https://doi.org/10.1038/s44319-024-00056-2

Converging synaptic and network dysfunctions in distinct autoimmune encephalitis

Daniel Hunter[1,5], Mar Petit-Pedrol[1,5], Dominique Fernandes[1], Nathan Bénac[1], Catarina Rodrigues[1], Jakob Kreye[2,3], Mihai Ceanga[4], Harald Prüs[2,3], Christian Geis[4], Laurent Groc[1]

[1]University of Bordeaux, CNRS, Interdisciplinary Institute for Neuroscience, IINS, UMR 5297, F-33000 Bordeaux, France.

[2]German Center for Neurodegenerative Diseases (DZNE) Berlin, 10117 Berlin, Germany.

[3]Department of Neurology and Experimental Neurology, Charité-Universitätsmedizin Berlin, Corporate Member of Freie Universität Berlin, Humboldt-Universität Berlin, 10117 Berlin, Germany.

[4]Hans-Berger Department of Neurology, Jena University Hospital, Jena, Germany.

[5]These authors contributed equally: Daniel Hunter, Mar Petit-Pedrol.

E-mail: laurent.groc@u-bordeaux.fr

Abstract

Psychiatric and neurological symptoms, as well as cognitive deficits, represent a prominent phenotype associated with variable forms of autoimmune encephalitis, regardless of the neurotransmitter receptor targeted by autoantibodies. The mechanistic underpinnings of these shared major neuropsychiatric symptoms remain however unclear. Here, we investigate the impacts of patient-derived monoclonal autoantibodies against the glutamatergic NMDAR (NMDAR mAb) and inhibitory GABAaR (GABAaR mAb) signalling in the hippocampal network. Unexpectedly, both excitatory and inhibitory synaptic receptor membrane dynamics, content and transmissions are altered by NMDAR or GABAaR mAb, irrespective of the affinity or antagonistic effect of the autoantibodies. The effect of NMDAR mAb on inhibitory synapses and GABAaR mAb on excitatory synapses requires neuronal activity and involves protein kinase signalling. At the cell level, both autoantibodies increase the excitation/inhibition balance of principal cell inputs. Furthermore,

NMDAR or GABAaR mAb leads to hyperactivation of hippocampal networks through distinct alterations of principal cell and interneuron properties. Thus, autoantibodies targeting excitatory NMDAR or inhibitory GABAaR trigger convergent network dysfunctions through a combination of shared and distinct mechanisms.

Additional publication 3

Published in Frontiers in Bioinformatics (2022). doi: 10.3389/fbinf.2022.813494

Multi-Dimensional Spectral Single Molecule Localization Microscopy

Corey Butler [1,2], G Ezequiel Saraceno [1], Adel Kechkar [3], Nathan Bénac [1], Vincent Studer [1], Julien P. Dupuis [1], Laurent Groc [1], Rémi Galland [1*] and Jean-Baptiste Sibarita [1*]

[1]Univ. Bordeaux, CNRS, Interdisciplinary Institute for Neuroscience, IINS, UMR 5297F-33000, F-33000, Bordeaux, France

[2]Imagine Optic, Orsay, France

[3]Ecole Nationale Supérieure de Biotechnologie, Laboratoire de Bioengineering, Constantine, El Khroub, Algeria

[*]Correspondence: Rémi Galland (remi.galland@u-bordeaux.fr), Jean-Baptiste Sibarita (jean-baptiste.sibarita@ u-bordeaux.fr)

Abstract

Single molecule localization (SML) and tracking (SPT) techniques, such as (spt) PALM, (u/ DNA) PAINT and quantum dot tracking, have given unprecedented insight into the nanoscale molecular organization and dynamics in living cells. They allow monitoring individual proteins with millisecond temporal resolution and high spatial resolution (< 30 nm) by precisely localizing the point spread function (PSF) of individual emitters and tracking their position over time. While SPT methods have been extended to study the temporal dynamics and co-organization of multiple proteins, conventional experimental setups are restricted in the number of proteins they can probe simultaneously and usually have to tradeoff between the number of colors, the spatio-temporal resolution, and the field of view. Yet, localizing and tracking several proteins simultaneously at high spatial and temporal resolution within large field of views can provide

important biological insights. By employing a dual-objective spectral imaging configuration compatible with live cell imaging combined with dedicated computation tools, we demonstrate simultaneous 3D single particle localization and tracking of multiple distinct species over large field of views to be feasible without compromising spatio-temporal resolution. The dispersive element introduced into the second optical path induces a spectrally dependent displacement, which we used to analytically separate up to five different fluorescent species of single emitters based on their emission spectra. We used commercially available microscope bodies aligned one on top of the other, offering biologists with a very ergonomic and flexible instrument covering a broad range of SMLM applications. Finally, we developed a powerful freely available software, called PALM Tracer, which allows to quantitatively assess 3D + t + λ SMLM data. We illustrate the capacity of our approach by performing multi-color 3D DNA-PAINT of fixed samples, and demonstrate simultaneous tracking of multiple receptors in live fibroblast and neuron cultures.

Bibliography

Abrahamsson, T., Chou, C.Y.C., Li, S.Y., Mancino, A., Costa, R.P., Brock, J.A., Nuro, E., Buchanan, K.A., Elgar, D., Blackman, A.V., Tudor-Jones, A., Oyrer, J., Farmer, W.T., Murai, K.K., Sjöström, P.J., 2017. Differential Regulation of Evoked and Spontaneous Release by Presynaptic NMDA Receptors. Neuron 96, 839-855.e5. https://doi.org/10.1016/j.neuron.2017.09.030

Abrahamsson, T., Gustafsson, B., Hanse, E., 2008. AMPA Silencing Is a Prerequisite for Developmental Long-Term Potentiation in the Hippocampal CA1 Region. J. Neurophysiol. 100, 2605–2614. https://doi.org/10.1152/jn.90476.2008

Abrahamsson, T., Gustafsson, B., Hanse, E., 2007. Reversible Synaptic Depression in Developing Rat CA3–CA1 Synapses Explained by a Novel Cycle of AMPA Silencing-Unsilencing. J. Neurophysiol. 98, 2604–2611. https://doi.org/10.1152/jn.00602.2007

Acuna, C., Liu, X., Südhof, T.C., 2016. How to Make an Active Zone: Unexpected Universal Functional Redundancy between RIMs and RIM-BPs. Neuron 91, 792–807. https://doi.org/10.1016/j.neuron.2016.07.042

Adesnik, H., Li, G., During, M.J., Pleasure, S.J., Nicoll, R.A., 2008. NMDA receptors inhibit synapse unsilencing during brain development. Proc. Natl. Acad. Sci. 105, 5597–5602. https://doi.org/10.1073/pnas.0800946105

Ahmari, S.E., Smith, S.J., 2002. Knowing a Nascent Synapse When You See It. Neuron 34, 333–336. https://doi.org/10.1016/S0896-6273(02)00685-2

Akashi, K., Kakizaki, T., Kamiya, H., Fukaya, M., Yamasaki, M., Abe, M., Natsume, R., Watanabe, M., Sakimura, K., 2009. NMDA Receptor GluN2B (GluRε2/NR2B) Subunit Is Crucial for Channel Function, Postsynaptic Macromolecular Organization, and Actin Cytoskeleton at Hippocampal CA3 Synapses. J. Neurosci. 29, 10869–10882. https://doi.org/10.1523/JNEUROSCI.5531-08.2009

Akazawa, C., Shigemoto, R., Bessho, Y., Nakanishi, S., Mizuno, N., 1994. Differential expression of five N-methyl-D-aspartate receptor subunit mRNAs in the cerebellum of developing and adult rats. J. Comp. Neurol. 347, 150–160. https://doi.org/10.1002/cne.903470112

Algar, W.R., Hildebrandt, N., Vogel, S.S., Medintz, I.L., 2019. FRET as a biomolecular research tool — understanding its potential while avoiding pitfalls. Nat. Methods 16, 815–829. https://doi.org/10.1038/s41592-019-0530-8

Allen, N.J., 2014. Astrocyte Regulation of Synaptic Behavior. Annu. Rev. Cell Dev. Biol. 30, 439–463. https://doi.org/10.1146/annurev-cellbio-100913-013053

Allen, N.J., Bennett, M.L., Foo, L.C., Wang, G.X., Chakraborty, C., Smith, S.J., Barres, B.A., 2012. Astrocyte glypicans 4 and 6 promote formation of excitatory synapses via GluA1 AMPA receptors. Nature 486, 410–414. https://doi.org/10.1038/nature11059

Aloisi, E., Le Corf, K., Dupuis, J., Zhang, P., Ginger, M., Labrousse, V., Spatuzza, M., Georg Haberl, M., Costa, L., Shigemoto, R., Tappe-Theodor, A., Drago, F., Vincenzo Piazza, P., Mulle, C., Groc, L., Ciranna, L., Catania, M.V., Frick, A., 2017. Altered surface mGluR5 dynamics provoke synaptic NMDAR dysfunction and cognitive defects in Fmr1 knockout mice. Nat. Commun. 8, 1103. https://doi.org/10.1038/s41467-017-01191-2

Aman, T.K., Maki, B.A., Ruffino, T.J., Kasperek, E.M., Popescu, G.K., 2014. Separate Intramolecular Targets for Protein Kinase A Control N-Methyl-d-aspartate Receptor Gating and Ca2+ Permeability *. J. Biol. Chem. 289, 18805–18817. https://doi.org/10.1074/jbc.M113.537282

Anderson, G.R., Maxeiner, S., Sando, R., Tsetsenis, T., Malenka, R.C., Südhof, T.C., 2017. Postsynaptic adhesion GPCR latrophilin-2 mediates target recognition in entorhinal-hippocampal synapse assembly. J. Cell Biol. 216, 3831–3846. https://doi.org/10.1083/jcb.201703042

Andrade-Talavera, Y., Duque-Feria, P., Paulsen, O., Rodríguez-Moreno, A., 2016. Presynaptic Spike Timing-Dependent Long-Term Depression in the Mouse Hippocampus. Cereb. Cortex 26, 3637–3654. https://doi.org/10.1093/cercor/bhw172

Andreae, L.C., Ben Fredj, N., Burrone, J., 2012. Independent Vesicle Pools Underlie Different Modes of Release during Neuronal Development. J. Neurosci. 32, 1867–1874. https://doi.org/10.1523/JNEUROSCI.5181-11.2012

Andreae, L.C., Burrone, J., 2018. The role of spontaneous neurotransmission in synapse and circuit development. J. Neurosci. Res. 96, 354–359. https://doi.org/10.1002/jnr.24154

Andreae, L.C., Burrone, J., 2015. Spontaneous Neurotransmitter Release Shapes Dendritic Arbors via Long-Range Activation of NMDA Receptors. Cell Rep. 10, 873–882. https://doi.org/10.1016/j.celrep.2015.01.032

Andreae, L.C., Burrone, J., 2014. The role of neuronal activity and transmitter release on synapse formation. Curr. Opin. Neurobiol. 27, 47–52. https://doi.org/10.1016/j.conb.2014.02.008

Andrianarivelo, A., Saint-Jour, E., Pousinha, P., Fernandez, S.P., Petitbon, A., De Smedt-Peyrusse, V., Heck, N., Ortiz, V., Allichon, M.-C., Kappès, V., Betuing, S., Walle, R., Zhu, Y., Joséphine, C., Bemelmans, A.-P., Turecki, G., Mechawar, N., Javitch, J.A., Caboche, J., Trifilieff, P., Barik, J., Vanhoutte, P., 2021. Disrupting D1-NMDA or D2-NMDA receptor heteromerization prevents cocaine's rewarding effects but preserves natural reward processing. Sci. Adv. 7, eabg5970. https://doi.org/10.1126/sciadv.abg5970

Anton, S.E., Kayser, C., Maiellaro, I., Nemec, K., Möller, J., Koschinski, A., Zaccolo, M., Annibale, P., Falcke, M., Lohse, M.J., Bock, A., 2022. Receptor-associated independent cAMP nanodomains mediate spatiotemporal specificity of GPCR signaling. Cell 185, 1130-1142.e11. https://doi.org/10.1016/j.cell.2022.02.011

Araki, K.Y., Sims, J.R., Bhide, P.G., 2007. Dopamine receptor mRNA and protein expression in the mouse corpus striatum and cerebral cortex during pre- and postnatal development. Brain Res. 1156, 31–45. https://doi.org/10.1016/j.brainres.2007.04.043

Arranz, A.M., Perkins, K.L., Irie, F., Lewis, D.P., Hrabe, J., Xiao, F., Itano, N., Kimata, K., Hrabetova, S., Yamaguchi, Y., 2014. Hyaluronan Deficiency Due to *Has3* Knock-Out Causes Altered Neuronal Activity and Seizures via Reduction in Brain Extracellular Space. J. Neurosci. 34, 6164–6176. https://doi.org/10.1523/JNEUROSCI.3458-13.2014

Artola, A., Bröcher, S., Singer, W., 1990. Different voltage-dependent thresholds for inducing long-term depression and long-term potentiation in slices of rat visual cortex. Nature 347, 69–72. https://doi.org/10.1038/347069a0

Ashby, M.C., Ibaraki, K., Henley, J.M., 2004. It's green outside: tracking cell surface proteins with pH-sensitive GFP. Trends Neurosci. 27, 257–261. https://doi.org/10.1016/j.tins.2004.03.010

Ashby, M.C., Maier, S.R., Nishimune, A., Henley, J.M., 2006. Lateral Diffusion Drives Constitutive Exchange of AMPA Receptors at Dendritic Spines and Is Regulated by Spine Morphology. J. Neurosci. 26, 7046–7055. https://doi.org/10.1523/JNEUROSCI.1235-06.2006

Asher, W.B., Geggier, P., Holsey, M.D., Gilmore, G.T., Pati, A.K., Meszaros, J., Terry, D.S., Mathiasen, S., Kaliszewski, M.J., McCauley, M.D., Govindaraju, A., Zhou, Z., Harikumar, K.G., Jaqaman, K., Miller, L.J., Smith, A.W., Blanchard, S.C., Javitch, J.A., 2021. Single-molecule FRET imaging of GPCR dimers in living cells. Nat. Methods 18, 397–405. https://doi.org/10.1038/s41592-021-01081-y

Asztely, F., Erdemli, G., Kullmann, D.M., 1997. Extrasynaptic Glutamate Spillover in the Hippocampus: Dependence on Temperature and the Role of Active Glutamate Uptake. Neuron 18, 281–293. https://doi.org/10.1016/S0896-6273(00)80268-8

Atasoy, D., Ertunc, M., Moulder, K.L., Blackwell, J., Chung, C., Su, J., Kavalali, E.T., 2008. Spontaneous and Evoked Glutamate Release Activates Two Populations of NMDA Receptors with Limited Overlap. J. Neurosci. 28, 10151–10166. https://doi.org/10.1523/JNEUROSCI.2432-08.2008

Atlason, P.T., Garside, M.L., Meddows, E., Whiting, P., McIlhinney, R.A.J., 2007. N-Methyl-d-aspartate (NMDA) Receptor Subunit NR1 Forms the Substrate for Oligomeric Assembly of the NMDA Receptor *. J. Biol. Chem. 282, 25299–25307. https://doi.org/10.1074/jbc.M702778200

Attardo, A., Fitzgerald, J.E., Schnitzer, M.J., 2015. Impermanence of dendritic spines in live adult CA1 hippocampus. Nature 523, 592–596. https://doi.org/10.1038/nature14467

Axelrod, D., Koppel, D.E., Schlessinger, J., Elson, E., Webb, W.W., 1976. Mobility measurement by analysis of fluorescence photobleaching recovery kinetics. Biophys. J. 16, 1055–1069. https://doi.org/10.1016/S0006-3495(76)85755-4

Axelrod, D, Ravdin, P., Koppel, D.E., Schlessinger, J., Webb, W.W., Elson, E.L., Podleski, T.R., 1976. Lateral motion of fluorescently labeled acetylcholine receptors in membranes of developing muscle fibers. Proc. Natl. Acad. Sci. 73, 4594–4598. https://doi.org/10.1073/pnas.73.12.4594

Bajar, B.T., Wang, E.S., Zhang, S., Lin, M.Z., Chu, J., 2016. A Guide to Fluorescent Protein FRET Pairs. Sensors 16, 1488. https://doi.org/10.3390/s16091488

Balasuriya, D., Stewart, A.P., Edwardson, J.M., 2013. The σ-1 Receptor Interacts Directly with GluN1 But Not GluN2A in the GluN1/GluN2A NMDA Receptor. J. Neurosci. 33, 18219–18224. https://doi.org/10.1523/JNEUROSCI.3360-13.2013

Balschun, D., Wetzel, W., 2002. Inhibition of mGluR5 blocks hippocampal LTP in vivo and spatial learning in rats. Pharmacol. Biochem. Behav., Metabotropic Glutamate Receptors 73, 375–380. https://doi.org/10.1016/S0091-3057(02)00847-X

Banerjee, A., Larsen, R.S., Philpot, B.D., Paulsen, O., 2016. Roles of Presynaptic NMDA Receptors in Neurotransmission and Plasticity. Trends Neurosci. 39, 26–39. https://doi.org/10.1016/j.tins.2015.11.001

Banker, G.A., 1980. Trophic Interactions Between Astroglial Cells and Hippocampal Neurons in Culture. Science 209, 809–810. https://doi.org/10.1126/science.7403847

Bard, L., Groc, L., 2011. Glutamate receptor dynamics and protein interaction: Lessons from the NMDA receptor. Mol. Cell. Neurosci. 48, 298–307. https://doi.org/10.1016/j.mcn.2011.05.009

Bard, L., Sainlos, M., Bouchet, D., Cousins, S., Mikasova, L., Breillat, C., Stephenson, F.A., Imperiali, B., Choquet, D., Groc, L., 2010. Dynamic and specific interaction between synaptic NR2-NMDA receptor and PDZ proteins. Proc. Natl. Acad. Sci. 107, 19561–19566. https://doi.org/10.1073/pnas.1002690107

Barria, A., Malinow, R., 2002. Subunit-Specific NMDA Receptor Trafficking to Synapses. Neuron 35, 345–353. https://doi.org/10.1016/S0896-6273(02)00776-6

Barrow, S.L., Constable, J.R., Clark, E., El-Sabeawy, F., McAllister, A.K., Washbourne, P., 2009. Neuroligin1: a cell adhesion molecule that recruits PSD-95 and NMDA receptors by distinct mechanisms during synaptogenesis. Neural Develop. 4. https://doi.org/10.1186/1749-8104-4-17

Bashir, Z.I., Bortolotto, Z.A., Davies, C.H., Berretta, N., Irving, A.J., Seal, A.J., Henley, J.M., Jane, D.E., Watkins, J.C., Collingridge, G.L., 1993a. Induction of LTP in the hippocampus needs synaptic activation of glutamate metabotropic receptors. Nature 363, 347–350. https://doi.org/10.1038/363347a0

Bashir, Z.I., Jane, D.E., Sunter, D.C., Watkins, J.C., Collingridge, G.L., 1993b. Metabotropic glutamate receptors contribute to the induction of long-term depression in the CA1 region of the hippocampus. Eur. J. Pharmacol. 239, 265–266. https://doi.org/10.1016/0014-2999(93)91009-C

Beghin, A., Kechkar, A., Butler, C., Levet, F., Cabillic, M., Rossier, O., Giannone, G., Galland, R., Choquet, D., Sibarita, J.-B., 2017. Localization-based super-resolution imaging meets high-content screening. Nat. Methods 14, 1184–1190. https://doi.org/10.1038/nmeth.4486

Bellone, C., Nicoll, R.A., 2007. Rapid Bidirectional Switching of Synaptic NMDA Receptors. Neuron 55, 779–785. https://doi.org/10.1016/j.neuron.2007.07.035

Bénac, N., Ezequiel Saraceno, G., Butler, C., Kuga, N., Nishimura, Y., Yokoi, T., Su, P., Sasaki, T., Petit-Pedrol, M., Galland, R., Studer, V., Liu, F., Ikegaya, Y., Sibarita, J.-B., Groc, L., 2024. Non-canonical interplay between glutamatergic NMDA and dopamine receptors shapes synaptogenesis. Nat. Commun. 15, 27. https://doi.org/10.1038/s41467-023-44301-z

Benke, T.A., Lüthi, A., Isaac, J.T.R., Collingridge, G.L., 1998. Modulation of AMPA receptor unitary conductance by synaptic activity. Nature 393, 793–797. https://doi.org/10.1038/31709

Berdiaki, A., Neagu, M., Spyridaki, I., Kuskov, A., Perez, S., Nikitovic, D., 2023. Hyaluronan and Reactive Oxygen Species Signaling—Novel Cues from the Matrix? Antioxidants 12, 824. https://doi.org/10.3390/antiox12040824

Bergson, C., Mrzljak, L., Smiley, J.F., Pappy, M., Levenson, R., Goldman-Rakic, P.S., 1995. Regional, cellular, and subcellular variations in the distribution of D1 and D5 dopamine receptors in primate brain. J. Neurosci. 15, 7821–7836. https://doi.org/10.1523/JNEUROSCI.15-12-07821.1995

Berry, K.P., Nedivi, E., 2017. Spine Dynamics: Are They All the Same? Neuron 96, 43–55. https://doi.org/10.1016/j.neuron.2017.08.008

Betzig, E., Patterson, G.H., Sougrat, R., Lindwasser, O.W., Olenych, S., Bonifacino, J.S., Davidson, M.W., Lippincott-Schwartz, J., Hess, H.F., 2006. Imaging Intracellular Fluorescent Proteins at Nanometer Resolution. Science 313, 1642–1645. https://doi.org/10.1126/science.1127344

Bhouri, M., Farrow, P.A., Motee, A., Yan, X., Battaglia, G., Menna, L.D., Riozzi, B., Nicoletti, F., Fitzjohn, S.M., Bashir, Z.I., 2014. mGlu1 Receptor-Induced LTD of NMDA Receptor Transmission Selectively at Schaffer Collateral-CA1 Synapses Mediates Metaplasticity. J. Neurosci. 34, 12223–12229. https://doi.org/10.1523/JNEUROSCI.0753-14.2014

Bi, G., Poo, M., 1998. Synaptic Modifications in Cultured Hippocampal Neurons: Dependence on Spike Timing, Synaptic Strength, and Postsynaptic Cell Type. J. Neurosci. 18, 10464–10472. https://doi.org/10.1523/JNEUROSCI.18-24-10464.1998

Biederer, T., Stagi, M., 2008. Signaling by synaptogenic molecules. Curr. Opin. Neurobiol., Signalling mechanisms 18, 261–269. https://doi.org/10.1016/j.conb.2008.07.014

Biermann, B., Sokoll, S., Klueva, J., Missler, M., Wiegert, J.S., Sibarita, J.-B., Heine, M., 2014. Imaging of molecular surface dynamics in brain slices using single-particle tracking. Nat. Commun. 5, 3024. https://doi.org/10.1038/ncomms4024

Birnbaum, J.H., Bali, J., Rajendran, L., Nitsch, R.M., Tackenberg, C., 2015. Calcium flux-independent NMDA receptor activity is required for Aβ oligomer-induced synaptic loss. Cell Death Dis. 6, e1791–e1791. https://doi.org/10.1038/cddis.2015.160

Blanpied, T.A., Scott, D.B., Ehlers, M.D., 2002. Dynamics and Regulation of Clathrin Coats at Specialized Endocytic Zones of Dendrites and Spines. Neuron 36, 435–449. https://doi.org/10.1016/S0896-6273(02)00979-0

Bodzęta, A., Scheefhals, N., MacGillavry, H.D., 2021. Membrane trafficking and positioning of mGluRs at presynaptic and postsynaptic sites of excitatory synapses. Neuropharmacology 200, 108799. https://doi.org/10.1016/j.neuropharm.2021.108799

Borgdorff, A.J., Choquet, D., 2002. Regulation of AMPA receptor lateral movements. Nature 417, 649–653. https://doi.org/10.1038/nature00780

Borroto-Escuela, D.O., Flajolet, M., Agnati, L.F., Greengard, P., Fuxe, K., 2013. Chapter 8 - Bioluminescence Resonance Energy Transfer Methods to Study G Protein-Coupled Receptor–Receptor Tyrosine Kinase Heteroreceptor Complexes, in: Conn, P.M. (Ed.), Methods in Cell Biology, Receptor-Receptor Interactions. Academic Press, pp. 141–164. https://doi.org/10.1016/B978-0-12-408143-7.00008-6

Bourgeron, T., 2015. From the genetic architecture to synaptic plasticity in autism spectrum disorder. Nat. Rev. Neurosci. 16, 551–563. https://doi.org/10.1038/nrn3992

Bourguignon, V., Flamion, B., 2016. Respective roles of hyaluronidases 1 and 2 in endogenous hyaluronan turnover. FASEB J. 30, 2108–2114. https://doi.org/10.1096/fj.201500178R

Bouvier, G., Bidoret, C., Casado, M., Paoletti, P., 2015. Presynaptic NMDA receptors: Roles and rules. Neuroscience 311, 322–340. https://doi.org/10.1016/j.neuroscience.2015.10.033

Bouvier, G., Larsen, R.S., Rodríguez-Moreno, A., Paulsen, O., Sjöström, P.J., 2018. Towards resolving the presynaptic NMDA receptor debate. Curr. Opin. Neurobiol., Cellular Neuroscience 51, 1–7. https://doi.org/10.1016/j.conb.2017.12.020

Bradbury, E.J., Moon, L.D.F., Popat, R.J., King, V.R., Bennett, G.S., Patel, P.N., Fawcett, J.W., McMahon, S.B., 2002. Chondroitinase ABC promotes functional recovery after spinal cord injury. Nature 416, 636–640. https://doi.org/10.1038/416636a

Brakeman, P.R., Lanahan, A.A., O'Brien, R., Roche, K., Barnes, C.A., Huganir, R.L., Worley, P.F., 1997. Homer: a protein that selectively binds metabotropic glutamate receptors. Nature 386, 284–288. https://doi.org/10.1038/386284a0

Bresler, T., Shapira, M., Boeckers, T., Dresbach, T., Futter, M., Garner, C.C., Rosenblum, K., Gundelfinger, E.D., Ziv, N.E., 2004. Postsynaptic Density Assembly Is Fundamentally Different from Presynaptic Active Zone Assembly. J. Neurosci. 24, 1507–1520. https://doi.org/10.1523/jneurosci.3819-03.2004

Budreck, E.C., Kwon, O.-B., Jung, J.H., Baudouin, S., Thommen, A., Kim, H.-S., Fukazawa, Y., Harada, H., Tabuchi, K., Shigemoto, R., Scheiffele, P., Kim, J.-H., 2013. Neuroligin-1 controls synaptic abundance of NMDA-type glutamate receptors through extracellular coupling. Proc. Natl. Acad. Sci. 110, 725–730. https://doi.org/10.1073/pnas.1214718110

Buffenstein, R., 2008. Negligible senescence in the longest living rodent, the naked mole-rat: insights from a successfully aging species. J. Comp. Physiol. B 178, 439–445. https://doi.org/10.1007/s00360-007-0237-5

Buffenstein, R., Jarvis, J.U.M., 2002. The Naked Mole Rat--A New Record for the Oldest Living Rodent. Sci. Aging Knowl. Environ. 2002, pe7–pe7. https://doi.org/10.1126/sageke.2002.21.pe7

Buffenstein, R., Park, T., Hanes, M., Artwohl, J.E., 2012. Chapter 45 - Naked Mole Rat, in: Suckow, M.A., Stevens, K.A., Wilson, R.P. (Eds.), The Laboratory Rabbit, Guinea Pig, Hamster, and Other Rodents, American College of Laboratory Animal Medicine. Academic Press, Boston, pp. 1055–1074. https://doi.org/10.1016/B978-0-12-380920-9.00045-6

Burlingham, S.R., Wong, N.F., Peterkin, L., Lubow, L., Dos Santos Passos, C., Benner, O., Ghebrial, M., Cast, T.P., Xu-Friedman, M.A., Südhof, T.C., Chanda, S., 2022. Induction of synapse formation by de novo neurotransmitter synthesis. Nat. Commun. 13, 3060. https://doi.org/10.1038/s41467-022-30756-z

Burnashev, N., Zhou, Z., Neher, E., Sakmann, B., 1995. Fractional calcium currents through recombinant GluR channels of the NMDA, AMPA and kainate receptor subtypes. J. Physiol. 485, 403–418. https://doi.org/10.1113/jphysiol.1995.sp020738

Butler, C., Saraceno, G.E., Kechkar, A., Bénac, N., Studer, V., Dupuis, J.P., Groc, L., Galland, R., Sibarita, J.-B., 2022. Multi-Dimensional Spectral Single Molecule Localization Microscopy. Front. Bioinforma. 2, 813494. https://doi.org/10.3389/fbinf.2022.813494

Cahill, E., Pascoli, V., Trifilieff, P., Savoldi, D., Kappès, V., Lüscher, C., Caboche, J., Vanhoutte, P., 2014. D1R/GluN1 complexes in the striatum integrate dopamine and glutamate signalling to control synaptic plasticity and cocaine-induced responses. Mol. Psychiatry 19, 1295–1304. https://doi.org/10.1038/mp.2014.73

Calabrese, B., Wilson, M.S., Halpain, S., 2006. Development and Regulation of Dendritic Spine Synapses. Physiology 21, 38–47. https://doi.org/10.1152/physiol.00042.2005

Calebiro, D., Rieken, F., Wagner, J., Sungkaworn, T., Zabel, U., Borzi, A., Cocucci, E., Zürn, A., Lohse, M.J., 2013. Single-molecule analysis of fluorescently labeled G-protein–coupled receptors reveals complexes with distinct dynamics and organization. Proc. Natl. Acad. Sci. 110, 743–748. https://doi.org/10.1073/pnas.1205798110

Callier, S., Snapyan, M., Le Crom, S., Prou, D., Vincent, J.-D., Vernier, P., 2003. Evolution and cell biology of dopamine receptors in vertebrates. Biol. Cell 95, 489–502. https://doi.org/10.1016/S0248-4900(03)00089-3

Camenisch, T.D., Spicer, A.P., Brehm-Gibson, T., Biesterfeldt, J., Augustine, M.L., Calabro, A., Kubalak, S., Klewer, S.E., McDonald, J.A., 2000. Disruption of hyaluronan synthase-2 abrogates normal cardiac morphogenesis and hyaluronan-mediated transformation of epithelium to mesenchyme. J. Clin. Invest. 106, 349–360. https://doi.org/10.1172/JCI10272

Campo, C.G., Sinagra, M., Verrier, D., Manzoni, O.J., Chavis, P., 2009. Reelin Secreted by GABAergic Neurons Regulates Glutamate Receptor Homeostasis. PLoS ONE 4, e5505. https://doi.org/10.1371/journal.pone.0005505

Cargill, R., Kohama, S.G., Struve, J., Su, W., Banine, F., Witkowski, E., Back, S.A., Sherman, L.S., 2012. Astrocytes in aged nonhuman primate brain gray matter synthesize excess hyaluronan. Neurobiol. Aging 33, 830.e13-830.e24. https://doi.org/10.1016/j.neurobiolaging.2011.07.006

Carulli, D., Pizzorusso, T., Kwok, J.C.F., Putignano, E., Poli, A., Forostyak, S., Andrews, M.R., Deepa, S.S., Glant, T.T., Fawcett, J.W., 2010. Animals lacking link protein have attenuated perineuronal nets and persistent plasticity. Brain 133, 2331–2347. https://doi.org/10.1093/brain/awq145

Carulli, D., Rhodes, K.E., Brown, D.J., Bonnert, T.P., Pollack, S.J., Oliver, K., Strata, P., Fawcett, J.W., 2006. Composition of perineuronal nets in the adult rat cerebellum and the cellular origin of their components. J. Comp. Neurol. 494, 559–577. https://doi.org/10.1002/cne.20822

Carulli, D., Verhaagen, J., 2021. An Extracellular Perspective on CNS Maturation: Perineuronal Nets and the Control of Plasticity. Int J Mol Sci.

Cepeda, C., Buchwald, N.A., Levine, M.S., 1993. Neuromodulatory actions of dopamine in the neostriatum are dependent upon the excitatory amino acid receptor subtypes activated. Proc. Natl. Acad. Sci. 90, 9576–9580. https://doi.org/10.1073/pnas.90.20.9576

Cepeda, C., Levine, M.S., 2012. Dopamine-NMDA Receptor Interactions: Twenty Years Later. Dev. Neurosci. 34, 2–4. https://doi.org/10.1159/000338590

Cepeda, C., Radisavljevic, Z., Peacock, W., Levine, M.S., Buchwald, N.A., 1992. Differential modulation by dopamine of responses evoked by excitatory amino acids in human cortex. Synapse 11, 330–341. https://doi.org/10.1002/syn.890110408

Cerpa, W., Gambrill, A., Inestrosa, N.C., Barria, A., 2011. Regulation of NMDA-Receptor Synaptic Transmission by Wnt Signaling. J. Neurosci. 31, 9466–9471. https://doi.org/10.1523/JNEUROSCI.6311-10.2011

Cerpa, W., Godoy, J.A., Alfaro, I., Farías, G.G., Metcalfe, M.J., Fuentealba, R., Bonansco, C., Inestrosa, N.C., 2008. Wnt-7a Modulates the Synaptic Vesicle Cycle and Synaptic Transmission in Hippocampal Neurons *. J. Biol. Chem. 283, 5918–5927. https://doi.org/10.1074/jbc.M705943200

Chalifoux, J.R., Carter, A.G., 2010. GABAB Receptors Modulate NMDA Receptor Calcium Signals in Dendritic Spines. Neuron 66, 101–113. https://doi.org/10.1016/j.neuron.2010.03.012

Chazot, P.L., Stephenson, F.A., 1997. Molecular Dissection of Native Mammalian Forebrain NMDA Receptors Containing the NR1 C2 Exon: Direct Demonstration of NMDA Receptors Comprising NR1, NR2A, and NR2B Subunits Within the Same Complex. J. Neurochem. 69, 2138–2144. https://doi.org/10.1046/j.1471-4159.1997.69052138.x

Cheadle, L., Biederer, T., 2012. The novel synaptogenic protein Farp1 links postsynaptic cytoskeletal dynamics and transsynaptic organization. J. Cell Biol. 199, 985–1001. https://doi.org/10.1083/jcb.201205041

Chen, L., Bohanick, J.D., Nishihara, M., Seamans, J.K., Yang, C.R., 2007. Dopamine D1/5 Receptor-Mediated Long-Term Potentiation of Intrinsic Excitability in Rat Prefrontal Cortical Neurons: Ca2+-Dependent Intracellular Signaling. J. Neurophysiol. 97, 2448–2464. https://doi.org/10.1152/jn.00317.2006

Chen, N., Moshaver, A., Raymond, L.A., 1997. Differential Sensitivity of RecombinantN-Methyl-d-Aspartate Receptor Subtypes to Zinc Inhibition. Mol. Pharmacol. 51, 1015–1023. https://doi.org/10.1124/mol.51.6.1015

Chen, P.E., Geballe, M.T., Katz, E., Erreger, K., Livesey, M.R., O'Toole, K.K., Le, P., Lee, C.J., Snyder, J.P., Traynelis, S.F., Wyllie, D.J.A., 2008. Modulation of glycine potency in rat recombinant NMDA receptors containing chimeric NR2A/2D subunits expressed in Xenopus laevis oocytes. J. Physiol. 586, 227–245. https://doi.org/10.1113/jphysiol.2007.143172

Chen, X., Wu, X., Wu, H., Zhang, M., 2020. Phase separation at the synapse. Nat. Neurosci. 23, 301–310. https://doi.org/10.1038/s41593-019-0579-9

Chen, Y., Liu, S., Jacobi, A.A., Jeng, G., Ulrich, J.D., Stein, I.S., Patriarchi, T., Hell, J.W., 2024. Rapid sequential clustering of NMDARs, CaMKII, and AMPARs upon activation of NMDARs at developing synapses. Front. Synaptic Neurosci. 16, 1291262. https://doi.org/10.3389/fnsyn.2024.1291262

Cheng, D., Hoogenraad, C.C., Rush, J., Ramm, E., Schlager, M.A., Duong, D.M., Xu, P., Wijayawardana, S.R., Hanfelt, J., Nakagawa, T., Sheng, M., Peng, J., 2006. Relative and Absolute Quantification of Postsynaptic Density Proteome Isolated from Rat Forebrain and Cerebellum. Mol. Cell. Proteomics 5, 1158–1170. https://doi.org/10.1074/mcp.D500009-MCP200

Chergui, K., Svenningsson, P., Greengard, P., 2005. Physiological Role for Casein Kinase 1 in Glutamatergic Synaptic Transmission. J. Neurosci. 25, 6601–6609. https://doi.org/10.1523/JNEUROSCI.1082-05.2005

Chih, B., Engelman, H., Scheiffele, P., 2005. Control of Excitatory and Inhibitory Synapse Formation by Neuroligins 307.

Choi, B.J., Imlach, W.L., Jiao, W., Wolfram, V., Wu, Y., Grbic, M., Cela, C., Baines, R.A., Nitabach, M.N., McCabe, B.D., 2014. Miniature Neurotransmission Regulates Drosophila Synaptic Structural Maturation. Neuron 82, 618–634. https://doi.org/10.1016/j.neuron.2014.03.012

Choi, D.I., Kaang, B.-K., 2022. Interrogating structural plasticity among synaptic engrams. Curr. Opin. Neurobiol. 75, 102552. https://doi.org/10.1016/j.conb.2022.102552

Choi, J.-H., Sim, S.-E., Kim, J., Choi, D.I., Oh, J., Ye, S., Lee, J., Kim, T., Ko, H.-G., Lim, C.-S., Kaang, B.-K., 2018. Interregional synaptic maps among engram cells underlie memory formation. Science 360, 430–435. https://doi.org/10.1126/science.aas9204

Choquet, D., 2018. Linking Nanoscale Dynamics of AMPA Receptor Organization to Plasticity of Excitatory Synapses and Learning. J. Neurosci. 38, 9318–9329. https://doi.org/10.1523/JNEUROSCI.2119-18.2018

Choquet, D., Sainlos, M., Sibarita, J.-B., 2021. Advanced imaging and labelling methods to decipher brain cell organization and function. Nat. Rev. Neurosci. 22, 237–255. https://doi.org/10.1038/s41583-021-00441-z

Choquet, D., Triller, A., 2013. The Dynamic Synapse. Neuron 80, 691–703. https://doi.org/10.1016/j.neuron.2013.10.013

Chou, V.T., Johnson, S.A., Van Vactor, D., 2020. Synapse development and maturation at the drosophila neuromuscular junction. Neural Develop. 15, 1–17. https://doi.org/10.1186/s13064-020-00147-5

Christopherson, K.S., Ullian, E.M., Stokes, C.C.A., Mullowney, C.E., Hell, J.W., Agah, A., Lawler, J., Mosher, D.F., Bornstein, P., Barres, B.A., 2005. Thrombospondins Are Astrocyte-Secreted Proteins that Promote CNS Synaptogenesis. Cell 120, 421–433. https://doi.org/10.1016/j.cell.2004.12.020

Chubykin, A.A., Atasoy, D., Etherton, M.R., Brose, N., Kavalali, E.T., Gibson, J.R., Südhof, T.C., 2007. Activity-Dependent Validation of Excitatory versus Inhibitory Synapses by Neuroligin-1 versus Neuroligin-2. Neuron 54, 919–931. https://doi.org/10.1016/j.neuron.2007.05.029

Chung, W.-S., Baldwin, K.T., Allen, N.J., 2024. Astrocyte Regulation of Synapse Formation, Maturation, and Elimination. Cold Spring Harb. Perspect. Biol. 16, a041352. https://doi.org/10.1101/cshperspect.a041352

Ciani, L., Boyle, K.A., Dickins, E., Sahores, M., Anane, D., Lopes, D.M., Gibb, A.J., Salinas, P.C., 2011. Wnt7a signaling promotes dendritic spine growth and synaptic strength through Ca2+/Calmodulin-dependent protein kinase II. Proc. Natl. Acad. Sci. 108, 10732–10737. https://doi.org/10.1073/pnas.1018132108

Cizeron, M., Qiu, Z., Koniaris, B., Gokhale, R., Komiyama, N.H., Fransén, E., Grant, S.G.N., 2020. A brainwide atlas of synapses across the mouse life span. Science 369, 270–275. https://doi.org/10.1126/science.aba3163

Clark, B.A., Cull-Candy, S.G., 2002. Activity-Dependent Recruitment of Extrasynaptic NMDA Receptor Activation at an AMPA Receptor-Only Synapse. J. Neurosci. 22, 4428–4436. https://doi.org/10.1523/JNEUROSCI.22-11-04428.2002

Clark, B.A., Farrant, M., Cull-Candy, S.G., 1997. A Direct Comparison of the Single-Channel Properties of Synaptic and Extrasynaptic NMDA Receptors. J. Neurosci. 17, 107–116. https://doi.org/10.1523/JNEUROSCI.17-01-00107.1997

Csoka, A.B., Frost, G.I., Stern, R., 2001. The six hyaluronidase-like genes in the human and mouse genomes. Matrix Biol. 20, 499–508. https://doi.org/10.1016/S0945-053X(01)00172-X

Dabrowski, A., Terauchi, A., Strong, C., Umemori, H., 2015. Distinct sets of FGF receptors sculpt excitatory and inhibitory synaptogenesis. Development 142, 1818–1830. https://doi.org/10.1242/dev.115568

Dahan, M., Lévi, S., Luccardini, C., Rostaing, P., Riveau, B., Triller, A., 2003. Diffusion Dynamics of Glycine Receptors Revealed by Single-Quantum Dot Tracking. Science 302, 442–445. https://doi.org/10.1126/science.1088525

Dai, Z., Peng, H.B., 1996. Dynamics of Synaptic Vesicles in Cultured Spinal Cord Neurons in Relationship to Synaptogenesis. Mol. Cell. Neurosci. 7, 443–452. https://doi.org/10.1006/mcne.1996.0032

Dalva, M.B., Takasu, M.A., Lin, M.Z., Shamah, S.M., Hu, L., Gale, N.W., Greenberg, M.E., 2000. EphB Receptors Interact with NMDA Receptors and Regulate Excitatory Synapse Formation. Cell 103, 945–956. https://doi.org/10.1016/S0092-8674(00)00197-5

Dan, Y., Poo, M.-M., 2006. Spike Timing-Dependent Plasticity: From Synapse to Perception. Physiol. Rev. 86, 1033–1048. https://doi.org/10.1152/physrev.00030.2005

Dankovich, T.M., Kaushik, R., Olsthoorn, L.H.M., Petersen, G.C., Giro, P.E., Kluever, V., Agüi-Gonzalez, P., Grewe, K., Bao, G., Beuermann, S., Hadi, H.A., Doeren, J., Klöppner, S., Cooper, B.H., Dityatev, A., Rizzoli, S.O., 2021. Extracellular matrix remodeling through endocytosis and resurfacing of Tenascin-R. Nat. Commun. 12, 7129. https://doi.org/10.1038/s41467-021-27462-7

Das, S., Sasaki, Y.F., Rothe, T., Premkumar, L.S., Takasu, M., Crandall, J.E., Dikkes, P., Conner, D.A., Rayudu, P.V., Cheung, W., Chen, H.-S.V., Lipton, S.A., Nakanishi, N., 1998. Increased NMDA current and spine density in mice lacking the NMDA receptor subunit NR3A. Nature 393, 377–381. https://doi.org/10.1038/30748

Dauth, S., Grevesse, T., Pantazopoulos, H., Campbell, P.H., Maoz, B.M., Berretta, S., Parker, K.K., 2016. Extracellular matrix protein expression is brain region dependent. J. Comp. Neurol. 524, 1309–1336. https://doi.org/10.1002/cne.23965

De Robertis, E.D.P., Bennett, H.S., 1955. SOME FEATURES OF THE SUBMICROSCOPIC MORPHOLOGY OF SYNAPSES IN FROG AND EARTHWORM. J. Biophys. Biochem. Cytol. 1, 47–58. https://doi.org/10.1083/jcb.1.1.47

Deepa, S.S., 2006. Composition of Perineuronal Net Extracellular Matrix in Rat Brain 281.

Del Marmol, D., Holtze, S., Kichler, N., Sahm, A., Bihin, B., Bourguignon, V., Dogné, S., Szafranski, K., Hildebrandt, T.B., Flamion, B., 2021. Abundance and size of hyaluronan in naked mole-rat tissues and plasma. Sci. Rep. 11, 7951. https://doi.org/10.1038/s41598-021-86967-9

Dembitskaya, Y., Gavrilov, N., Kraev, I., Doronin, M., Tang, Y., Li, L., Semyanov, A., 2021. Attenuation of the extracellular matrix increases the number of synapses but suppresses synaptic plasticity through upregulation of SK channels. Cell Calcium 96, 102406. https://doi.org/10.1016/j.ceca.2021.102406

Derkach, V., Barria, A., Soderling, T.R., 1999. Ca2+/calmodulin-kinase II enhances channel conductance of α-amino-3-hydroxy-5-methyl-4-isoxazolepropionate type glutamate receptors. Proc. Natl. Acad. Sci. 96, 3269–3274. https://doi.org/10.1073/pnas.96.6.3269

Dityatev, A., Brückner, G., Dityateva, G., Grosche, J., Kleene, R., Schachner, M., 2007. Activity-dependent formation and functions of chondroitin sulfate-rich extracellular matrix of perineuronal nets. Dev. Neurobiol. 67, 570–588. https://doi.org/10.1002/dneu.20361

Dityatev, A., Dityateva, G., Sytnyk, V., Delling, M., Toni, N., Nikonenko, I., Muller, D., Schachner, M., 2004. Polysialylated Neural Cell Adhesion Molecule Promotes Remodeling and Formation of Hippocampal Synapses. J. Neurosci. 24, 9372–9382. https://doi.org/10.1523/JNEUROSCI.1702-04.2004

Dityatev, A., Rusakov, D.A., 2011. Molecular signals of plasticity at the tetrapartite synapse. Curr. Opin. Neurobiol. 21, 353–359. https://doi.org/10.1016/j.conb.2010.12.006

Dityatev, A., Schachner, M., 2003. Extracellular matrix molecules and synaptic plasticity. Nat. Rev. Neurosci. 4, 456–468. https://doi.org/10.1038/nrn1115

Dityatev, A., Schachner, M., Sonderegger, P., 2010. The dual role of the extracellular matrix in synaptic plasticity and homeostasis. Nat. Rev. Neurosci. 11, 735–746. https://doi.org/10.1038/nrn2898

Donelan, W., Dominguez-Gutierrez, P.R., Kusmartsev, S., 2022. Deregulated hyaluronan metabolism in the tumor microenvironment drives cancer inflammation and tumor-associated immune suppression. Front. Immunol. 13. https://doi.org/10.3389/fimmu.2022.971278

Dore, K., Aow, J., Malinow, R., 2016. The Emergence of NMDA Receptor Metabotropic Function: Insights from Imaging. Front. Synaptic Neurosci. 8. https://doi.org/10.3389/fnsyn.2016.00020

Dore, K., Aow, J., Malinow, R., 2015. Agonist binding to the NMDA receptor drives movement of its cytoplasmic domain without ion flow. Proc. Natl. Acad. Sci. 112, 14705–14710. https://doi.org/10.1073/pnas.1520023112

Dorsch, S., Klotz, K.-N., Engelhardt, S., Lohse, M.J., Bünemann, M., 2009. Analysis of receptor oligomerization by FRAP microscopy. Nat. Methods 6, 225–230. https://doi.org/10.1038/nmeth.1304

Druckmann, S., Feng, L., Lee, B., Yook, C., Zhao, T., Magee, J.C., Kim, J., 2014. Structured Synaptic Connectivity between Hippocampal Regions. Neuron 81, 629–640. https://doi.org/10.1016/j.neuron.2013.11.026

Dudek, S.M., Bear, M.F., 1992. Homosynaptic long-term depression in area CA1 of hippocampus and effects of N-methyl-D-aspartate receptor blockade. Proc. Natl. Acad. Sci. 89, 4363–4367. https://doi.org/10.1073/pnas.89.10.4363

Dudman, J.T., Eaton, M.E., Rajadhyaksha, A., Macías, W., Taher, M., Barczak, A., Kameyama, K., Huganir, R., Konradi, C., 2003. Dopamine D1 receptors mediate CREB phosphorylation via phosphorylation of the NMDA receptor at Ser897–NR1. J. Neurochem. 87, 922–934. https://doi.org/10.1046/j.1471-4159.2003.02067.x

Dumanis, S.B., Cha, H.-J., Song, J.M., Trotter, J.H., Spitzer, M., Lee, J.-Y., Weeber, E.J., Turner, R.S., Pak, D.T.S., Rebeck, G.W., Hoe, H.-S., 2011. ApoE Receptor 2 Regulates Synapse and Dendritic Spine Formation. PLoS ONE 6, e17203. https://doi.org/10.1371/journal.pone.0017203

Dunaevsky, A., Tashiro, A., Majewska, A., Mason, C., Yuste, R., 1999. Developmental regulation of spine motility in the mammalian central nervous system. Proc. Natl. Acad. Sci. 96, 13438–13443. https://doi.org/10.1073/pnas.96.23.13438

Dunah, A.W., Standaert, D.G., 2001. Dopamine D1 Receptor-Dependent Trafficking of Striatal NMDA Glutamate Receptors to the Postsynaptic Membrane. J. Neurosci. 21, 5546–5558. https://doi.org/10.1523/JNEUROSCI.21-15-05546.2001

Dupuis, J.P., Groc, L., 2020. Surface trafficking of neurotransmitter receptors: From cultured neurons to intact brain preparations. Neuropharmacology 169, 107642. https://doi.org/10.1016/j.neuropharm.2019.05.019

Dupuis, J.P., Ladepeche, L., Seth, H., Bard, L., Varela, J., Mikasova, L., Bouchet, D., Rogemond, V., Honnorat, J., Hanse, E., Groc, L., 2014a. Surface dynamics of GluN2B-NMDA receptors controls plasticity of maturing glutamate synapses. EMBO J. 33, 842–861. https://doi.org/10.1002/embj.201386356

Dupuis, J.P., Ladepeche, L., Seth, H., Bard, L., Varela, J., Mikasova, L., Bouchet, D., Rogemond, V., Honnorat, J., Hanse, E., Groc, L., 2014b. Surface dynamics of GluN2B-NMDA receptors controls plasticity of maturing glutamate synapses. EMBO J. 33, 842–861. https://doi.org/10.1002/embj.201386356

Dupuis, J.P., Nicole, O., Groc, L., 2023. NMDA receptor functions in health and disease: Old actor, new dimensions. Neuron 111, 2312–2328. https://doi.org/10.1016/j.neuron.2023.05.002

Durand, G.M., Gregor, P., Zheng, X., Bennett, M.V., Uhl, G.R., Zukin, R.S., 1992. Cloning of an apparent splice variant of the rat N-methyl-D-aspartate receptor NMDAR1 with altered sensitivity to polyamines and activators of protein kinase C. Proc. Natl. Acad. Sci. 89, 9359–9363. https://doi.org/10.1073/pnas.89.19.9359

Durand, G.M., Kovalchuk, Y., Konnerth, A., 1996. Long-term potentiation and functional synapse induction in developing hippocampus. Nature 381, 71–75. https://doi.org/10.1038/381071a0

Edrey, Y.H., Medina, D.X., Gaczynska, M., Osmulski, P.A., Oddo, S., Caccamo, A., Buffenstein, R., 2013. Amyloid beta and the longest-lived rodent: the naked mole-rat as a model for natural protection from Alzheimer's disease. Neurobiol. Aging 34, 2352–2360. https://doi.org/10.1016/j.neurobiolaging.2013.03.032

Ehlers, M.D., 2000. Reinsertion or Degradation of AMPA Receptors Determined by Activity-Dependent Endocytic Sorting. Neuron 28, 511–525. https://doi.org/10.1016/S0896-6273(00)00129-X

Elegheert, J., Cvetkovska, V., Clayton, A.J., Heroven, C., Vennekens, K.M., Smukowski, S.N., Regan, M.C., Jia, W., Smith, A.C., Furukawa, H., Savas, J.N., De Wit, J., Begbie, J., Craig, A.M., Aricescu, A.R., 2017. Structural Mechanism for Modulation of Synaptic Neuroligin-Neurexin Signaling by MDGA Proteins. Neuron 95, 896-913.e10. https://doi.org/10.1016/j.neuron.2017.07.040

El-Husseini, A.E.-D., Schnell, E., Chetkovich, D.M., Nicoll, R.A., Bredt, D.S., 2000. PSD-95 Involvement in Maturation of Excitatory Synapses. Science 290, 1364–1368. https://doi.org/10.1126/science.290.5495.1364

Elia, L.P., Yamamoto, M., Zang, K., Reichardt, L.F., 2006. p120 Catenin Regulates Dendritic Spine and Synapse Development through Rho-Family GTPases and Cadherins. Neuron 51, 43–56. https://doi.org/10.1016/j.neuron.2006.05.018

Elias, G.M., Elias, L.A.B., Apostolides, P.F., Kriegstein, A.R., Nicoll, R.A., 2008. Differential trafficking of AMPA and NMDA receptors by SAP102 and PSD-95 underlies synapse development. Proc. Natl. Acad. Sci. 105, 20953–20958. https://doi.org/10.1073/pnas.0811025106

Emperador-Melero, J., De Nola, G., Kaeser, P.S., 2021. Intact synapse structure and function after combined knockout of PTPδ, PTPσ, and LAR. eLife 10. https://doi.org/10.7554/elife.66638

Emperador-Melero, J., Kaeser, P.S., 2020. Assembly of the presynaptic active zone. Curr. Opin. Neurobiol. 63, 95–103. https://doi.org/10.1016/j.conb.2020.03.008

Engelman, D.M., 2005. Membranes are more mosaic than fluid. Nature 438, 578–580. https://doi.org/10.1038/nature04394

Engler, A.J., Sen, S., Sweeney, H.L., Discher, D.E., 2006. Matrix Elasticity Directs Stem Cell Lineage Specification. Cell 126, 677–689. https://doi.org/10.1016/j.cell.2006.06.044

Erami, Z., Herrmann, D., Warren, S.C., Nobis, M., McGhee, E.J., Lucas, M.C., Leung, W., Reischmann, N., Mrowinska, A., Schwarz, J.P., Kadir, S., Conway, J.R.W., Vennin, C., Karim, S.A., Campbell, A.D., Gallego-Ortega, D., Magenau, A., Murphy, K.J., Ridgway, R.A., Law, A.M., Walters, S.N., Grey, S.T., Croucher, D.R., Zhang, L., Herzog, H., Hardeman, E.C., Gunning, P.W., Ormandy, C.J., Evans, T.R.J., Strathdee, D., Sansom, O.J., Morton, J.P., Anderson, K.I., Timpson, P., 2016. Intravital FRAP Imaging using an E-cadherin-GFP Mouse Reveals Disease- and Drug-Dependent Dynamic Regulation of Cell-Cell Junctions in Live Tissue. Cell Rep. 14, 152–167. https://doi.org/10.1016/j.celrep.2015.12.020

Eroglu, Ç., Allen, N.J., Susman, M.W., O'Rourke, N.A., Park, C.Y., Özkan, E., Chakraborty, C., Mulinyawe, S.B., Annis, D.S., Huberman, A.D., Green, E.M., Lawler, J., Dolmetsch, R., Garcia, K.C., Smith, S.J., Luo, Z.D., Rosenthal, A., Mosher, D.F., Barres, B.A., 2009. Gabapentin Receptor α2δ-1 Is a Neuronal Thrombospondin Receptor Responsible for Excitatory CNS Synaptogenesis. Cell 139, 380–392. https://doi.org/10.1016/j.cell.2009.09.025

Erreger, K., Geballe, M.T., Kristensen, A., Chen, P.E., Hansen, K.B., Lee, C.J., Yuan, H., Le, P., Lyuboslavsky, P.N., Micale, N., Jørgensen, L., Clausen, R.P., Wyllie, D.J.A., Snyder, J.P., Traynelis, S.F., 2007. Subunit-Specific Agonist Activity at NR2A-, NR2B-, NR2C-, and NR2D-

Containing N-Methyl-d-aspartate Glutamate Receptors. Mol. Pharmacol. 72, 907–920. https://doi.org/10.1124/mol.107.037333

Espana, A., Seth, H., Jézéquel, J., Huang, T., Bouchet, D., Lepleux, M., Gréa, H., Bechter, K., Schneider, M., Hanse, E., Groc, L., 2021. Alteration of NMDA receptor trafficking as a cellular hallmark of psychosis. Transl. Psychiatry 11, 444. https://doi.org/10.1038/s41398-021-01549-7

Evanko, S., Tammi, M., Tammi, R., Wight, T., 2007. Hyaluronan-dependent pericellular matrix. Adv. Drug Deliv. Rev. 59, 1351–1365. https://doi.org/10.1016/j.addr.2007.08.008

Fallacara, A., Baldini, E., Manfredini, S., Vertuani, S., 2018. Hyaluronic Acid in the Third Millennium. Polymers 10, 701. https://doi.org/10.3390/polym10070701

Fang, H., Bygrave, A.M., Roth, R.H., Johnson, R.C., Huganir, R.L., 2021. An optimized CRISPR/Cas9 approach for precise genome editing in neurons. eLife 10, e65202. https://doi.org/10.7554/eLife.65202

Farhy-Tselnicker, I., Boisvert, M.M., Liu, H., Dowling, C., Erikson, G.A., Blanco-Suarez, E., Farhy, C., Shokhirev, M.N., Ecker, J.R., Allen, N.J., 2021. Activity-dependent modulation of synapse-regulating genes in astrocytes. eLife 10, e70514. https://doi.org/10.7554/eLife.70514

Farhy-Tselnicker, I., Casteren, A.C.M. van, Lee, A., Chang, V.T., Aricescu, A.R., Allen, N.J., 2017. Astrocyte-Secreted Glypican 4 Regulates Release of Neuronal Pentraxin 1 from Axons to Induce Functional Synapse Formation. Neuron 96, 428-445.e13. https://doi.org/10.1016/j.neuron.2017.09.053

Farías, G.G., Alfaro, I.E., Cerpa, W., Grabowski, C.P., Godoy, J.A., Bonansco, C., Inestrosa, N.C., 2009. Wnt-5a/JNK Signaling Promotes the Clustering of PSD-95 in Hippocampal Neurons *. J. Biol. Chem. 284, 15857–15866. https://doi.org/10.1074/jbc.M808986200

Faulkes, C.G., Davies, K.T.J., Rossiter, S.J., Bennett, N.C., 2015. Molecular evolution of the hyaluronan synthase 2 gene in mammals: implications for adaptations to the subterranean niche and cancer resistance. Biol. Lett. 11, 20150185. https://doi.org/10.1098/rsbl.2015.0185

Feinberg, E.H., VanHoven, M.K., Bendesky, A., Wang, G., Fetter, R.D., Shen, K., Bargmann, C.I., 2008. GFP Reconstitution Across Synaptic Partners (GRASP) Defines Cell Contacts and Synapses in Living Nervous Systems. Neuron 57, 353–363. https://doi.org/10.1016/j.neuron.2007.11.030

Fejtova, A., Davydova, D., Bischof, F., Lazarevic, V., Altrock, W.D., Romorini, S., Schöne, C., Zuschratter, W., Kreutz, M.R., Garner, C.C., Ziv, N.E., Gundelfinger, E.D., 2009. Dynein light chain regulates axonal trafficking and synaptic levels of Bassoon. J. Cell Biol. 185, 341–355. https://doi.org/10.1083/jcb.200807155

Ferhat, L., Au Louis, N.C., Jorquera, I., Niquet, J., Khrestchatisky, M., Ben-Ari, Y., Represa, A., 1996. Transient increase of tenascin-C in immature hippocampus: astroglial and neuronal expression. J. Neurocytol. 25, 53–66. https://doi.org/10.1007/BF02284785

Ferraguti, F., Shigemoto, R., 2006. Metabotropic glutamate receptors. Cell Tissue Res. 326, 483–504. https://doi.org/10.1007/s00441-006-0266-5

Ferreira, J.S., Dupuis, J.P., Kellermayer, B., Bénac, N., Manso, C., Bouchet, D., Levet, F., Butler, C., Sibarita, J.-B., Groc, L., 2020. Distance-dependent regulation of NMDAR nanoscale organization along hippocampal neuron dendrites. Proc. Natl. Acad. Sci. 117, 24526–24533. https://doi.org/10.1073/pnas.1922477117

Ferreira, J.S., Kellermayer, B., Carvalho, A.L., Groc, L., 2021. Interplay between NMDA receptor dynamics and the synaptic proteasome. Eur. J. Neurosci. 54, 6000–6011. https://doi.org/10.1111/ejn.15427

Ferreira, J.S., Papouin, T., Ladépêche, L., Yao, A., Langlais, V.C., Bouchet, D., Dulong, J., Mothet, J.-P., Sacchi, S., Pollegioni, L., Paoletti, P., Oliet, S.H.R., Groc, L., 2017. Co-agonists differentially tune GluN2B-NMDA receptor trafficking at hippocampal synapses. eLife 6, e25492. https://doi.org/10.7554/eLife.25492

Ferrer-Ferrer, M., Dityatev, A., 2018. Shaping Synapses by the Neural Extracellular Matrix. Front. Neuroanat. 12, 40. https://doi.org/10.3389/fnana.2018.00040

Fiala, J.C., Feinberg, M., Popov, V., Harris, K.M., 1998. Synaptogenesis Via Dendritic Filopodia in Developing Hippocampal Area CA1. J. Neurosci. 18, 8900–8911. https://doi.org/10.1523/JNEUROSCI.18-21-08900.1998

Fietz, S.A., Lachmann, R., Brandl, H., Kircher, M., Samusik, N., Schröder, R., Lakshmanaperumal, N., Henry, I., Vogt, J., Riehn, A., Distler, W., Nitsch, R., Enard, W., Pääbo, S., Huttner, W.B., 2012. Transcriptomes of germinal zones of human and mouse fetal neocortex suggest a role of extracellular matrix in progenitor self-renewal. Proc. Natl. Acad. Sci. 109, 11836–11841. https://doi.org/10.1073/pnas.1209647109

Fiorentini, C., Gardoni, F., Spano, P., Di Luca, M., Missale, C., 2003. Regulation of Dopamine D1 Receptor Trafficking and Desensitization by Oligomerization with Glutamate N-Methyl-D-aspartate Receptors. J. Biol. Chem. 278, 20196–20202. https://doi.org/10.1074/jbc.M213140200

Flanagan, L.A., Ju, Y.-E., Marg, B., Osterfield, M., Janmey, P.A., 2002. Neurite branching on deformable substrates. NeuroReport 13, 2411.

Flavell, S.W., Cowan, C.W., Kim, T.-K., Greer, P.L., Lin, Y., Paradis, S., Griffith, E.C., Hu, L.S., Chen, C., Greenberg, M.E., 2006. Activity-Dependent Regulation of MEF2 Transcription Factors Suppresses Excitatory Synapse Number. Science 311, 1008–1012. https://doi.org/10.1126/science.1122511

Forero, A., Pipicelli, F., Moser, S., Baumann, N., Grätz, C., Pisfil, M.G., Pfaffl, M.W., Pütz, B., Kielkowski, P., Cernilogar, F.M., Maccarrone, G., Giaimo, R.D., Cappello, S., 2024. Extracellular vesicle-mediated trafficking of molecular cues during human brain development. Cell Rep. 43. https://doi.org/10.1016/j.celrep.2024.114755

Fossati, G., Pozzi, D., Canzi, A., Mirabella, F., Valentino, S., Morini, R., Ghirardini, E., Filipello, F., Moretti, M., Gotti, C., Annis, D.S., Mosher, D.F., Garlanda, C., Bottazzi, B., Taraboletti, G., Mantovani, A., Matteoli, M., Menna, E., 2019. Pentraxin 3 regulates synaptic function by inducing AMPA receptor clustering via ECM remodeling and β1-integrin. EMBO J. 38, e99529. https://doi.org/10.15252/embj.201899529

Fowke, T.M., Karunasinghe, R.N., Bai, J.-Z., Jordan, S., Gunn, A.J., Dean, J.M., 2017. Hyaluronan synthesis by developing cortical neurons in vitro. Sci. Rep. 7, 44135. https://doi.org/10.1038/srep44135

Fowler, D.K., Peters, J.H., Williams, C., Washbourne, P., 2017. Redundant Postsynaptic Functions of SynCAMs 1–3 during Synapse Formation. Front. Mol. Neurosci. 10. https://doi.org/10.3389/fnmol.2017.00024

Frederick, A.L., Yano, H., Trifilieff, P., Vishwasrao, H.D., Biezonski, D., Mészáros, J., Urizar, E., Sibley, D.R., Kellendonk, C., Sonntag, K.C., Graham, D.L., Colbran, R.J., Stanwood, G.D., Javitch, J.A., 2015. Evidence against dopamine D1/D2 receptor heteromers. Mol. Psychiatry 20, 1373–1385. https://doi.org/10.1038/mp.2014.166

Frischknecht, R., Heine, M., Perrais, D., Seidenbecher, C.I., Choquet, D., Gundelfinger, E.D., 2009. Brain extracellular matrix affects AMPA receptor lateral mobility and short-term synaptic plasticity. Nat. Neurosci. 12, 897–904. https://doi.org/10.1038/nn.2338

Froemke, R.C., Dan, Y., 2002. Spike-timing-dependent synaptic modification induced by natural spike trains. Nature 416, 433–438. https://doi.org/10.1038/416433a

Fukata, Y., Adesnik, H., Iwanaga, T., Bredt, D.S., Nicoll, R.A., Fukata, M., 2006. Epilepsy-Related Ligand/Receptor Complex LGI1 and ADAM22 Regulate Synaptic Transmission. Science 313, 1792–1795. https://doi.org/10.1126/science.1129947

Gambrill, A.C., Barria, A., 2011. NMDA receptor subunit composition controls synaptogenesis and synapse stabilization. Proc. Natl. Acad. Sci. 108, 5855–5860. https://doi.org/10.1073/pnas.1012676108

Gan, K.J., Südhof, T.C., 2020. SPARCL1 Promotes Excitatory But Not Inhibitory Synapse Formation and Function Independent of Neurexins and Neuroligins. J. Neurosci. 40, 8088–8102. https://doi.org/10.1523/JNEUROSCI.0454-20.2020

Gan, K.J., Südhof, T.C., 2019. Specific factors in blood from young but not old mice directly promote synapse formation and NMDA-receptor recruitment. Proc. Natl. Acad. Sci. 116, 12524–12533. https://doi.org/10.1073/pnas.1902672116

Gangarossa, G., Longueville, S., De Bundel, D., Perroy, J., Hervé, D., Girault, J.-A., Valjent, E., 2012. Characterization of dopamine D1 and D2 receptor-expressing neurons in the mouse hippocampus. Hippocampus 22, 2199–2207. https://doi.org/10.1002/hipo.22044

García-López, P., García-Marín, V., Freire, M., 2010. Dendritic Spines and Development: Towards a Unifying Model of Spinogenesis—A Present Day Review of Cajal's Histological Slides and Drawings. Neural Plast. 2010, 769207. https://doi.org/10.1155/2010/769207

Gardoni, F., Boraso, M., Zianni, E., Corsini, E., Galli, C.L., Cattabeni, F., Marinovich, M., Di Luca, M., Viviani, B., 2011. Distribution of interleukin-1 receptor complex at the synaptic membrane driven by interleukin-1β and NMDA stimulation. J. Neuroinflammation 8, 14. https://doi.org/10.1186/1742-2094-8-14

Gardoni, F., Di Luca, M., 2021. Protein-protein interactions at the NMDA receptor complex: From synaptic retention to synaptonuclear protein messengers. Neuropharmacology 190, 108551. https://doi.org/10.1016/j.neuropharm.2021.108551

Gautier, A., Juillerat, A., Heinis, C., Corrêa, I.R., Kindermann, M., Beaufils, F., Johnsson, K., 2008. An Engineered Protein Tag for Multiprotein Labeling in Living Cells. Chem. Biol. 15, 128–136. https://doi.org/10.1016/j.chembiol.2008.01.007

Georges, P.C., Miller, W.J., Meaney, D.F., Sawyer, E.S., Janmey, P.A., 2006. Matrices with Compliance Comparable to that of Brain Tissue Select Neuronal over Glial Growth in Mixed Cortical Cultures. Biophys. J. 90, 3012–3018. https://doi.org/10.1529/biophysj.105.073114

Gerrow, K., Romorini, S., Nabi, S.M., Colicos, M.A., Sala, C., El-Husseini, A., 2006. A Preformed Complex of Postsynaptic Proteins Is Involved in Excitatory Synapse Development. Neuron 49, 547–562. https://doi.org/10.1016/j.neuron.2006.01.015

Ghosh, I., Hamilton, A.D., Regan, L., 2000. Antiparallel Leucine Zipper-Directed Protein Reassembly: Application to the Green Fluorescent Protein. J. Am. Chem. Soc. 122, 5658–5659. https://doi.org/10.1021/ja994421w

Gielen, M., Retchless, B.S., Mony, L., Johnson, J.W., Paoletti, P., 2009. Mechanism of differential control of NMDA receptor activity by NR2 subunits. Nature 459, 703–707. https://doi.org/10.1038/nature07993

Godin, A.G., Varela, J.A., Gao, Z., Danné, N., Dupuis, J.P., Lounis, B., Groc, L., Cognet, L., 2017. Single-nanotube tracking reveals the nanoscale organization of the extracellular space in the live brain. Nat. Nanotechnol. 12, 238–243. https://doi.org/10.1038/nnano.2016.248

Gogolla, N., Caroni, P., Lüthi, A., Herry, C., 2009. Perineuronal Nets Protect Fear Memories from Erasure. Science 325, 1258–1261. https://doi.org/10.1126/science.1174146

Goldman-Rakic, P.S., Leranth, C., Williams, S.M., Mons, N., Geffard, M., 1989. Dopamine synaptic complex with pyramidal neurons in primate cerebral cortex. Proc. Natl. Acad. Sci. 86, 9015–9019. https://doi.org/10.1073/pnas.86.22.9015

González-González, I.M., Gray, J.A., Ferreira, J., Conde-Dusman, M.J., Bouchet, D., Perez-Otaño, I., Groc, L., 2023. GluN3A subunit tunes NMDA receptor synaptic trafficking and content during postnatal brain development. Cell Rep. 42, 112477. https://doi.org/10.1016/j.celrep.2023.112477

Good, M.C., Zalatan, J.G., Lim, W.A., 2011. Scaffold Proteins: Hubs for Controlling the Flow of Cellular Information. Science 332, 680–686. https://doi.org/10.1126/science.1198701

Grand, T., Abi Gerges, S., David, M., Diana, M.A., Paoletti, P., 2018. Unmasking GluN1/GluN3A excitatory glycine NMDA receptors. Nat. Commun. 9, 4769. https://doi.org/10.1038/s41467-018-07236-4

Grassi, D., Idziak, A., Lee, A., Calaresu, I., Sibarita, J.-B., Cognet, L., Nägerl, U.V., Groc, L., 2023. Nanoscale and functional heterogeneity of the hippocampal extracellular space. Cell Rep. 42, 112478. https://doi.org/10.1016/j.celrep.2023.112478

Gray, J.A., Shi, Y., Usui, H., During, M.J., Sakimura, K., Nicoll, R.A., 2011. Distinct Modes of AMPA Receptor Suppression at Developing Synapses by GluN2A and GluN2B: Single-Cell NMDA Receptor Subunit Deletion In Vivo. Neuron 71, 1085–1101. https://doi.org/10.1016/j.neuron.2011.08.007

Greenwald, E.C., Mehta, S., Zhang, J., 2018. Genetically Encoded Fluorescent Biosensors Illuminate the Spatiotemporal Regulation of Signaling Networks. Chem. Rev. 118, 11707–11794. https://doi.org/10.1021/acs.chemrev.8b00333

Groc, L., Choquet, D., 2020. Linking glutamate receptor movements and synapse function. Science 368, eaay4631. https://doi.org/10.1126/science.aay4631

Groc, L., Choquet, D., Chaouloff, F., 2008. The stress hormone corticosterone conditions AMPAR surface trafficking and synaptic potentiation. Nat. Neurosci. 11, 868–870. https://doi.org/10.1038/nn.2150

Groc, L., Choquet, D., Stephenson, F.A., Verrier, D., Manzoni, O.J., Chavis, P., 2007a. NMDA Receptor Surface Trafficking and Synaptic Subunit Composition Are Developmentally Regulated by the Extracellular Matrix Protein Reelin. J. Neurosci. 27, 10165–10175. https://doi.org/10.1523/JNEUROSCI.1772-07.2007

Groc, L., Gustafsson, B., Hanse, E., 2006a. AMPA signalling in nascent glutamatergic synapses: there and not there! Trends Neurosci. 29, 132–139. https://doi.org/10.1016/j.tins.2006.01.005

Groc, L., Heine, M., Cognet, L., Brickley, K., Stephenson, F.A., Lounis, B., Choquet, D., 2004. Differential activity-dependent regulation of the lateral mobilities of AMPA and NMDA receptors. Nat. Neurosci. 7, 695–696. https://doi.org/10.1038/nn1270

Groc, L., Heine, M., Cousins, S.L., Stephenson, F.A., Lounis, B., Cognet, L., Choquet, D., 2006b. NMDA receptor surface mobility depends on NR2A-2B subunits. Proc. Natl. Acad. Sci. 103, 18769–18774. https://doi.org/10.1073/pnas.0605238103

Groc, L., Lafourcade, M., Heine, M., Renner, M., Racine, V., Sibarita, J.-B., Lounis, B., Choquet, D., Cognet, L., 2007b. Surface Trafficking of Neurotransmitter Receptor: Comparison between Single-Molecule/Quantum Dot Strategies. J. Neurosci. 27, 12433–12437. https://doi.org/10.1523/JNEUROSCI.3349-07.2007

Grosshans, D.R., Clayton, D.A., Coultrap, S.J., Browning, M.D., 2002. LTP leads to rapid surface expression of NMDA but not AMPA receptors in adult rat CA1. Nat. Neurosci. 5, 27–33. https://doi.org/10.1038/nn779

Gu, Y., Huganir, R.L., 2016. Identification of the SNARE complex mediating the exocytosis of NMDA receptors. Proc. Natl. Acad. Sci. 113, 12280–12285. https://doi.org/10.1073/pnas.1614042113

Haas, K.T., Compans, B., Letellier, M., Bartol, T.M., Grillo-Bosch, D., Sejnowski, T.J., Sainlos, M., Choquet, D., Thoumine, O., Hosy, E., 2018. Pre-post synaptic alignment through neuroligin-1 tunes synaptic transmission efficiency. eLife 7, e31755. https://doi.org/10.7554/eLife.31755

Hafner, A.-S., Donlin-Asp, P.G., Leitch, B., Herzog, E., Schuman, E.M., 2019. Local protein synthesis is a ubiquitous feature of neuronal pre- and postsynaptic compartments.

Hallett, P.J., Spoelgen, R., Hyman, B.T., Standaert, D.G., Dunah, A.W., 2006. Dopamine D1 Activation Potentiates Striatal NMDA Receptors by Tyrosine Phosphorylation-Dependent Subunit Trafficking. J. Neurosci. 26, 4690–4700. https://doi.org/10.1523/JNEUROSCI.0792-06.2006

Halt, A.R., Dallapiazza, R.F., Zhou, Y., Stein, I.S., Qian, H., Juntti, S., Wojcik, S., Brose, N., Silva, A.J., Hell, J.W., 2012. CaMKII binding to GluN2B is critical during memory consolidation. EMBO J. 31, 1203–1216. https://doi.org/10.1038/emboj.2011.482

Hama, H., Hara, C., Yamaguchi, K., Miyawaki, A., 2004. PKC Signaling Mediates Global Enhancement of Excitatory Synaptogenesis in Neurons Triggered by Local Contact with Astrocytes. Neuron 41, 405–415. https://doi.org/10.1016/S0896-6273(04)00007-8

Hanse, E., Seth, H., Riebe, I., 2013. AMPA-silent synapses in brain development and pathology. Nat. Rev. Neurosci. 14, 839–850. https://doi.org/10.1038/nrn3642

Hansen, K.B., Yi, F., Perszyk, R.E., Furukawa, H., Wollmuth, L.P., Gibb, A.J., Traynelis, S.F., 2018. Structure, function, and allosteric modulation of NMDA receptors. J. Gen. Physiol. 150, 1081–1105. https://doi.org/10.1085/jgp.201812032

Hanus, C., Geptin, H., Tushev, G., Garg, S., Alvarez-Castelao, B., Sambandan, S., Kochen, L., Hafner, A.-S., Langer, J.D., Schuman, E.M., 2016. Unconventional secretory processing diversifies neuronal ion channel properties. eLife 5, e20609. https://doi.org/10.7554/eLife.20609

Hardingham, G.E., Bading, H., 2010. Synaptic versus extrasynaptic NMDA receptor signalling: implications for neurodegenerative disorders. Nat. Rev. Neurosci. 11, 682–696. https://doi.org/10.1038/nrn2911

Harms, K.J., Craig, A.M., 2005. Synapse composition and organization following chronic activity blockade in cultured hippocampal neurons. J. Comp. Neurol. 490, 72–84. https://doi.org/10.1002/cne.20635

Harney, S.C., Rowan, M., Anwyl, R., 2006. Long-Term Depression of NMDA Receptor-Mediated Synaptic Transmission Is Dependent on Activation of Metabotropic Glutamate Receptors and Is Altered to Long-Term Potentiation by Low Intracellular Calcium Buffering. J. Neurosci. 26, 1128–1132. https://doi.org/10.1523/JNEUROSCI.2753-05.2006

Harris, A.Z., Pettit, D.L., 2007. Extrasynaptic and synaptic NMDA receptors form stable and uniform pools in rat hippocampal slices. J. Physiol. 584, 509–519. https://doi.org/10.1113/jphysiol.2007.137679

Hayashi, M.K., Nishioka, T., Shimizu, H., Takahashi, K., Kakegawa, W., Mikami, T., Hirayama, Y., Koizumi, S., Yoshida, S., Yuzaki, M., Tammi, M., Sekino, Y., Kaibuchi, K., Shigemoto-Mogami, Y., Yasui, M., Sato, K., 2019. Hyaluronan synthesis supports glutamate transporter activity. J. Neurochem. 150, 249–263. https://doi.org/10.1111/jnc.14791

Hayashi, M.K., Tang, C., Verpelli, C., Narayanan, R., Stearns, M.H., Xu, R.-M., Li, H., Sala, C., Hayashi, Y., 2009. The Postsynaptic Density Proteins Homer and Shank Form a Polymeric Network Structure. Cell 137, 159–171. https://doi.org/10.1016/j.cell.2009.01.050

Heatley, F., Scott, J.E., 1988. A water molecule participates in the secondary structure of hyaluronan. Biochem. J. 254, 489–493. https://doi.org/10.1042/bj2540489

Heine, M., Groc, L., Frischknecht, R., Béïque, J.-C., Lounis, B., Rumbaugh, G., Huganir, R.L., Cognet, L., Choquet, D., 2008. Surface Mobility of Postsynaptic AMPARs Tunes Synaptic Transmission. Science 320, 201–205. https://doi.org/10.1126/science.1152089

Henderson, J.T., Georgiou, J., Jia, Z., Robertson, J., Elowe, S., Roder, J.C., Pawson, T., 2001. The Receptor Tyrosine Kinase EphB2 Regulates NMDA-Dependent Synaptic Function. Neuron 32, 1041–1056. https://doi.org/10.1016/S0896-6273(01)00553-0

Henkemeyer, M., Itkis, O.S., Ngo, M., Hickmott, P.W., Ethell, I.M., 2003. Multiple EphB receptor tyrosine kinases shape dendritic spines in the hippocampus. J. Cell Biol. 163, 1313–1326. https://doi.org/10.1083/jcb.200306033

Henson, M.A., Larsen, R.S., Lawson, S.N., Pérez-Otaño, I., Nakanishi, N., Lipton, S.A., Philpot, B.D., 2012. Genetic Deletion of NR3A Accelerates Glutamatergic Synapse Maturation. PLoS ONE 7, e42327. https://doi.org/10.1371/journal.pone.0042327

Herber, J., Njavro, J., Feederle, R., Schepers, U., Müller, U.C., Bräse, S., Müller, S.A., Lichtenthaler, S.F., 2018. Click Chemistry-mediated Biotinylation Reveals a Function for the Protease BACE1 in Modulating the Neuronal Surface Glycoproteome. Mol. Cell. Proteomics 17, 1487–1501. https://doi.org/10.1074/mcp.RA118.000608

Hering, H., Sheng, M., 2001. DENDRITIC SPINES: STRUCTURE, DYNAMICS AND REGULATION.

Hern, J.A., Baig, A.H., Mashanov, G.I., Birdsall, B., Corrie, J.E.T., Lazareno, S., Molloy, J.E., Birdsall, N.J.M., 2010. Formation and dissociation of M_1 muscarinic receptor dimers seen by total internal reflection fluorescence imaging of single molecules. Proc. Natl. Acad. Sci. 107, 2693–2698. https://doi.org/10.1073/pnas.0907915107

Hess, S.T., Girirajan, T.P.K., Mason, M.D., 2006. Ultra-High Resolution Imaging by Fluorescence Photoactivation Localization Microscopy. Biophys. J. 91, 4258–4272. https://doi.org/10.1529/biophysj.106.091116

Higley, M.J., Sabatini, B.L., 2010. Competitive regulation of synaptic Ca2+ influx by D2 dopamine and A2A adenosine receptors. Nat. Neurosci. 13, 958–966. https://doi.org/10.1038/nn.2592

Hoe, H.-S., Pocivavsek, A., Chakraborty, G., Fu, Z., Vicini, S., Ehlers, M.D., Rebeck, G.W., 2006. Apolipoprotein E Receptor 2 Interactions with the N-Methyl-D-aspartate Receptor *. J. Biol. Chem. 281, 3425–3431. https://doi.org/10.1074/jbc.M509380200

Holler, S., Köstinger, G., Martin, K.A.C., Schuhknecht, G.F.P., Stratford, K.J., 2021. Structure and function of a neocortical synapse. Nature 591, 111–116. https://doi.org/10.1038/s41586-020-03134-2

Hollmann, M., Boulter, J., Maron, C., Beasley, L., Sullivan, J., Pecht, G., Heinemann, S., 1993. Zinc potentiates agonist-lnduced currents at certain splice variants of the NMDA receptor. Neuron 10, 943–954. https://doi.org/10.1016/0896-6273(93)90209-A

Holtmaat, A., Svoboda, K., 2009. Experience-dependent structural synaptic plasticity in the mammalian brain. Nat. Rev. Neurosci. 10, 647–658. https://doi.org/10.1038/nrn2699

Horak, M., Petralia, R.S., Kaniakova, M., Sans, N., 2014. ER to synapse trafficking of NMDA receptors. Front. Cell. Neurosci. 8. https://doi.org/10.3389/fncel.2014.00394

Horak, M., Wenthold, R.J., 2009. Different Roles of C-terminal Cassettes in the Trafficking of Full-length NR1 Subunits to the Cell Surface. J. Biol. Chem. 284, 9683–9691. https://doi.org/10.1074/jbc.M807050200

Horn, K.E., Xu, B., Gobert, D., Hamam, B.N., Thompson, K.M., Wu, C., Bouchard, J., Uetani, N., Racine, R.J., Tremblay, M.L., Ruthazer, E.S., Chapman, C.A., Kennedy, T.E., 2012. Receptor protein tyrosine phosphatase sigma regulates synapse structure, function and plasticity. J. Neurochem. 122, 147–161. https://doi.org/10.1111/j.1471-4159.2012.07762.x

Hosokawa, T., Liu, P.-W., Cai, Q., Ferreira, J.S., Levet, F., Butler, C., Sibarita, J.-B., Choquet, D., Groc, L., Hosy, E., Zhang, M., Hayashi, Y., 2021. CaMKII activation persistently segregates postsynaptic proteins via liquid phase separation. Nat. Neurosci. 24, 777–785. https://doi.org/10.1038/s41593-021-00843-3

Hotulainen, P., Hoogenraad, C.C., 2010. Actin in dendritic spines: connecting dynamics to function. J. Cell Biol. 189, 619–629. https://doi.org/10.1083/jcb.201003008

Hou, L., Klann, E., 2004. Activation of the Phosphoinositide 3-Kinase-Akt-Mammalian Target of Rapamycin Signaling Pathway Is Required for Metabotropic Glutamate Receptor-Dependent Long-Term Depression. J. Neurosci. 24, 6352–6361. https://doi.org/10.1523/JNEUROSCI.0995-04.2004

Howell, M.D., Gottschall, P.E., 2012. Lectican proteoglycans, their cleaving metalloproteinases, and plasticity in the central nervous system extracellular microenvironment. Neuroscience 217, 6–18. https://doi.org/10.1016/j.neuroscience.2012.05.034

Hruska, M., Dalva, M.B., 2012. Ephrin regulation of synapse formation, function and plasticity. Mol. Cell. Neurosci. 50, 35–44. https://doi.org/10.1016/j.mcn.2012.03.004

Hu, J.-L., Liu, G., Li, Y.-C., Gao, W.-J., Huang, Y.-Q., 2010. Dopamine D1 receptor-mediated NMDA receptor insertion depends on Fyn but not Src kinase pathway in prefrontal cortical neurons. Mol. Brain 3, 20. https://doi.org/10.1186/1756-6606-3-20

Huang, K., Park, S., 2021. Heparan Sulfated Glypican-4 Is Released from Astrocytes by Proteolytic Shedding and GPI-Anchor Cleavage Mechanisms. eNeuro 8. https://doi.org/10.1523/ENEURO.0069-21.2021

Huganir, R.L., Nicoll, R.A., 2013. AMPARs and Synaptic Plasticity: The Last 25 Years. Neuron 80, 704–717. https://doi.org/10.1016/j.neuron.2013.10.025

Hunt, D.L., Puente, N., Grandes, P., Castillo, P.E., 2013. Bidirectional NMDA receptor plasticity controls CA3 output and heterosynaptic metaplasticity. Nat. Neurosci. 16, 1049–1059. https://doi.org/10.1038/nn.3461

Hunter, D., Petit-Pedrol, M., Fernandes, D., Bénac, N., Rodrigues, C., Kreye, J., Ceanga, M., Prüss, H., Geis, C., Groc, L., 2024. Converging synaptic and network dysfunctions in distinct autoimmune encephalitis. EMBO Rep. 25, 1623–1649. https://doi.org/10.1038/s44319-024-00056-2

Iacobucci, G.J., Popescu, G.K., 2019. Spatial Coupling Tunes NMDA Receptor Responses via Ca^{2+} Diffusion. J. Neurosci. 39, 8831–8844. https://doi.org/10.1523/JNEUROSCI.0901-19.2019

Incontro, S., Díaz-Alonso, J., Iafrati, J., Vieira, M., Asensio, C.S., Sohal, V.S., Roche, K.W., Bender, K.J., Nicoll, R.A., 2018. The CaMKII/NMDA receptor complex controls hippocampal synaptic transmission by kinase-dependent and independent mechanisms. Nat. Commun. 9, 2069. https://doi.org/10.1038/s41467-018-04439-7

Isaac, J.T.R., Nicoll, R.A., Malenka, R.C., 1995. Evidence for silent synapses: Implications for the expression of LTP. Neuron 15, 427–434. https://doi.org/10.1016/0896-6273(95)90046-2

Ito-Ishida, A., Miura, E., Emi, K., Matsuda, K., Iijima, T., Kondo, T., Kohda, K., Watanabe, M., Yuzaki, M., 2008. Cbln1 Regulates Rapid Formation and Maintenance of Excitatory Synapses in Mature Cerebellar Purkinje Cells In Vitro and In Vivo. J. Neurosci. 28, 5920–5930. https://doi.org/10.1523/JNEUROSCI.1030-08.2008

Iwata, R., Casimir, P., Erkol, E., Boubakar, L., Planque, M., Gallego López, I.M., Ditkowska, M., Gaspariunaite, V., Beckers, S., Remans, D., Vints, K., Vandekeere, A., Poovathingal, S., Bird, M., Vlaeminck, I., Creemers, E., Wierda, K., Corthout, N., Vermeersch, P., Carpentier, S., Davie, K., Mazzone, M., Gounko, N.V., Aerts, S., Ghesquière, B., Fendt, S.-M., Vanderhaeghen, P., 2023. Mitochondria metabolism sets the species-specific tempo of neuronal development. Science 379, eabn4705. https://doi.org/10.1126/science.abn4705

Iwata, R., Casimir, P., Vanderhaeghen, P., 2020. Mitochondrial dynamics in postmitotic cells regulate neurogenesis. Science 369, 858–862. https://doi.org/10.1126/science.aba9760

Jacobson, K., Liu, P., Lagerholm, B.C., 2019. The Lateral Organization and Mobility of Plasma Membrane Components. Cell 177, 806–819. https://doi.org/10.1016/j.cell.2019.04.018

Jakovcevski, I., Miljkovic, D., Schachner, M., Andjus, P.R., 2013. Tenascins and inflammation in disorders of the nervous system. Amino Acids 44, 1115–1127. https://doi.org/10.1007/s00726-012-1446-0

Jamet, Z., Mergaux, C., Meras, M., Bouchet, D., Villega, F., Kreye, J., Prüss, H., Groc, L., 2024. NMDA receptor autoantibodies primarily impair the extrasynaptic compartment. Brain awae163. https://doi.org/10.1093/brain/awae163

Jenkins, H.G., Bachelard, H.S., 1988. Developmental and Age-Related Changes in Rat Brain Glycosaminoglycans. J. Neurochem. 51, 1634–1640. https://doi.org/10.1111/j.1471-4159.1988.tb01134.x

Jézéquel, J., Johansson, E.M., Dupuis, J.P., Rogemond, V., Gréa, H., Kellermayer, B., Hamdani, N., Le Guen, E., Rabu, C., Lepleux, M., Spatola, M., Mathias, E., Bouchet, D., Ramsey, A.J., Yolken, R.H., Tamouza, R., Dalmau, J., Honnorat, J., Leboyer, M., Groc, L., 2017. Dynamic disorganization of synaptic NMDA receptors triggered by autoantibodies from psychotic patients. Nat. Commun. 8, 1791. https://doi.org/10.1038/s41467-017-01700-3

Jiang, D., Liang, J., Fan, J., Yu, S., Chen, S., Luo, Y., Prestwich, G.D., Mascarenhas, M.M., Garg, H.G., Quinn, D.A., Homer, R.J., Goldstein, D.R., Bucala, R., Lee, P.J., Medzhitov, R., Noble, P.W., 2005. Regulation of lung injury and repair by Toll-like receptors and hyaluronan. Nat. Med. 11, 1173–1179. https://doi.org/10.1038/nm1315

Jobin, M.-L., Siddig, S., Koszegi, Z., Lanoiselée, Y., Khayenko, V., Sungkaworn, T., Werner, C., Seier, K., Misigaiski, C., Mantovani, G., Sauer, M., Maric, H.M., Calebiro, D., 2023. Filamin A organizes γ-aminobutyric acid type B receptors at the plasma membrane. Nat. Commun. 14, 34. https://doi.org/10.1038/s41467-022-35708-1

Joester, A., Faissner, A., 2001. The structure and function of tenascins in the nervous system. Matrix Biol. 20, 13–22. https://doi.org/10.1016/S0945-053X(00)00136-0

Johansson, E.M., Bouchet, D., Tamouza, R., Ellul, P., Morr, As., Avignone, E., Germi, R., Leboyer, M., Perron, H., Groc, L., 2020. Human endogenous retroviral protein triggers deficit in glutamate synapse maturation and behaviors associated with psychosis. Sci. Adv. 6, eabc0708. https://doi.org/10.1126/sciadv.abc0708

Jones, F.S., Jones, P.L., 2000. The tenascin family of ECM glycoproteins: Structure, function, and regulation during embryonic development and tissue remodeling. Dev. Dyn. 218, 235–259. https://doi.org/10.1002/(SICI)1097-0177(200006)218:2<235::AID-DVDY2>3.0.CO;2-G

Jones, G.A., Bradshaw, D.S., 2019. Resonance Energy Transfer: From Fundamental Theory to Recent Applications. Front. Phys. 7. https://doi.org/10.3389/fphy.2019.00100

Kaboord, B., Perr, M., 2008. Isolation of Proteins and Protein Complexes by Immunoprecipitation, in: Posch, A. (Ed.), 2D PAGE: Sample Preparation and Fractionation. Humana Press, Totowa, NJ, pp. 349–364. https://doi.org/10.1007/978-1-60327-064-9_27

Kaniakova, M., Krausova, B., Vyklicky, V., Korinek, M., Lichnerova, K., Vyklicky, L., Horak, M., 2012. Key Amino Acid Residues within the Third Membrane Domains of NR1 and NR2 Subunits Contribute to the Regulation of the Surface Delivery of N-methyl-d-aspartate Receptors *. J. Biol. Chem. 287, 26423–26434. https://doi.org/10.1074/jbc.M112.339085

Karakas, E., Furukawa, H., 2014. Crystal structure of a heterotetrameric NMDA receptor ion channel. Science 344, 992–997. https://doi.org/10.1126/science.1251915

Kasai, R.S., Suzuki, K.G.N., Prossnitz, E.R., Koyama-Honda, I., Nakada, C., Fujiwara, T.K., Kusumi, A., 2011. Full characterization of GPCR monomer–dimer dynamic equilibrium by single molecule imaging. J. Cell Biol. 192, 463–480. https://doi.org/10.1083/jcb.201009128

Kasthuri, N., Hayworth, K.J., Berger, D.R., Schalek, R.L., Conchello, J.A., Knowles-Barley, S., Lee, D., Vázquez-Reina, A., Kaynig, V., Jones, T.R., Roberts, M., Morgan, J.L., Tapia, J.C., Seung, H.S., Roncal, W.G., Vogelstein, J.T., Burns, R., Sussman, D.L., Priebe, C.E., Pfister, H., Lichtman, J.W., 2015. Saturated Reconstruction of a Volume of Neocortex. Cell 162, 648–661. https://doi.org/10.1016/j.cell.2015.06.054

Kavalali, E.T., 2015. The mechanisms and functions of spontaneous neurotransmitter release. Nat. Rev. Neurosci. 16, 5–16. https://doi.org/10.1038/nrn3875

Kayser, M.S., McClelland, A.C., Hughes, E.G., Dalva, M.B., 2006. Intracellular and Trans-Synaptic Regulation of Glutamatergic Synaptogenesis by EphB Receptors. J. Neurosci. 26, 12152–12164. https://doi.org/10.1523/JNEUROSCI.3072-06.2006

Kegel, L., Aunin, E., Meijer, D., Bermingham, J.R., 2013. LGI Proteins in the Nervous System. ASN Neuro 5, AN20120095. https://doi.org/10.1042/AN20120095

Kehoe, L.A., Bellone, C., De Roo, M., Zandueta, A., Dey, P.N., Perez-Otano, I., Muller, D., 2014. GluN3A Promotes Dendritic Spine Pruning and Destabilization during Postnatal Development. J. Neurosci. 34, 9213–9221. https://doi.org/10.1523/JNEUROSCI.5183-13.2014

Kellermayer, B., Ferreira, J.S., Dupuis, J., Levet, F., Grillo-Bosch, D., Bard, L., Linarès-Loyez, J., Bouchet, D., Choquet, D., Rusakov, D.A., Bon, P., Sibarita, J.-B., Cognet, L., Sainlos, M., Carvalho, A.L., Groc, L., 2018. Differential Nanoscale Topography and Functional Role of

GluN2-NMDA Receptor Subtypes at Glutamatergic Synapses. Neuron 100, 106-119.e7. https://doi.org/10.1016/j.neuron.2018.09.012

Kempadoo, K.A., Mosharov, E.V., Choi, S.J., Sulzer, D., Kandel, E.R., 2016. Dopamine release from the locus coeruleus to the dorsal hippocampus promotes spatial learning and memory. Proc. Natl. Acad. Sci. 113, 14835–14840. https://doi.org/10.1073/pnas.1616515114

Kessler, S.P., Obery, D.R., De La Motte, C., 2015. Hyaluronan Synthase 3 Null Mice Exhibit Decreased Intestinal Inflammation and Tissue Damage in the DSS-Induced Colitis Model. Int. J. Cell Biol. 2015, 1–13. https://doi.org/10.1155/2015/745237

Kim, D.I., Roux, K.J., 2016. Filling the Void: Proximity-Based Labeling of Proteins in Living Cells. Trends Cell Biol. 26, 804–817. https://doi.org/10.1016/j.tcb.2016.09.004

Kim, J., Zhao, T., Petralia, R.S., Yu, Y., Peng, H., Myers, E., Magee, J.C., 2012. mGRASP enables mapping mammalian synaptic connectivity with light microscopy. Nat. Methods 9, 96–102. https://doi.org/10.1038/nmeth.1784

Konopka, A., Zeug, A., Skupien, A., Kaza, B., Mueller, F., Chwedorowicz, A., Ponimaskin, E., Wilczynski, G.M., Dzwonek, J., 2016. Cleavage of Hyaluronan and CD44 Adhesion Molecule Regulate Astrocyte Morphology via Rac1 Signalling. PLOS ONE 11, e0155053. https://doi.org/10.1371/journal.pone.0155053

Kornau, H.-C., Schenker, L.T., Kennedy, M.B., Seeburg, P.H., 1995. Domain Interaction Between NMDA Receptor Subunits and the Postsynaptic Density Protein PSD-95. Science 269, 1737–1740. https://doi.org/10.1126/science.7569905

Kortus, S., Rehakova, K., Klima, M., Kolcheva, M., Ladislav, M., Langore, E., Barackova, P., Netolicky, J., Misiachna, A., Hemelikova, K., Humpolickova, J., Chalupska, D., Silhan, J., Kaniakova, M., Krausova, B.H., Boura, E., Zapotocky, M., Horak, M., 2023. Subunit-Dependent Surface Mobility and Localization of NMDA Receptors in Hippocampal Neurons Measured Using Nanobody Probes. J. Neurosci. 43, 4755–4774. https://doi.org/10.1523/JNEUROSCI.2014-22.2023

Kotecha, S.A., Jackson, M.F., Al-Mahrouki, A., Roder, J.C., Orser, B.A., MacDonald, J.F., 2003. Co-stimulation of mGluR5 and N-Methyl-D-aspartate Receptors Is Required for Potentiation of Excitatory Synaptic Transmission in Hippocampal Neurons *. J. Biol. Chem. 278, 27742–27749. https://doi.org/10.1074/jbc.M301946200

Kraszewski, K., Mundigl, O., Daniell, L., Verderio, C., Matteoli, M., Camilli, P.D., 1995. Synaptic vesicle dynamics in living cultured hippocampal neurons visualized with CY3-conjugated antibodies directed against the lumenal domain of synaptotagmin. J. Neurosci. 15, 4328–4342. https://doi.org/10.1523/JNEUROSCI.15-06-04328.1995

Kucukdereli, H., Allen, N.J., Lee, A.T., Feng, A., Ozlu, M.I., Conatser, L.M., Chakraborty, C., Workman, G., Weaver, M., Sage, E.H., Barres, B.A., Eroglu, C., 2011. Control of excitatory CNS synaptogenesis by astrocyte-secreted proteins Hevin and SPARC. Proc. Natl. Acad. Sci. 108. https://doi.org/10.1073/pnas.1104977108

Kulaberoglu, Y., Bhushan, B., Hadi, F., Chakrabarti, S., Khaled, W.T., Rankin, K.S., Smith, E.St.J., Frankel, D., 2019. The material properties of naked mole-rat hyaluronan. Sci. Rep. 9, 6632. https://doi.org/10.1038/s41598-019-43194-7

Kultti, A., Rilla, K., Tiihonen, R., Spicer, A.P., Tammi, R.H., Tammi, M.I., 2006. Hyaluronan Synthesis Induces Microvillus-like Cell Surface Protrusions. J. Biol. Chem. 281, 15821–15828. https://doi.org/10.1074/jbc.M512840200

Kuner, T., Schoepfer, R., 1996. Multiple Structural Elements Determine Subunit Specificity of Mg2+ Block in NMDA Receptor Channels. J. Neurosci. 16, 3549–3558. https://doi.org/10.1523/JNEUROSCI.16-11-03549.1996

Kusumi, A., Fujiwara, T.K., Chadda, R., Xie, M., Tsunoyama, T.A., Kalay, Z., Kasai, R.S., Suzuki, K.G.N., 2012. Dynamic Organizing Principles of the Plasma Membrane that Regulate Signal Transduction: Commemorating the Fortieth Anniversary of Singer and Nicolson's Fluid-Mosaic Model. Annu. Rev. Cell Dev. Biol. 28, 215–250. https://doi.org/10.1146/annurev-cellbio-100809-151736

Kwon, H.-B., Sabatini, B.L., 2011. Glutamate induces de novo growth of functional spines in developing cortex. Nature 474, 100–104. https://doi.org/10.1038/nature09986

Ladepeche, L., Dupuis, J.P., Bouchet, D., Doudnikoff, E., Yang, L., Campagne, Y., Bézard, E., Hosy, E., Groc, L., 2013. Single-molecule imaging of the functional crosstalk between surface NMDA and dopamine D1 receptors. Proc. Natl. Acad. Sci. 110, 18005–18010. https://doi.org/10.1073/pnas.1310145110

Lagardère, M., Chamma, I., Bouilhol, E., Nikolski, M., Thoumine, O., 2020. FluoSim: simulator of single molecule dynamics for fluorescence live-cell and super-resolution imaging of membrane proteins. Sci. Rep. 10, 19954. https://doi.org/10.1038/s41598-020-75814-y

Lan, J., Skeberdis, V.A., Jover, T., Grooms, S.Y., Lin, Y., Araneda, R.C., Zheng, X., Bennett, M.V.L., Zukin, R.S., 2001. Protein kinase C modulates NMDA receptor trafficking and gating. Nat. Neurosci. 4, 382–390. https://doi.org/10.1038/86028

Larance, M., Lamond, A.I., 2015. Multidimensional proteomics for cell biology. Nat. Rev. Mol. Cell Biol. 16, 269–280. https://doi.org/10.1038/nrm3970

Larsen, R.S., Smith, I.T., Miriyala, J., Han, J.E., Corlew, R.J., Smith, S.L., Philpot, B.D., 2014. Synapse-Specific Control of Experience-Dependent Plasticity by Presynaptic NMDA Receptors. Neuron 83, 879–893. https://doi.org/10.1016/j.neuron.2014.07.039

Lau, C.G., Takayasu, Y., Rodenas-Ruano, A., Paternain, A.V., Lerma, J., Bennett, M.V.L., Zukin, R.S., 2010. SNAP-25 Is a Target of Protein Kinase C Phosphorylation Critical to NMDA Receptor Trafficking. J. Neurosci. 30, 242–254. https://doi.org/10.1523/JNEUROSCI.4933-08.2010

Lau, C.G., Zukin, R.S., 2007. NMDA receptor trafficking in synaptic plasticity and neuropsychiatric disorders. Nat. Rev. Neurosci. 8, 413–426. https://doi.org/10.1038/nrn2153

Laurie, D.J., Seeburg, P.H., 1994. Regional and developmental heterogeneity in splicing of the rat brain NMDAR1 mRNA. J. Neurosci. 14, 3180–3194. https://doi.org/10.1523/JNEUROSCI.14-05-03180.1994

Lavezzari, G., McCallum, J., Dewey, C.M., Roche, K.W., 2004. Subunit-Specific Regulation of NMDA Receptor Endocytosis. J. Neurosci. 24, 6383–6391. https://doi.org/10.1523/JNEUROSCI.1890-04.2004

Lee, C.-H., Lü, W., Michel, J.C., Goehring, A., Du, J., Song, X., Gouaux, E., 2014. NMDA receptor structures reveal subunit arrangement and pore architecture. Nature 511, 191–197. https://doi.org/10.1038/nature13548

Lee, F.J.S., Xue, S., Pei, L., Vukusic, B., Chéry, N., Wang, Y., Wang, Y.T., Niznik, H.B., Yu, X., Liu, F., 2002. Dual Regulation of NMDA Receptor Functions by Direct Protein-Protein Interactions with the Dopamine D1 Receptor. Cell 111, 219–230. https://doi.org/10.1016/S0092-8674(02)00962-5

Lee, S.H., Jin, C., Cai, E., Ge, P., Ishitsuka, Y., Teng, K.W., De Thomaz, A.A., Nall, D., Baday, M., Jeyifous, O., Demonte, D., Dundas, C.M., Park, S., Delgado, J.Y., Green, W.N., Selvin, P.R., 2017. Super-resolution imaging of synaptic and Extra-synaptic AMPA receptors with different-sized fluorescent probes. eLife 6, e27744. https://doi.org/10.7554/eLife.27744

Lee, S.-J., Wei, M., Zhang, C., Maxeiner, S., Pak, C., Botelho, S.C., Trotter, J., Sterky, F.H., Südhof, T.C., 2017. Presynaptic Neuronal Pentraxin Receptor Organizes Excitatory and Inhibitory Synapses. J. Neurosci. 37, 1062–1080. https://doi.org/10.1523/JNEUROSCI.2768-16.2016

Leemhuis, J., Bouché, E., Frotscher, M., Henle, F., Hein, L., Herz, J., Meyer, D.K., Pichler, M., Roth, G., Schwan, C., Bock, H.H., 2010. Reelin Signals through Apolipoprotein E Receptor 2 and Cdc42 to Increase Growth Cone Motility and Filopodia Formation. J. Neurosci. 30, 14759–14772. https://doi.org/10.1523/JNEUROSCI.4036-10.2010

Lehmenkühler, A., Syková, E., Svoboda, J., Zilles, K., Nicholson, C., 1993. Extracellular space parameters in the rat neocortex and subcortical white matter during postnatal development determined by diffusion analysis. Neuroscience 55, 339–351. https://doi.org/10.1016/0306-4522(93)90503-8

Lesept, F., Chevilley, A., Jezequel, J., Ladépêche, L., Macrez, R., Aimable, M., Lenoir, S., Bertrand, T., Rubrecht, L., Galea, P., Lebouvier, L., Petersen, K.-U., Hommet, Y., Maubert, E., Ali, C., Groc, L., Vivien, D., 2016. Tissue-type plasminogen activator controls neuronal death by raising surface dynamics of extrasynaptic NMDA receptors. Cell Death Dis. 7, e2466–e2466. https://doi.org/10.1038/cddis.2016.279

Leshchyns'ka, I., Sytnyk, V., Morrow, J.S., Schachner, M., 2003. Neural cell adhesion molecule (NCAM) association with PKCβ2 via βI spectrin is implicated in NCAM-mediated neurite outgrowth. J. Cell Biol. 161, 625–639. https://doi.org/10.1083/jcb.200303020

Letourneau, P.C., Condic, M.L., Snow, D.M., 1992. Extracellular matrix and neurite outgrowth. Curr. Opin. Genet. Dev. 2, 625–634. https://doi.org/10.1016/S0959-437X(05)80183-2

Levet, F., Hosy, E., Kechkar, A., Butler, C., Beghin, A., Choquet, D., Sibarita, J.-B., 2015. SR-Tesseler: a method to segment and quantify localization-based super-resolution microscopy data. Nat. Methods 12, 1065–1071. https://doi.org/10.1038/nmeth.3579

Levey, A.I., Hersch, S.M., Rye, D.B., Sunahara, R.K., Niznik, H.B., Kitt, C.A., Price, D.L., Maggio, R., Brann, M.R., Ciliax, B.J., 1993. Localization of D1 and D2 dopamine receptors in brain with subtype-specific antibodies. Proc. Natl. Acad. Sci. 90, 8861–8865. https://doi.org/10.1073/pnas.90.19.8861

Levy, A.D., Omar, M.H., Koleske, A.J., 2014. Extracellular matrix control of dendritic spine and synapse structure and plasticity in adulthood. Front. Neuroanat. 8. https://doi.org/10.3389/fnana.2014.00116

Li, S., Li, Z., Pei, L., Le, A.D., Liu, F., 2012. The α7nACh–NMDA receptor complex is involved in cue-induced reinstatement of nicotine seeking. J. Exp. Med. 209, 2141–2147. https://doi.org/10.1084/jem.20121270

Li, Y.-C., Liu, G., Hu, J.-L., Gao, W.-J., Huang, Y.-Q., 2010. Dopamine D1 receptor-mediated enhancement of NMDA receptor trafficking requires rapid PKC-dependent synaptic insertion in the prefrontal neurons. J. Neurochem. 114, 62–73. https://doi.org/10.1111/j.1471-4159.2010.06720.x

Liao, D., Zhang, X., O'Brien, R., Ehlers, M.D., Huganir, R.L., 1999. Regulation of morphological postsynaptic silent synapses in developing hippocampal neurons. Nat. Neurosci. 2, 37–43. https://doi.org/10.1038/4540

Lichtenthaler, S.F., Lemberg, M.K., Fluhrer, R., 2018. Proteolytic ectodomain shedding of membrane proteins in mammals—hardware, concepts, and recent developments. EMBO J. 37, e99456. https://doi.org/10.15252/embj.201899456

Lin, J.-S., Ali, J., Lai, E.-M., 2024. Protein–Protein Interactions: Co-immunoprecipitation, in: Journet, L., Cascales, E. (Eds.), Bacterial Secretion Systems : Methods and Protocols. Springer US, New York, NY, pp. 273–283. https://doi.org/10.1007/978-1-0716-3445-5_18

Lisman, J., 1989. A mechanism for the Hebb and the anti-Hebb processes underlying learning and memory. Proc. Natl. Acad. Sci. 86, 9574–9578. https://doi.org/10.1073/pnas.86.23.9574

Liu, F., Ma, X.-H., Ule, J., Bibb, J.A., Nishi, A., DeMaggio, A.J., Yan, Z., Nairn, A.C., Greengard, P., 2001. Regulation of cyclin-dependent kinase 5 and casein kinase 1 by metabotropic glutamate receptors. Proc. Natl. Acad. Sci. 98, 11062–11068. https://doi.org/10.1073/pnas.191353898

Liu, F., Virshup, D.M., Nairn, A.C., Greengard, P., 2002. Mechanism of Regulation of Casein Kinase I Activity by Group I Metabotropic Glutamate Receptors. J. Biol. Chem. 277, 45393–45399. https://doi.org/10.1074/jbc.M204499200

Liu, X.-B., Murray, K.D., Jones, E.G., 2004. Switching of NMDA Receptor 2A and 2B Subunits at Thalamic and Cortical Synapses during Early Postnatal Development. J. Neurosci. 24, 8885–8895. https://doi.org/10.1523/JNEUROSCI.2476-04.2004

Lohmann, C., Bonhoeffer, T., 2008. A Role for Local Calcium Signaling in Rapid Synaptic Partner Selection by Dendritic Filopodia. Neuron 59, 253–260. https://doi.org/10.1016/j.neuron.2008.05.025

Long, K.R., Huttner, W.B., 2019. How the extracellular matrix shapes neural development. Open Biol. 9, 180216. https://doi.org/10.1098/rsob.180216

López-Murcia, F.J., Terni, B., Llobet, A., 2015. SPARC triggers a cell-autonomous program of synapse elimination. Proc. Natl. Acad. Sci. 112, 13366–13371. https://doi.org/10.1073/pnas.1512202112

Low, C.-M., Lyuboslavsky, P., French, A., Le, P., Wyatte, K., Thiel, W.H., Marchan, E.M., Igarashi, K., Kashiwagi, K., Gernert, K., Williams, K., Traynelis, S.F., Zheng, F., 2003. Molecular

Determinants of Proton-Sensitive N-Methyl-d-aspartate Receptor Gating. Mol. Pharmacol. 63, 1212–1222. https://doi.org/10.1124/mol.63.6.1212

Lundell, A., Olin, A.I., Mörgelin, M., al-Karadaghi, S., Aspberg, A., Logan, D.T., 2004. Structural Basis for Interactions between Tenascins and Lectican C-Type Lectin Domains. Structure 12, 1495–1506. https://doi.org/10.1016/j.str.2004.05.021

Luo, J., Wang, Y., Yasuda, R.P., Dunah, A.W., Wolfe, B.B., 1997. The Majority of *N* -Methyl-d-Aspartate Receptor Complexes in Adult Rat Cerebral Cortex Contain at Least Three Different Subunits (NR1/NR2A/NR2B). Mol. Pharmacol. 51, 79–86. https://doi.org/10.1124/mol.51.1.79

Lüscher, C., Huber, K.M., 2010. Group 1 mGluR-Dependent Synaptic Long-Term Depression: Mechanisms and Implications for Circuitry and Disease. Neuron 65, 445–459. https://doi.org/10.1016/j.neuron.2010.01.016

Lüscher, C., Malenka, R.C., 2012. NMDA Receptor-Dependent Long-Term Potentiation and Long-Term Depression (LTP/LTD). Cold Spring Harb. Perspect. Biol. 4, a005710. https://doi.org/10.1101/cshperspect.a005710

Lussier, M.P., Sanz-Clemente, A., Roche, K.W., 2015. Dynamic Regulation of N-Methyl-d-aspartate (NMDA) and α-Amino-3-hydroxy-5-methyl-4-isoxazolepropionic Acid (AMPA) Receptors by Posttranslational Modifications. J. Biol. Chem. 290, 28596–28603. https://doi.org/10.1074/jbc.R115.652750

MacGillavry, H.D., Song, Y., Raghavachari, S., Blanpied, T.A., 2013. Nanoscale Scaffolding Domains within the Postsynaptic Density Concentrate Synaptic AMPA Receptors. Neuron 78, 615–622. https://doi.org/10.1016/j.neuron.2013.03.009

Malenka, R.C., Bear, M.F., 2004. LTP and LTD: An Embarrassment of Riches. Neuron 44, 5–21. https://doi.org/10.1016/j.neuron.2004.09.012

Margolis, R.U., Margolis, R.K., Chang, L.B., Preti, C., 1975. Glycosaminoglycans of brain during development. Biochemistry 14, 85–88. https://doi.org/10.1021/bi00672a014

Martel, M.-A., Ryan, T.J., Bell, K.F.S., Fowler, J.H., McMahon, A., Al-Mubarak, B., Komiyama, N.H., Horsburgh, K., Kind, P.C., Grant, S.G.N., Wyllie, D.J.A., Hardingham, G.E., 2012. The Subtype of GluN2 C-terminal Domain Determines the Response to Excitotoxic Insults. Neuron 74, 543–556. https://doi.org/10.1016/j.neuron.2012.03.021

Martín-de-Saavedra, M.D., Dos Santos, M., Culotta, L., Varea, O., Spielman, B.P., Parnell, E., Forrest, M.P., Gao, R., Yoon, S., McCoig, E., Jalloul, H.A., Myczek, K., Khalatyan, N., Hall, E.A., Turk, L.S., Sanz-Clemente, A., Comoletti, D., Lichtenthaler, S.F., Burgdorf, J.S., Barbolina, M.V., Savas, J.N., Penzes, P., 2022a. Shed CNTNAP2 ectodomain is detectable in CSF and regulates Ca2+ homeostasis and network synchrony via PMCA2/ATP2B2. Neuron 110, 627-643.e9. https://doi.org/10.1016/j.neuron.2021.11.025

Martín-de-Saavedra, M.D., Santos, M.D., Penzes, P., 2022b. Intercellular signaling by ectodomain shedding at the synapse. Trends Neurosci. 45, 483–498. https://doi.org/10.1016/j.tins.2022.03.004

Matsumoto-Miyai, K., Sokolowska, E., Zurlinden, A., Gee, C.E., Lüscher, D., Hettwer, S., Wölfel, J., Ladner, A.P., Ster, J., Gerber, U., Rülicke, T., Kunz, B., Sonderegger, P., 2009. Coincident

Pre- and Postsynaptic Activation Induces Dendritic Filopodia via Neurotrypsin-Dependent Agrin Cleavage. Cell 136, 1161–1171. https://doi.org/10.1016/j.cell.2009.02.034

Matta, J.A., Ashby, M.C., Sanz-Clemente, A., Roche, K.W., Isaac, J.T.R., 2011. mGluR5 and NMDA Receptors Drive the Experience- and Activity-Dependent NMDA Receptor NR2B to NR2A Subunit Switch. Neuron 70, 339–351. https://doi.org/10.1016/j.neuron.2011.02.045

Matteoli, M., Takei, K., Perin, M., Südhof, T., De Camilli, P., 1992. Exo-endocytotic recycling of synaptic vesicles in developing processes of cultured hippocampal neurons. J. Cell Biol. 117, 849–861. https://doi.org/10.1083/jcb.117.4.849

Mayford, M., Wang, J., Kandel, E.R., O'Dell, T.J., 1995. CaMKII regulates the frequency-response function of hippocampal synapses for the production of both LTD and LTP. Cell 81, 891–904. https://doi.org/10.1016/0092-8674(95)90009-8

McAllister, A.K., 2007. Dynamic Aspects of CNS Synapse Formation. Annu. Rev. Neurosci. 30, 425–450. https://doi.org/10.1146/annurev.neuro.29.051605.112830

McKay, S., Ryan, T.J., McQueen, J., Indersmitten, T., Marwick, K.F.M., Hasel, P., Kopanitsa, M.V., Baxter, P.S., Martel, M.-A., Kind, P.C., Wyllie, D.J.A., O'Dell, T.J., Grant, S.G.N., Hardingham, G.E., Komiyama, N.H., 2018. The Developmental Shift of NMDA Receptor Composition Proceeds Independently of GluN2 Subunit-Specific GluN2 C-Terminal Sequences. Cell Rep. 25, 841-851.e4. https://doi.org/10.1016/j.celrep.2018.09.089

McQuate, A., Barria, A., 2020. Rapid exchange of synaptic and extrasynaptic NMDA receptors in hippocampal CA1 neurons. J. Neurophysiol. 123, 1004–1014. https://doi.org/10.1152/jn.00458.2019

McQueen, J., Ryan, T.J., McKay, S., Marwick, K., Baxter, P., Carpanini, S.M., Wishart, T.M., Gillingwater, T.H., Manson, J.C., Wyllie, D.J.A., Grant, S.G.N., McColl, B.W., Komiyama, N.H., Hardingham, G.E., 2017. Pro-death NMDA receptor signaling is promoted by the GluN2B C-terminus independently of Dapk1. eLife 6, e17161. https://doi.org/10.7554/eLife.17161

Meier, J., Vannier, C., Sergé, A., Triller, A., Choquet, D., 2001. Fast and reversible trapping of surface glycine receptors by gephyrin. Nat. Neurosci. 4, 253–260. https://doi.org/10.1038/85099

Michaluk, P., Mikasova, L., Groc, L., Frischknecht, R., Choquet, D., Kaczmarek, L., 2009. Matrix Metalloproteinase-9 Controls NMDA Receptor Surface Diffusion through Integrin β1 Signaling. J. Neurosci. 29, 6007–6012. https://doi.org/10.1523/JNEUROSCI.5346-08.2009

Mikasova, L., De Rossi, P., Bouchet, D., Georges, F., Rogemond, V., Didelot, A., Meissirel, C., Honnorat, J., Groc, L., 2012. Disrupted surface cross-talk between NMDA and Ephrin-B2 receptors in anti-NMDA encephalitis. Brain 135, 1606–1621. https://doi.org/10.1093/brain/aws092

Mikasova, L., Xiong, H., Kerkhofs, A., Bouchet, D., Krugers, H.J., Groc, L., 2017. Stress hormone rapidly tunes synaptic NMDA receptor through membrane dynamics and mineralocorticoid signalling. Sci. Rep. 7, 8053. https://doi.org/10.1038/s41598-017-08695-3

Milev, P., Maurel, P., Chiba, A., Mevissen, M., Popp, S., Yamaguchi, Y., Margolis, R.K., Margolis, R.U., 1998. Differential Regulation of Expression of Hyaluronan-Binding Proteoglycans in

Developing Brain: Aggrecan, Versican, Neurocan, and Brevican. Biochem. Biophys. Res. Commun. 247, 207–212. https://doi.org/10.1006/bbrc.1998.8759

Milligan, G., Bouvier, M., 2005. Methods to monitor the quaternary structure of G protein-coupled receptors. FEBS J. 272, 2914–2925. https://doi.org/10.1111/j.1742-4658.2005.04731.x

Milnerwood, A.J., Gladding, C.M., Pouladi, M.A., Kaufman, A.M., Hines, R.M., Boyd, J.D., Ko, R.W.Y., Vasuta, O.C., Graham, R.K., Hayden, M.R., Murphy, T.H., Raymond, L.A., 2010. Early Increase in Extrasynaptic NMDA Receptor Signaling and Expression Contributes to Phenotype Onset in Huntington's Disease Mice. Neuron 65, 178–190. https://doi.org/10.1016/j.neuron.2010.01.008

Minakami, R., Iida, K., Hirakawa, N., Sugiyama, H., 1995. The Expression of Two Splice Variants of Metabotropic Glutamate Receptor Subtype 5 in the Rat Brain and Neuronal Cells During Development. J. Neurochem. 65, 1536–1542. https://doi.org/10.1046/j.1471-4159.1995.65041536.x

Mizuno, T., Kanazawa, I., Sakurai, M., 2001. Differential induction of LTP and LTD is not determined solely by instantaneous calcium concentration: an essential involvement of a temporal factor. Eur. J. Neurosci. 14, 701–708. https://doi.org/10.1046/j.0953-816x.2001.01679.x

Mondin, M., Labrousse, V., Hosy, E., Heine, M., Tessier, B., Levet, F., Poujol, C., Blanchet, C., Choquet, D., Thoumine, O., 2011. Neurexin-Neuroligin Adhesions Capture Surface-Diffusing AMPA Receptors through PSD-95 Scaffolds. J. Neurosci. 31, 13500–13515. https://doi.org/10.1523/JNEUROSCI.6439-10.2011

Monteiro, P., Feng, G., 2017. SHANK proteins: roles at the synapse and in autism spectrum disorder. Nat. Rev. Neurosci. 18, 147–157. https://doi.org/10.1038/nrn.2016.183

Monyer, H., Burnashev, N., Laurie, D.J., Sakmann, B., Seeburg, P.H., 1994. Developmental and regional expression in the rat brain and functional properties of four NMDA receptors. Neuron 12, 529–540. https://doi.org/10.1016/0896-6273(94)90210-0

Monyer, H., Sprengel, R., Schoepfer, R., Herb, A., Higuchi, M., Lomeli, H., Burnashev, N., Sakmann, B., Seeburg, P.H., 1992. Heteromeric NMDA Receptors: Molecular and Functional Distinction of Subtypes. Science 256, 1217–1221. https://doi.org/10.1126/science.256.5060.1217

Moon, L.D.F., Asher, R.A., Rhodes, K.E., Fawcett, J.W., 2001. Regeneration of CNS axons back to their target following treatment of adult rat brain with chondroitinase ABC. Nat. Neurosci. 4, 465–466. https://doi.org/10.1038/87415

Moutin, E., Raynaud, F., Roger, J., Pellegrino, E., Homburger, V., Bertaso, F., Ollendorff, V., Bockaert, J., Fagni, L., Perroy, J., 2012. Dynamic remodeling of scaffold interactions in dendritic spines controls synaptic excitability. J. Cell Biol. 198, 251–263. https://doi.org/10.1083/jcb.201110101

Myers, J.P., Santiago-Medina, M., Gomez, T.M., 2011. Regulation of axonal outgrowth and pathfinding by integrin–ecm interactions. Dev. Neurobiol. 71, 901–923. https://doi.org/10.1002/dneu.20931

Nabavi, S., Kessels, H.W., Alfonso, S., Aow, J., Fox, R., Malinow, R., 2013. Metabotropic NMDA receptor function is required for NMDA receptor-dependent long-term depression. Proc. Natl. Acad. Sci. 110, 4027–4032. https://doi.org/10.1073/pnas.1219454110

Nägerl, U.V., Köstinger, G., Anderson, J.C., Martin, K.A.C., Bonhoeffer, T., 2007. Protracted Synaptogenesis after Activity-Dependent Spinogenesis in Hippocampal Neurons. J. Neurosci. 27, 8149–8156. https://doi.org/10.1523/JNEUROSCI.0511-07.2007

Nagy, J., Hacking, J., Frankenstein, U., Turley, E., 1995. Requirement of the hyaluronan receptor RHAMM in neurite extension and motility as demonstrated in primary neurons and neuronal cell lines. J. Neurosci. 15, 241–252. https://doi.org/10.1523/JNEUROSCI.15-01-00241.1995

Nahir, B., Jahr, C.E., 2013. Activation of Extrasynaptic NMDARs at Individual Parallel Fiber–Molecular Layer Interneuron Synapses in Cerebellum. J. Neurosci. 33, 16323–16333. https://doi.org/10.1523/JNEUROSCI.1971-13.2013

Nai, Q., Li, S., Wang, S.-H., Liu, J., Lee, F.J.S., Frankland, P.W., Liu, F., 2010. Uncoupling the D1-N-Methyl-D-Aspartate (NMDA) Receptor Complex Promotes NMDA-Dependent Long-Term Potentiation and Working Memory. Biol. Psychiatry 67, 246–254. https://doi.org/10.1016/j.biopsych.2009.08.011

Nair, D., Hosy, E., Petersen, J.D., Constals, A., Giannone, G., Choquet, D., Sibarita, J.-B., 2013. Super-Resolution Imaging Reveals That AMPA Receptors Inside Synapses Are Dynamically Organized in Nanodomains Regulated by PSD95. J. Neurosci. 33, 13204–13224. https://doi.org/10.1523/JNEUROSCI.2381-12.2013

Nakanishi, M., Nomura, J., Ji, X., Tamada, K., Arai, T., Takahashi, E., Bućan, M., Takumi, T., 2017. Functional significance of rare neuroligin 1 variants found in autism. PLOS Genet. 13, e1006940. https://doi.org/10.1371/journal.pgen.1006940

Nakanishi, N., Axel, R., Shneider, N.A., 1992. Alternative splicing generates functionally distinct N-methyl-D-aspartate receptors. Proc. Natl. Acad. Sci. 89, 8552–8556. https://doi.org/10.1073/pnas.89.18.8552

Nakatsu, F., Ohno, H., 2003. Adaptor Protein Complexes as the Key Regulators of Protein Sorting in the Post-Golgi Network. Cell Struct. Funct. 28, 419–429. https://doi.org/10.1247/csf.28.419

Navakkode, S., Sajikumar, S., Frey, J.U., 2007. Synergistic requirements for the induction of dopaminergic D1/D5-receptor-mediated LTP in hippocampal slices of rat CA1 in vitro. Neuropharmacology 52, 1547–1554. https://doi.org/10.1016/j.neuropharm.2007.02.010

Neyman, S., Manahan-Vaughan, D., 2008. Metabotropic glutamate receptor 1 (mGluR1) and 5 (mGluR5) regulate late phases of LTP and LTD in the hippocampal CA1 region in vitro. Eur. J. Neurosci. 27, 1345–1352. https://doi.org/10.1111/j.1460-9568.2008.06109.x

Nguyen, T.A., Lehr, A.W., Roche, K.W., 2020. Neuroligins and Neurodevelopmental Disorders: X-Linked Genetics. Front. Synaptic Neurosci. 12, 33. https://doi.org/10.3389/fnsyn.2020.00033

Nicoll, R.A., Schulman, H., 2023. Synaptic memory and CaMKII. Physiol. Rev. 103, 2897–2945. https://doi.org/10.1152/physrev.00034.2022

Niederauer, C., Nguyen, C., Wang-Henderson, M., Stein, J., Strauss, S., Cumberworth, A., Stehr, F., Jungmann, R., Schwille, P., Ganzinger, K.A., 2023. Dual-color DNA-PAINT single-particle tracking enables extended studies of membrane protein interactions. Nat. Commun. 14, 4345. https://doi.org/10.1038/s41467-023-40065-8

Nishida, H., Okabe, S., 2007. Direct Astrocytic Contacts Regulate Local Maturation of Dendritic Spines. J. Neurosci. 27, 331–340. https://doi.org/10.1523/JNEUROSCI.4466-06.2007

Niu, S., Renfro, A., Quattrocchi, C.C., Sheldon, M., D'Arcangelo, G., 2004. Reelin Promotes Hippocampal Dendrite Development through the VLDLR/ApoER2-Dab1 Pathway. Neuron 41, 71–84. https://doi.org/10.1016/S0896-6273(03)00819-5

Niu, S., Yabut, O., D'Arcangelo, G., 2008. The Reelin Signaling Pathway Promotes Dendritic Spine Development in Hippocampal Neurons. J. Neurosci. 28, 10339–10348. https://doi.org/10.1523/JNEUROSCI.1917-08.2008

Nolt, M.J., Lin, Y., Hruska, M., Murphy, J., Sheffler-Colins, S.I., Kayser, M.S., Passer, J., Bennett, M.V.L., Zukin, R.S., Dalva, M.B., 2011. EphB Controls NMDA Receptor Function and Synaptic Targeting in a Subunit-Specific Manner. J. Neurosci. 31, 5353–5364. https://doi.org/10.1523/JNEUROSCI.0282-11.2011

Nonaka, H., Sakamoto, S., Shiraiwa, K., Ishikawa, M., Tamura, T., Okuno, K., Kondo, T., Kiyonaka, S., Susaki, E.A., Shimizu, C., Ueda, H.R., Kakegawa, W., Arai, I., Yuzaki, M., Hamachi, I., 2024. Bioorthogonal chemical labeling of endogenous neurotransmitter receptors in living mouse brains. Proc. Natl. Acad. Sci. 121, e2313887121. https://doi.org/10.1073/pnas.2313887121

Nong, Y., Huang, Y.-Q., Ju, W., Kalia, L.V., Ahmadian, G., Wang, Y.T., Salter, M.W., 2003. Glycine binding primes NMDA receptor internalization. Nature 422, 302–307. https://doi.org/10.1038/nature01497

Nörenberg, U., Hubert, M., Rathjen, F.G., 1996. STRUCTURAL AND FUNCTIONAL CHARACTERIZATION OF TENASCIN-R (RESTRICTIN), AN EXTRACELLULAR MATRIX GLYCOPROTEIN OF GLIAL CELLS AND NEURONS. Int. J. Dev. Neurosci. 14, 217–231. https://doi.org/10.1016/0736-5748(96)00009-3

O'Brien, R., Xu, D., Mi, R., Tang, X., Hopf, C., Worley, P., 2002. Synaptically Targeted Narp Plays an Essential Role in the Aggregation of AMPA Receptors at Excitatory Synapses in Cultured Spinal Neurons. J. Neurosci. 22, 4487–4498. https://doi.org/10.1523/JNEUROSCI.22-11-04487.2002

O'Brien, R.J., Xu, D., Petralia, R.S., Steward, O., Huganir, R.L., Worley, P., 1999. Synaptic Clustering of AMPA Receptors by the Extracellular Immediate-Early Gene Product Narp. Neuron 23, 309–323. https://doi.org/10.1016/S0896-6273(00)80782-5

Okawa, H., Hoon, M., Yoshimatsu, T., Della Santina, L., Wong, R.O.L., 2014. Illuminating the Multifaceted Roles of Neurotransmission in Shaping Neuronal Circuitry. Neuron 83, 1303–1318. https://doi.org/10.1016/j.neuron.2014.08.029

Oliet, S.H.R., Malenka, R.C., Nicoll, R.A., 1997. Two Distinct Forms of Long-Term Depression Coexist in CA1 Hippocampal Pyramidal Cells. Neuron 18, 969–982. https://doi.org/10.1016/S0896-6273(00)80336-0

Oliferenko, S., Kaverina, I., Small, J.V., Huber, L.A., 2000. Hyaluronic Acid (Ha) Binding to Cd44 Activates Rac1 and Induces Lamellipodia Outgrowth. J. Cell Biol. 148, 1159–1164. https://doi.org/10.1083/jcb.148.6.1159

Omar, M.H., Campbell, M.K., Xiao, X., Zhong, Q., Brunken, W.J., Miner, J.H., Greer, C.A., Koleske, A.J., 2017. CNS Neurons Deposit Laminin α5 to Stabilize Synapses. Cell Rep. 21, 1281–1292. https://doi.org/10.1016/j.celrep.2017.10.028

Ooki, T., Murata-Kamiya, N., Takahashi-Kanemitsu, A., Wu, W., Hatakeyama, M., 2019. High-Molecular-Weight Hyaluronan Is a Hippo Pathway Ligand Directing Cell Density-Dependent Growth Inhibition via PAR1b. Dev. Cell 49, 590-604.e9. https://doi.org/10.1016/j.devcel.2019.04.018

Orr, M.E., Garbarino, V.R., Salinas, A., Buffenstein, R., 2016. Extended Postnatal Brain Development in the Longest-Lived Rodent: Prolonged Maintenance of Neotenous Traits in the Naked Mole-Rat Brain. Front. Neurosci. 10. https://doi.org/10.3389/fnins.2016.00504

Otmakhova, N.A., Lisman, J.E., 1996. D1/D5 Dopamine Receptor Activation Increases the Magnitude of Early Long-Term Potentiation at CA1 Hippocampal Synapses. J. Neurosci. 16, 7478–7486. https://doi.org/10.1523/JNEUROSCI.16-23-07478.1996

Pagano, J., Giona, F., Beretta, S., Verpelli, C., Sala, C., 2021. N-methyl-d-aspartate receptor function in neuronal and synaptic development and signaling. Curr. Opin. Pharmacol. 56, 93–101. https://doi.org/10.1016/j.coph.2020.12.006

Paoletti, P., Bellone, C., Zhou, Q., 2013. NMDA receptor subunit diversity: impact on receptor properties, synaptic plasticity and disease. Nat. Rev. Neurosci. 14, 383–400. https://doi.org/10.1038/nrn3504

Papa, M., Bundman, M., Greenberger, V., Segal, M., 1995. Morphological analysis of dendritic spine development in primary cultures of hippocampal neurons. J. Neurosci. 15, 1–11. https://doi.org/10.1523/JNEUROSCI.15-01-00001.1995

Papouin, T., Ladépêche, L., Ruel, J., Sacchi, S., Labasque, M., Hanini, M., Groc, L., Pollegioni, L., Mothet, J.-P., Oliet, S.H.R., 2012. Synaptic and Extrasynaptic NMDA Receptors Are Gated by Different Endogenous Coagonists. Cell 150, 633–646. https://doi.org/10.1016/j.cell.2012.06.029

Parsons, M.P., Raymond, L.A., 2014. Extrasynaptic NMDA Receptor Involvement in Central Nervous System Disorders. Neuron 82, 279–293. https://doi.org/10.1016/j.neuron.2014.03.030

Patel, M.R., Weaver, A.M., 2021. Astrocyte-derived small extracellular vesicles promote synapse formation via fibulin-2-mediated TGF-β signaling. Cell Rep. 34. https://doi.org/10.1016/j.celrep.2021.108829

Paupard, M.-C., Friedman, L.K., Zukin, R.S., 1997. Developmental regulation and cell-specific expression of N-methyl-d-aspartate receptor splice variants in rat hippocampus. Neuroscience 79, 399–409. https://doi.org/10.1016/S0306-4522(96)00677-X

Paviolo, C., Ferreira, J.S., Lee, A., Hunter, D., Calaresu, I., Nandi, S., Groc, L., Cognet, L., 2022. Near-Infrared Carbon Nanotube Tracking Reveals the Nanoscale Extracellular Space around Synapses. Nano Lett. 22, 6849–6856. https://doi.org/10.1021/acs.nanolett.1c04259

Pei, L., Lee, F.J.S., Moszczynska, A., Vukusic, B., Liu, F., 2004. Regulation of Dopamine D1 Receptor Function by Physical Interaction with the NMDA Receptors. J. Neurosci. 24, 1149–1158. https://doi.org/10.1523/JNEUROSCI.3922-03.2004

Peixoto, R.T., Kunz, P.A., Kwon, H., Mabb, A.M., Sabatini, B.L., Philpot, B.D., Ehlers, M.D., 2012. Transsynaptic Signaling by Activity-Dependent Cleavage of Neuroligin-1. Neuron 76, 396–409. https://doi.org/10.1016/j.neuron.2012.07.006

Pennacchietti, F., Vascon, S., Nieus, T., Rosillo, C., Das, S., Tyagarajan, S.K., Diaspro, A., Bue, A.D., Petrini, E.M., Barberis, A., Zanacchi, F.C., 2017. Nanoscale Molecular Reorganization of the Inhibitory Postsynaptic Density Is a Determinant of GABAergic Synaptic Potentiation. J. Neurosci. 37, 1747–1756. https://doi.org/10.1523/JNEUROSCI.0514-16.2016

Penz, O.K., Fuzik, J., Kurek, A.B., Romanov, R., Larson, J., Park, T.J., Harkany, T., Keimpema, E., 2015. Protracted brain development in a rodent model of extreme longevity. Sci. Rep. 5, 11592. https://doi.org/10.1038/srep11592

Perez de Arce, K., Schrod, N., Metzbower, S.W.R., Allgeyer, E., Kong, G.K.-W., Tang, A.-H., Krupp, A.J., Stein, V., Liu, X., Bewersdorf, J., Blanpied, T.A., Lucić, V., Biederer, T., 2015. Topographic Mapping of the Synaptic Cleft into Adhesive Nanodomains. Neuron 88, 1165–1172. https://doi.org/10.1016/j.neuron.2015.11.011

Pérez-Otaño, I., Larsen, R.S., Wesseling, J.F., 2016. Emerging roles of GluN3-containing NMDA receptors in the CNS. Nat. Rev. Neurosci. 17, 623–635. https://doi.org/10.1038/nrn.2016.92

Perroy, J., Raynaud, F., Homburger, V., Rousset, M.-C., Telley, L., Bockaert, J., Fagni, L., 2008. Direct Interaction Enables Cross-talk between Ionotropic and Group I Metabotropic Glutamate Receptors. J. Biol. Chem. 283, 6799–6805. https://doi.org/10.1074/jbc.M705661200

Petanjek, Z., Judaš, M., Šimić, G., Rašin, M.R., Uylings, H.B.M., Rakic, P., Kostović, I., 2011. Extraordinary neoteny of synaptic spines in the human prefrontal cortex. Proc. Natl. Acad. Sci. 108, 13281–13286. https://doi.org/10.1073/pnas.1105108108

Peterson, B.L., Park, T.J., Larson, J., 2012. Adult naked mole-rat brain retains the NMDA receptor subunit GluN2D associated with hypoxia tolerance in neonatal mammals. Neurosci. Lett. 506, 342–345. https://doi.org/10.1016/j.neulet.2011.11.042

Petit-Pedrol, M., Groc, L., 2021. Regulation of membrane NMDA receptors by dynamics and protein interactions. J. Cell Biol. 220, e202006101. https://doi.org/10.1083/jcb.202006101

Petralia, R.S., Esteban, J.A., Wang, Y. –X., Partridge, J.G., Zhao, H. –M., Wenthold, R.J., Malinow, R., 1999. Selective acquisition of AMPA receptors over postnatal development suggests a molecular basis for silent synapses. Nat. Neurosci. 2, 31–36. https://doi.org/10.1038/4532

Petralia, R.S., Wang, Y., Wenthold, R.J., 2003. Internalization at glutamatergic synapses during development. Eur. J. Neurosci. 18, 3207–3217. https://doi.org/10.1111/j.1460-9568.2003.03074.x

Petralia, R.S., Wang, Y.X., Hua, F., Yi, Z., Zhou, A., Ge, L., Stephenson, F.A., Wenthold, R.J., 2010. Organization of NMDA receptors at extrasynaptic locations. Neuroscience 167, 68–87. https://doi.org/10.1016/j.neuroscience.2010.01.022

Pfeiffer, T., Poll, S., Bancelin, S., Angibaud, J., Inavalli, V.K., Keppler, K., Mittag, M., Fuhrmann, M., Nägerl, U.V., 2018. Chronic 2P-STED imaging reveals high turnover of dendritic spines in the hippocampus in vivo. eLife 7, e34700. https://doi.org/10.7554/eLife.34700

Pfleger, K.D.G., Seeber, R.M., Eidne, K.A., 2006. Bioluminescence resonance energy transfer (BRET) for the real-time detection of protein-protein interactions. Nat. Protoc. 1, 337–345. https://doi.org/10.1038/nprot.2006.52

Pfrieger, F.W., Barres, B.A., 1997. Synaptic Efficacy Enhanced by Glial Cells in Vitro. Science 277, 1684–1687. https://doi.org/10.1126/science.277.5332.1684

Pin, J.-P., Neubig, R., Bouvier, M., Devi, L., Filizola, M., Javitch, J.A., Lohse, M.J., Milligan, G., Palczewski, K., Parmentier, M., Spedding, M., 2007. International Union of Basic and Clinical Pharmacology. LXVII. Recommendations for the Recognition and Nomenclature of G Protein-Coupled Receptor Heteromultimers. Pharmacol. Rev. 59, 5–13. https://doi.org/10.1124/pr.59.1.5

Pipicelli, F., Baumann, N., Di Giaimo, R., Forero-Echeverry, A., Kyrousi, C., Bonrath, R., Maccarrone, G., Jabaudon, D., Cappello, S., 2023. Non–cell-autonomous regulation of interneuron specification mediated by extracellular vesicles. Sci. Adv. 9, eadd8164. https://doi.org/10.1126/sciadv.add8164

Pizzorusso, T., Medini, P., Berardi, N., Chierzi, S., Fawcett, J.W., Maffei, L., 2002. Reactivation of Ocular Dominance Plasticity in the Adult Visual Cortex. Science 298, 1248–1251. https://doi.org/10.1126/science.1072699

Pizzorusso, T., Medini, P., Landi, S., Baldini, S., Berardi, N., Maffei, L., 2006. Structural and functional recovery from early monocular deprivation in adult rats. Proc. Natl. Acad. Sci. 103, 8517–8522. https://doi.org/10.1073/pnas.0602657103

Polansky, J.R., Toole, B.P., Gross, J., 1974. Brain Hyaluronidase: Changes in Activity during Chick Development. Science 183, 862–864. https://doi.org/10.1126/science.183.4127.862

Potier, M., Georges, F., Brayda-Bruno, L., Ladépêche, L., Lamothe, V., Al Abed, A.S., Groc, L., Marighetto, A., 2016. Temporal Memory and Its Enhancement by Estradiol Requires Surface Dynamics of Hippocampal CA1 N-Methyl-D-Aspartate Receptors. Biol. Psychiatry 79, 735–745. https://doi.org/10.1016/j.biopsych.2015.07.017

Prybylowski, K., Chang, K., Sans, N., Kan, L., Vicini, S., Wenthold, R.J., 2005. The Synaptic Localization of NR2B-Containing NMDA Receptors Is Controlled by Interactions with PDZ Proteins and AP-2. Neuron 47, 845–857. https://doi.org/10.1016/j.neuron.2005.08.016

Pucadyil, T.J., Kalipatnapu, S., Harikumar, K.G., Rangaraj, N., Karnik, S.S., Chattopadhyay, A., 2004. G-Protein-Dependent Cell Surface Dynamics of the Human Serotonin1A Receptor Tagged to Yellow Fluorescent Protein. Biochemistry 43, 15852–15862. https://doi.org/10.1021/bi0480887

Puighermanal, E., Cutando, L., Boubaker-Vitre, J., Honoré, E., Longueville, S., Hervé, D., Valjent, E., 2017. Anatomical and molecular characterization of dopamine D1 receptor-expressing neurons of the mouse CA1 dorsal hippocampus. Brain Struct. Funct. 222, 1897–1911. https://doi.org/10.1007/s00429-016-1314-x

Pujadas, L., Gruart, A., Bosch, C., Delgado, L., Teixeira, C.M., Rossi, D., De Lecea, L., Martínez, A., Delgado-García, J.M., Soriano, E., 2010. Reelin Regulates Postnatal Neurogenesis and Enhances Spine Hypertrophy and Long-Term Potentiation. J. Neurosci. 30, 4636–4649. https://doi.org/10.1523/JNEUROSCI.5284-09.2010

Qian, A., Buller, A.L., Johnson, J.W., 2005. NR2 subunit-dependence of NMDA receptor channel block by external Mg2+. J. Physiol. 562, 319–331. https://doi.org/10.1113/jphysiol.2004.076737

Qiu, S., Zhang, X., Cao, J., Yang, W., Yan, Y., Shan, L., Zheng, J., Luo, J., 2009. An Endoplasmic Reticulum Retention Signal Located in the Extracellular Amino-terminal Domain of the NR2A Subunit of N-Methyl-d-aspartate Receptors *. J. Biol. Chem. 284, 20285–20298. https://doi.org/10.1074/jbc.M109.004960

Qiu, S., Zhao, L.F., Korwek, K.M., Weeber, E.J., 2006. Differential Reelin-Induced Enhancement of NMDA and AMPA Receptor Activity in the Adult Hippocampus. J. Neurosci. 26, 12943–12955. https://doi.org/10.1523/JNEUROSCI.2561-06.2006

Rao, A., Craig, A.M., 1997. Activity Regulates the Synaptic Localization of the NMDA Receptor in Hippocampal Neurons. Neuron 19, 801–812. https://doi.org/10.1016/S0896-6273(00)80962-9

Rasmussen, A.H., Rasmussen, H.B., Silahtaroglu, A., 2017. The DLGAP family: neuronal expression, function and role in brain disorders. Mol. Brain 10, 43. https://doi.org/10.1186/s13041-017-0324-9

Rasse, T.M., Fouquet, W., Schmid, A., Kittel, R.J., Mertel, S., Sigrist, C.B., Schmidt, M., Guzman, A., Merino, C., Qin, G., Quentin, C., Madeo, F.F., Heckmann, M., Sigrist, S.J., 2005. Glutamate receptor dynamics organizing synapse formation in vivo. Nat. Neurosci. 8, 898–905. https://doi.org/10.1038/nn1484

Rauch, U., 2004. Extracellular matrix components associated with remodeling processes in brain 61.

Rebola, N., Lujan, R., Cunha, R.A., Mulle, C., 2008. Adenosine A2A Receptors Are Essential for Long-Term Potentiation of NMDA-EPSCs at Hippocampal Mossy Fiber Synapses. Neuron 57, 121–134. https://doi.org/10.1016/j.neuron.2007.11.023

Reed, M.J., Damodarasamy, M., Pathan, J.L., Erickson, M.A., Banks, W.A., Vernon, R.B., 2018. The Effects of Normal Aging on Regional Accumulation of Hyaluronan and Chondroitin Sulfate Proteoglycans in the Mouse Brain. J. Histochem. Cytochem. 66, 697–707. https://doi.org/10.1369/0022155418774779

Reese, A.L., Kavalali, E.T., 2016. Single synapse evaluation of the postsynaptic NMDA receptors targeted by evoked and spontaneous neurotransmission. eLife 5, e21170. https://doi.org/10.7554/eLife.21170

Reiner, A., Levitz, J., 2018. Glutamatergic Signaling in the Central Nervous System: Ionotropic and Metabotropic Receptors in Concert. Neuron 98, 1080–1098. https://doi.org/10.1016/j.neuron.2018.05.018

Rhee, H.-W., Zou, P., Udeshi, N.D., Martell, J.D., Mootha, V.K., Carr, S.A., Ting, A.Y., 2013. Proteomic Mapping of Mitochondria in Living Cells via Spatially Restricted Enzymatic Tagging. Science 339, 1328–1331. https://doi.org/10.1126/science.1230593

Rilla, K., Tiihonen, R., Kultti, A., Tammi, M., Tammi, R., 2008. Pericellular Hyaluronan Coat Visualized in Live Cells With a Fluorescent Probe Is Scaffolded by Plasma Membrane Protrusions. J. Histochem. Cytochem. 56, 901–910. https://doi.org/10.1369/jhc.2008.951665

Risher, W.C., Kim, N., Koh, S., Choi, J.-E., Mitev, P., Spence, E.F., Pilaz, L.-J., Wang, D., Feng, G., Silver, D.L., Soderling, S.H., Yin, H.H., Eroglu, C., 2018. Thrombospondin receptor α2δ-1 promotes synaptogenesis and spinogenesis via postsynaptic Rac1. J. Cell Biol. 217, 3747–3765. https://doi.org/10.1083/jcb.201802057

Rizalar, F.S., Roosen, D.A., Haucke, V., 2021. A Presynaptic Perspective on Transport and Assembly Mechanisms for Synapse Formation. Neuron 109, 27–41. https://doi.org/10.1016/j.neuron.2020.09.038

Robbins, E.M., Krupp, A.J., Perez De Arce, K., Ghosh, A.K., Fogel, A.I., Boucard, A., Südhof, T.C., Stein, V., Biederer, T., 2010. SynCAM 1 Adhesion Dynamically Regulates Synapse Number and Impacts Plasticity and Learning. Neuron 68, 894–906. https://doi.org/10.1016/j.neuron.2010.11.003

Roche, K.W., Standley, S., McCallum, J., Ly, C.D., Ehlers, M.D., Wenthold, R.J., 2001. Molecular determinants of NMDA receptor internalization. Nat. Neurosci. 4.

Rodriguez, L., Yi, C., Chu, C., Duriez, Q., Watanabe, S., Ryu, M., Reyes, B., Asatryan, L., Boué-Grabot, E., Davies, D., 2020. Cross-Talk between P2X and NMDA Receptors. Int. J. Mol. Sci. 21, 7187. https://doi.org/10.3390/ijms21197187

Rodríguez-Muñoz, M., Sánchez-Blázquez, P., Vicente-Sánchez, A., Berrocoso, E., Garzón, J., 2012. The Mu-Opioid Receptor and the NMDA Receptor Associate in PAG Neurons: Implications in Pain Control. Neuropsychopharmacology 37, 338–349. https://doi.org/10.1038/npp.2011.155

Rodríguez-Ruiz, M., Moreno, E., Moreno-Delgado, D., Navarro, G., Mallol, J., Cortés, A., Lluís, C., Canela, E.I., Casadó, V., McCormick, P.J., Franco, R., 2017. Heteroreceptor Complexes Formed by Dopamine D1, Histamine H3, and N-Methyl-D-Aspartate Glutamate Receptors as Targets to Prevent Neuronal Death in Alzheimer's Disease. Mol. Neurobiol. 54, 4537–4550. https://doi.org/10.1007/s12035-016-9995-y

Romano, C., Sesma, M.A., McDonald, C.T., O'malley, K., van den Pol, A.N., Olney, J.W., 1995. Distribution of metabotropic glutamate receptor mGluR5 immunoreactivity in rat brain. J. Comp. Neurol. 355, 455–469. https://doi.org/10.1002/cne.903550310

Rosenmund, C., Feltz, A., Westbrook, G., 1995. Synaptic NMDA receptor channels have a low open probability. J. Neurosci. 15, 2788–2795. https://doi.org/10.1523/JNEUROSCI.15-04-02788.1995

Roszkowska, M., Skupien, A., Wójtowicz, T., Konopka, A., Gorlewicz, A., Kisiel, M., Bekisz, M., Ruszczycki, B., Dolezyczek, H., Rejmak, E., Knapska, E., Mozrzymas, J.W., Wlodarczyk, J., Wilczynski, G.M., Dzwonek, J., 2016. CD44: a novel synaptic cell adhesion molecule

regulating structural and functional plasticity of dendritic spines. Mol. Biol. Cell 27, 4055–4066. https://doi.org/10.1091/mbc.E16-06-0423

Rothmond, D.A., Weickert, C.S., Webster, M.J., 2012. Developmental changes in human dopamine neurotransmission: cortical receptors and terminators. BMC Neurosci. 13, 18. https://doi.org/10.1186/1471-2202-13-18

Roux, K.J., Kim, D.I., Raida, M., Burke, B., 2012. A promiscuous biotin ligase fusion protein identifies proximal and interacting proteins in mammalian cells. J. Cell Biol. 196, 801–810. https://doi.org/10.1083/jcb.201112098

Rowlands, D., Lensjø, K.K., Dinh, T., Yang, S., Andrews, M.R., Hafting, T., Fyhn, M., Fawcett, J.W., Dick, G., 2018. Aggrecan Directs Extracellular Matrix-Mediated Neuronal Plasticity. J. Neurosci. 38, 10102–10113. https://doi.org/10.1523/JNEUROSCI.1122-18.2018

Ruby, J.G., Smith, M., Buffenstein, R., 2018. Naked mole-rat mortality rates defy Gompertzian laws by not increasing with age. eLife 7, e31157. https://doi.org/10.7554/eLife.31157

Ryan, T.A., Myers, J., Holowka, D., Baird, B., Webb, W.W., 1988. Molecular Crowding on the Cell Surface. Science 239, 61–64. https://doi.org/10.1126/science.2962287

Ryan, T.J., Kopanitsa, M.V., Indersmitten, T., Nithianantharajah, J., Afinowi, N.O., Pettit, C., Stanford, L.E., Sprengel, R., Saksida, L.M., Bussey, T.J., O'Dell, T.J., Grant, S.G.N., Komiyama, N.H., 2013. Evolution of GluN2A/B cytoplasmic domains diversified vertebrate synaptic plasticity and behavior. Nat. Neurosci. 16, 25–32. https://doi.org/10.1038/nn.3277

Sabo, S.L., Gomes, R.A., McAllister, A.K., 2006. Formation of Presynaptic Terminals at Predefined Sites along Axons. J. Neurosci. 26, 10813–10825. https://doi.org/10.1523/JNEUROSCI.2052-06.2006

Sahores, M., Gibb, A., Salinas, P.C., 2010. Frizzled-5, a receptor for the synaptic organizer Wnt7a, regulates activity-mediated synaptogenesis. Development 137, 2215–2225. https://doi.org/10.1242/dev.046722

Sando, R., Bushong, E., Zhu, Y., Huang, M., Considine, C., Phan, S., Ju, S., Uytiepo, M., Ellisman, M., Maximov, A., 2017. Assembly of Excitatory Synapses in the Absence of Glutamatergic Neurotransmission. Neuron 94, 312-321.e3. https://doi.org/10.1016/j.neuron.2017.03.047

Sanes, J.R., Zipursky, S.L., 2020. Synaptic Specificity, Recognition Molecules, and Assembly of Neural Circuits. Cell 181, 536–556. https://doi.org/10.1016/j.cell.2020.04.008

Sans, N., Petralia, R.S., Wang, Y.-X., Blahos, J., Hell, J.W., Wenthold, R.J., 2000. A Developmental Change in NMDA Receptor-Associated Proteins at Hippocampal Synapses. J. Neurosci. 20, 1260–1271. https://doi.org/10.1523/JNEUROSCI.20-03-01260.2000

Sapudom, J., Nguyen, K.-T., Martin, S., Wippold, T., Möller, S., Schnabelrauch, M., Anderegg, U., Pompe, T., 2020. Biomimetic tissue models reveal the role of hyaluronan in melanoma proliferation and invasion. Biomater. Sci. 8, 1405–1417. https://doi.org/10.1039/C9BM01636H

Sara, Y., Bal, M., Adachi, M., Monteggia, L.M., Kavalali, E.T., 2011. Use-Dependent AMPA Receptor Block Reveals Segregation of Spontaneous and Evoked Glutamatergic Neurotransmission. J. Neurosci. 31, 5378–5382. https://doi.org/10.1523/JNEUROSCI.5234-10.2011

Saulière-Nzeh, A.N., Millot, C., Corbani, M., Mazères, S., Lopez, A., Salomé, L., 2010. Agonist-selective Dynamic Compartmentalization of Human Mu Opioid Receptor as Revealed by Resolutive FRAP Analysis *. J. Biol. Chem. 285, 14514–14520. https://doi.org/10.1074/jbc.M109.076695

Scanziani, M., Malenka, R.C., Nicoll, R.A., 1996. Role of intercellular interactions in heterosynaptic long-term depression. Nature 380, 446–450. https://doi.org/10.1038/380446a0

Scarselli, M., Annibale, P., McCormick, P.J., Kolachalam, S., Aringhieri, S., Radenovic, A., Corsini, G.U., Maggio, R., 2016. Revealing G-protein-coupled receptor oligomerization at the single-molecule level through a nanoscopic lens: methods, dynamics and biological function. FEBS J. 283, 1197–1217. https://doi.org/10.1111/febs.13577

Scheefhals, N., MacGillavry, H.D., 2018. Functional organization of postsynaptic glutamate receptors. Mol. Cell. Neurosci. 91, 82–94. https://doi.org/10.1016/j.mcn.2018.05.002

Scheefhals, N., Westra, M., MacGillavry, H.D., 2023. mGluR5 is transiently confined in perisynaptic nanodomains to shape synaptic function. Nat. Commun. 14, 244. https://doi.org/10.1038/s41467-022-35680-w

Scheiffele, P., Fan, J., Choih, J., Fetter, R., Serafini, T., 2000. Neuroligin Expressed in Nonneuronal Cells Triggers Presynaptic Development in Contacting Axons. Cell 101, 657–669. https://doi.org/10.1016/S0092-8674(00)80877-6

Schlessinger, J., Koppel, D.E., Axelrod, D., Jacobson, K., Webb, W.W., Elson, E.L., 1976. Lateral transport on cell membranes: mobility of concanavalin A receptors on myoblasts. Proc. Natl. Acad. Sci. 73, 2409–2413. https://doi.org/10.1073/pnas.73.7.2409

Schmalfeldt, M., Bandtlow, C.E., Dours-Zimmermann, M.T., Winterhalter, K.H., Zimmermann, D.R., 2000. Brain derived versican V2 is a potent inhibitor of axonal growth. J. Cell Sci. 113, 807–816. https://doi.org/10.1242/jcs.113.5.807

Schmidt-Salzmann, C., Li, L., Bischofberger, J., 2014. Functional properties of extrasynaptic AMPA and NMDA receptors during postnatal hippocampal neurogenesis. J. Physiol. 592, 125–140. https://doi.org/10.1113/jphysiol.2013.267203

Schweitzer, B., Singh, J., Fejtova, A., Groc, L., Heine, M., Frischknecht, R., 2017. Hyaluronic acid based extracellular matrix regulates surface expression of GluN2B containing NMDA receptors. Sci. Rep. 7, 10991. https://doi.org/10.1038/s41598-017-07003-3

Sclip, A., Südhof, T.C., 2020. LAR receptor phospho-tyrosine phosphatases regulate NMDA-receptor responses. eLife 9, e53406. https://doi.org/10.7554/eLife.53406

Scott, D.B., Blanpied, T.A., Swanson, G.T., Zhang, C., Ehlers, M.D., 2001. An NMDA Receptor ER Retention Signal Regulated by Phosphorylation and Alternative Splicing. J. Neurosci. 21, 3063–3072. https://doi.org/10.1523/JNEUROSCI.21-09-03063.2001

Scott, L., Kruse, M.S., Forssberg, H., Brismar, H., Greengard, P., Aperia, A., 2002. Selective up-regulation of dopamine D1 receptors in dendritic spines by NMDA receptor activation. Proc. Natl. Acad. Sci. 99, 1661–1664. https://doi.org/10.1073/pnas.032654599

Scott, L., Zelenin, S., Malmersjö, S., Kowalewski, J.M., Markus, E.Z., Nairn, A.C., Greengard, P., Brismar, H., Aperia, A., 2006. Allosteric changes of the NMDA receptor trap diffusible

dopamine 1 receptors in spines. Proc. Natl. Acad. Sci. 103, 762–767. https://doi.org/10.1073/pnas.0505557103

Sebastianutto, I., Goyet, E., Andreoli, L., Font-Ingles, J., Moreno-Delgado, D., Bouquier, N., Jahannault-Talignani, C., Moutin, E., Menna, L.D., Maslava, N., Pin, J.-P., Fagni, L., Nicoletti, F., Ango, F., Cenci, M.A., Perroy, J., 2020. D1-mGlu5 heteromers mediate noncanonical dopamine signaling in Parkinson's disease. J. Clin. Invest. 130, 1168–1184. https://doi.org/10.1172/JCI126361

Seidlits, S.K., Khaing, Z.Z., Petersen, R.R., Nickels, J.D., Vanscoy, J.E., Shear, J.B., Schmidt, C.E., 2010. The effects of hyaluronic acid hydrogels with tunable mechanical properties on neural progenitor cell differentiation. Biomaterials 31, 3930–3940. https://doi.org/10.1016/j.biomaterials.2010.01.125

Sekino, Y., Tanaka, S., Hanamura, K., Yamazaki, H., Sasagawa, Y., Xue, Y., Hayashi, K., Shirao, T., 2006. Activation of *N*-methyl-d-aspartate receptor induces a shift of drebrin distribution: Disappearance from dendritic spines and appearance in dendritic shafts. Mol. Cell. Neurosci. 31, 493–504. https://doi.org/10.1016/j.mcn.2005.11.003

Shalizi, A., Gaudillière, B., Yuan, Z., Stegmüller, J., Shirogane, T., Ge, Q., Tan, Y., Schulman, B., Harper, J.W., Bonni, A., 2006. A Calcium-Regulated MEF2 Sumoylation Switch Controls Postsynaptic Differentiation. Science 311, 1012–1017. https://doi.org/10.1126/science.1122513

Shapira, M., Zhai, R.G., Dresbach, T., Bresler, T., Torres, V.I., Gundelfinger, E.D., Ziv, N.E., Garner, C.C., 2003. Unitary Assembly of Presynaptic Active Zones from Piccolo-Bassoon Transport Vesicles. Neuron 38, 237–252. https://doi.org/10.1016/s0896-6273(03)00207-1

Sharma, P., Mesci, P., Carromeu, C., McClatchy, D.R., Schiapparelli, L., Yates, J.R., Muotri, A.R., Cline, H.T., 2019. Exosomes regulate neurogenesis and circuit assembly. Proc. Natl. Acad. Sci. 116, 16086–16094. https://doi.org/10.1073/pnas.1902513116

Sharonov, A., Hochstrasser, R.M., 2006. Wide-field subdiffraction imaging by accumulated binding of diffusing probes. Proc. Natl. Acad. Sci. 103, 18911–18916. https://doi.org/10.1073/pnas.0609643104

Shibata, M., Pattabiraman, K., Muchnik, S.K., Kaur, N., Morozov, Y.M., Cheng, X., Waxman, S.G., Sestan, N., 2021. Hominini-specific regulation of CBLN2 increases prefrontal spinogenesis. Nature 598, 489–494. https://doi.org/10.1038/s41586-021-03952-y

Shuster, S.A., Li, J., Chon, Ur., Sinantha-Hu, M.C., Luginbuhl, D.J., Udeshi, N.D., Carey, D.K., Takeo, Y.H., Xie, Q., Xu, C., Mani, D.R., Han, S., Ting, A.Y., Carr, S.A., Luo, L., 2022. *In situ* cell-type-specific cell-surface proteomic profiling in mice. Neuron 110, 3882-3896.e9. https://doi.org/10.1016/j.neuron.2022.09.025

Sigler, A., Oh, W.C., Imig, C., Altas, B., Kawabe, H., Cooper, B.H., Kwon, H.-B., Rhee, J.-S., Brose, N., 2017. Formation and Maintenance of Functional Spines in the Absence of Presynaptic Glutamate Release. Neuron 94, 304-311.e4. https://doi.org/10.1016/j.neuron.2017.03.029

Sillivan, S.E., Konradi, C., 2011. Expression and function of dopamine receptors in the developing medial frontal cortex and striatum of the rat. Neuroscience 199, 501–514. https://doi.org/10.1016/j.neuroscience.2011.10.004

Simms, B.A., Zamponi, G.W., 2014. Neuronal Voltage-Gated Calcium Channels: Structure, Function, and Dysfunction. Neuron 82, 24–45. https://doi.org/10.1016/j.neuron.2014.03.016

Singer, S.J., Nicolson, G.L., 1972. The Fluid Mosaic Model of the Structure of Cell Membranes: Cell membranes are viewed as two-dimensional solutions of oriented globular proteins and lipids. Science 175, 720–731. https://doi.org/10.1126/science.175.4023.720

Singh, S.K., Stogsdill, J.A., Pulimood, N.S., Dingsdale, H., Kim, Y.H., Pilaz, L.-J., Kim, I.H., Manhaes, A.C., Rodrigues, W.S., Pamukcu, A., Enustun, E., Ertuz, Z., Scheiffele, P., Soderling, S.H., Silver, D.L., Ji, R.-R., Medina, A.E., Eroglu, C., 2016. Astrocytes Assemble Thalamocortical Synapses by Bridging NRX1α and NL1 via Hevin. Cell 164, 183–196. https://doi.org/10.1016/j.cell.2015.11.034

Skeberdis, V.A., Chevaleyre, V., Lau, C.G., Goldberg, J.H., Pettit, D.L., Suadicani, S.O., Lin, Y., Bennett, M.V.L., Yuste, R., Castillo, P.E., Zukin, R.S., 2006. Protein kinase A regulates calcium permeability of NMDA receptors. Nat. Neurosci. 9, 501–510. https://doi.org/10.1038/nn1664

Skulachev, V.P., Holtze, S., Vyssokikh, M.Y., Bakeeva, L.E., Skulachev, M.V., Markov, A.V., Hildebrandt, T.B., Sadovnichii, V.A., 2017. Neoteny, Prolongation of Youth: From Naked Mole Rats to “Naked Apes” (Humans). Physiol. Rev. 97, 699–720. https://doi.org/10.1152/physrev.00040.2015

Skupien, A., Konopka, A., Trzaskoma, P., Labus, J., Gorlewicz, A., Swiech, L., Babraj, M., Dolezyczek, H., Figiel, I., Ponimaskin, E., Wlodarczyk, J., Jaworski, J., Wilczynski, G.M., Dzwonek, J., 2014. CD44 regulates dendrite morphogenesis through Src tyrosine kinase-dependent positioning of the Golgi. Development 141, e2407–e2407. https://doi.org/10.1242/dev.119990

Smith, L.R., Cho, S., Discher, D.E., 2018. Stem Cell Differentiation is Regulated by Extracellular Matrix Mechanics. Physiology 33, 16–25. https://doi.org/10.1152/physiol.00026.2017

Söderberg, O., Gullberg, M., Jarvius, M., Ridderstråle, K., Leuchowius, K.-J., Jarvius, J., Wester, K., Hydbring, P., Bahram, F., Larsson, L.-G., Landegren, U., 2006. Direct observation of individual endogenous protein complexes in situ by proximity ligation. Nat. Methods 3, 995–1000. https://doi.org/10.1038/nmeth947

Söderberg, O., Leuchowius, K.-J., Gullberg, M., Jarvius, M., Weibrecht, I., Larsson, L.-G., Landegren, U., 2008. Characterizing proteins and their interactions in cells and tissues using the *in situ* proximity ligation assay. Methods, Visualization of molecular processes in cells using fluorescence imaging 45, 227–232. https://doi.org/10.1016/j.ymeth.2008.06.014

Soria, F.N., Paviolo, C., Doudnikoff, E., Arotcarena, M.-L., Lee, A., Danné, N., Mandal, A.K., Gosset, P., Dehay, B., Groc, L., Cognet, L., Bezard, E., 2020. Synucleinopathy alters nanoscale organization and diffusion in the brain extracellular space through hyaluronan remodeling. Nat. Commun. 11, 3440. https://doi.org/10.1038/s41467-020-17328-9

Specht, C.G., Izeddin, I., Rodriguez, P.C., El Beheiry, M., Rostaing, P., Darzacq, X., Dahan, M., Triller, A., 2013. Quantitative Nanoscopy of Inhibitory Synapses: Counting Gephyrin Molecules and Receptor Binding Sites. Neuron 79, 308–321. https://doi.org/10.1016/j.neuron.2013.05.013

Spicer, A.P., Joo, A., Bowling, R.A., 2003. A Hyaluronan Binding Link Protein Gene Family Whose Members Are Physically Linked Adjacent to Chrondroitin Sulfate Proteoglycan Core Protein Genes. J. Biol. Chem. 278, 21083–21091. https://doi.org/10.1074/jbc.M213100200

Standley, S., Roche, K.W., McCallum, J., Sans, N., Wenthold, R.J., 2000. PDZ Domain Suppression of an ER Retention Signal in NMDA Receptor NR1 Splice Variants. Neuron 28, 887–898. https://doi.org/10.1016/S0896-6273(00)00161-6

Stein, I.S., Gray, J.A., Zito, K., 2015. Non-Ionotropic NMDA Receptor Signaling Drives Activity-Induced Dendritic Spine Shrinkage. J. Neurosci. 35, 12303–12308. https://doi.org/10.1523/JNEUROSCI.4289-14.2015

Stein, I.S., Park, D.K., Claiborne, N., Zito, K., 2021. Non-ionotropic NMDA receptor signaling gates bidirectional structural plasticity of dendritic spines. Cell Rep. 34, 108664. https://doi.org/10.1016/j.celrep.2020.108664

Stein, I.S., Park, D.K., Flores, J.C., Jahncke, J.N., Zito, K., 2020. Molecular Mechanisms of Non-ionotropic NMDA Receptor Signaling in Dendritic Spine Shrinkage. J. Neurosci. 40, 3741–3750. https://doi.org/10.1523/JNEUROSCI.0046-20.2020

Stogsdill, J.A., Ramirez, J., Liu, D., Kim, Y.H., Baldwin, K.T., Enustun, E., Ejikeme, T., Ji, R.-R., Eroglu, C., 2017. Astrocytic neuroligins control astrocyte morphogenesis and synaptogenesis. Nature 551, 192–197. https://doi.org/10.1038/nature24638

Strack, S., McNeill, R.B., Colbran, R.J., 2000. Mechanism and Regulation of Calcium/Calmodulin-dependent Protein Kinase II Targeting to the NR2B Subunit of the N-Methyl-d-aspartate Receptor. J. Biol. Chem. 275, 23798–23806. https://doi.org/10.1074/jbc.M001471200

Stroebel, D., Mony, L., Paoletti, P., 2021. Glycine agonism in ionotropic glutamate receptors. Neuropharmacology 193, 108631. https://doi.org/10.1016/j.neuropharm.2021.108631

Stroebel, D., Paoletti, P., 2021. Architecture and function of NMDA receptors: an evolutionary perspective. J. Physiol. 599, 2615–2638. https://doi.org/10.1113/JP279028

Südhof, T.C., 2021. The cell biology of synapse formation. J. Cell Biol. 220, e202103052. https://doi.org/10.1083/jcb.202103052

Südhof, T.C., 2018. Towards an Understanding of Synapse Formation. Neuron 100, 276–293. https://doi.org/10.1016/j.neuron.2018.09.040

Südhof, T.C., 2017. Synaptic Neurexin Complexes: A Molecular Code for the Logic of Neural Circuits. Cell 171, 745–769. https://doi.org/10.1016/j.cell.2017.10.024

Südhof, T.C., Rothman, J.E., 2009. Membrane Fusion: Grappling with SNARE and SM Proteins. Science 323, 474–477. https://doi.org/10.1126/science.1161748

Sugihara, H., Moriyoshi, K., Ishii, T., Masu, M., Nakanishi, S., 1992. Structures and properties of seven isoforms of the NMDA receptor generated by alternative splicing. Biochem. Biophys. Res. Commun. 185, 826–832. https://doi.org/10.1016/0006-291X(92)91701-Q

Suh, Y.H., Terashima, A., Petralia, R.S., Wenthold, R.J., Isaac, J.T.R., Roche, K.W., Roche, P.A., 2010. A neuronal role for SNAP-23 in postsynaptic glutamate receptor trafficking. Nat. Neurosci. 13, 338–343. https://doi.org/10.1038/nn.2488

Sungkaworn, T., Jobin, M.-L., Burnecki, K., Weron, A., Lohse, M.J., Calebiro, D., 2017. Single-molecule imaging reveals receptor–G protein interactions at cell surface hot spots. Nature 550, 543–547. https://doi.org/10.1038/nature24264

Suttkus, A., Rohn, S., Weigel, S., Glöckner, P., Arendt, T., Morawski, M., 2014. Aggrecan, link protein and tenascin-R are essential components of the perineuronal net to protect neurons against iron-induced oxidative stress. Cell Death Dis. 5, e1119–e1119. https://doi.org/10.1038/cddis.2014.25

Suzuki, K., Hayashi, Y., Nakahara, S., Kumazaki, H., Prox, J., Horiuchi, K., Zeng, M., Tanimura, S., Nishiyama, Y., Osawa, S., Sehara-Fujisawa, A., Saftig, P., Yokoshima, S., Fukuyama, T., Matsuki, N., Koyama, R., Tomita, T., Iwatsubo, T., 2012. Activity-Dependent Proteolytic Cleavage of Neuroligin-1. Neuron 76, 410–422. https://doi.org/10.1016/j.neuron.2012.10.003

Swulius, M.T., Kubota, Y., Forest, A., Waxham, M.N., 2010. Structure and composition of the postsynaptic density during development. J. Comp. Neurol. 518, 4243–4260. https://doi.org/10.1002/cne.22451

Syková, E., Nicholson, C., 2008. Diffusion in Brain Extracellular Space. Physiol. Rev. 88, 1277–1340. https://doi.org/10.1152/physrev.00027.2007

Tabor, A., Weisenburger, S., Banerjee, A., Purkayastha, N., Kaindl, J.M., Hübner, H., Wei, L., Grömer, T.W., Kornhuber, J., Tschammer, N., Birdsall, N.J.M., Mashanov, G.I., Sandoghdar, V., Gmeiner, P., 2016. Visualization and ligand-induced modulation of dopamine receptor dimerization at the single molecule level. Sci. Rep. 6, 33233. https://doi.org/10.1038/srep33233

Takahashi, H., Sekino, Y., Tanaka, S., Mizui, T., Kishi, S., Shirao, T., 2003. Drebrin-Dependent Actin Clustering in Dendritic Filopodia Governs Synaptic Targeting of Postsynaptic Density-95 and Dendritic Spine Morphogenesis. J. Neurosci. 23, 6586–6595. https://doi.org/10.1523/JNEUROSCI.23-16-06586.2003

Takamori, S., Holt, M., Stenius, K., Lemke, E.A., Grønborg, M., Riedel, D., Urlaub, H., Schenck, S., Brügger, B., Ringler, P., Müller, S.A., Rammner, B., Gräter, F., Hub, J.S., De Groot, B.L., Mieskes, G., Moriyama, Y., Klingauf, J., Grubmüller, H., Heuser, J., Wieland, F., Jahn, R., 2006. Molecular Anatomy of a Trafficking Organelle. Cell 127, 831–846. https://doi.org/10.1016/j.cell.2006.10.030

Takano, T., Wallace, J.T., Baldwin, K.T., Purkey, A.M., Uezu, A., Courtland, J.L., Soderblom, E.J., Shimogori, T., Maness, P.F., Eroglu, C., Soderling, S.H., 2020. Chemico-genetic discovery of astrocytic control of inhibition in vivo. Nature 588, 296–302. https://doi.org/10.1038/s41586-020-2926-0

Takasu, M.A., Dalva, M.B., Zigmond, R.E., Greenberg, M.E., 2002. Modulation of NMDA Receptor-Dependent Calcium Influx and Gene Expression Through EphB Receptors. Science 295, 491–495. https://doi.org/10.1126/science.1065983

Takechi, M., Oshima, K., Nadano, D., Kitagawa, H., Matsuda, T., Miyata, S., 2020. A pericellular hyaluronan matrix is required for the morphological maturation of cortical neurons. Biochim. Biophys. Acta BBA - Gen. Subj. 1864, 129679. https://doi.org/10.1016/j.bbagen.2020.129679

Takeuchi, T., Duszkiewicz, A.J., Sonneborn, A., Spooner, P.A., Yamasaki, M., Watanabe, M., Smith, C.C., Fernández, G., Deisseroth, K., Greene, R.W., Morris, R.G.M., 2016. Locus coeruleus and dopaminergic consolidation of everyday memory. Nature 537, 357–362. https://doi.org/10.1038/nature19325

Talantova, M., Sanz-Blasco, S., Zhang, X., Xia, P., Akhtar, M.W., Okamoto, S., Dziewczapolski, G., Nakamura, T., Cao, G., Pratt, A.E., Kang, Y.-J., Tu, S., Molokanova, E., McKercher, S.R., Hires, S.A., Sason, H., Stouffer, D.G., Buczynski, M.W., Solomon, J.P., Michael, S., Powers, E.T., Kelly, J.W., Roberts, A., Tong, G., Fang-Newmeyer, T., Parker, J., Holland, E.A., Zhang, D., Nakanishi, N., Chen, H.-S.V., Wolosker, H., Wang, Y., Parsons, L.H., Ambasudhan, R., Masliah, E., Heinemann, S.F., Piña-Crespo, J.C., Lipton, S.A., 2013. Aβ induces astrocytic glutamate release, extrasynaptic NMDA receptor activation, and synaptic loss. Proc. Natl. Acad. Sci. 110, E2518–E2527. https://doi.org/10.1073/pnas.1306832110

Tam, J.Z., Palumbo, T., Miwa, J.M., Chen, B.Y., 2022. Analysis of Protein-Protein Interactions for Intermolecular Bond Prediction. Molecules 27, 6178. https://doi.org/10.3390/molecules27196178

Tanaka, C., Nishizuka, Y., 1994. The Protein Kinase C Family for Neuronal Signaling. Annu. Rev. Neurosci. 17, 551–567. https://doi.org/10.1146/annurev.ne.17.030194.003003

Tang, A.-H., Chen, H., Li, T.P., Metzbower, S.R., MacGillavry, H.D., Blanpied, T.A., 2016. A trans-synaptic nanocolumn aligns neurotransmitter release to receptors. Nature 536, 210–214. https://doi.org/10.1038/nature19058

Tao-Cheng, J.-H., Azzam, R., Crocker, V., Winters, C.A., Reese, T., 2015. Depolarization of Hippocampal Neurons Induces Formation of Nonsynaptic NMDA Receptor Islands Resembling Nascent Postsynaptic Densities. eNeuro 2. https://doi.org/10.1523/ENEURO.0066-15.2015

Thevalingam, D., Naik, A.A., Hrabe, J., McCloskey, D.P., Hrabětová, S., 2021. Brain extracellular space of the naked mole-rat expands and maintains normal diffusion under ischemic conditions. Brain Res. 1771, 147646. https://doi.org/10.1016/j.brainres.2021.147646

Thomas, P., Mortensen, M., Hosie, A.M., Smart, T.G., 2005. Dynamic mobility of functional GABAA receptors at inhibitory synapses. Nat. Neurosci. 8, 889–897. https://doi.org/10.1038/nn1483

Tian, X., Azpurua, J., Hine, C., Vaidya, A., Myakishev-Rempel, M., Ablaeva, J., Mao, Z., Nevo, E., Gorbunova, V., Seluanov, A., 2013. High-molecular-mass hyaluronan mediates the cancer resistance of the naked mole rat. Nature 499, 346–349. https://doi.org/10.1038/nature12234

Tingley, W.G., Ehlers, M.D., Kameyama, K., Doherty, C., Ptak, J.B., Riley, C.T., Huganir, R.L., 1997. Characterization of Protein Kinase A and Protein Kinase C Phosphorylation of the N-Methyl-D-aspartate Receptor NR1 Subunit Using Phosphorylation Site-specific Antibodies *. J. Biol. Chem. 272, 5157–5166. https://doi.org/10.1074/jbc.272.8.5157

Tissir, F., Goffinet, A.M., 2003. Reelin and brain development. Nat. Rev. Neurosci. 4, 496–505. https://doi.org/10.1038/nrn1113

Togashi, H., Abe, K., Mizoguchi, A., Takaoka, K., Chisaka, O., Takeichi, M., 2002. Cadherin Regulates Dendritic Spine Morphogenesis. Neuron 35, 77–89. https://doi.org/10.1016/S0896-6273(02)00748-1

Tønnesen, J., Hrabětová, S., Soria, F.N., 2023. Local diffusion in the extracellular space of the brain. Neurobiol. Dis. 177, 105981. https://doi.org/10.1016/j.nbd.2022.105981

Toole, B.P., 2004. Hyaluronan: from extracellular glue to pericellular cue. Nat. Rev. Cancer 4, 528–539. https://doi.org/10.1038/nrc1391

Toole, B.P., 2001. Hyaluronan in morphogenesis. Semin. Cell Dev. Biol. 12, 79–87. https://doi.org/10.1006/scdb.2000.0244

Tovar, K.R., Westbrook, G.L., 2002. Mobile NMDA Receptors at Hippocampal Synapses. Neuron 34, 255–264. https://doi.org/10.1016/S0896-6273(02)00658-X

Tovar, K.R., Westbrook, G.L., 1999. The Incorporation of NMDA Receptors with a Distinct Subunit Composition at Nascent Hippocampal Synapses *In Vitro*. J. Neurosci. 19, 4180–4188. https://doi.org/10.1523/JNEUROSCI.19-10-04180.1999

Tran, T.S., Rubio, M.E., Clem, R.L., Johnson, D., Case, L., Tessier-Lavigne, M., Huganir, R.L., Ginty, D.D., Kolodkin, A.L., 2009. Secreted semaphorins control spine distribution and morphogenesis in the postnatal CNS. Nature 462, 1065–1069. https://doi.org/10.1038/nature08628

Traynelis, S.F., Wollmuth, L.P., McBain, C.J., Menniti, F.S., Vance, K.M., Ogden, K.K., Hansen, K.B., Yuan, H., Myers, S.J., Dingledine, R., 2010. Glutamate Receptor Ion Channels: Structure, Regulation, and Function. Pharmacol. Rev. 62, 405–496. https://doi.org/10.1124/pr.109.002451

Trifilieff, P., Rives, M.-L., Urizar, E., Piskorowski, R.A., Vishwasrao, H.D., Castrillon, J., Schmauss, C., Slättman, M., Gullberg, M., Javitch, J.A., 2011. Detection of Antigen Interactions Ex Vivo by Proximity Ligation Assay: Endogenous Dopamine D2-Adenosine A2A Receptor Complexes in the Striatum. BioTechniques 51, 111–118. https://doi.org/10.2144/000113719

Trinkle-Mulcahy, L., Boulon, S., Lam, Y.W., Urcia, R., Boisvert, F.-M., Vandermoere, F., Morrice, N.A., Swift, S., Rothbauer, U., Leonhardt, H., Lamond, A., 2008. Identifying specific protein interaction partners using quantitative mass spectrometry and bead proteomes. J. Cell Biol. 183, 223–239. https://doi.org/10.1083/jcb.200805092

Tritsch, N.X., Sabatini, B.L., 2012. Dopaminergic Modulation of Synaptic Transmission in Cortex and Striatum. Neuron 76, 33–50. https://doi.org/10.1016/j.neuron.2012.09.023

Tsai, Y.-X., Chang, N.-E., Reuter, K., Chang, H.-T., Yang, T.-J., Von Bülow, S., Sehrawat, V., Zerrouki, N., Tuffery, M., Gecht, M., Grothaus, I.L., Colombi Ciacchi, L., Wang, Y.-S., Hsu, M.-F., Khoo, K.-H., Hummer, G., Hsu, S.-T.D., Hanus, C., Sikora, M., 2024. Rapid simulation of glycoprotein structures by grafting and steric exclusion of glycan conformer libraries. Cell 187, 1296-1311.e26. https://doi.org/10.1016/j.cell.2024.01.034

Tsui, C.C., Copeland, N.G., Gilbert, D.J., Jenkins, N.A., Barnes, C., Worley, P.F., 1996. Narp, a novel member of the pentraxin family, promotes neurite outgrowth and is dynamically regulated

by neuronal activity. J. Neurosci. 16, 2463–2478. https://doi.org/10.1523/JNEUROSCI.16-08-02463.1996

Tu, W., Xu, X., Peng, L., Zhong, X., Zhang, Wenfeng, Soundarapandian, M.M., Belal, C., Wang, M., Jia, N., Zhang, Wen, Lew, F., Chan, S.L., Chen, Y., Lu, Y., 2010. DAPK1 Interaction with NMDA Receptor NR2B Subunits Mediates Brain Damage in Stroke. Cell 140, 222–234. https://doi.org/10.1016/j.cell.2009.12.055

Uchigashima, M., Ohtsuka, T., Kobayashi, K., Watanabe, M., 2016. Dopamine synapse is a neuroligin-2–mediated contact between dopaminergic presynaptic and GABAergic postsynaptic structures. Proc. Natl. Acad. Sci. 113, 4206–4211. https://doi.org/10.1073/pnas.1514074113

Ullian, E.M., Sapperstein, S.K., Christopherson, K.S., Barres, B.A., 2001. Control of Synapse Number by Glia. Sci. New Ser. 291, 657–661.

Um, J.W., Ko, J., 2013. LAR-RPTPs: synaptic adhesion molecules that shape synapse development. Trends Cell Biol. 23, 465–475. https://doi.org/10.1016/j.tcb.2013.07.004

Van Oostrum, M., Campbell, B., Seng, C., Müller, M., Tom Dieck, S., Hammer, J., Pedrioli, P.G.A., Földy, C., Tyagarajan, S.K., Wollscheid, B., 2020. Surfaceome dynamics reveal proteostasis-independent reorganization of neuronal surface proteins during development and synaptic plasticity. Nat. Commun. 11, 4990. https://doi.org/10.1038/s41467-020-18494-6

Vardalaki, D., Chung, K., Harnett, M.T., 2022. Filopodia are a structural substrate for silent synapses in adult neocortex. Nature 612, 323–327. https://doi.org/10.1038/s41586-022-05483-6

Varela, J.A., Dupuis, J.P., Etchepare, L., Espana, A., Cognet, L., Groc, L., 2016. Targeting neurotransmitter receptors with nanoparticles in vivo allows single-molecule tracking in acute brain slices. Nat. Commun. 7, 10947. https://doi.org/10.1038/ncomms10947

Varela, J.A., Hirsch, S.J., Chapman, D., Leverich, L.S., Greene, R.W., 2009. D1/D5 Modulation of Synaptic NMDA Receptor Currents. J. Neurosci. 29, 3109–3119. https://doi.org/10.1523/JNEUROSCI.4746-08.2009

Varela-Nallar, L., Alfaro, I.E., Serrano, F.G., Parodi, J., Inestrosa, N.C., 2010. Wingless-type family member 5A (Wnt-5a) stimulates synaptic differentiation and function of glutamatergic synapses. Proc. Natl. Acad. Sci. 107, 21164–21169. https://doi.org/10.1073/pnas.1010011107

Varoqueaux, F., Aramuni, G., Rawson, R.L., Mohrmann, R., Missler, M., Gottmann, K., Zhang, W., Südhof, T.C., Brose, N., 2006. Neuroligins Determine Synapse Maturation and Function. Neuron 51, 741–754. https://doi.org/10.1016/j.neuron.2006.09.003

Verhage, M., Maia, A.S., Plomp, J.J., Brussaard, A.B., Heeroma, J.H., Vermeer, H., Toonen, R.F., Hammer, R.E., Van Den, T.K., Berg, Missler, M., Geuze, H.J., Südhof, T.C., 2000. Synaptic Assembly of the Brain in the Absence of Neurotransmitter Secretion. Science 287, 864–869. https://doi.org/10.1126/science.287.5454.864

Verney, C., Baulac, M., Berger, B., Alvarez, C., Vigny, A., Helle, K.B., 1985. Morphological evidence for a dopaminergic terminal field in the hippocampal formation of young and adult rat. Neuroscience 14, 1039–1052. https://doi.org/10.1016/0306-4522(85)90275-1

Vicini, S., Wang, J.F., Li, J.H., Zhu, W.J., Wang, Y.H., Luo, J.H., Wolfe, B.B., Grayson, D.R., 1998. Functional and Pharmacological Differences Between RecombinantN-Methyl-d-Aspartate Receptors. J. Neurophysiol. 79, 555–566. https://doi.org/10.1152/jn.1998.79.2.555

Vieira, M., Yong, X.L.H., Roche, K.W., Anggono, V., 2020. Regulation of NMDA glutamate receptor functions by the GluN2 subunits. J. Neurochem. 154, 121–143. https://doi.org/10.1111/jnc.14970

Vigetti, D., Karousou, E., Viola, M., Deleonibus, S., De Luca, G., Passi, A., 2014. Hyaluronan: Biosynthesis and signaling. Biochim. Biophys. Acta BBA - Gen. Subj. 1840, 2452–2459. https://doi.org/10.1016/j.bbagen.2014.02.001

Vissel, B., Krupp, J.J., Heinemann, S.F., Westbrook, G.L., 2001. A use-dependent tyrosine dephosphorylation of NMDA receptors is independent of ion flux. Nat. Neurosci. 4, 587–596. https://doi.org/10.1038/88404

Vukoja, A., Rey, U., Petzoldt, A.G., Ott, C., Vollweiter, D., Quentin, C., Puchkov, D., Reynolds, E., Lehmann, M., Hohensee, S., Rosa, S., Lipowsky, R., Sigrist, S.J., Haucke, V., 2018. Presynaptic Biogenesis Requires Axonal Transport of Lysosome-Related Vesicles. Neuron 99, 1216-1232.e7. https://doi.org/10.1016/j.neuron.2018.08.004

Wakayama, S., Kiyonaka, S., Arai, I., Kakegawa, W., Matsuda, S., Ibata, K., Nemoto, Y.L., Kusumi, A., Yuzaki, M., Hamachi, I., 2017. Chemical labelling for visualizing native AMPA receptors in live neurons. Nat. Commun. 8, 14850. https://doi.org/10.1038/ncomms14850

Walling, M.A., Novak, J.A., Shepard, J.R.E., 2009. Quantum Dots for Live Cell and In Vivo Imaging. Int. J. Mol. Sci. 10, 441–491. https://doi.org/10.3390/ijms10020441

Wang, M., Wong, A.H., Liu, F., 2012. Interactions between NMDA and dopamine receptors: A potential therapeutic target. Brain Res. 1476, 154–163. https://doi.org/10.1016/j.brainres.2012.03.029

Wang, X., Hu, B., Zieba, A., Neumann, N.G., Kasper-Sonnenberg, M., Honsbein, A., Hultqvist, G., Conze, T., Witt, W., Limbach, C., Geitmann, M., Danielson, H., Kolarow, R., Niemann, G., Lessmann, V., Kilimann, M.W., 2009. A Protein Interaction Node at the Neurotransmitter Release Site: Domains of Aczonin/Piccolo, Bassoon, CAST, and Rim Converge on the N-Terminal Domain of Munc13-1. J. Neurosci. 29, 12584–12596. https://doi.org/10.1523/JNEUROSCI.1255-09.2009

Washbourne, P., 2015. Synapse Assembly and Neurodevelopmental Disorders. Neuropsychopharmacology 40, 4–15. https://doi.org/10.1038/npp.2014.163

Washbourne, P., Bennett, J.E., McAllister, A.K., 2002. Rapid recruitment of NMDA receptor transport packets to nascent synapses. Nat. Neurosci. 5, 751–759. https://doi.org/10.1038/nn883

Washbourne, P., Liu, X.-B., Jones, E.G., McAllister, A.K., 2004. Cycling of NMDA Receptors during Trafficking in Neurons before Synapse Formation. J. Neurosci. 24, 8253–8264. https://doi.org/10.1523/JNEUROSCI.2555-04.2004

Washburn, H.R., Xia, N.L., Zhou, W., Mao, Y.-T., Dalva, M.B., 2020. Positive surface charge of GluN1 N-terminus mediates the direct interaction with EphB2 and NMDAR mobility. Nat. Commun. 11, 570. https://doi.org/10.1038/s41467-020-14345-6

Watanabe, M., Inoue, Y., Sakimura, K., Mishina, M., 1992. Developmental changes in distribution of NMDA receptor channel subunit mRNAs. NeuroReport 3, 1138.

Waugh, D.F., 1954. Protein-Protein Interactions, in: Anson, M.L., Bailey, K., Edsall, J.T. (Eds.), Advances in Protein Chemistry. Academic Press, pp. 325–437. https://doi.org/10.1016/S0065-3233(08)60210-7

Wei, X., Ma, T., Cheng, Y., Huang, C.C.Y., Wang, X., Lu, J., Wang, J., 2018. Dopamine D1 or D2 receptor-expressing neurons in the central nervous system. Addict. Biol. 23, 569–584. https://doi.org/10.1111/adb.12512

Weigel, P.H., Baggenstoss, B.A., 2017. What is special about 200 kDa hyaluronan that activates hyaluronan receptor signaling? Glycobiology 27, 868–877. https://doi.org/10.1093/glycob/cwx039

Weigel, P.H., Hascall, V.C., Tammi, M., 1997. Hyaluronan Synthases. J. Biol. Chem. 272, 13997–14000. https://doi.org/10.1074/jbc.272.22.13997

Willems, J., De Jong, A.P.H., Scheefhals, N., Mertens, E., Catsburg, L.A.E., Poorthuis, R.B., De Winter, F., Verhaagen, J., Meye, F.J., MacGillavry, H.D., 2020. ORANGE: A CRISPR/Cas9-based genome editing toolbox for epitope tagging of endogenous proteins in neurons. PLOS Biol. 18, e3000665. https://doi.org/10.1371/journal.pbio.3000665

Wilson, E., Knudson, W., Newell-Litwa, K., 2020. Hyaluronan regulates synapse formation and function in developing neural networks. Sci. Rep. 10, 16459. https://doi.org/10.1038/s41598-020-73177-y

Wollmuth, L.P., 2018. Ion permeation in ionotropic glutamate receptors: still dynamic after all these years. Curr. Opin. Physiol., Ion Channels 2, 36–41. https://doi.org/10.1016/j.cophys.2017.12.003

Woods, A.S., Ciruela, F., Fuxe, K., Agnati, L.F., Lluis, C., Franco, R., Ferré, S., 2005. Role of Electrostatic Interaction in Receptor–Receptor Heteromerization. J. Mol. Neurosci. 26, 125–132. https://doi.org/10.1385/JMN:26:2-3:125

Wu, G.-Y., Malinow, R., Cline, H.T., 1996. Maturation of a Central Glutamatergic Synapse. Science 274, 972–976. https://doi.org/10.1126/science.274.5289.972

Wu, X., Cai, Q., Shen, Z., Chen, X., Zeng, M., Du, S., Zhang, M., 2019. RIM and RIM-BP Form Presynaptic Active-Zone-like Condensates via Phase Separation. Mol. Cell 73, 971-984.e5. https://doi.org/10.1016/j.molcel.2018.12.007

Wu, Y., Jiang, T., 2022. Developments in FRET- and BRET-Based Biosensors. Micromachines 13, 1789. https://doi.org/10.3390/mi13101789

Wyllie, D.J.A., Béhé, P., Colquhoun, D., 1998. Single-channel activations and concentration jumps: comparison of recombinant NR1a/NR2A and NR1a/NR2D NMDA receptors. J. Physiol. 510, 1–18. https://doi.org/10.1111/j.1469-7793.1998.001bz.x

Xiao, M.-Y., Wasling, P., Hanse, E., Gustafsson, B., 2004. Creation of AMPA-silent synapses in the neonatal hippocampus. Nat. Neurosci. 7, 236–243. https://doi.org/10.1038/nn1196

Xie, L., Kang, H., Xu, Q., Chen, M.J., Liao, Y., Thiyagarajan, M., O'Donnell, J., Christensen, D.J., Nicholson, C., Iliff, J.J., Takano, T., Deane, R., Nedergaard, M., 2013. Sleep Drives

Metabolite Clearance from the Adult Brain. Science 342, 373–377. https://doi.org/10.1126/science.1241224

Xu, D., Hopf, C., Reddy, R., Cho, R.W., Guo, L., Lanahan, A., Petralia, R.S., Wenthold, R.J., O'Brien, R.J., Worley, P., 2003. Narp and NP1 Form Heterocomplexes that Function in Developmental and Activity-Dependent Synaptic Plasticity. Neuron 39, 513–528. https://doi.org/10.1016/S0896-6273(03)00463-X

Xu, J., Xiao, N., Xia, J., 2010. Thrombospondin 1 accelerates synaptogenesis in hippocampal neurons through neuroligin 1. Nat. Neurosci. 13, 22–24. https://doi.org/10.1038/nn.2459

Yamaguchi, Y., 2000. Lecticans: organizers of the brain extracellular matrix: Cell. Mol. Life Sci. 57, 276–289. https://doi.org/10.1007/PL00000690

Yamashita, N., Morita, A., Uchida, Y., Nakamura, F., Usui, H., Ohshima, T., Taniguchi, M., Honnorat, J., Thomasset, N., Takei, K., Takahashi, T., Kolattukudy, P., Goshima, Y., 2007. Regulation of Spine Development by Semaphorin3A through Cyclin-Dependent Kinase 5 Phosphorylation of Collapsin Response Mediator Protein 1. J. Neurosci. 27, 12546–12554. https://doi.org/10.1523/JNEUROSCI.3463-07.2007

Yan, J., Bengtson, C.P., Buchthal, B., Hagenston, A.M., Bading, H., 2020. Coupling of NMDA receptors and TRPM4 guides discovery of unconventional neuroprotectants. Science 370, eaay3302. https://doi.org/10.1126/science.aay3302

Yang, C., Cao, M., Liu, H., He, Y., Xu, J., Du, Y., Liu, Y., Wang, W., Cui, L., Hu, J., Gao, F., 2012. The High and Low Molecular Weight Forms of Hyaluronan Have Distinct Effects on CD44 Clustering. J. Biol. Chem. 287, 43094–43107. https://doi.org/10.1074/jbc.M112.349209

Yang, W., Steen, H., Freeman, M.R., 2008. Proteomic approaches to the analysis of multiprotein signaling complexes. PROTEOMICS 8, 832–851. https://doi.org/10.1002/pmic.200700650

Yi, Z., Petralia, R.S., Fu, Z., Swanwick, C.C., Wang, Y.-X., Prybylowski, K., Sans, N., Vicini, S., Wenthold, R.J., 2007. The Role of the PDZ Protein GIPC in Regulating NMDA Receptor Trafficking. J. Neurosci. 27, 11663–11675. https://doi.org/10.1523/JNEUROSCI.3252-07.2007

Yoshii, A., Constantine-Paton, M., 2007. BDNF induces transport of PSD-95 to dendrites through PI3K-AKT signaling after NMDA receptor activation. Nat. Neurosci. 10, 702–711. https://doi.org/10.1038/nn1903

Young, S.H., Poo, M., 1983. Spontaneous release of transmitter from growth cones of embryonic neurones. Nature 305, 634–637. https://doi.org/10.1038/305634a0

Yu, S.P., Jiang, M.Q., Shim, S.S., Pourkhodadad, S., Wei, L., 2023. Extrasynaptic NMDA receptors in acute and chronic excitotoxicity: implications for preventive treatments of ischemic stroke and late-onset Alzheimer's disease. Mol. Neurodegener. 18, 43. https://doi.org/10.1186/s13024-023-00636-1

Yuan, H., Hansen, K.B., Vance, K.M., Ogden, K.K., Traynelis, S.F., 2009. Control of NMDA Receptor Function by the NR2 Subunit Amino-Terminal Domain. J. Neurosci. 29, 12045–12058. https://doi.org/10.1523/JNEUROSCI.1365-09.2009

Yuste, R., 2015. The discovery of dendritic spines by Cajal. Front. Neuroanat. 9. https://doi.org/10.3389/fnana.2015.00018

Yuste, R., Bonhoeffer, T., 2004. Genesis of dendritic spines: insights from ultrastructural and imaging studies. Nat. Rev. Neurosci. 5, 24–34. https://doi.org/10.1038/nrn1300

Yuzaki, M., 2018. Two Classes of Secreted Synaptic Organizers in the Central Nervous System. Annu. Rev. Physiol. 80, 243–262. https://doi.org/10.1146/annurev-physiol-021317-121322

Zakharenko, S., Chang, S., O'Donoghue, M., Popov, S.V., 1999. Neurotransmitter Secretion along Growing Nerve Processes: Comparison with Synaptic Vesicle Exocytosis. J. Cell Biol. 144, 507–518. https://doi.org/10.1083/jcb.144.3.507

Zakusilo, F.T., Kerry O'Banion, M., Gelbard, H.A., Seluanov, A., Gorbunova, V., 2021. Matters of size: Roles of hyaluronan in CNS aging and disease. Ageing Res. Rev. 72, 101485. https://doi.org/10.1016/j.arr.2021.101485

Zeng, M., Chen, X., Guan, D., Xu, J., Wu, H., Tong, P., Zhang, M., 2018. Reconstituted Postsynaptic Density as a Molecular Platform for Understanding Synapse Formation and Plasticity. Cell 174, 1172-1187.e16. https://doi.org/10.1016/j.cell.2018.06.047

Zeng, M., Shang, Y., Araki, Y., Guo, T., Huganir, R.L., Zhang, M., 2016. Phase Transition in Postsynaptic Densities Underlies Formation of Synaptic Complexes and Synaptic Plasticity. Cell 166, 1163-1175.e12. https://doi.org/10.1016/j.cell.2016.07.008

Zhang, H., Li, T., Li, S., Liu, F., 2016. Cross-talk between α7 nAchR and NMDAR revealed by protein profiling. J. Proteomics 131, 113–121. https://doi.org/10.1016/j.jprot.2015.10.018

Zhang, H., Tsui, C.K., Garcia, G., Joe, L.K., Wu, H., Maruichi, A., Fan, W., Pandovski, S., Yoon, P.H., Webster, B.M., Durieux, J., Frankino, P.A., Higuchi-Sanabria, R., Dillin, A., 2024. The extracellular matrix integrates mitochondrial homeostasis. Cell S009286742400638X. https://doi.org/10.1016/j.cell.2024.05.057

Zhang, J., Guan, X., Li, Q., Meredith, A.L., Pan, H.-L., Yan, J., 2018. Glutamate-activated BK channel complexes formed with NMDA receptors. Proc. Natl. Acad. Sci. 115, E9006–E9014. https://doi.org/10.1073/pnas.1802567115

Zhang, J., Xu, T.-X., Hallett, P.J., Watanabe, M., Grant, S.G.N., Isacson, O., Yao, W.-D., 2009. PSD-95 Uncouples Dopamine–Glutamate Interaction in the D_1 /PSD-95/NMDA Receptor Complex. J. Neurosci. 29, 2948–2960. https://doi.org/10.1523/JNEUROSCI.4424-08.2009

Zhang, Z., Tian, X., Lu, J.Y., Boit, K., Ablaeva, J., Zakusilo, F.T., Emmrich, S., Firsanov, D., Rydkina, E., Biashad, S.A., Lu, Q., Tyshkovskiy, A., Gladyshev, V.N., Horvath, S., Seluanov, A., Gorbunova, V., 2023. Increased hyaluronan by naked mole-rat Has2 improves healthspan in mice. Nature 621, 196–205. https://doi.org/10.1038/s41586-023-06463-0

Zhao, Y., Qiao, S., Zhang, B., Cao, Y., Tian, H., Liu, R., Sun, L., Wang, C., Li, Liang, Wang, R., Chen, Y., Hou, X., Li, Y., Zhou, J., Li, Liyi, Tian, W., 2022. A novel neuroinflammation-responsive hydrogel based on mimicking naked mole rat brain microenvironment retards neurovascular dysfunction and cognitive decline in Alzheimer's disease. Chem. Eng. J. 430, 133090. https://doi.org/10.1016/j.cej.2021.133090

Zhao, Y., Zheng, Z., Zhang, Z., Xu, Y., Hillpot, E., Lin, Y.S., Zakusilo, F.T., Lu, J.Y., Ablaeva, J., Biashad, S.A., Miller, R.A., Nevo, E., Seluanov, A., Gorbunova, V., 2023. Evolution of high-molecular-

mass hyaluronic acid is associated with subterranean lifestyle. Nat. Commun. 14, 8054. https://doi.org/10.1038/s41467-023-43623-2

Zhou, Q., Homma, K.J., Poo, M., 2004. Shrinkage of Dendritic Spines Associated with Long-Term Depression of Hippocampal Synapses. Neuron 44, 749–757. https://doi.org/10.1016/j.neuron.2004.11.011

Zhu, J., Shang, Y., Zhang, M., 2016. Mechanistic basis of MAGUK-organized complexes in synaptic development and signalling. Nat. Rev. Neurosci. 17, 209–223. https://doi.org/10.1038/nrn.2016.18

Zhu, J.J., Malinow, R., 2002. Acute versus chronic NMDA receptor blockade and synaptic AMPA receptor delivery. Nat. Neurosci. 5, 513–514. https://doi.org/10.1038/nn0602-850

Zieger, H.L., Choquet, D., 2021. Nanoscale synapse organization and dysfunction in neurodevelopmental disorders. Neurobiol. Dis. 158, 105453. https://doi.org/10.1016/j.nbd.2021.105453

Zimmermann, D.R., Dours-Zimmermann, M.T., 2008. Extracellular matrix of the central nervous system: from neglect to challenge. Histochem. Cell Biol. 130, 635–653. https://doi.org/10.1007/s00418-008-0485-9

Zito, K., Scheuss, V., Knott, G., Hill, T., Svoboda, K., 2009. Rapid Functional Maturation of Nascent Dendritic Spines. Neuron 61, 247–258. https://doi.org/10.1016/j.neuron.2008.10.054

Ziv, N.E., Smith, S.J., 1996. Evidence for a Role of Dendritic Filopodia in Synaptogenesis and Spine Formation. Neuron 17, 91–102. https://doi.org/10.1016/S0896-6273(00)80283-4

Zong, P., Feng, J., Yue, Z., Li, Y., Wu, G., Sun, B., He, Y., Miller, B., Yu, A.S., Su, Z., Xie, J., Mori, Y., Hao, B., Yue, L., 2022. Functional coupling of TRPM2 and extrasynaptic NMDARs exacerbates excitotoxicity in ischemic brain injury. Neuron 110, 1944-1958.e8. https://doi.org/10.1016/j.neuron.2022.03.021